



Durham E-Theses

Chiral lanthanide complexes as probe of nucleic acids

Mathieu, Celine E.

How to cite:

Mathieu, Celine E. (2001) *Chiral lanthanide complexes as probe of nucleic acids*, Durham theses, Durham University. Available at Durham E-Theses Online: <http://etheses.dur.ac.uk/3812/>

Use policy

The full-text may be used and/or reproduced, and given to third parties in any format or medium, without prior permission or charge, for personal research or study, educational, or not-for-profit purposes provided that:

- a full bibliographic reference is made to the original source
- a [link](#) is made to the metadata record in Durham E-Theses
- the full-text is not changed in any way

The full-text must not be sold in any format or medium without the formal permission of the copyright holders.

Please consult the [full Durham E-Theses policy](#) for further details.

University of DURHAM

Department of Chemistry

Chiral Lanthanide Complexes
as Probe of Nucleic Acids

Céline E. Mathieu

The copyright of this thesis rests with the author. No quotation from it should be published in any form, including Electronic and the Internet, without the author's prior written consent. All information derived from this thesis must be acknowledged appropriately.

A thesis submitted for the degree of Doctor of Philosophy



2001

- 8 MAR 2002

Declaration

The work described herein was carried out in the Department of Chemistry, University of Durham, between October 1997 and September 2000. All the work is my own unless otherwise stated, and no part of it has been submitted for a degree at this or any other university.

Statement of copyright

The copyright of this thesis rests with the author. No quotation should be published without prior consent and information derived from it must be acknowledged.

To my Grand Dad
A mon grand-père, René Baderot

Acknowledgements

I would like to express my sincere thanks to Prof. David Parker for his constant encouragement, help and patience through the past three years, and for giving me the opportunity to come to Durham to achieve my PhD.

I am very grateful to Dr Guiliano Siligardi for his advice and patience in setting-up CD experiments.

I would like to thank Dr R. Peacock, S. Lopinski and Prof. J. Riehl for running CPL experiments.

I would like to thank Lara Turner and Dr. Mike Jones for their help and advice in the Mass Spectrometry Lab.

I would like to address my thanks to Alison Jones for her valuable help in running luminescence experiments.

I would like to express my special thanks to friends who have made my time in Durham so great especially Linda, Rachel, Sharon & Martin, Karima, Thorri, people from DARC and Marie-Anne.

I would like to thank all my colleagues from CG 27 for the wonderful ambience everyone has brought to the lab from all over the world. It has been so nice to work with all of you, and special thanks to Kanthi for all her help with synthesis and her sympathy.

I would like to express my gratitude to my parents and brothers for their precious and enthusiastic support, and for understanding my choices.

And finally I am especially thankful to Eric for his patience, encouragement and optimism through the past three years.

Abstract

A series of kinetically stable chiral lanthanide complexes has been developed, with a view to developing responsive probes for use in analysis and in seeking chiral complexes exhibiting selectivity in their interaction with nucleic acids.

Firstly a pH sensitive complex has been modified with the aim of tuning the pH range to which it responds to the physiologically useful regime. The synthesis was undertaken of relatively lipophilic 6-butylphenanthridinyl complexes. Their photophysical behaviour was investigated by absorbance and luminescence spectroscopy and the modulation of their emission examined in the pH range 4.5 to 7.5.

In addition to their luminescent properties, enantiomerically pure chiral lanthanide complexes permit chiroptical techniques to be used, allowing their interactions with other chiral species to be addressed (e.g. nucleic acids, oligonucleotides).

The first series of enantiopure lanthanide complexes has been devised that show several interesting features in binding to oligonucleotides and nucleic acids. These macrocyclic tris- and tetra-amide lanthanide (Eu, Tb or Yb) complexes contain an N-alkyl phenanthridinium unit that allows intercalation between the base pairs of the DNA. Their binding to $[(AT)_6]_2$, $[(CG)_6]_2$ and CT-DNA was monitored by changes in the ligand and metal based luminescence, and in the characteristic CD bands of the oligonucleotides. Binding affinities were assessed using intrinsic methods and the McGhee-von Hippel analysis. Marked differences have been observed in the binding of Eu and Yb complexes as a function of the Δ and Λ helicity of the complexes, which is itself determined by the configuration of the remote amide substituents. Binding of the Δ -Eu complex was over 50 times stronger to $[(CG)_6]_2$ compared to $[(AT)_6]_2$, while the left handed Λ -Yb complex showed a different pattern of selectivity. In the europium complex of a related heptadentate tris-amide ligand, the coordination of a DNA phosphate group to the lanthanide centre was suggested by emission and lifetime changes.

Another series of chiral tetraamide complexes linked to the 6 position of the phenanthridine moiety was synthesised and studied. An additional stereogenic centre at carbon, alpha to the phenanthridine group was introduced with the aim of tuning the selectivity of binding. A set of four diastereoisomeric ligands was separated and their lanthanide complexes characterised. The binding of their Eu and Yb complexes was evaluated and differences between Eu and Yb complexes persisted. The additional chiral centre did not appear to modify the binding affinity of this series of complexes. Finally, a series of 6-phenanthridinyl complexes was investigated in which the phenanthridine N atom was directly bound to the lanthanide centre.. Their affinity for DNA was found to be relatively low, which may be related to their rigid structure.

2-3.1	<i>Synthesis of europium(III) and terbium(III) complexes</i>	44
2-3.2	<i>Luminescence properties of these complexes</i>	47
2-3.2.1	<i>Determination of acidity constant</i>	47
2-3.2.2	<i>Lifetimes and quantum yields</i>	52
Chapter 3: 2-Phenanthridinyl based ligands for DNA interaction		57
3-1	Bases	58
3-1.1	<i>Description of the chiral complexes</i>	58
3-1.2	<i>Interaction with oligonucleotides</i>	60
3-1.3	<i>Photophysical aspects of the interaction</i>	60
3-1.4	<i>McGhee and von Hippel method of binding constant determination</i>	61
3-2	Interaction of 2-phenanthridinium Δ and Λ complexes with oligonucleotides	64
3-2.1	<i>Affinities towards [(CG)₆]₂ and [(AT)₆]₂</i>	64
3-2.1.1	<i>Europium complexes Δ and Λ-[LnL¹]⁴⁺</i>	64
3-2.1.1.1	<i>Absorbance spectroscopy</i>	64
3-2.1.1.2	<i>Luminescence spectroscopy</i>	65
3-2.1.1.3	<i>Circular dichroism spectroscopy</i>	68
3-2.1.2	<i>Ytterbium complexes: Δ and Λ [YbL¹]⁴⁺</i>	71
3-2.1.3	<i>Mass spectrometry</i>	73
3-2.1.4	<i>Binding affinities of Δ and Λ-Ln complexes to [(CG)₆]₂ and [(AT)₆]₂</i>	75
3-2.2	<i>Control experiments</i>	77
3-2.2.1	<i>Quenching of fluorescence from complexes Δ and Λ</i>	77
3-2.2.2	<i>Control CD studies of the Δ and Λ-tetraamide complexes</i>	81
3-2.3	<i>Dependence of affinity on salt concentration</i>	83
3-3	Control studies examining the unmethylated complexes, Δ and Λ-[LnL³]³⁺	85
3-3.1	<i>Binding affinities: absorbance, fluorescence quenching and CD studies</i>	86
3-3.2	<i>Salt concentration effect</i>	91
3-4	A diaqua Δ-L⁴ Europium complex	93
3-4.1	<i>Spectroscopic titrations</i>	94
3-4.2	<i>Binding affinities for Δ-[EuL⁴]⁴⁺ with [(CG)₆]₂ and [(AT)₆]₂</i>	99
3-4.3	<i>Lifetime measurements</i>	99

Chapter 4: 6-Phenanthridinyl based ligands for DNA interaction.....	102
4-1 A new series of chiral phenanthridinyl complexes.....	102
4-1.1 Aims and objectives.....	102
4-1.2 Synthesis of a series of chiral complexes.....	103
4-1.3 Interaction with nucleic acids.....	107
4-1.3.1 Absorbance and fluorescence spectroscopies.....	107
4-1.3.2 CD titrations.....	113
4-1.3.3 Ionic strength influence.....	117
4-2 Mono and bis chiral phenanthridinyl complexes.....	119
4-2.1 Synthesis of a series of chiral complexes.....	120
4-2.2 Characterisation of the complexes $[EuL^9]^{3+}$ $[EuL^{10}]^{3+}$ and $[EuL^{11}]^{3+}$	122
4-2.2.1 Circularly Polarized Light.....	122
4-2.2.2 Halide effect quenching.....	124
4-2.2.3 Variable temperature NMR.....	125
4-2.3 Interaction with nucleic acids.....	127
4-2.3.1 Absorbance spectroscopy.....	127
4-2.3.2 Luminescence spectroscopy.....	128
Chapter 5: Experimental.....	132
Conclusion.....	165
Appendix.....	167

List of abbreviations

Bn	Benzyl
bpy	Bipyridine
Calc	Calculated
CD	Circular Dichroism
cyclen	1,4,7,11-tetraazacyclododecane
DMF	Dimethylformamide
DNA	Deoxyribo Nucleic Acid
DOTA	1,4,7,11-tetraazacyclododecane-N,N',N'',N'''-tetraacetic acid
dppz	Dipyridophenazine
DTPA	Ethylene diamine pentaacetic acid
EDCI	[1-(3-Dimethylaminopropyl)-3-ethyl-carbodiimide hydrochloride]
EDTA	Ethylenediamine tetraacetic acid
em	Emission
ESMS	Electrospray Mass Spectrometry
exc	Excitation
Expt	Experimental
FAB	Fast Atom Bombardment
HOBt	Hydroxybenzotriazole
HEPES	[4-(2-hydroxyethyl)-1-piperazineethane sulfonic acid]
IC	Internal Conversion
Int	Intensity
ISC	Inter System Crossing
LD	Linear Dichroism
MRI	Magnetic Resonance Imaging
NBS	N-Bromosuccinimide
phen	Phenanthroline
phi	Phenanthrene-9,10-diimine
RNA	Ribonucleic acid
TFA	Trifluoroacetic acid
THF	Tetrahydrofuran
Cu-TMPy	Copper tetramethyl porphyrin
12-N ₄	1,4,7,11-Tetraazacyclododecane

Introduction

The DeoxyriboNucleic Acid DNA represents the richest source of information within a living organism. The genotype of each cell locked into its DNA sequence encodes protein and enzyme synthesis. It is composed of two separated chains that are usually wrapped around each other to form the double helix. They are connected to each other by hydrogen bonding interactions between the base units.

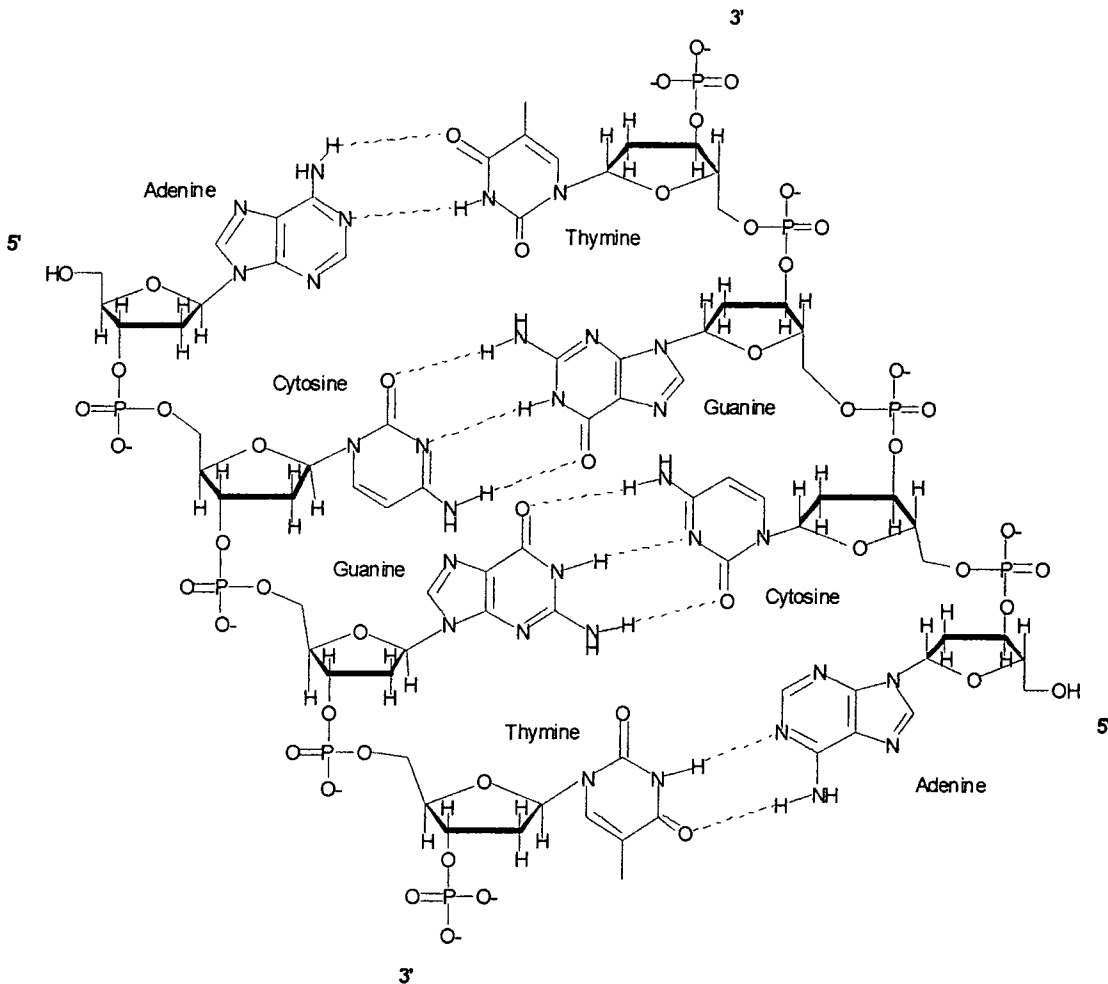
1-1 DNA

1-1.1 : Building-blocks of DNA

DNA can be regarded as a polymer made from four kind of monomers. The nucleosides, formed by a purine or pyrimidine base and a deoxyribose sugar, are linked to each other by a phosphate bridge. The four bases are Adenine, Cytosine, Guanine and Thymine (which is replaced by Uracil in the case of RNA), and are hydrogen bonded in a self-complementary manner, as shown in Scheme 1.1. In 1953, Watson and Crick proposed a model for the DNA structure with two strands in an anti parallel double helix with 10 base pairs per turn. The pairing of the bases by hydrogen bonding is strictly Cytosine-Guanine and Thymine-Adenine.¹

Because the sugar molecules are asymmetric, each sugar-phosphate motif has a polarity denoted as -5' or -3'. Thus the two individual nucleotide chains have opposite polarity, and are complementary. The paired bases are stacked on the top of each other along the axis of the helix and allow strong Van der Waals interactions between them. Each base pair is rotated by 36° (in B-DNA) with respect to the next. The phosphate groups sit outside and with the sugar form the backbone. The conformation of the sugar ring, which can be C2' *ENDO* or C3' *ENDO*, as well the position of the glycosidic bond, *SYN* or *ANTI*, affects the geometry of the double helix.² The bases at the axis of the helix can be approached through two deep spiral grooves, called the *major* and *minor grooves*. Their existence is due to the asymmetry in the base pairing. The phosphate groups and the sugars form the walls of the groove, and the bases the floor, producing a hydrophobic compartment.



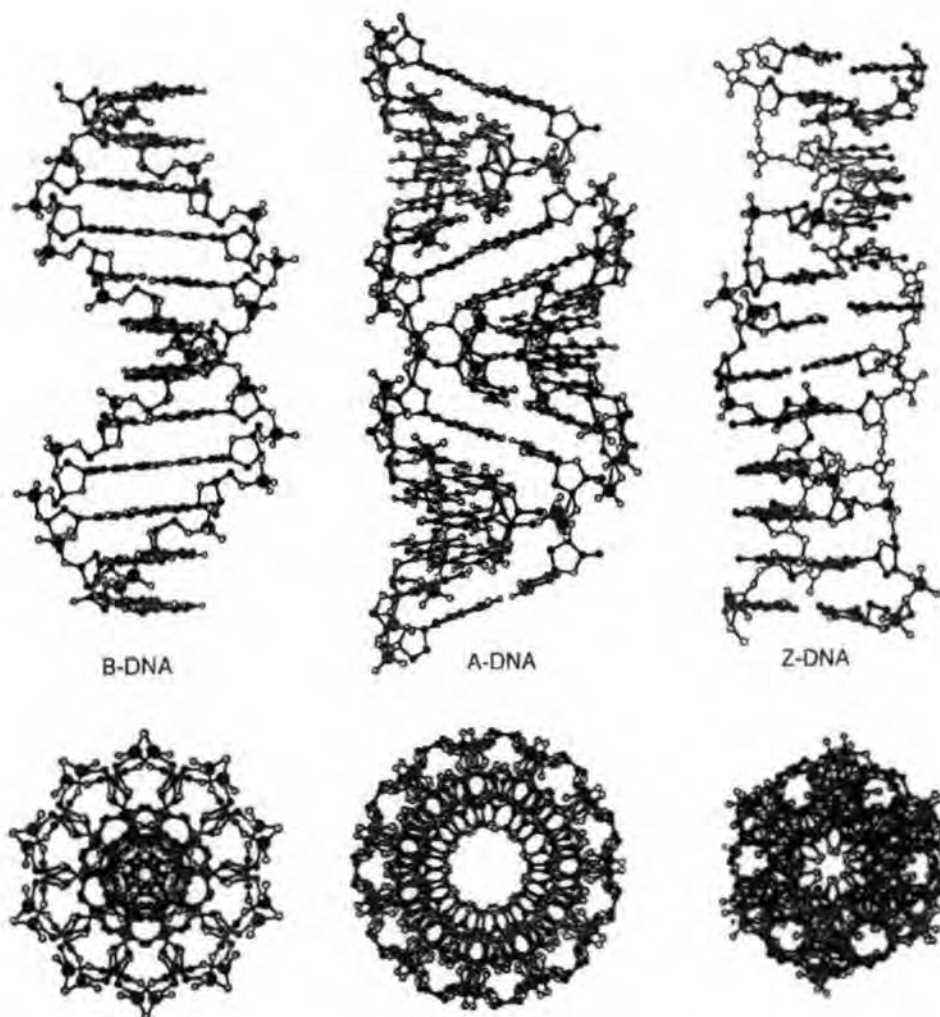


Scheme 1.1 : Arrangement of the nucleobases in the DNA double strand

1-1.2 : Different kinds of helix

1-1.2.1 : A, B, Z helices

The most common form of DNA helix is the 'so-called' B-DNA. It is the one found at a relative high humidity, as expected for the aqueous milieu of the cell. But there also exists the A and Z forms. Although the B helix is indeed the form of DNA found in cells, the A helix is also important biologically. Double strand RNA always forms the A structure, and so do DNA-RNA hybrid duplexes.³ The standard A and B forms can occur with most sequences, depending for example on the degree of humidity ; the A form is found at relative low humidity (65-75%) and B form at a higher humidity level (>92%). The conformational changes in the duplexes have been studied by X-ray,⁴ proton NMR⁵ and circular dichroism (CD).⁶ The three forms are distinguished by the size of their grooves and their helicity.



Scheme 1.2: The 3 forms of DNA

	A Form	B Form	Z Form
Direction of helix rotation	Right	Right	Left
Number of residue per turn (n)	11	10	12 (6 dimers)
Rotation per residue ($360/n$)	33°	36°	-60° per dimer
Rise in helix per residue (h)	0.255 nm	0.34 nm	0.37 nm
Pitch of helix (nh)	2.8 nm	3.4 nm	4.5 nm
Major groove	Deep & Narrow	Deep & Wide	Shallow & Wide
Minor groove	Shallow & Wide	Same Depth & Width	Deep & Narrow

Table 1.1 : Parameters of polynucleotides.

These structural parameters have been determined by NMR and X-ray crystallography.

1-1.2.2 : Unusual secondary structures

Triplex and Quadruplex

The first triple helix discovered was poly(U)-poly(A)-poly(U), containing two pyrimidine strands and one purine strand.⁷ Such a structure involves both a Watson-Crick pairing and a Hoogsteen-type base pairing. This is called *H-form* and can be found in any structure showing an 'all pyrimidine strand' and one 'all purine strand'.

Evidence has also been found for a quadruple helix, involving runs of guanine nucleosides.⁸ The tetrad G-G bases are paired via a Hoogsteen model in the same plane, in anti-parallel or parallel arrangements.

Hairpins and cruciforms

Most RNA molecules are single strand but many have self complementary regions that form hairpin structures : the bases sequence allow the chain to fold back on itself and form a base-paired antiparallel helix. Double hairpins are also called cruciforms.

1-1.3 : Stability of DNA

The major polynucleotide secondary structures (A and B forms) are relatively stable under physiological conditions. Yet they must not be too stable because many biochemical processes require the double helix opening. This loss of secondary structure is called *denaturation*. The major factors which favour dissociation of the double helix, are the electrostatic repulsion between the chains (as they are charged equally), and the increase in the entropy factor.

Nevertheless, the double helix is well held together by different kinds of interaction.⁹ First there is the stacking of the aromatic bases, where one π -system overlaps with the next one, resulting in the stabilization of the helix.¹⁰ Secondly, the hydrogen bonding between the bases is critical to the stability, even if the energy of stabilisation is low ; this reflects the competition with water molecules.¹¹ The hydration of DNA is essential for the maintenance

of its structural activity. Permanent electrostatic effects, induced dipole interactions, and solvophobic effects may also play a role in the stabilization of DNA.¹²

1-2 Binding to DNA

Because of the features of their tertiary structure, the different forms of DNA do not interact in the same way with drugs. The hydrophobic part constituted by the bases is not accessible to the same extent in the three main cases of binding, depending on the size of the grooves. The interactions with the bases are favoured in the case where one of the grooves is wide enough to allow the molecule to bind to it. For each form of DNA the phosphate groups make up a polyanionic backbone on the outside surface allowing interaction with the aqueous milieu. The edges of the bases have hydrogen bonding potential, which is only partially satisfied by the pairing, and is therefore available for recognition by ligands.

1-2.1 : Interest of binding drugs to DNA

DNA controls the genotype of each cell and so, consists of a library where 'all the recipes' are stored. Without it, it would be impossible for cells to replicate themselves. This is the case not only for healthy cells but also for malignant cells. One approach to cancer therapy involves the use of cytotoxic agents, which reduce the proliferative drive to the tumour.¹³ Many compounds with good tumour cell-killing activity have been discovered, but relatively few have found a clinical use because of the lack of discrimination between tumour and normal tissue.

The mode of action of cell-killing drugs is believed to involve the binding to DNA inside the cell, to stop the replication process. Replication is the process wherein the DNA is read base after base, translated into a codon, which codes for a particular amino acid.¹⁴ If one base is missing or is the wrong one, the resulting nucleic acid chain or peptide, in the protein synthesis, would be different, this is called *mutation*,¹⁵ and may lead to the death of the cell. There are two ways for the cytotoxic agents to act : the first is to bind covalently or non-covalently to the double strand and so block the RNA pathway to the replication, or more readily to cleave the strand directly.

1-2.2 : Types of binding

The affinity of drugs for nucleic acids depends on the physicochemical characteristics of the ligands (usually a molecular weight less than 1000) as well as the way they fit around the DNA helix. Their charge, hydrophilicity, and geometry are important factors to consider. The three main types of non-covalent interactions that have been identified are illustrated in Scheme 1-3.



Scheme 1-3 : Binding modes of small molecules to DNA.

Electrostatic interaction :

This type of binding is favoured in cases where a cationic ligand is electrostatically attracted to the negatively charged phosphate groups found at the surface of the DNA helix, so fairly accessible. The ligand displaces the counter ion (typically Na^+ or Mg^{2+}) around the double strand. The type of cationic ligand ranges from simple aqua ions to charged organic ions or complexes, since each presents a positive charge. The energy of this attraction varies inversely with the distance and so this can be a longer-range interaction. This force could therefore be an important factor to direct the ligand to a given region of the sequence.

Groove binding :

The driving force for this interaction is the solvophobic effect which in turn is related to the hydrophobicity of the ligand. The molecule adapts its conformation to sit along the groove, stabilized by Van der Waals interactions and hydrogen bonding,¹⁶ and hidden from

external solvent. Groove interaction involves the concave curvature of the inner surface of the drug molecule complementing the convex surface of the groove floor. This surface matching has been termed isohelicity¹⁷ since both the groove floor and the drug inner surface have twists in their curvature. This concept has been found useful in the design of new groove-binding agents. A great number of compounds showing a preference for AT regions have been classified as groove-binders, and bind exclusively to the minor groove of B-DNA. They do not significantly perturb DNA structure, in contrast to intercalative drugs.

Intercalation :

The intercalation process is characterized by the interaction of an extended electron-deficient, planar aromatic ring system. The intercalation hypothesis, first proposed by Lerman,¹⁸ suggests that the planar chromophore has been inserted between adjacent base pairs of the DNA. The resultant complex is stabilized by Van der Waals interactions between the aromatic ring of the chromophore and the π -system of the bases surrounding it. This results in an extension of the helix by 3.4 Å, and a change in the helical twist.¹⁹ Furthermore the intercalator becomes rigidly held and oriented with the planar moiety perpendicular to the helical axis. Another feature in intercalation is the 'neighbourhood exclusion principle', where the intercalation of two molecules adjacent to each other is strongly disfavoured.^{17a}

1-2.3 : Drugs which bind to DNA

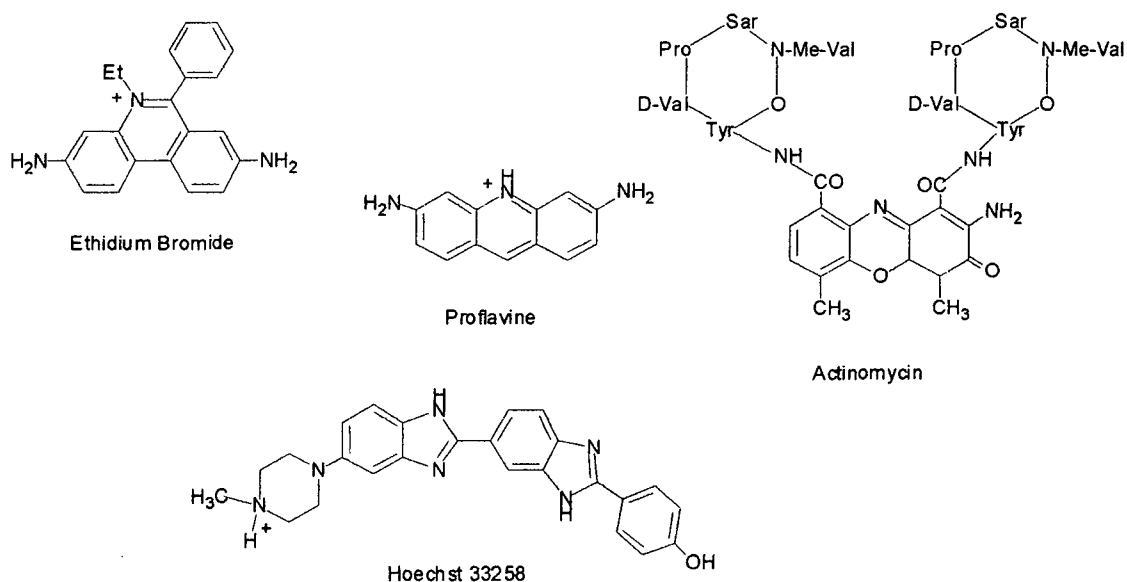
Ethidium bromide is probably the best known intercalating agent.²⁰ Its planar aromatic unit is able to slide between the base pairs and form a strong complex. Consequently the replication of the DNA is impossible and it is lethal for the cell.²¹ A fluorimetric method for determining DNA and RNA concentrations using the fluorescence enhancement of ethidium bromide on binding to double strand nucleic-acids was proposed by LePecq and Paoletti in 1966.²²

In the same family of intercalating drugs are acridine²³ and proflavine.²⁴ They possess not only charged planar heteroaromatic rings but also amino groups able to form hydrogen bonds to acceptor sites on the DNA. Not all of the acridines are intercalative agents. The conditions of temperature and concentration can also affect the binding. At high concentration, the acridine dyes saturate the intercalative sites, after which they bind on the backbone surface.

The synthetic dye HOECHST 33258 is widely used¹ as a fluorescent cytological stain for DNA, because it binds strongly to AT-rich sequences from the minor groove.²⁵ This binding is stabilized by Van der Waals interactions between the two benzimidazole rings and the sugar (O4'), and hydrogen bonds between benzimidazole NH groups and proximal Adenine (N3) and Thymine (O2). This groove binder is base-pair selective, by specific hydrogen bonding with the bases in the bottom of the groove, and it is particularly selective for AT pairs in DNA.

As an example of these kinds of groove binders, Dervan *et al.* developed analogues of netropsin. The parent molecule contains a succession of pyrrole and imidazole rings interacting with the bases by specific hydrogen bonds, which targets specifically a sequence by formation of a third helix sitting in the minor groove.²⁶ These polyamides, because they have a higher affinity and specificity than naturally occurring DNA binding proteins, have the potential to control gene expression.²⁷

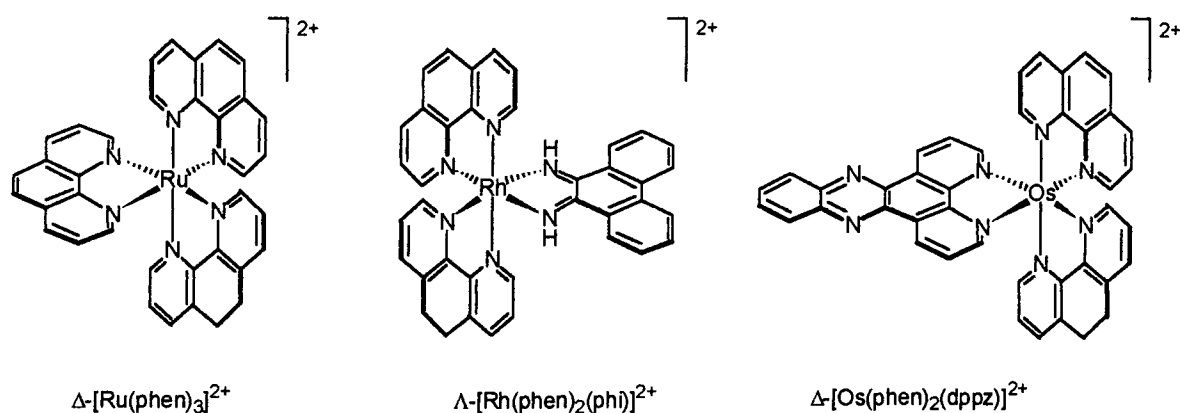
Actinomycin D is an intercalative antitumour drug which has also attached amino-acid side chains. It acts as a groove binder.²⁸ The peptide chains reside in the DNA groove, while the heterocyclic unit stacks between the base pairs. This is an example of an intercalator appended with a groove binding tail.



Scheme 1.4 : Small molecules interacting with DNA

Transition-metal complexes :

Numerous studies of DNA interactions with chiral tris-chelate complexes ML_3 have been inspired by the possibility of discriminating DNA handedness.²⁹ ML_3 complexes are shaped like three-bladed propellers, and have two enantiomeric forms, right- (Δ) and left- (Λ) , that might be expected to interact differently with DNA. The nature of the polyaromatic ligands determines the type of interaction that the complex can make with the double helix. Furthermore, due to their metal-ligand charge transfer transitions (MLCT), providing a spectroscopic handle, osmium(II), rhenium(I), rhodium(III) and ruthenium(II) complexes are very sensitive luminescent reporters of DNA in aqueous solutions.³⁰ The best documented examples of such complexes are ruthenium tris-phenanthroline $[Ru(phen)_3]^{2+}$ and the mixed complex $[Ru(phen)_2(dppz)]^{2+}$ (Scheme 1.5).



Scheme 1.5 : Chiral transition-metal complexes

Much work has been done on ruthenium(II) tris-(1,10-phenanthroline) complexes and its binding to various kinds of DNA helix. The first conclusions postulated following photophysical studies,³¹ and concerning the 'enantioselective binding' to right handed DNA, were that the two opposite enantiomers display two different binding modes with different affinities : one involving intercalation and the other, surface binding. In contradiction to these conclusions, Nordén has shown using NMR, LD and CD experiments³² that there is no preferential intercalation of the Δ -enantiomer over the Λ to B-DNA, and so no discrimination

of DNA handedness. Both enantiomers have been found to be groove-binders with similar strengths as a function of the base-pair composition.

The two enantiomers of $[\text{Ru}(\text{phen})_2(\text{dppz})]^{2+}$, presenting an extended aromatic system, bind with comparable strengths to DNA, by intercalation of the (dppz) chelate wing inserted between the base-pairs, but with no enantiospecificity.^{26a,33} A lot of reports³⁴ on the binding of these complexes with DNA have appeared describing the interaction using different methods. The precise definition of from where the intercalation occurs, i.e. from the major or minor groove, remains unresolved.

A large series of ruthenium,³⁵ rhenium,³⁶ rhodium,³⁷ cobalt or osmium^{26b,38} complexes have been synthesized, aiming to study DNA binding, and for some of them, photocleavage of the double strand. The increase in the ligand surface area, for example from phenanthroline (phen) or bipyridine (bpy), to dipyrrophenazine (dppz) or phenanthrene-9,10-diimine (phi) leads to a substantial increase in intercalative binding affinity.

Another large heterocyclic surface used for DNA interaction is the electron-poor aromatic porphyrin ring system. It has been known for some time that porphyrins bind to DNA but the mode of binding is still debated.³⁹ Spectroscopic data indicates that porphyrins bind to CG-rich regions intercalatively, while they take on an external binding mode interacting with AT-rich regions.⁴⁰ The nature of porphyrin intercalation has been defined from the crystal structure of a hexamer with a copper meso-substituted porphyrin.⁴¹ Often porphyrins intercalate by flipping out a cytosine from the oligonucleotide helix. In these conditions, the intercalation of such metal complex represents a substantial perturbation of the DNA helical structure. A feature of metalloporphyrins is their use as cleavage agents by oxo-transfer on DNA bases (usually guanine).

Cis-Platin⁴² provides a typical example of a covalent interaction with DNA which blocks replication and translation process. But the first step is an electrostatic attraction of a doubled charged complex with the backbone of the DNA. This drug is clinically used in the treatment of ovarian and testicular cancer.

1-3 Techniques used to study conformational changes in DNA upon binding

The study of the interaction of a drug with DNA is crucial in understanding how this could act as therapeutic agent. Relatively few techniques are available to visualize how the non-covalent binding of a small molecule can affect the DNA helix. The elucidation of the structure of such a drug-DNA complex has been a goal for many researchers, from physical chemists to biologists.

1-3.1 : X-ray crystallography

Fibre diffraction provided many answers concerning the structure of DNA, but also concerning its interaction with drugs by relating the structure to the function. X-ray crystallographic studies⁴³ of a DNA-drug system provides a lot of help in understanding how the drug interacts with DNA. They help to define the nature of the binding interaction which may be linked to the mode of action of the drug, and where along the oligonucleotide the ligand binds. The binding geometry and the ratio of ligand bound can as well be deduced from a fibre diffraction study of a crystal. Because it gives a view of the ensemble, X-ray structures can visualize the effects of the binding on the structural properties of the helix : its length, twist, and bending.

This technique of investigation probing the interaction between a ligand and DNA expanded in the late 1970's, with the development of solid phase oligonucleotide synthesis, providing pure defined oligonucleotide sequences for crystallisation attempts. The structure of the first fully base-paired full turn of double helix to be determined by a single crystal method, was that of the sequence d(CGCGAATTCGCG) at 1.9 Å resolution.⁴⁴ However a limitation to this technique is the conditions under which the crystals were grown. To obtain crystals of an oligonucleotide requires most of the time, a different system of counter-ions, a different humidity level, or a different temperature than the physiological milieu. This means that the 'picture' of the interaction from the X-ray structure may differ from the actual milieu.

Crystallographic studies have concentrated on the intercalative and minor-groove categories of complexes : The first drug-DNA crystal structures to be determined were of

simple intercalating molecules, typified by the acridine, proflavine.²³ The structure showed the planar chromophore sandwiched between the two base-pairs of the dinucleotide duplex. The study was unable to address issues of conformational change beyond the immediate intercalation site. Intercalation at the centre of an extended sequence was also observed for the antibiotic actinomycin, showing it to interact at the central GpC site of the sequence d(GAAGCTTC). The two cyclic pentapeptides lie in the minor groove, showing as well a predicted set of hydrogen bonds between the threonine of the side chain and the two central guanines.^{27b}

Many studies have been carried out on the intercalation of meso-substituted porphyrins with DNA. In particular, the crystal structure of Cu-TMPy with the sequence d(CGTACG)⁴⁰ shows that hemi-intercalation of the bulky ring displaces a cytosine residue from the helix.

Other structural studies have focused on groove-binding drugs like pentamidine or berenil defining their specificity to bind to AT-rich sequences of B-DNA.⁴⁵ It appears from the crystal structures of these drug-DNA complexes that hydrophobic interaction with hydrogen atoms from the nucleotide backbone are in a large part responsible for the AT-selectivity of these drugs.

Only two covalently-linked drug-DNA complexes crystal structures have been reported.⁴⁶ That of clinically-important antitumour drug 'cis-platin' has the platinum linked to two adjacent guanines of a dodecamer. Except for the one cited previously, no crystal structure of non-covalently bound metal complexes with nucleic acids have been reported so far. There is yet no structural data on any drug-DNA-protein ternary complex, raising the question of the relevance of structural studies on drug-DNA complexes alone.

1-3.2 : NMR Spectroscopy

NMR spectroscopy is a method of choice to evaluate the binding of a ligand with nucleic acids, but also to know where exactly the interaction occurs along the oligonucleotide, with what geometry and affinity. High resolution NMR can afford very detailed information on various features, such as the electronic effects in the base-pairs induced upon binding, the structural changes of the backbone, or the hydrogen bonding the drug establishes with the bases or the sugar moieties. This technique is accessible to monitor ligand-DNA interactions because the kinetics of these reversible binding associations are slow compared to the time

scale of an NMR experiment. Binding of drugs to nucleic acids has been studied in various cases by NMR.^{33b, 47,48}

Proton NMR shifts are directly linked to their structural and electronic environment, and consequently provide informations on the type of binding involved in a drug-DNA interaction. Shifts to lower frequency in the aromatic protons of the intercalated molecule result from the anisotropy cone of the stacked aromatic bases, which is generally associated with an intercalative binding mode.^{18a,b,33b} In contrast, a molecule bound in a groove does not induce such dramatic electronic changes ; its binding is mainly governed by hydrogen bond formation between the drug and some adjacent bases, which is reflected by the shift to higher frequency of NH or OH protons involved in hydrogen bonding. Shifts to higher frequency in the phosphorus NMR spectrum of the phosphodiester backbone are indicative of a substantial perturbation of the sugar-phosphate backbone, that accompanies intercalation.^{33b}

The NOE experiment being a probe for measuring distances between two nuclei in 3D space, can be very informative concerning the environment of the drug and the DNA^{6a,31b,36c} ; this can reflect, how closely nucleobase or sugar nuclei approached the drug-protons.

Line width measurements may also be used to study the conformation of nucleic acids : this reflects the magnetic spin-spin interactions with nearby proton, nitrogen, and phosphorus nuclei. For exchangeable NH and OH protons the increased line width may reflect differing exchange rates with solvent and is a measure of the relative stability of the local duplex structure. The saturation recovery method is particularly useful for evaluating the exchange rates of NH and OH protons.

1-3.3 : Circular and Linear Dichroism

Circular Dichroism (CD) and Linear Dichroism (LD) are important chiroptical techniques that provide information about molecular structure and about interactions between chiral molecules⁴⁹ : CD is the difference in absorption between *right* and *left circularly polarized light*, and LD is the difference in absorption of light *linearly polarized parallel* and *perpendicular* to an orientation axis, as shown in Scheme 1.6.

$$\text{CD} = A_l - A_r$$

$$\text{LD} = A_{//} - A_{\perp}$$

Scheme 1.6 : Definition of CD and LD

In monitoring the interaction between small molecules and DNA, CD and LD appear to be very sensitive techniques to probe the changes in conformation of chiral macromolecules, such as DNA or peptides. Furthermore CD experiments deal with the solution phase, which is suitable to study changes in conformation, in contrast to the way that crystallization may modify the structure, especially for DNA. Another advantage is that the shorter timescale (10^{-15}s^{-1}) and the lower concentration are more advantageous for CD than with NMR.

The origin of the CD absorption bands in double-stranded oligonucleotides is the $\pi \rightarrow \pi^*$ transitions from the *achiral* purine and pyrimidine bases, linked by the *chiral* sugar moiety, each of which is part of a *chiral* biopolymer.⁵⁰ In this way, the conformation of DNA at different temperatures⁵¹ or at high concentration of various salts⁵² may be identified. For example, the B to Z transition in the conformation of DNA is accompanied by a dramatic change in the CD spectrum.⁵³ The spectrum of B-form DNA shows a negative band at 250 nm and a positive one at 280 nm, while the spectrum of Z-form presents a positive band at 265 nm, and a negative one at 290 nm.

The application of the CD technique to study DNA structure has been extended to intercalating⁵⁴ and non-intercalating DNA binding agents associated in most cases with induced CD bands.⁵⁵ These effects permit a characterization of the binding mode.

The intercalation of ethidium bromide into DNA has been studied by CD⁵⁶: the spectra show characteristic induced CD bands between 300 and 360 nm, outside the DNA spectral range. With actinomycin, intercalation has also been studied by CD,⁵⁷ as well as its competition with other intercalative agents, or its sequence specificity.

For a series of porphyrin derivatives, drastic changes were obtained in the ultraviolet region of the CD spectra of DNA upon binding, which was accompanied by a characteristic induced CD band in the visible region. In addition to an intercalative binding mechanism, an

external binding mode has been suggested, based on the positive band in the visible region, associated with a selective interaction on dA-dT sequences.^{58,39c}

The binding of non-intercalating ligands can also be investigated by CD. A dA-dT base pair preference for the binding of Hoechst 33258 was suggested by extensive CD studies, in addition to several other measurements which have contributed to the elucidation of the groove binding mechanism.⁵⁹

An additional feature of nucleic acid structure that is particularly relevant in LD studies is the relative orientation of the bases to each other. Variations in the LD spectra upon binding with drugs can be used as a proof of an intercalative binding mode.

The use of CD or LD to investigate the type of DNA binding involving chiral metal complexes, including UV-active ligands has been extensively reviewed.^{31b,32a,33b,35d-f}

1-3.4 : Electrospray Mass Spectrometry

In recent years, mass spectrometry (MS) has been introduced as a sensitive and specific tool for the analysis of specific, non-covalent complexes involving biopolymers. The use of MS to probe the interaction between oligonucleotides and drugs became possible owing to the development of extremely mild techniques of ionization, such as electrospray ionization (ESI) and pneumatically assisted ESI or ionspray (IS), which allowed the preservation of even weak interactions during the transfer of ions from the liquid to the gas phase, and the subsequent mass analysis of the whole complex.⁶⁰ This promising development in MS avoids the use of a viscous environment, as in FAB or solid matrices in MALDI, and allows the direct analysis of biological samples.

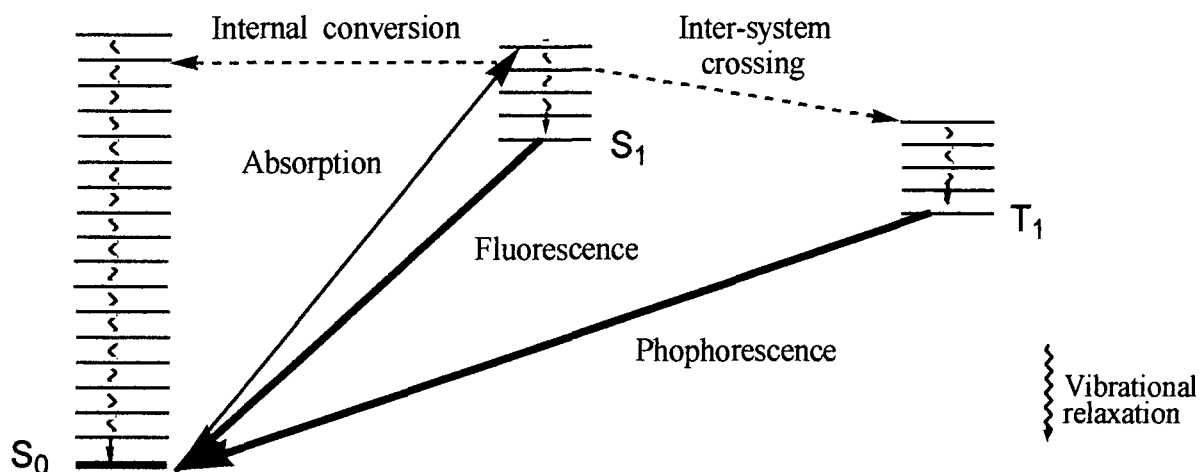
The goal of such an experiment is to determine the stoichiometry of the binding, and it may allow an evaluation of the affinity of similar drugs with a given oligonucleotide. However this type of experiment is not able to give any information about the binding mode, because it is simply related to the relative stability of the system in solution. In the detection chamber of a mass spectrometer, the stability of the ion-complexes in the gas phase cannot be assumed to be the same as in solution.

The groove-binder distamycin has been studied by ionspray spectroscopy with a dodecamer and the stoichiometry of binding was shown to involve both 1 :1 and 1 :2 complex formation. The stoichiometry of intercalation of daunorubicin in a hexamer has also been investigated.⁶¹

1-4 Luminescence

1-4.1 : General features

Photoluminescence⁶² is the emission of energy from an electronically excited state of an atom or a molecule following the absorption of light. The emission can be subdivided into fluorescence and phosphorescence (Scheme 1.7). The radiative process which occurs between the singlet excited state S_1 and the ground state S_0 is termed *fluorescence* and lasts for 10^{-9} - 10^{-6} s. In the case of *phosphorescence*, emission of light is preceded by inter-system crossing (ISC) from the singlet excited state to the triplet excited state. The subsequent transition which arises from a triplet-to-singlet transition (different spin multiplicity), is characterised by a small natural radiative rate constant (i.e. long lifetime of 10^{-4} -1 s). The excited state can also be deactivated by non-radiative de-excitation pathways, such as internal conversion (IC) or vibrational quenching.



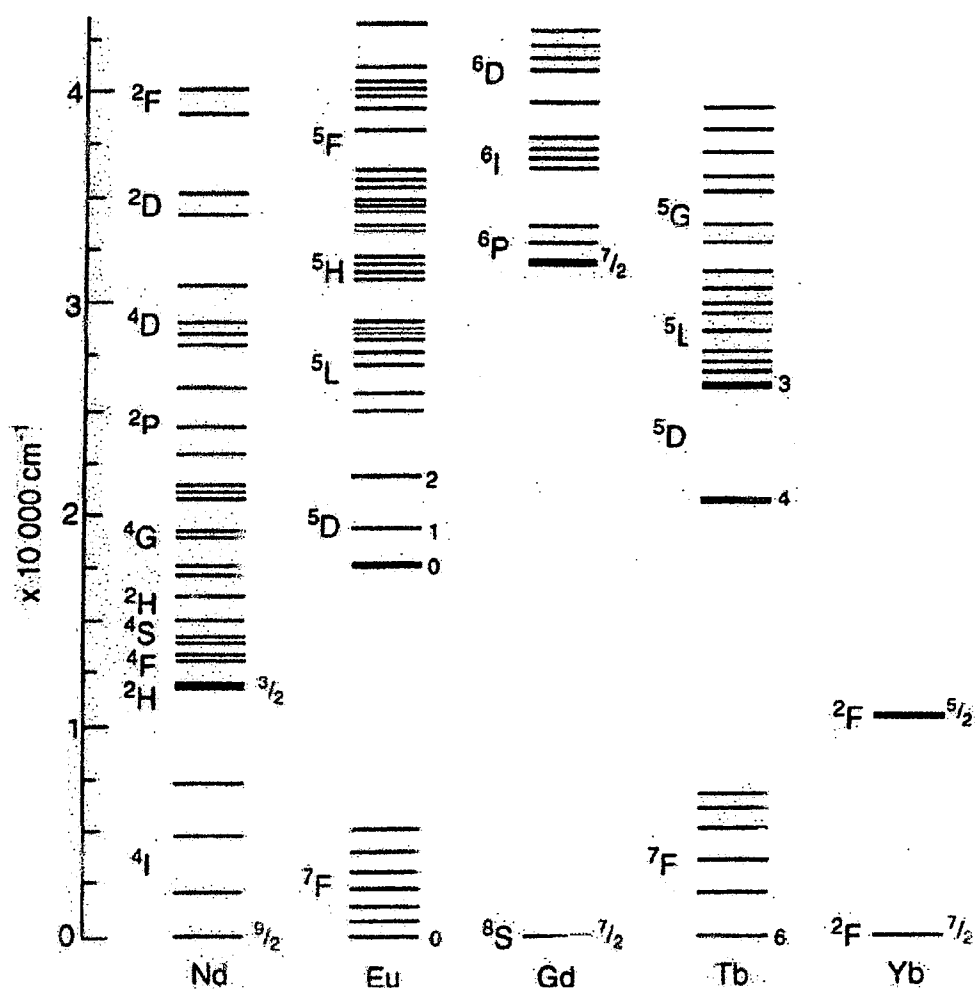
Scheme 1.7: Simplified Jablonski diagram

1-4.2 : Luminescence of lanthanides ions

Most of lanthanides are known to luminesce, particularly in the solid state. Lanthanide(III) ions contain partially-filled 4f shells and so, are paramagnetic, except La and Lu which are diamagnetic. Their luminescence properties are characterised by sharp emission bands, that is due to the transitions between the lowest lying orbitals, which have a $4f^n$

electronic configuration. According to the Russell-Sanders coupling scheme, the f-f transitions of the lanthanides are spin-forbidden ($\Delta S \neq 0$, Laporte parity rule).⁶³ However this scheme fails in the case of heavy ions, because of the large spin-orbit interactions. In consequence the extinction coefficients associated with these transitions are very small (of the order of $1 \text{ M}^{-1}\text{cm}^{-1}$).

The luminescence spectra of lanthanides exhibit very sharp emission bands, which are related to the small ligand field effect to which the 4f electrons are subjected. Another feature of certain f-f transitions in lanthanide ions is their sensitivity in intensity or shape towards the environment, they are called *hypersensitive transitions*.⁶⁴ Such transition, like $^5\text{D}_0 \rightarrow ^7\text{F}_2$ ($\Delta J = 2$), or $^5\text{D}_0 \rightarrow ^7\text{F}_4$ ($\Delta J = 4$) of Eu^{3+} can be used to study the composition of the first coordination sphere.



Scheme 1.8 : Energy levels of selected lanthanides ions

The relatively long lifetimes are directly related to the observed small line widths. The splitting of the energy levels of the lanthanide ions results in many possible transitions between the different states after excitation of the ion (Scheme 1.8). Therefore the emission spectrum of a lanthanide ion consists of a series of distinct frequencies each corresponding to the transition from the lowest excited state to one of the sublevels of the ground state ; these frequencies are characteristic of each ion. The most intense luminescence band is usually used to determine the luminescence lifetime of the lanthanide ion. The luminescence lifetime τ is defined by Equation 1.1:

$$I(t) = I_0 \exp(-t/\tau) \quad (\text{Eq. 1.1})$$

where $I(t)$ and I_0 are the luminescence intensities at $t = t$ and $t = 0$, respectively.

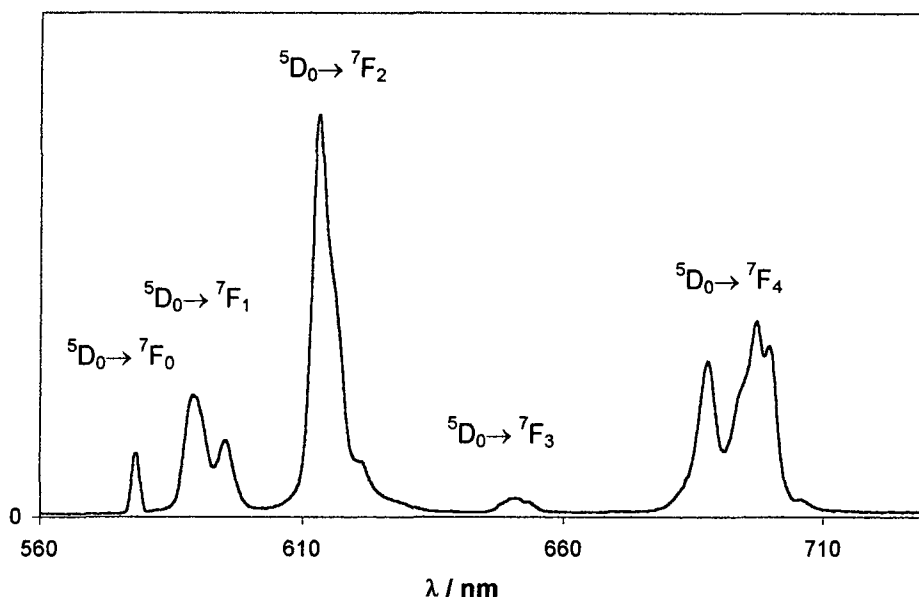
Monitoring the emission at a given emission wavelength, while scanning the excitation wavelength, gives information about the transitions from the ground state, which populate the emitting state, either directly or via higher-lying energy levels.⁶⁵

Deactivation of luminescent excited state

The luminescent lifetimes in aqueous solutions for the emissive level of Eu typically lie in the range of the 0.1-2.0 ms. Other non-radiative processes involving vibrational energy transfer can decrease the lifetimes. The high energy vibrational oscillator can couple vibrationally to the excited states of the lanthanide ions, and efficiently deactivate the luminescent state. It is well known that O-H, N-H and C-H oscillators quench the excited states energy. However O-D oscillators are at least 100 times less efficient than O-H oscillators, and so measurements of excited state lifetimes in H₂O and D₂O can be used to find the hydration state, q , of a lanthanide complex.⁶⁶

Europium luminescence

Of all the lanthanide ions Eu³⁺ is the most commonly studied for its luminescent properties. The main luminescent transitions of Eu occur between ⁵D₀ and ⁷F_J levels. The more intense emission bands generally arise from the transitions, ⁵D₀ → ⁷F₁ at 590 nm and ⁵D₀ → ⁷F₂ at 610 nm.



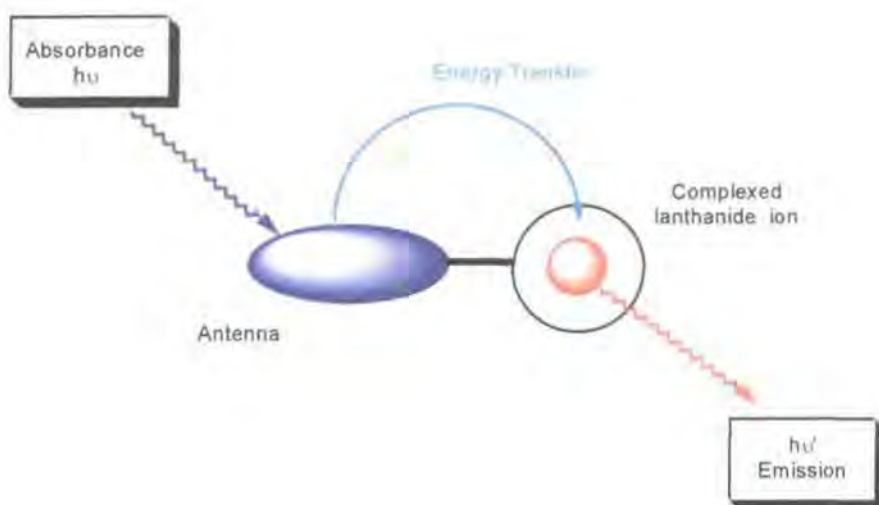
Scheme 1.9 : Typical luminescence spectrum of an Eu(III) complex.

The $^5D_0 \rightarrow ^7F_1$ transition has magnetic dipole character, and so is essentially independent of the ligand environment but is very sensitive to the symmetry of the complex. In the case of $^5D_0 \rightarrow ^7F_2$, its nature being predominantly electric dipolar, this transition is hypersensitive to the ligand environment. It is very weak or even not visible if the Eu ion lies on an inversion centre. As the level 7F_0 is non-degenerate, only a single transition is allowed to this state, the allowedness of the transition being a sensitive function of the complex symmetry.

1-4.3 : Sensitised emission

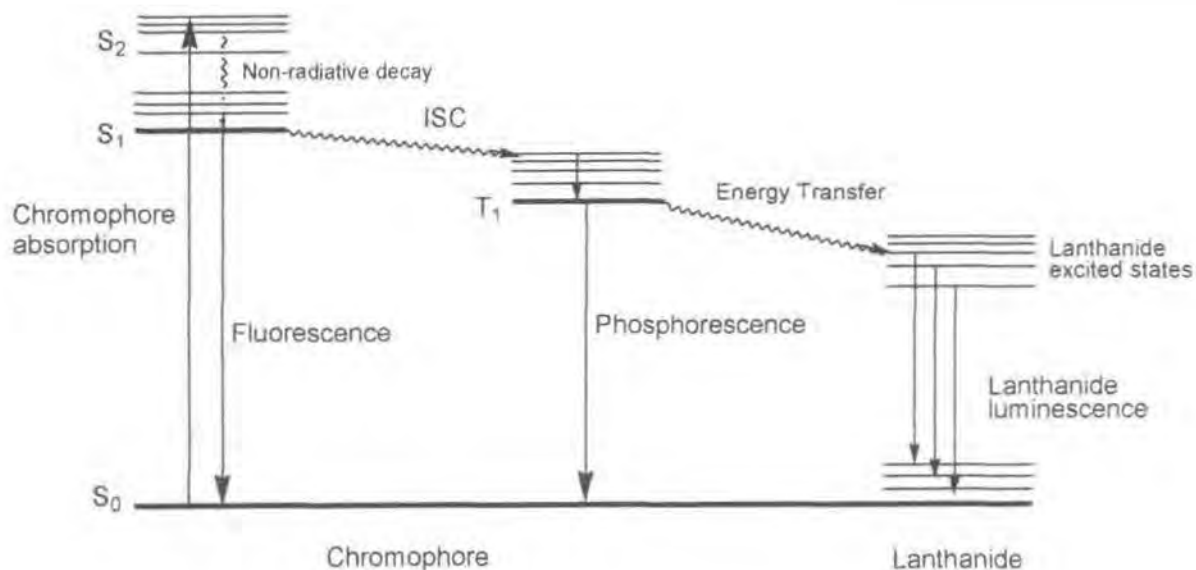
As discussed before, the main drawback of lanthanide luminescence is the lack of efficiency of direct excitation because of the low molar extinction coefficients ($\epsilon = 1 \text{ M}^{-1} \cdot \text{cm}^{-1}$). A way to overcome that problem is using an antenna as a relay to absorb energy and transfer it to populate the excited states of lanthanides. A two component system combines a lanthanide ion binding subunit with a suitable aromatic chromophore ('antenna').

The sensitizer absorbs the excitation energy at an appropriate wavelength, and transfers this excited state energy directly to the lanthanide excited state, resulting in *sensitised emission*.⁶⁷



Scheme 1.10 : Sensitised emission or 'antenna effect'

The first step in sensitised emission involves the absorption of the excitation light by the sensitizer, as a result the sensitizer is excited to its singlet excited state (S_1). The second step comprises an InterSystem Crossing (ISC) from the first excited state (S_1) to the triplet excited state (T_1) of the sensitizer. This triplet state can populate a luminescent state of the lanthanide ion by energy transfer. The excited lanthanide can then emit light at longer wavelength as it returns to the ground state.



Scheme 1.11 : Modified Jablonski diagram for sensitised emission

The efficiency of the luminescence from the lanthanide is determined by the following processes :

- Light absorption by the antenna (high extinction coefficient at the excitation wavelength)
- Efficiency of intersystem crossing : Φ_{ISC}
- Efficiency of energy transfer from the antenna to the lanthanide : η_{ET}
- Efficiency of lanthanide luminescence : Φ_{Ln}

The quantum yield as the product of these steps is given by equation 1.2:

$$\Phi_{overall} = \Phi_{ISC} * \eta_{ET} * \Phi_{Ln} \quad (\text{Eq 1.2})$$

The quantum yield for emission from the excited lanthanide ions (Φ_{Ln}) is usually high as long as vibronic quenching by XH oscillators is minimised. The efficiency of the intersystem crossing is very high for diarylketones, but more modest for planar aromatics such as phenanthrenes.

Energy transfer is the process by which the excited state of a molecule or ion relaxes its energy to a lower-lying state. Such a process requires an electronic interaction between the donor (antenna) and the acceptor. Two mechanisms have been postulated to occur :

- A coulombic predominantly dipole-dipole interaction via the electromagnetic field renders energy transfer from the sensitiser to the acceptor ; this is called the *Förster mechanism*⁶⁸ and represents an action at distance.
- The exchange interaction occurs via overlap of the electronic orbitals, and hence requires closer contact. Simultaneously an electron from the excited sensitiser is transferred to the acceptor, while a ground state electron from the acceptor goes back to ground state of the sensitiser ; this is called the *Dexter mechanism*⁶⁹.

The energy transfer is often accompanied by competing quenching processes, and therefore it can be difficult to determine the efficiency of the energy transfer process.

1-4.4 : Ligands for lanthanide ions

The coordination properties of lanthanides ions are associated with the nature of the 4f valence electrons which are located in the inner orbitals and are therefore not directly accessible for bonding. The lanthanide contraction is at the origin of the gradual increase in

effective nuclear charge and oxidation potential, and a contraction of the ionic radius along the lanthanide series (La^{3+} to Lu^{3+}). The 'hard acid' character of lanthanide ions favours an electrostatic interaction with ligands containing 'hard donor atoms', such as oxygen, nitrogen or fluoride. The high charge density of a lanthanide(III) ion enhances the binding with polyanionic ligands such as carboxylates, phosphinates or phosphates. The coordination number and the geometry of their complexes is rather flexible in comparison to the constraints imposed by the ligand-metal orbital overlap in many transition-metal complexes. Lanthanide ions commonly present a coordination number from 7 to 10, with 8 and 9 coordination number predominating. The potential use of such complexes as luminescent probe for immunofluoroassays⁷⁰ requires a high thermodynamic and kinetic stability in aqueous solution.

The vibrational quenching of lanthanide ion luminescence also initiated an interest in coordinating ligands able to encapsulate and shield the lanthanide centre from the deactivating effect of coordinating OH oscillators (eg. H_2O , alcohols).

A class of ligands often cited comprises some acyclic polyamino polyacetic acids like EDTA or DTPA,⁷¹ but the main drawback of these complexing agents was the relatively low kinetic stability of their complexes to be good candidates for immunofluoroassays. Various acyclic ligands using pyridine, or 2,2'-bipyridine⁷² present a chromophore which can act as a sensitiser for the lanthanide ion they complex, and they have the advantage of shielding the metal centre efficiently from the solvent, although their hydrophobic nature limits their solubility in aqueous media.

To overcome these effects of poor kinetic stability or solubility in water, macrocyclic ligands such as cryptands and azacrowns, have been developed and have been shown to form thermodynamically and kinetically stable complexes with lanthanides. Their ability to encapsulate the lanthanide ion inhibits deactivation by solvent oscillators. Furthermore, the functionalisation, especially with carboxylate pendent arms, can increase their solubility in aqueous media, and by increasing the number of donor atoms more stable complexes are obtained. Expansion of ligand denticity allows scope to introduce a sensitiser to improve luminescence properties.

In the case of cryptands, the donor atoms are already somewhat preorganized for complexation, and this can result in a completely shielded metal centre. The original [2.2.1]

cryptand⁷³ consisting of three oxyethylene bridges which, when replaced by bipyridine units⁷⁴ afford useful antennae to increase the luminescence from the bound lanthanide ion.

Porphyrins are other biological compounds that form lanthanide complexes of special interest. Two texaphyrin complexes are undergoing clinical trials ; a gadolinium compound is an effective radiation sensitiser for tumour cells, whilst the corresponding lutetium compound that absorbs light in the far-red end of the the visible spectrum is in phase II trials for photodynamic therapy for brain tumours and breast cancer.⁷⁵

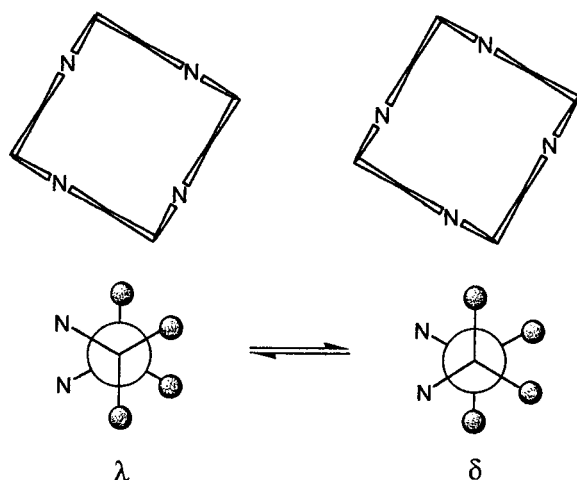
In the aza-crown class, many derivatives of DOTA (1,4,7,11-tetraazacyclododecane-N,N',N'',N'''-tetraacetic acid) exist where the pendent carboxylic arms have been replaced by phosphate, phosphinate, amide or ester groups. The different coordinating arms have an influence on the luminescence spectra of their europium complexes spectra, which demonstrates the effect of varying the symmetry around the metal centre⁷⁶.

1-4.4.1 : Cyclen as a ligand system

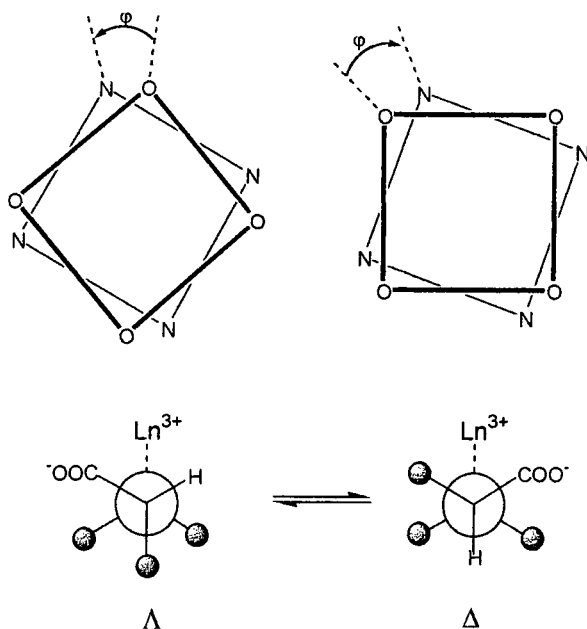
Macrocyclic octadentate ligands derived from a 1,4,7,11-tetraazacyclododecane ring (cyclen) have received attention as a result of their ability to form stable and non-labile complexes with metal ions, especially lanthanide cations. In particular, one of the most successful ligands, DOTA, whose Gd(III) complex is widely used as a contrast agent for MRI and biomedical applications, has been investigated through the whole f block series.

1-4.4.2 : Isomerism of DOTA complexes

The X-ray characterization of Ln³⁺ complexes of DOTA reveals that the eight coordination sites, four nitrogens and four oxygens, provided by these ligands, are arranged in two parallel squares, twisted by an angle ϕ . There are two limiting structures defined by the value of this twist angle : a square antiprismatic geometry is associated with an angle of ca. 40°, while a value of nearer 29° defines the twisted square antiprismatic isomer. These isomeric structures emanate from the minimum energy values of the ring N-C-C-N torsion angles ($\pm 60^\circ$) and the side arm N-C-C-O angles ($\pm 30^\circ$). The enantiomeric ring conformers are referred to as ($\delta\delta\delta\delta$) and ($\lambda\lambda\lambda\lambda$) (Scheme 1.12),⁷⁷ while the interconversion of Δ (right-handed) and Λ (left-handed) isomers proceeds via arm rotation (Scheme 1.13).⁷⁸

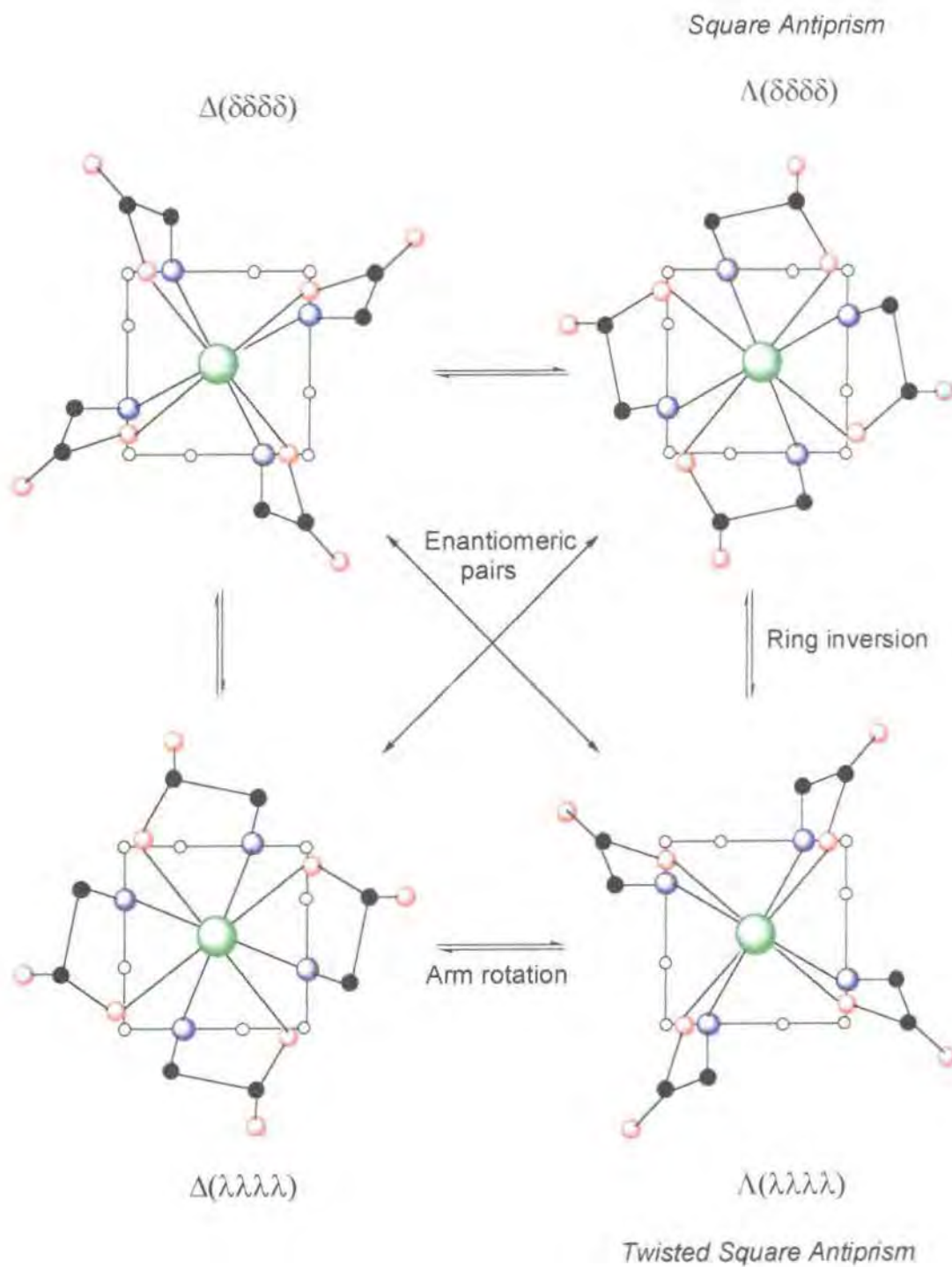


Scheme 1.12 : Equilibria between δ and λ forms of the cyclen ring by cooperative ring inversion



Scheme 1.13 : Equilibria between the Δ and Λ isomers following arm rotation in DOTA type complexes.

These two elements of symmetry therefore give rise to four stereoisomers related as two pairs of enantiomers, which may interconvert in solution via ring inversion $\delta\delta\delta\delta \rightarrow \lambda\lambda\lambda\lambda$ or arm rotation ($\Lambda \rightarrow \Delta$). The former motion occurs typically at a rate of 50s^{-1} (298K) in water (Scheme 1.14).



Scheme 1.14: Stereoisomerism of $[Ln.DOTA]$ complexes.

The relative proportion of the two isomers, square antiprism and twisted square antiprism, varies as a function of the substituent in the ligand and of lanthanide size⁷⁹.

1-4.5 : Sensitiser

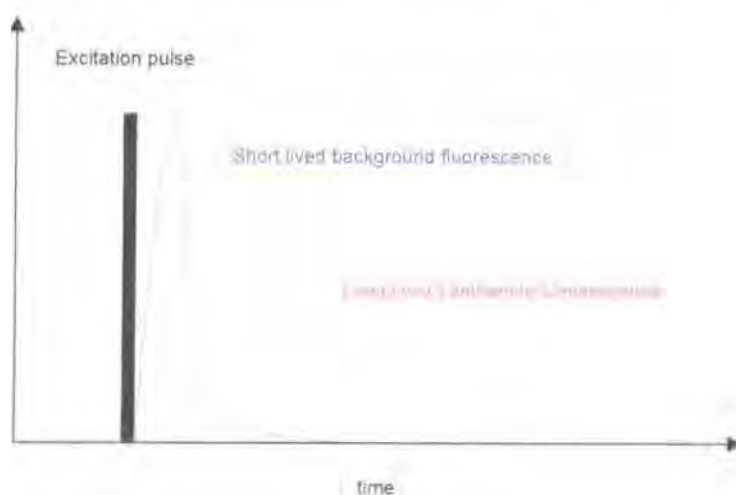
The efficiency of the photosensitisation process depends on the properties of the sensitiser to make a practical luminescent probe. Even when the energy transfer from the organic chromophore to the lanthanide ion is only moderately efficient, it may still offer a considerable advantage over direct excitation. The selection of a suitable antenna chromophore should be based on the following points :

- The triplet energy level of the antenna should preferably be 2000 cm^{-1} above the luminescent level of the lanthanide to ensure that the energy transfer process is effectively irreversible under ambient conditions.
- A high extinction coefficient in the UV-visible region with possible excitation at wavelengths greater than 340 nm (to avoid quartz optics and overlap with the absorption region of biological aromatic compounds).
- The singlet excited state should not be readily oxidized, to avoid the quenching of the excited state lanthanide by electron transfer (oxidation potential E^0 for $\text{Eu}^{3+}/\text{Eu}^{2+} = -0.35\text{V}$ for the aqua ion and ca. -1.1V for typical complexes).
- An efficient intersystem crossing from the antenna singlet excited state to the triplet excited state.

1-5 Luminescent probes using lanthanide ions*1-5.1 : General features*

Lanthanides are valuable spectroscopic probes because of not only the drastic changes they bring to the NMR spectra of their ligands, but also their luminescence properties. Furthermore, calcium and lanthanides possess very similar ionic radii, and are likely to occupy the same type of coordination sites in biological macromolecules. Lanthanides can enter into reaction with biologically active compounds, replacing ions of calcium, and due to their specific spectroscopic properties, can serve as probes providing information on these molecules and the biological processes occurring in them.⁸⁰ The main advantage of lanthanide luminescent probes is their high sensitivity, allowing them to act as both structural and analytical probes in physiological media.

Time-resolved luminescence minimises the interference with the biological milieu. The fluorescence arising from the biological background (amino acids etc...) has a short decay of the order of nanosecond, while the lanthanide luminescence decays much more slowly, of the order of milliseconds. For this reason the utilisation of lanthanide luminescence has stimulated considerable interest over the "conventional" fluorophores.



Scheme 1.15 : Schematic representation of time-resolved detection

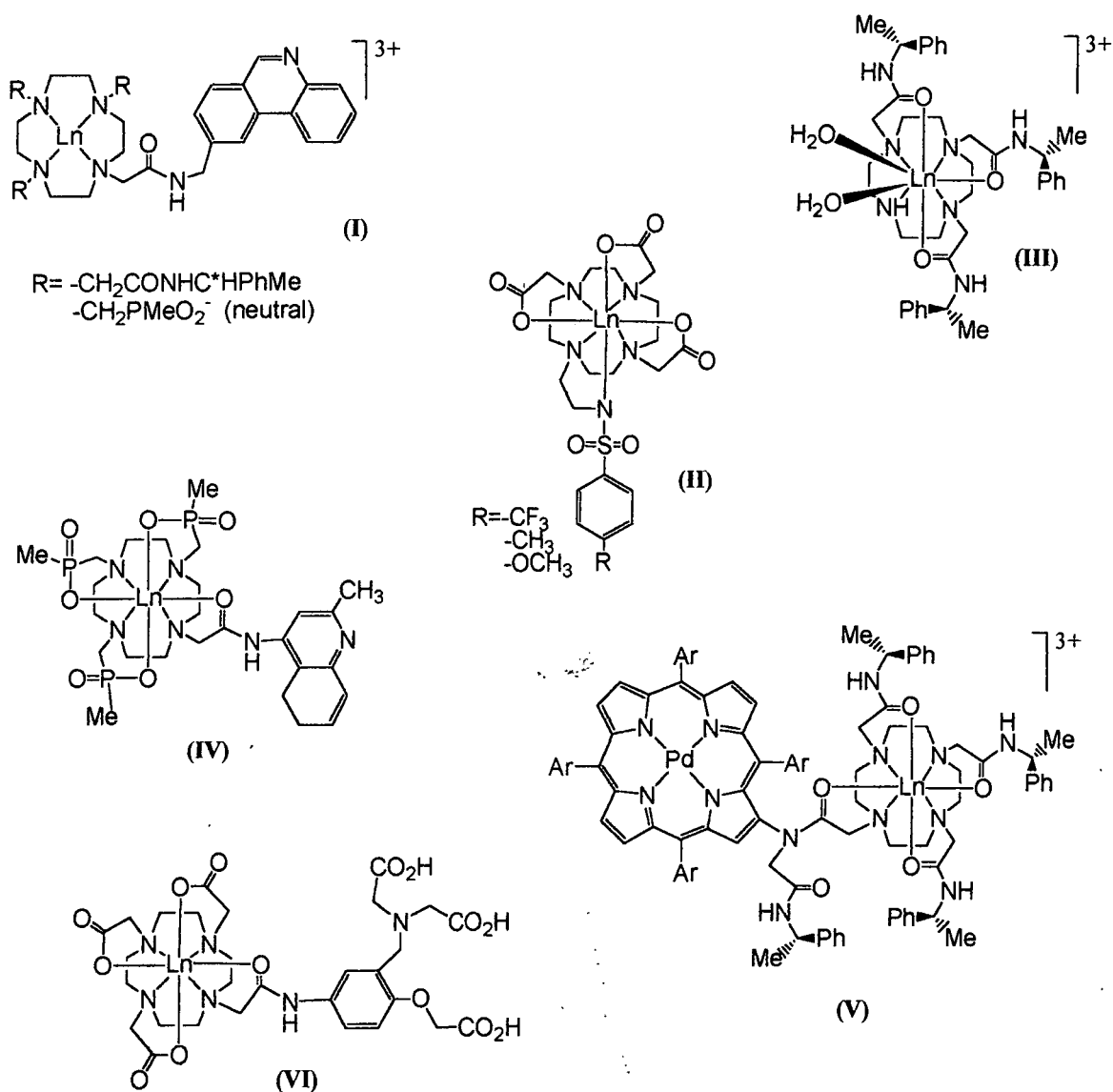
Responsive lanthanide complexes are used to signal variations occurring at the metal centre or in the local environment of the sensitiser. Three parameters can be monitored to signal binding of an analyte: emission intensity, lifetime and polarization. The most important role in biochemical studies is held by Eu(III) and Tb(III) ions, because of their favourable energy gap between their lowest emission level and their ground state. Sufficient stability towards metal ion dissociation in aqueous solution at physiological pH and temperature is required for the use of lanthanide complexes as probes in biological tissues. The use of a specific sensitiser, for example recognizing a given analyte, may signal changes in analyte concentration by a change in its emission spectrum following energy transfer to the lanthanide.⁸¹

The technique of immunological assay is based on the process of binding of an analyte (antigen) with an appropriate antibody. A lanthanide chelate suitable for immunofluoroassays should be water-soluble and should contain functional groups capable of entering in covalent bond formation with an immunologically active compound (antigen or antibody). Moreover it should be characterized by a high stability constant, a suitable excitation spectrum (high

absorbance of the ligand) and an efficient energy transfer process from the ligand to the lanthanide ion.

Lanthanide chelates are employed in different commercially available fluoroimmunoassays: DELFIA (Dissociation-Enhanced Lanthanide FluoroImmunoAssay) and FIAgen (FluoroImmunoAssay).⁸²

In Durham, lanthanide probes based on variously substituted cyclen including triphosphinates, tetraamides and tricarboxylates⁸¹ (Scheme 1.16), have been developed with the aim of signalling anion binding, pH, pO₂, metal ions or the interaction with biomolecules, such as nucleic acids.



Scheme 1.16 : Selected Responsive Lanthanide Complexes developed in Durham

Sensing pH involves two approaches : the first is the protonation-deprotonation of the antenna before energy transfer, that may modulate the luminescence from Eu(III) or Tb(III) ions, e.g. for **(I)**⁸³ and **(IV)**.⁸⁴ The second involves the coordination of the fourth pendent arm to the lanthanide which is sensitive to pH in the range of 5.5 to 7.5, e.g. **(II)**.⁸⁵

The luminescence intensity and the shape of the emission spectrum in diaqua complexes, e.g. **(III)**, is also affected by the presence of anions. Carbonate, acetate, lactate/citrate, malonate and phosphate each can bind to the lanthanide centre displacing water molecules and perturbing the lifetime and emission intensity.⁸⁶ Halides have also been shown to act as efficient quenchers of the antenna fluorescence and lanthanide luminescence in **(I)**. In Tb complexes of **(I)** the sensitivity to molecular oxygen is reflected by quenching of emission ; this could be useful to determine pO₂ in aqueous solution.⁸⁷

The presence of nucleic acids is signalled by an enhancement of the luminescence intensity of **(V)**, where the porphyrin unit sensitizes the Yb³⁺ ion complexed by a chiral tetraamide cyclen.⁸⁸

The complex **(VI)** has been developed with the aim of responding selectively to changes in zinc concentration occurring at physiological pH, by modulation of Tb luminescence.⁸⁹

1-5.2 : Lanthanide probes of nucleic acids

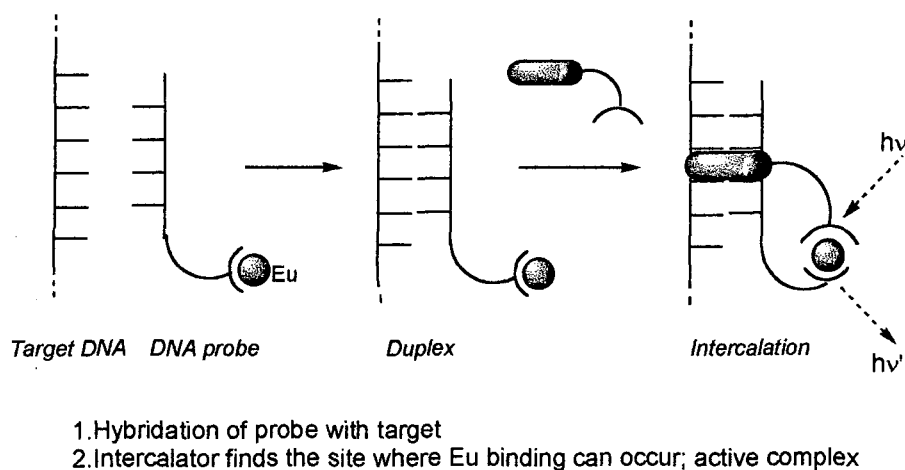
The literature of lanthanide-nucleic acid interactions is sparse when compared with lanthanide-protein studies. The effects of the aquated lanthanide ions on the structure of oligonucleotide duplex have been studied by many research groups.⁹⁰ Energy transfer from nucleic acids to the Tb(III) ion has been studied to investigate the geometry of the binding of ions to the nucleobases, and by extension the selective detection of base mismatches in a given oligonucleotide.⁹¹ Cleavage of the DNA strand by lanthanide ions is also a well documented area of research.⁹²

Lanthanide chelates have recently been shown to be promising probes for the structure and the composition of polynucleotides. An example of the use of lanthanide complexes for the detection of nucleic-acids is the technique involving a ternary complex of Tb(III) with diethylenetriamidopentaacetic and p-aminosalicylic acids bound with single-stranded DNA.⁹³ In such a system, the intensity of Tb(III) emission increases with increasing concentration of

DNA. An other method proposed for the direct determination of nucleic acids involves an Eu(III) complex of terpyridine-bis(methyleneamine)tetraacetic acid,⁹⁴ and on agarose gel, an Eu(III) complex of BCPDA was employed.⁹⁵

Sensitised emission from Eu(III) and Tb(III) has also found application in the detection of single/doubled strand nucleic acids containing guanine, thymine or xanthine by liquid chromatography.⁹⁶ The suitable energy levels of excited states of these bases allow an energy transfer from the bases to the lanthanide ions.

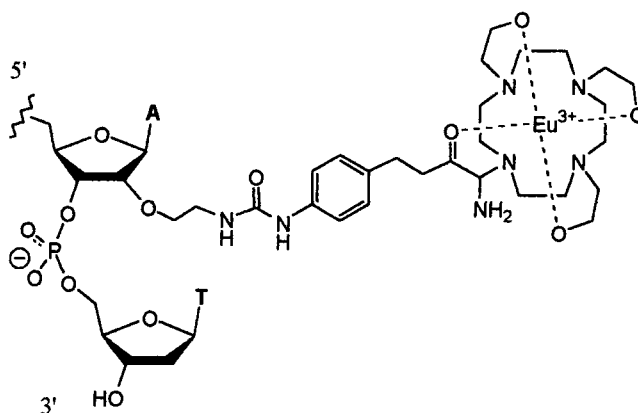
Sammes *et al.* developed one of the first methods for the direct *in situ* identification of mutations in a target strand of DNA.⁹⁷ The probe is composed of a complementary sequence of bases that can hybridise with the target DNA and to which is attached at one end, a short linker molecule bearing a chelated europium ion. The chelator used is EDTA which binds quite strongly to the europium ion, but does not fill its coordination sphere. A second component is a sensitiser that works with further encapsulation around the metal ion to which is attached a phenanthridinium intercalating group (Scheme 1.17). The emission from the europium shows a decrease in intensity when the probe is bound to the mis-match compared to the matched (complementary) sequence.



Scheme 1.17 : Sammes probe

An other example of oligonucleotide-europium complex conjugate has been developed by Baker *et al.* aiming the selective cleavage of the phosphate bond for an anti-sense activity in cells.⁹⁸ The Eu(III) ion is complexed by a trishydroxyethyl substituted cyclen linked to the

oligonucleotide (Scheme 1.18). The cleavage is alleged to occur by nucleophilic attack of the phosphate linkage by the Eu complex. Details are lacking however and the ligand is unlikely to form very stable complexes with Eu at ambient pH.



Scheme 1.18 : Oligonucleotide Eu-conjugate

Hurskainen et al. have developed an europium-labelled DNA probe, using a derivatised *N,N'*-biscarboxymethylaminomethylpyridine chelate.⁹⁹ The Eu chelate was introduced on transaminated λ DNA, and the hybridisation assays were carried out on the solid phase. The advantages of their detection method is the use of time resolved fluorescence to quantify and interpret easily the probe response over a range of target DNA and at a fairly high probe concentration (up to 500 ng/ml).

- ¹ J. D. Watson, F. H. C. Crick, *Nature*, **1953**, 171, 737.
- ² S. Neidle, *DNA structure and recognition*, **1994**, In focus, Oxford University Press.
- ³ C. K. Matthews, K. E. van Holde, *Biochemistry*, **1996**, 2nd Ed, Chap. IV.
- ⁴ a) R. M. Wing, H. R. Drew, T. Takano, C. Broka, S. Takana, K. Itakura, R. E. Dickerson, *Nature*, **1980**, 287, 755.
b) S. Fujii, A. H. J. Wang, G. J. Quigley, H. Westerink, G. van der Marel, J. H. Boom, A. Rich, *Biopolymers*, **1985**, 24, 243.
c) M. McCall, T. Brown, W. N. Hunter, O. Kennard, *Nature*, **1986**, 322, 661.
- ⁵ a) M. G. Kubinec, D. E. Wemmer, *J. Am. Chem. Soc.*, **1992**, 114, 8739.
b) G. R. Clark, D. G. Brown, M. R. Sanderson, T. Chwalinski, S. Neidle, J. M. Veal, R. L. Jones, W. D. Wilson, G. Zon, E. Garman, D. I. Stuart, *Nucleic Acids Research*, **1990**, 18, 5521.
- ⁶ a) D. J. Patel, A. Pardi, K. Itakura, *Science*, **1982**, 216, 581-590.
b) L. Fairall, S. Martin, D. Rhodes, *The EMBO Journal*, **1989**, 8, 1809.
- ⁷ G. Felsenfeld, D. R. Davies, A. Rich, *J. Am. Chem. Soc.*, **1957**, 79, 2023.
- ⁸ S. Arnott, R. Chandrasekaran, C. M. Marttila, *Biochem. J.*, **1974**, 141, 537.
- ⁹ T. Lindahl, *Nature*, **1993**, 362, 709-715.
- ¹⁰ H. DeVoe, I. Tinoco, *J. Mol. Biol.*, **1962**, 4, 500.
- ¹¹ E. T. Kool, J. C. Morales, K. M. Guckian, *Angew. Chem. Int. Ed.*, **2000**, 39, 990-1009.
- ¹² a) I. R. Gould, P. R. Kollman, *J. Am. Chem. Soc.*, **1994**, 116, 2493-2499.
b) Y. P. Pang, J.L. Miller, P. A. Kollman, *J. Am. Chem. Soc.*, **1999**, 121, 1717-1725.
- ¹³ F. T. Boyle, G. F. Costello, *Chemical Society Reviews*, **1998**, 27, 251-261.
- ¹⁴ R. S. Hawley, C. A. Mori, *The Human Genome*, **1999**, Ed. Academic Press, 21-44.
- ¹⁵ U. Diederichsen, *Angew. Chem. Int. Ed.*, **1998**, 37, 12, 1655-1657.
- ¹⁶ R. R. Sauers, *Bioorganic & Medicinal Chemistry Letters*, **1995**, 5, 21, 2573-2576.
- ¹⁷ D. Goodsell, R. E. Dickerson, *J. Med. Chem.*, **1986**, 29, 727.
- ¹⁸ L. S. Lerman, *Journal of Mol. Biol.*, **1961**, 3, 18.
- ¹⁹ a) E. C. Long, J. K. Barton, *Acc. Chem. Res.*, **1990**, 23, 271.
b) J. Sartorius, H.-J. Schneider, *J. Chem. Soc., Perkin Trans. 2*, **1997**, 2319-2327.
c) M. J. Waring, *J. Mol. Biol.*, **1970**, 54, 247.
- ²⁰ T.-C. Tang, H.-J. Huang, *Electroanalysis*, **1999**, 11, 16, 1185-1190.
- ²¹ H. W. Zimmermann, *Angew. Chem. Int. Ed.*, **1986**, 25, 115-130.
- ²² a) Le Pecq, C. Paoletti, *Anal. Biochem*, **1966**, 17, 100-107.
b) K. G. Strothkamp, R. E. Strothkamp, *J. Chem. Educ.*, **1990**, 71, 1, 77-79.
- ²³ a) E. Fredericq, C. Houssier, *Biopolymers*, **1972**, 11, 2281.
b) B. Gardner, S. Mason, *Biopolymers*, **1967**, 5, 79.
- ²⁴ a) J. M. Rosenberg, N. C. Seeman, R. O. Day, A. Rich, *J. Mol. Biol.*, **1976**, 104, 145.
b) H. M. Berman, W. Stallings, H. L. Carrell, J. P. Glusker, S. Neidle, G. Taylor, A. Achari, *Biopolymers*, **1979**, 18, 2405.
- ²⁵ a) M. Teng, N. Usman, C. A. Frederick, A. H. J. Wang, *Nucleic Acids Res.*, **1988**, 16, 2671.
b) N. Spink, D. G. Brown, J. V. Skelly, S. Neidle, *Nucleic Acids Res.*, **1994**, 22, 1607.
c) A. A. Wood, C. M. Nunn, A. Czarny, D. W. Boykin, S. Neidle, *Nucleic Acids Res.*, **1995**, 23, 3678.
- ²⁶ D. M. Hermann, E. E. Baird, P. B. Dervan, *Chem. Eur. J.*, **1999**, 5, 3, 975-983.
- ²⁷ a) J. M. Gottesfeld, L. Nealy, J. W. Trauger, E. E. Baird, P. B. Dervan, *Nature*, **1997**, 387, 202.
b) L. A. Dickinson, R. J. Gulizia, J. W. Trauger, E. E. Baird, D. E. Mosier, J. M. Gottesfeld, P. B. Dervan, *Proc. Natl. Acad. Sci. USA*, **1998**, 95, 12890.
- ²⁸ a) S. Kamitori, F. Takusagawa, *Journal of Mol. Biol.*, **1992**, 225, 445.
b) S. Kamitori, F. Takusagawa, *J. Am. Chem. Soc.*, **1994**, 116, 4154.
- ²⁹ K. E. Erkkila, D. T. Odom, J.K. Barton, *Chem. Rev.*, **1999**, 99, 2777-2795.
- ³⁰ a) Y. Jenkins, A. E. Friedman, N. J. Turro, J. K. Barton, *Biochemistry*, **1992**, 313, 10809-10816.
b) R. E. Holming, J. A. Yao, J. K. Barton, *Inorg. Chem.*, **1999**, 38, 174-198.
c) A. M. Pyle, J. P. Rehmann, R. Meshoyrer, C. V. Kumar, N. J. Turro, J. K. Barton, *J. Am. Chem. Soc.*, **1989**, 111, 3051-3058.
d) R. B. Nair, E. S. Teng, S. L. Kirkland, C. J. Murphy, *Inorg. Chem.*, **1998**, 37, 139-141.
- ³¹ a) J. K. Barton, J. J. Dannenberg, A. L. Raphael, *J. Am. Chem. Soc.*, **1982**, 104, 4967-4969.
b) J. K. Barton, A. T. Danishefski, J. M. Goldberg, *J. Am. Chem. Soc.*, **1984**, 106, 2172-2176.
c) J. K. Barton, J. M. Goldberg, C. V. Kumar, N. J. Turro, *J. Am. Chem. Soc.*, **1986**, 108, 2081-2088.
- ³² a) C. Hiort, B. Nordén, A. Rodger, *J. Am. Chem. Soc.*, **1990**, 112, 1971-1982.
b) M. Eriksson, M. Leijon, C. Hiort, B. Nordén, A. Graslund, *J. Am. Chem. Soc.*, **1992**, 114, 4933-4934.
- ³³ a) R. M. Hartshorn, J. K. Barton, *J. Am. Chem. Soc.*, **1992**, 114, 5919-5925.

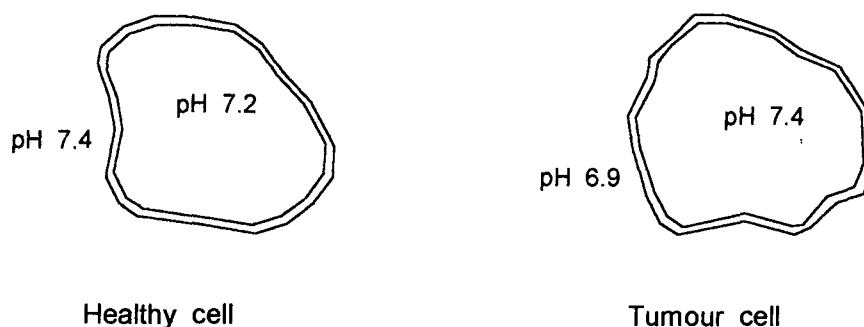
- b) C. Hiort, P. Lincoln, B. Nordén, *J. Am. Chem. Soc.*, **1993**, 115, 3448-3454.
- ³⁴ a) E. Tuite, P. Lincoln, B. Nordén, *J. Am. Chem. Soc.*, **1997**, 119, 239-240.
b) C. M. Dupureur, J. K. Barton, *J. Am. Chem. Soc.*, **1994**, 116, 10286-10287.
c) R. E. Holmlin, E. D. A. Stemp, J. K. Barton, *Inorg. Chem.*, **1998**, 37, 29-34.
- ³⁵ a) H.-Y. Mei, J. K. Barton, *J. Am. Chem. Soc.*, **1986**, 108, 7414-7416.
b) A. E. Friedman, J.-C. Chambron, J.-P. Sauvage, N. J. Turro, J. K. Barton, *J. Am. Chem. Soc.*, **1990**, 112, 4960-4962.
c) A. E. Friedman, C. V. Kumar, N. J. Turro, J. K. Barton, *Nucleic Acids Res.*, **1991**, 19, 10, 2595-2602.
d) H.-K. Kim, P. Lincoln, B. Nordén, E. Tuite, *Chem. Commun.*, **1997**, 2375-2376.
e) P. Lincoln, B. Nordén, *J. Phys. Chem. B*, **1998**, 102, 9583-9594.
f) B. Önfelt, P. Lincoln, B. Nordén, *J. Am. Chem. Soc.*, **1999**, 121, 10846-10847.
g) F. M. O'Reilly, J. M. Kelly, *New J. Chem.*, **1998**, 215-217.
h) O. Van Gijte, A. Kirch-De Mesmaescker, *J. Chem. Soc., Dalton Trans.*, **1999**, 951-956.
i) K. Wiederholt, L. W. McLaughlin, *Nucleic Acids Res.*, **1999**, 27, 12, 2487-2493.
- ³⁶ a) H. D. Stoeffler, N. B. Thornton, S. L. Temkin, K. S. Schanze, *J. Am. Chem. Soc.*, **1995**, 117, 7119-7128.
b) V. W.-W. Yam, K. K.-W. Lo, K.-K. Cheung, R. Y.-C. Kong, *Chem. Commun.*, **1995**, 1191.
c) V. W.-W. Yam, K. K.-W. Lo, K.-K. Cheung, R. Y.-C. Kong, *J. Chem. Soc., Dalton Trans.*, **1997**, 2067.
- ³⁷ a) B. A. Jackson, J. K. Barton, *J. Am. Chem. Soc.*, **1997**, 119, 12986-12987.
b) B. A. Jackson, V. Y. Alekseyev, J. K. Barton, *Biochemistry*, **1999**, 38, 4655-4662.
c) S. S. David, J. K. Barton, *J. Am. Chem. Soc.*, **1993**, 115, 2984-2985.
d) P. Lincoln, E. Tuite, B. Nordén, *J. Am. Chem. Soc.*, **1997**, 119, 1454-1455.
e) B. P. Hudson, J. K. Barton, *J. Am. Chem. Soc.*, **1998**, 120, 6877-6888.
f) E. C. Theil, *New J. Chem.*, **1994**, 18, 435-441.
- ³⁸ S. Content, A. Kirsch-De Mesmaeker, *J. Chem. Soc., Faraday Trans.*, **1997**, 93(6), 1089-1094.
- ³⁹ a) R. J. Fiel, J. C. Howard, E. H. Mark, N. Datta Gupta, *Nucleic Acids Res.*, **1979**, 6, 3093.
b) M. Sirish, H.-J. Schneider, *Chem. Commun.*, **2000**, 23-24.
c) P. Kubat, K. Lang, P. Anzenbacher, K. Jursikova, V. Kral, B. Ehrenberg, *J. Chem. Soc., Perkin Trans. 1*, **2000**, 933-941.
- ⁴⁰ R. F. Pasternack, P. Garrity, B. Ehrlich, C. B. Davis, E. J. Gibbs, G. Orloff, A. Giartosio, C. Turano, *Nucleic Acids Res.*, **1986**, 14, 5919.
- ⁴¹ L. A. Lipscomb, F. X. Zhou, S. R. Presnell, R. J. Woo, M. E. Peek, R. R. Plaskon, L. D. Williams, *Biochemistry*, **1996**, 35, 2818.
- ⁴² a) B. Rosenberg, J. van Camp, J. E. Trosko, V. H. Mansour, *Nature*, **1969**, 222, 385.
b) R. M. Wing, P. Pjura, H. R. Drew, R. E. Dickerson, *The EMBO Journal*, **1984**, 3, 1201-1206.
c) S. R. Rajski, R. M. Williams, *Chem. Rev.*, **1998**, 98, 2723-2795.
- ⁴³ S. Neidle, C. N. Nunn, *Natural Product Reports*, **1998**, 1-15.
- ⁴⁴ R. E. Dickerson, H. R. Drew, *J. Mol. Biol.*, **1981**, 149, 761.
- ⁴⁵ C. A. Loughton, F. Tanius, C. M. Nunn, B. Boykin, W. D. Wilson, S. Neidle, *Biochemistry*, **1996**, 35, 5655.
- ⁴⁶ a) P.M. Takahara, A. C. Rosenzweig, C. A. Frederick, S. J. Lippard, *Nature*, **1995**, 377, 649.
b) P.M. Takahara, C. A. Frederick, S. J. Lippard, *J. Am. Chem. Soc.*, **1996**, 118, 12309.
- ⁴⁷ M. S. Searle, *Progress in NMR Spectroscopy*, **1993**, 25, 403-480.
- ⁴⁸ A. Ali, M. Gasiorek, H.-J. Schneider, *Angew. Chem. Int. Ed.*, **1998**, 37, 21, 3016-3019.
- ⁴⁹ A. Rodger, B. Nordén, *Circular Dichroism and Linear Dichroism*, **1997**, Oxford University Press.
- ⁵⁰ a) R. Lyng, A. Rodger, B. Nordén, *Biopolymers*, **1991**, 31, 1709-1720.
b) R. Lyng, A. Rodger, B. Nordén, *Biopolymers*, **1992**, 32, 1201-1214.
- ⁵¹ J. A. Taboury, E. Taillandier, *Nucleic Acids Res.*, **1985**, 13, 4469-4483.
- ⁵² K. B. Hall, M. F. Meastre, *Biopolymers*, **1984**, 23, 2127-2139.
- ⁵³ a) V. I. Ivanov, E. E. Minyat, *Nucleic Acids Res.*, **1981**, 9, 4783-4798.
b) M. Vorlickova, P. Sedlacek, J. Pypr, J. Sponar, *Nucleic Acids Res.*, **1982**, 10, 6969-6979.
- ⁵⁴ a) R. Lyng, T. Hård, B. Nordén, *Biopolymers*, **1987**, 26, 1327-1345.
b) G. Colmenarejo, A. Holmén, B. Nordén, *J. Phys. Chem. B*, **1997**, 101, 5196-5204.
c) H.-C. Becker, B. Nordén, *J. Am. Chem. Soc.*, **1997**, 119, 5798-5803.
- ⁵⁵ C. Zimmer, G. Luck, *Advances in DNA Sequence specific Agents*, 1992, Vol 1, 51-88.
- ⁵⁶ G. T. Walker, M. P. Stone, T. R. Krugh, *Biochemistry*, **1985**, 24, 7462-7471.
- ⁵⁷ F. S. Allen, R. P. Moen, U. Hollstein, *J. Am. Chem. Soc.*, **1976**, 98, 864-865.
- ⁵⁸ M. J. Carvlin, R. J. Fiel, *Nucleic Acids Res.*, **1983**, 11, 6121-6138.
- ⁵⁹ M. V. Mikhailov, A. S. Zasedatelev, A. M. Kolchinsky, G. V. Gurky, *Molec. Biol. (SSSR)*, **1981**, 15, 690-705.
- ⁶⁰ E. Bayer, T. Bauer, K. Schmeer, K. Bleicher, M. Maier, H.-J. Gaus, *Anal. Chem.*, **1994**, 66, 3858-3863.
- ⁶¹ A. Triolo, F. M. Arcamone, A. Raffealli, P. Salvadori, *J. Mass Spectrom.*, **1997**, 32, 1186-1194.

- ⁶² P. W. Atkins, *Physical Chemistry*, Third Edition, 1986, Oxford University Press.
- ⁶³ V. Balzani, J.-M. Lehn, N. Sabbatini, R. Therörde, R. Ziessel, *Helv. Chim. Acta.*, 1990, 73, 2083.
- ⁶⁴ R. D. Peacock, *Struct. Bonding (Berlin)*, 1975, 22, 83.
- ⁶⁵ W. DeW. Horrocks, M. Albin, *Prog. Inorg. Chem.*, 1984, 31, 1.
- ⁶⁶ a) A. Beeby, I. M. Clarkson, R. S. Dickins, S. Faulkner, D. Parker, L. Royle, A. S. de Sousa, J. A. G. Williams, M. Woods, *J. Chem. Soc., Perkin Trans. 2*, 1999, 493-503.
b) D. Parker, J. A. G. Williams, *J. Chem. Soc., Dalton Trans.*, 1996, 3613.
c) W. DeW. Horrocks, D. R. Sudnick, *J. Am. Chem. Soc.*, 1979, 101, 334.
d) W. DeW. Horrocks, D. R. Sudnick, *Acc. Res. Chem.*, 1981, 14, 384.
- ⁶⁷ S. I. J. Weisman, *Chem. Phys.*, 1942, 10, 214.
- ⁶⁸ T. Förster, *Discuss. Faraday Soc.*, 1959, 27, 7.
- ⁶⁹ D. L. Dexter, *J. Chem. Phys.*, 1953, 21, 836.
- ⁷⁰ E. F. G. Dickson, A. Pollak, E. P. Diamantis, *Photochem. Photobiol.*, 1995, 27, 3.
- ⁷¹ a) D. Parker, *Chem. Soc. Rev.*, 1990, 19, 271.
b) R. B. Lauffer, *Chem. Rev.*, 1987, 87, 901.
- ⁷² a) R. Ziessel, J.-M. Lehn, *Helv. Chim. Acta*, 1990, 73, 1149.
b) V. Balzani, E. Berghmans, J.-M. Lehn, N. Sabbatini, R. Terörde, R. Ziessel, *Helv. Chim. Acta*, 1990, 73, 2083.
- ⁷³ a) N. Sabbatini, S. Dellonte, M. Ciano, A. Bonazzi, V. Balzani, *Chem. Phys. Lett.*, 1984, 107, 212.
b) N. Sabbatini, S. Dellonte, G. Blasse, *Chem. Phys. Lett.*, 1986, 129, 541.
- ⁷⁴ B. Alpha, J.-M. Lehn, G. Mathis, *Angew. Chem. Int. Ed.*, 1987, 26, 266.
- ⁷⁵ A. Adams, *Science*, 1998, 279, 1307.
- ⁷⁶ S. Aime, M. Botta, D. Parker, J. A. G. Williams, *J. Chem. Soc., Dalton Trans.*, 1996, 17.
- ⁷⁷ S. Hoefl, K. Roth, *Chem. Ber.*, 1993, 126, 869-873.
- ⁷⁸ D. H. Metcalf, J.M. McD. Stewart, S. W. Snyder, C. M. Grisham, F. S. Richardson, *Inorg. Chem.*, 1992, 31, 2445-2455.
- ⁷⁹ a) S. Aime, M. Botta, G. Ermondi, *Inorg. Chem.*, 1992, 31, 4291-4299.
b) S. Aime, M. Botta, M. Fasano, M. P. M. Marques, C. F. G. C. Geraldés, D. Pubanz, A. E. Merbach, *Inorg. Chem.*, 1997, 36, 2059-2068.
- ⁸⁰ a) W. DeW. Horrocks Jr., D. R. Sudnick, *Acc. Chem. Res.*, 1981, 14, 384-392.
b) M. Elbanowski, B. Makowska, *J. Photochem. Photobiol. A*, 1996, 85-92.
- ⁸¹ D. Parker, *Coordination Chem. Rev.*, 2000, 205, 109-130.
- ⁸² E. P. Diamantis, R. C. Morton, *J. Immunol. Methods*, 1988, 112, 43-52.
- ⁸³ D. Parker, P. K. Senanayake, J. A. G. Williams, *J. Chem. Soc., Perkin Trans. 2*, 1998, 2129-2140.
- ⁸⁴ a) T. Gunnlaugsson, D. Parker, *Chem. Commun.*, 1998, 511-512.
b) T. Gunnlaugsson, D. Mc Dónail, D. Parker, *Chem. Commun.*, 2000, 93-94.
- ⁸⁵ M. P. Lowe, D. Parker, *J. Chem. Soc., Chem. Commun.*, 2000, 707-708.
- ⁸⁶ J. I. Bruce, R. S. Dickins, T. Gunnlaugsson, S. Lopinski, M. P. Lowe, D. Parker, R. B. Peacock, J.B.B. Perry, S. Aime, M. Botta, *J. Am. Chem. Soc.*, 2000, 122, 9674-9684.
- ⁸⁷ D. Parker, J. A. G. Williams, *Chem. Commun.*, 1998, 245-246.
- ⁸⁸ A. Beeby, R. S. Dickins, S. Fitzgerald, L. J. Govenlock, C. L. Maupin, D. Parker, J. P. Riehl, G. Siligardi, J. A. G. Williams, *Chem. Commun.*, 2000, 1183-1184.
- ⁸⁹ O. Reany, T. Gunnlaugsson, D. Parker, *Chem. Commun.*, 2000, 473-474.
- ⁹⁰ a) S. L. Klakamp, W. DeW. Horrocks, Jr., *J. Inorg. Chem.*, 1992, 46, 175-192.
b) S. L. Klakamp, W. DeW. Horrocks, Jr., *J. Inorg. Chem.*, 1992, 46, 193-205.
c) S. L. Klakamp, W. DeW. Horrocks, Jr., *Biopolymers*, 1990, 30, 33-43.
- ⁹¹ P. K.-L. Fu, C. Turro, *J. Am. Chem. Soc.*, 1999, 121, 1, 1-7.
- ⁹² a) M. Komiyama, N. Takeda, H. Shigekawa, *Chem. Commun.*, 1999, 1443-1451.
b) R. Hettich, H.-J. Schneider, *J. Chem. Soc., Perkin Trans. 2*, 1997, 2069-2072.
- ⁹³ S. S. Saavedra, E. G. Picozza, *Analyst*, 1989, 114, 835.
- ⁹⁴ A. K. Saha, K. Kross, Kloszewski, D. A. Upson, J. L. Toner, R. Snow, C.D.V. Black, V.C. Desai, *J. Am. Chem. Soc.*, 1993, 115, 11032.
- ⁹⁵ A. Chan, E. P. Diamandis, M. Kraiden, *Anal. Chem.*, 1993, 65, 158.
- ⁹⁶ T. J. Wenzel, L. M. Colette, *J. Chromatogr.*, 1988, 436, 299.
- ⁹⁷ a) J. Coates, P. G. Sammes, R. M. West, *J. Chem. Soc., Chem. Commun.*, 1995, 1107-1108.
b) J. Coates, P. G. Sammes, G. Yahioğlu, R. M. West, A. J. Garman, *J. Chem. Soc., Chem. Commun.*, 1994, 2311-2312.
c) S. T. Mullins, P. G. Sammes, R. M. West, G. Yahioğlu, *J. Chem. Soc., Perkin Trans. 1*, 1995, 75-81.
d) J. Coates, P. G. Sammes, R. M. West, *J. Chem. Soc., Perkin Trans. 2*, 1996, 1275-1282.

-
- e) J. Coates, P. G. Sammes, R. M. West, *J. Chem. Soc., Perkin Trans. 2*, **1996**, 1283-1287.
- ⁹⁸ a) L. Huang, L. L. Chappell, O. Iranzo, B. F. Baker, J. R. Morrow, *J. Biol. Inorg. Chem.*, **2000**, 5, 85-92.
b) B. F. Baker, S. S. Lot, J. Kringlel, S. Cheng-Flournoy, P. Villiet, H. M. Sasmor, A. M. Siwkowski, L. L. Chappell, J. R. Morrow, *Nucleic Acids Res.*, **1999**, 27, 6, 1547-1551.
- ⁹⁹ P. Hurskainen, P. Dahlén, J. Ylikoski, M. Kwiatkowski, H. Siitari, T. Lövgren, *Nucleic Acids Res.*, **1991**, 19, 5, 1057-1061.

pH Responsive Lanthanide Probes

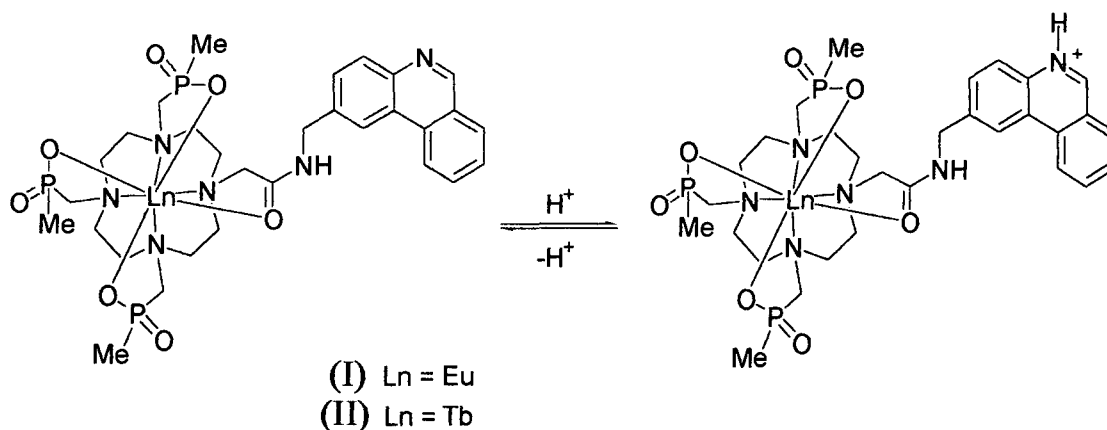
Because the growth of tumour cells often is accompanied by variation in local pH, signalling a change in acidity in human body is an important feature of cancer diagnosis (Scheme 2.1). Consequently the design of a pH probe which responds precisely to that pH range (typically 6.8-7.5) is critical for potential uses such as micro-scale pH measurements. Chemically robust single-component luminescent sensors are thus needed for studying this and related changes in ionic concentrations in living cells.



Scheme 2.1: Intra and extra cellular pH in a healthy and tumour cell

2-1: Previous work on pH sensors.

In 1997, Parker *et al.* designed various macrocyclic lanthanide complexes, involving 1,4,7,10-tetraazacyclododecane (cyclen) bearing a phenanthridine chromophore which acted as a sensitizer for the bound lanthanide ion (Scheme 2.2).¹

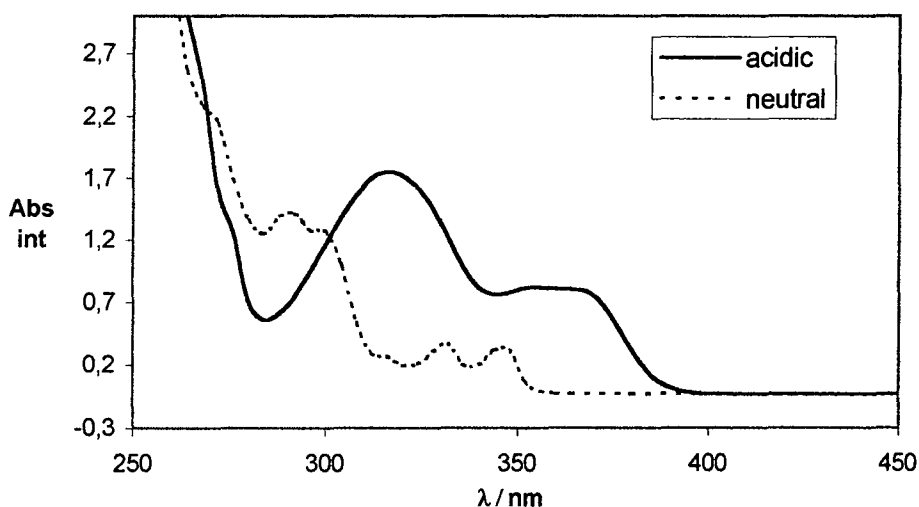


Scheme 2.2: Phenanthridinium lanthanide conjugates

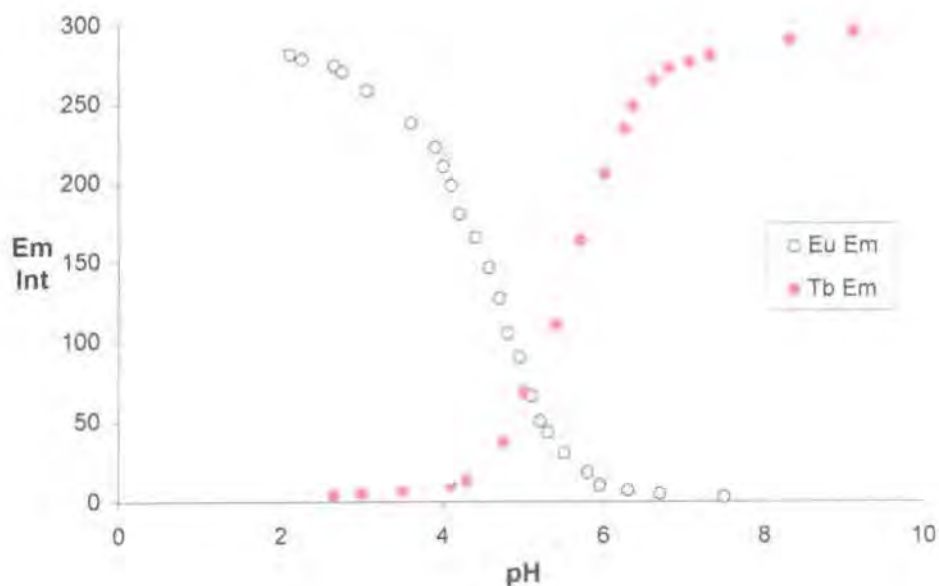
This chromophore was chosen for its property of allowing excitation in biological media: it is possible to excite the sensitiser at wavelengths of over 350 nm minimising the associated background fluorescence from excited biomolecules. The sensitising chromophore serves a dual function: its singlet or triplet excited states may be reversibly perturbed by changes in the local environment, in particular pH changes leading to the protonation of the phenanthridine.

These monoamide triphosphinate complexes are kinetically stable in aqueous media, and exist as one major stereoisomer in water. Upon protonation the phenanthridinyl absorption spectrum exhibits distinctive changes: the three absorption bands visible at neutral pH become only two in acidic conditions, increase in intensity and shift to longer wavelengths, from 350 nm to 370 nm (Scheme 2.3). Consequently, the Eu(III) luminescence sensitised at 370 nm by the phenanthridinyl group increases by a factor of over 500 by protonation of the antenna. The fluorescence spectrum from the phenanthridine group also undergoes changes as the phenanthridinyl nitrogen is protonated: the intensity increases by 300% and there is a shift to longer wavelength of 40 nm. The variation in the intensity of the phenanthridine fluorescence ($\lambda_{\text{em}} = 405 \text{ nm}$, $\lambda_{\text{exc}} = 320 \text{ nm}$) and of the Eu emission ($\lambda_{\text{em}} = 594 \text{ nm}$, $\lambda_{\text{exc}} = 370 \text{ nm}$) with pH allowed an estimate of the $\text{p}K_{\text{a}}$ of the singlet excited state of the complex. A value of 4.4 was found for both parameters monitored, which is, according to the literature, fairly similar to the $\text{p}K_{\text{a}}$ value of 4.45 reported for the phenanthridine ground state.²

The Tb complex responds differently to acidic conditions³: the luminescence from Tb drops upon protonation of the phenanthridine (Scheme 2.4). The phenanthridine based fluorescence increases by a factor of three by protonation of phenanthridinyl nitrogen, as observed with (I).

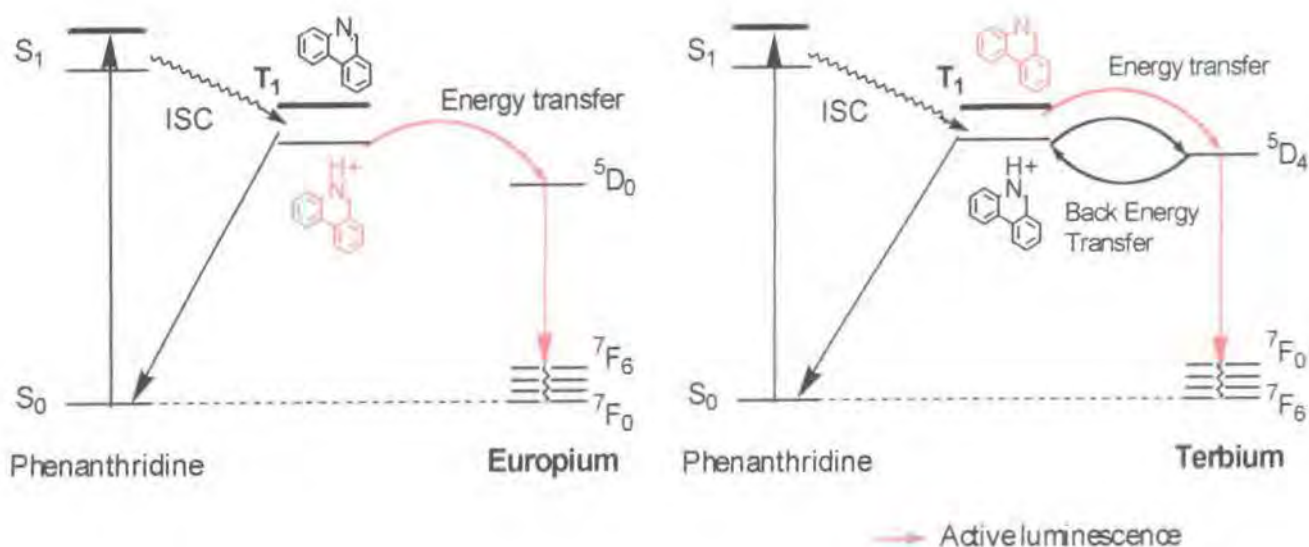


Scheme 2.3: UV-vis absorbance spectra of phenanthridine in neutral and acidic media



Scheme 2.4: Emission from the lanthanide centre in the europium and terbium complexes **I** and **II** as a function of pH (298K, $I = 0.1 \text{ NMe}_4\text{NO}_3$)

The different behaviour displayed by the Eu(III) and the Tb(III) complexes can be explained by considering the energies of the appropriate excited states (Scheme 2.5).



Scheme 2.5: Representation of energy levels for Eu and Tb complexes **I** and **II**

Under acidic conditions the phenanthridine triplet state lies only 800 cm^{-1} above the $^5\text{D}_4$ energy level of Tb. Such proximity leads to efficient deactivation through thermally activated back energy transfer from the metal to the sensitiser at the expense of the lanthanide emission. Such a process does not occur in the case of Eu, owing to the larger energy gap between the two levels. When unprotonated the triplet state of phenanthridine is 1500 cm^{-1} higher than the Tb $^5\text{D}_4$ level; the rate of back energy transfer in the Tb complex is then very much reduced, and no longer competes effectively with the rate of intramolecular energy transfer and hence lanthanide emission. The excited state $\text{p}K_a$ of 5.75 for the Tb complex, as determined from the dependence of the metal luminescence, is close to the $\text{p}K_a$ value reported for the triplet state of phenanthridine itself ($\text{p}K_a(\text{T}_1)=5.75$). The complementarity of these two lanthanide complexes is evident in their potential use as luminescent pH probes.⁴

2-2: Modification of the phenanthridine chromophore

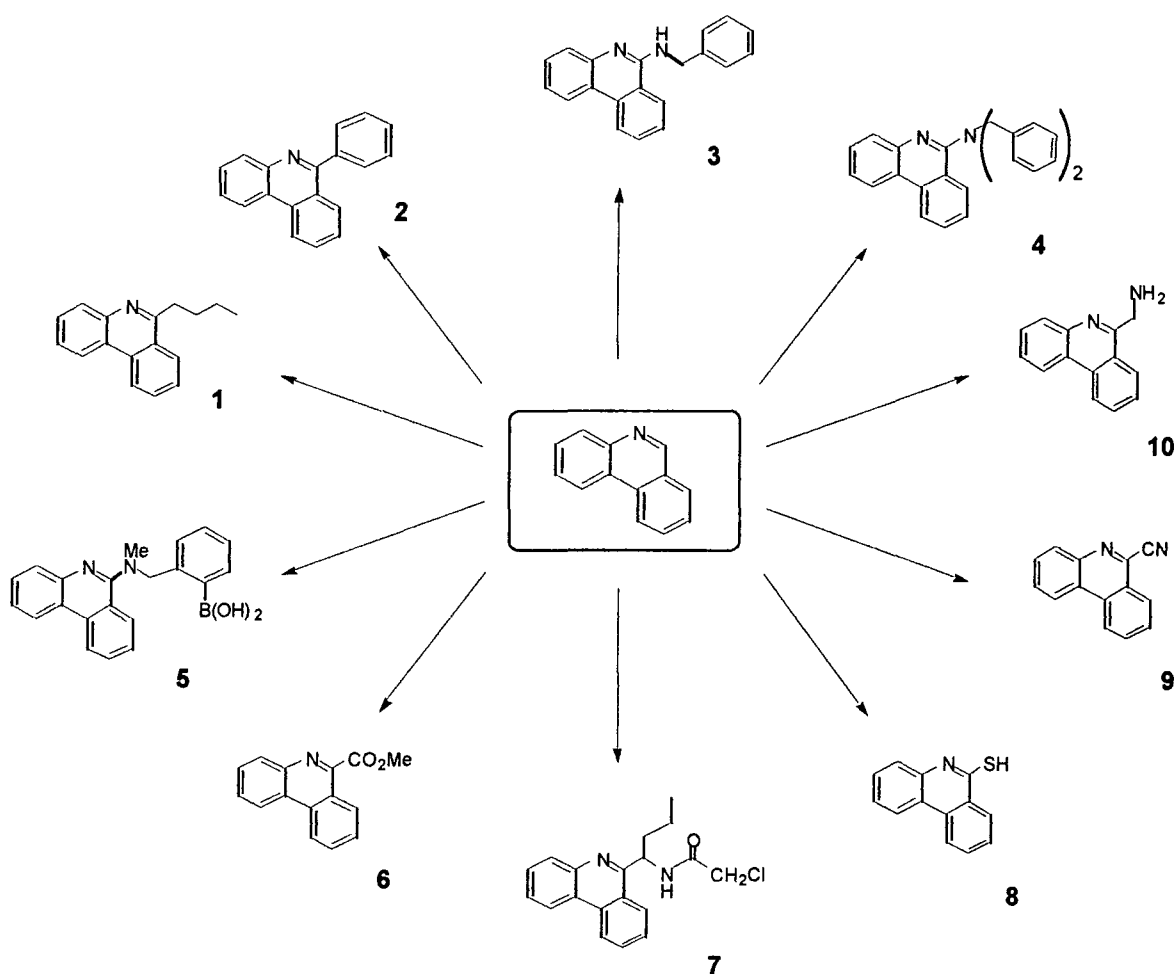
The phenanthridine chromophore possesses very useful characteristics in its excited energy levels, thereby allowing the sensitisation of both Eu and Tb ions. Thus there is a relatively low lying first excited state and absorption of light at wavelengths of around 350 nm occurs fairly efficiently ($\epsilon > 10^3\text{ M}^{-1}\text{cm}^{-1}$). Moreover there is a fairly small singlet triplet energy gap, allowing a fast rate of intersystem crossing to populate the triplet which, in turn, is sufficiently high in energy to allow intramolecular energy transfer to a proximate Eu or Tb ion. Furthermore the “switching” process operated by the protonation/deprotonation of the phenanthridinyl nitrogen occurs at pH 5.7, which is relatively close to the physiologically useful pH range (pH 5.5 to 7.5). Because the change at which this effect occurs is controlled by the modification of the molecular structure of the antenna, it was expected that substitution α to the nitrogen (i.e. at the 6-position) would perturb the $\text{p}K_a$ of the phenanthridine, without affecting its triplet energy too much.

Therefore, a series of simple alkyl and both electron-withdrawing and electron-releasing groups were considered. Initially the effect on the singlet and triplet energy levels was screened.

2-2.1: Introduction of substituents in 6 position: synthesis

Alkylation or arylation of the phenanthridine at the 6-position was expected to modulate the $\text{p}K_a$ of the sensitiser. The positive inductive effect of the butyl group should

raise the pK_a , but could also affect the protonation equilibrium through a steric effect via steric inhibition of solvation of the phenanthridinium conjugate acid. Likewise a phenyl group could perturb the value in the required direction despite its small negative inductive effect. Amination has a negative inductive effect, but the lone-pair conjugation could increase favourably the absorbance λ_{max} . The introduction of an electron-withdrawing ester group was expected to lead to a decrease of the pK_a , but was also likely to affect negatively the triplet energy. Cyanation should have a negative inductive effect, but the highly conjugated chromophore would absorb to longer wavelength.

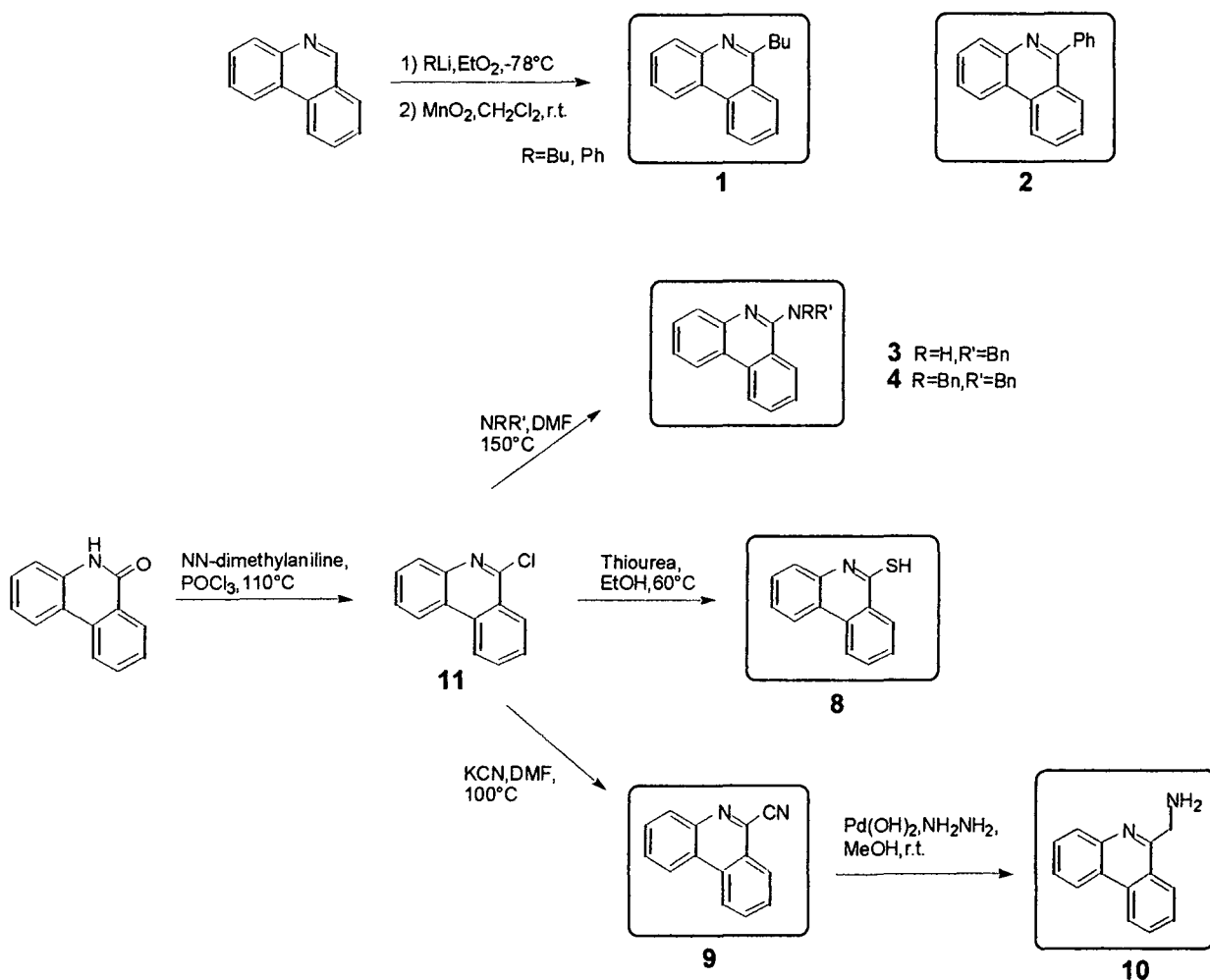


Scheme 2.6: 6-Substituted phenanthridines

Synthesis of 6-substituted phenanthridines

6-Butyl and 6-phenyl phenanthridine were obtained following the Gilman procedure,⁵ by nucleophilic attack of the appropriate lithium reagent at low temperature. The re-aromatisation step was carried out using manganese (IV) oxide as an oxidising agent.

A series of 6-substituted compounds was prepared by the nucleophilic substitution of chloride from 6-chlorophenanthridine. 6-Chlorophenanthridine itself was obtained according to the literature method,⁶ by reaction of phenanthridinone with phosphorus oxychloride in the presence of *N,N*-dimethylaniline. The next step involved the nucleophilic substitution of the chloride by cyanide, benzylamine, dibenzylamine, or a thiol, which allowed respectively 6-cyanophenanthridine, 6-benzylaminephenanthridine, 6-dibenzylamine phenanthridine and 6-thiophenanthridine to be obtained. The benzylamine and dibenzylamine substitutions were also carried out using only minor variations to the literature procedure.⁷ 6-Aminomethylenamine phenanthridine **10** was prepared by reduction of 6-cyanophenanthridine **9** using Pearlman's catalyst and hydrazine hydrate. 6-*N*-methyl-*N'*-[2-boroxymethyl] phenanthridine, **5**, and 6-carboxymethyl phenanthridine, **6**, were made available to the author and were given generously. The synthesis of 6-(*N*-chloroacetyl-1'-amino)-butyl phenanthridine **7** is detailed in chapter 4.



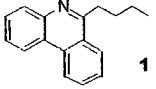
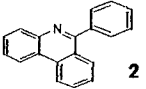
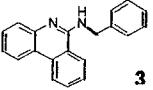
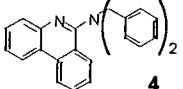
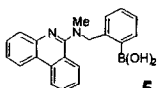
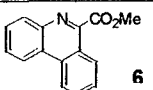
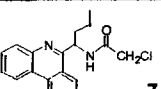
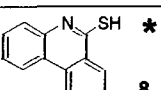
Scheme 2.7: Synthesis of substituted phenanthridines

2-2.2: Photophysical aspects of the chromophore

The effect of each of these different substitutions on the pK_a of the 6-substituted phenanthridine has been investigated by monitoring the variation of absorbance and fluorescence upon protonation. The changes in absorbance as a function of pH allowed the determination of the pK_a of the ground state S_0 , for each of the substituted phenanthridines. The variation of fluorescence intensity with pH similarly allowed the determination of the singlet excited state (S_1) pK_a . The more representative value for a pH responsive probe is the pK_a of the singlet because the variations in its population are echoed by changes in the emission of the lanthanide excited state following intramolecular energy transfer. The value of the pK_a is obviously crucial in the selection of the substituent group, but the energy level of the triplet excited state has also to be considered.

The singlet state energies of neutral and protonated species can be established from their UV-visible absorbance spectra at room temperature. Their triplet state energies were measured from phosphorescence spectra, at 77K in a diethyl ether/pentane/ethanol glass. The values obtained for the various substituted phenanthridines are listed in Table 2.1.

In order to identify an appropriate substituted phenanthridine for pH measurements, an increase in the pK_a value was sought without affecting significantly the triplet energy. The butyl chain allowed the phenanthridine pK_a of compound **1** to rise to 5 for the singlet excited state, and the singlet and triplet energies remain unchanged compared to those of the phenanthridine itself; both effects were considered suitable. The phenyl group, **2**, had only a slight increasing effect on the pK_a value compared to the butyl substitution, probably due to the small negative inductive effect of the aromatic ring. The effect on the energy levels was minor. In the case of the amino-substituted compounds, their strong electron-donating character allowed the pK_a to be raised up to 5.5 (only the pK_a of 6-benzylamine phenanthridine was determined; it was expected to be fairly similar for compounds **4** and **5**). This type of substitution had a dramatic effect on the triplet energy, raising it up to 23000-24000 cm^{-1} . This value is too high to allow an efficient energy transfer. The carboxymethyl substituted compound, **6**, had a similar increasing effect on the triplet state energy. This would also tend not to favour energy transfer to the metal. Compound **7** had a pK_a which was well beyond the useful range. In this case, steric inhibition of hydration of the phenanthridinium ion may play a part. The triplet energy of 6-thiolphenanthridine, **8**, is slightly lower than the parent unsubstituted phenanthridine.

6-Substituted Phenanthridine	pK _a (S ₀)	pK _a (S ₁)	E singlet (cm ⁻¹)		E triplet (cm ⁻¹)	
			Neutral	Acidic	Neutral	Acidic
Phenanthridine	3.4	3.6	28200	26300	22000	21300
 1	4.6	5	28600	26600	21600	21000
 2	3.4	3.9	28200	25600	20700	20500
 3	5.5	5.5	28600	26600	23400	21700
 4	-	-	28000	-	23800	23600
 5	-	-	28000	-	23800	22600
 6	-	-	28000	-	20100	19900
 7	2.3	2.5	28200	25900	21800	21000
 8	-	-	24300	-	19800	19800
	-	-	-	-	21600	21400
	4.8	4.9	28600	26300	-	-

* This may exist as the thioamide tautomeric form :

Table 2.1 : Acidity constants and singlet excited state and triplet excited state energies for a series of 6-substituted phenanthridine

A cyano group (compound **9**) being electron-withdrawing is not expected to increase the pK_a of the phenanthridine nitrogen, but lowered the singlet energy, allowing excitation at wavelengths in the range 360-380 nm. The reduction of the cyano group in **9** provided a route to 6-aminomethylphenanthridine (compound **10**). This amine possessed a pK_a which was fairly similar to that measured for 6-butyl phenanthridine, consistent with a small electron-releasing effect of the aminomethyl moiety.

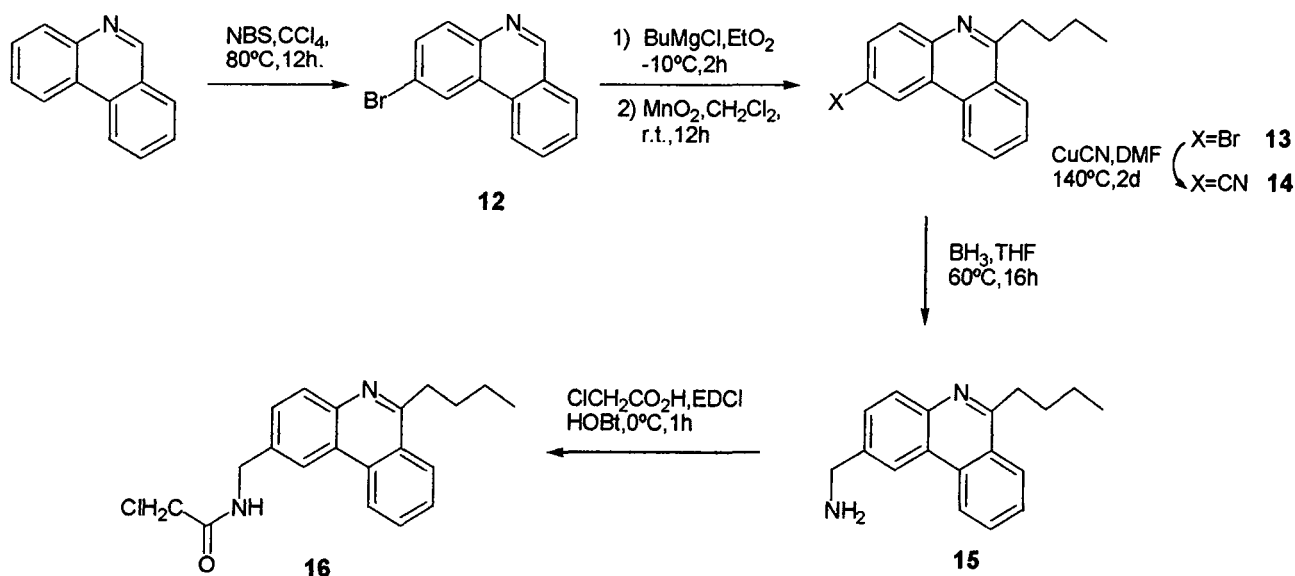
Taking all these facts into consideration, the more suitable substitution for increasing the pK_a value without introducing too much modification of the photochemical properties of the sensitiser, i.e. singlet and triplet energies, is the substitution by a simple alkyl group, and the butyl substituent was considered the most appropriate.

2-3: A pH probe based on 6-butyl phenanthridine

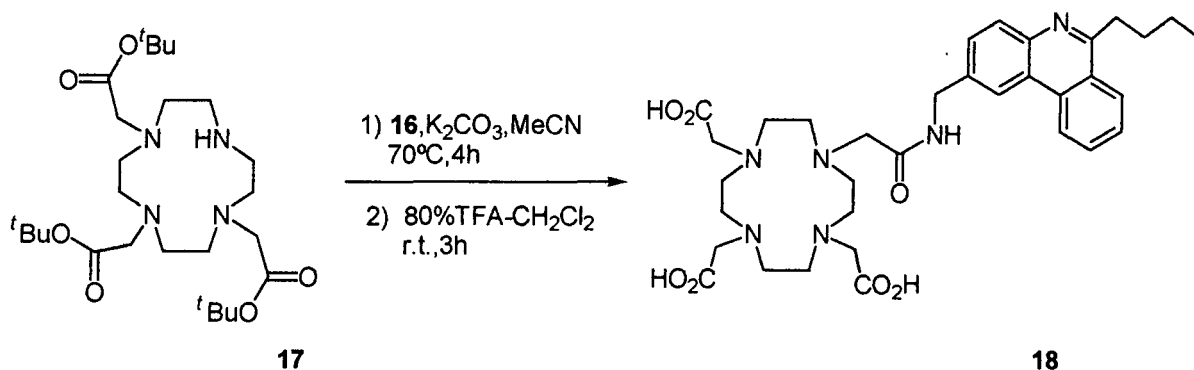
The target complexes for pH sensing are based on a cyclen macrocyclic ligand functionalised with three carboxylate or phosphinate pendent arms; such a ligand forms neutral complexes with lanthanide(III) ions.

2-3.1: Synthesis of europium(III) and terbium(III) complexes

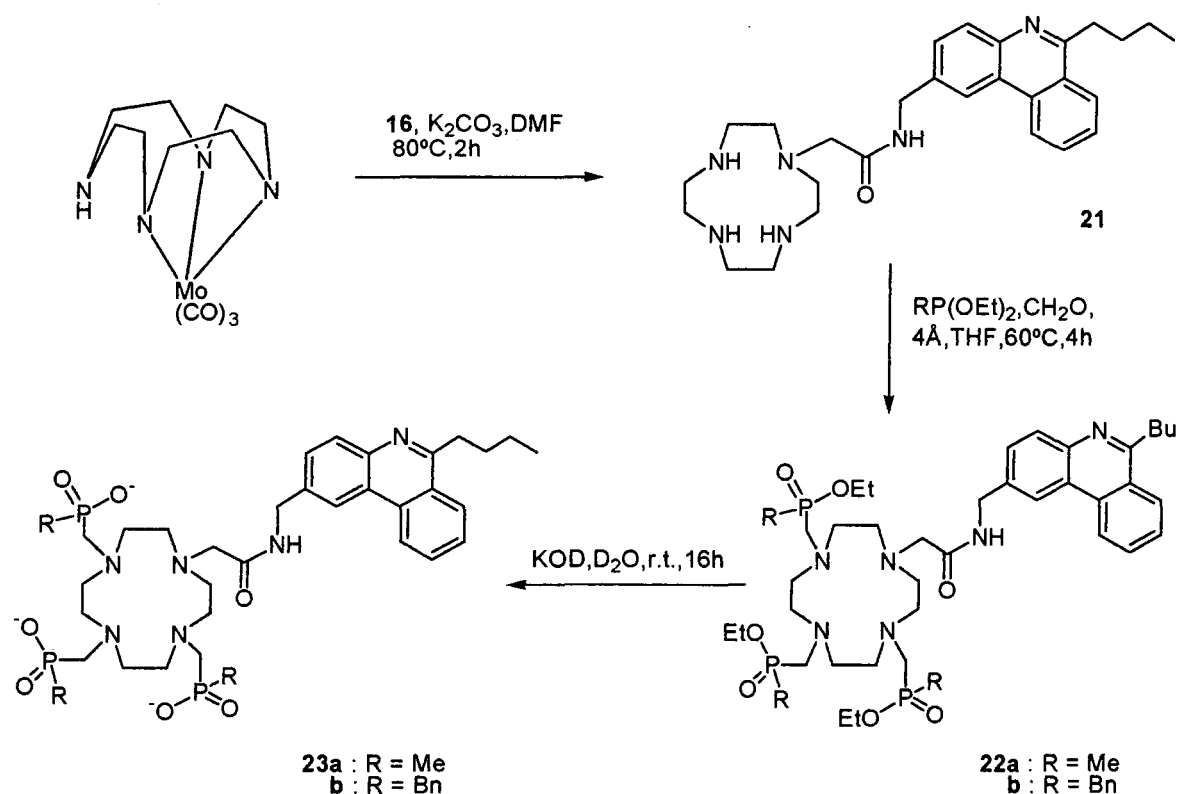
The synthesis, developed with the acknowledged assistance of Dr. Kanthi Senanayake, was based on a route established for the original unsubstituted phenanthridine probe,⁴ introducing the butyl group in an early synthetic step. The first step involved the bromination of the phenanthridine ring (**12**), which occurs selectively in the 2 position with NBS.⁴ The nucleophilic alkylation in the 6 position was undertaken using related method involving butylmagnesium chloride to avoid a putative bromide-lithium exchange in the case of the organolithium reaction. In an oxidative work-up step, the re-aromatisation of the ring was effected using manganese(IV) dioxide as an oxidising agent. Thereafter a nucleophilic substitution of the bromide (**13**) by a cyano group (**14**) was achieved using cuprous cyanide and the primary amine **15** was isolated after reduction with borane-THF. The peptide coupling with α -chloroacetic acid was carried out in THF in the presence of EDC and hydroxybenzotriazole, allowing the formation of **16**.

Scheme 2.8: Synthesis of the α -haloamide chromophore

The carboxylate ligand **18** was prepared by alkylation of the α -haloamide **16** with the tri-ester cyclen derivative **17**, in which the *tert*-butyl protection was subsequently removed under acidic conditions (Scheme 2.9).

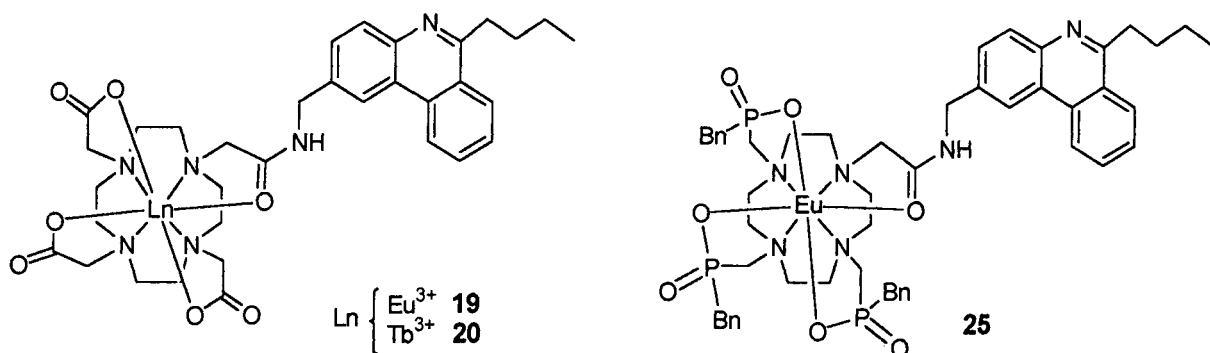
Scheme 2.9: Synthesis of the carboxylate ligand **18**

The phosphinate ligand **23** was obtained after protection of three of the cyclen ring nitrogens using established methodology⁸ in which a molybdenum-tricarbonyl complex is formed, which leaves one amine free for the alkylation reaction with the phenanthridine α -haloamide, **16**. Subsequent phosphinoxybenzylation using formaldehyde in the presence of molecular sieves, followed by hydrolysis of the phosphoester led to the triphosphinate ligand **23** (Scheme 2.10). The benzyl phosphinate ligand **23b** was obtained in a parallel manner to the methyl phosphinate ligand **23a**.



Scheme 2.10: Synthesis of the phosphinate ligand 23a and 23b

The last step involved the complexation of both ligands with lanthanide(III) salts in acetonitrile; for the monoamide tricarboxylate ligand 18, europium(III) (or terbium) acetate was used, and europium(III) nitrate was employed in the case of the monoamide triphosphinate ligand 23. The neutral complexes 19, 20, 24 and 25 that formed were purified on a short alumina chromatography column.



Scheme 2.11: Europium and terbium complexes

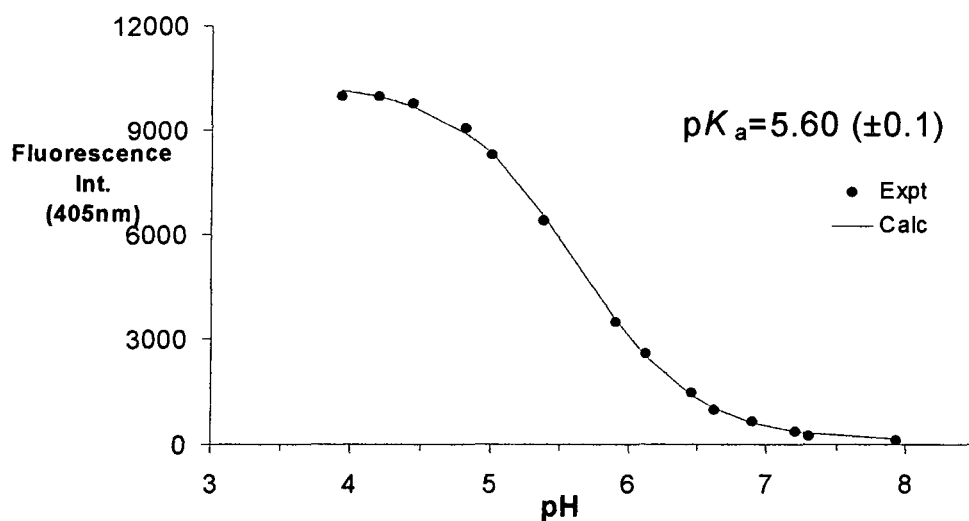
2-3.2: Luminescence properties of these complexes

2-3.2.1: Determination of acidity constant

Absorption spectra for Eu(III) and Tb(III) complexes were recorded in acidic ($\text{pH} < 2$) and neutral media ($\text{pH} > 7$). The protonation caused a marked shift to longer wavelength and a hyperchromism with an isosbestic point at 306 nm. Monitoring the changes in absorbance at 365 nm as a function of pH allowed the ground state $\text{p}K_a$ to be determined (295K, $I = 0.1 \text{ M NMe}_4\text{NO}_3$). The $\text{p}K_a$ of the singlet excited state was also estimated by monitoring the change in fluorescence emission from the phenanthridinyl group. The $\text{p}K_a$ value determined by monitoring the changes in metal emission was the same as the one from fluorescence emission changes, previously described.

➤ *Europium(III) tricarboxylate complex 19*

The absorbance spectra recorded for the europium complex **19** were typical of the phenanthridine group, showing a shift to longer wavelength of about 20 nm and a significant hyperchromism in acidic solution, compared to the spectra obtained in neutral conditions. A $\text{p}K_a$ of 5.4 was determined for the ground state of this 6-substituted complex, that is 1.2 units higher than for the analogous unsubstituted complex (**I**), (described in part 2-1).

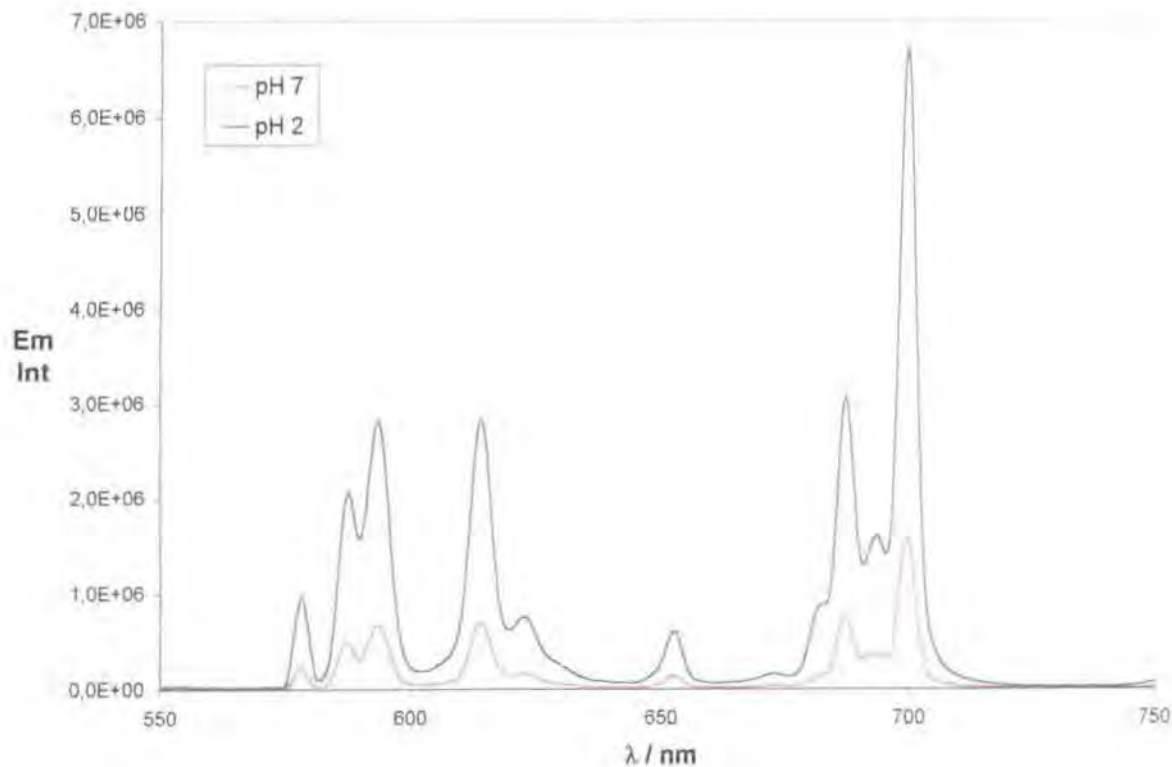


Scheme 2.12: Variation of fluorescence intensity ($\lambda_{em} = 405 \text{ nm}$) as a function of pH for **19**, showing the fit to the experimental data points (295K, $I = 0.1 \text{ M NMe}_4\text{NO}_3$, $\lambda_{exc} = 304 \text{ nm}$)

The pH dependence of the fluorescence emission raised from the phenanthridine group ($\lambda_{\text{exc}} = 365 \text{ nm}$, $\lambda_{\text{em}} = 405 \text{ nm}$) allowed an estimate of the $\text{p}K_{\text{a}}$ of the singlet excited state, and was found to be 5.6 (Scheme 2.12). Again this value represented an increase of 1.2 units from that observed for (**1**).

The phenanthridinyl group sensitised emission from the metal following excitation at 365 nm. Therefore Eu emission spectra were also recorded as a function of pH ($\lambda_{\text{exc}} = 304 \text{ nm}$, $\lambda_{\text{em}} = 580, 592 \text{ or } 615 \text{ nm}$, $\Delta J = 0, 1, 2$) (Scheme 2.13). The variation in intensity with pH of any of the europium emission bands reflected the singlet excited state $\text{p}K_{\text{a}}$ value of 5.6, similar to that obtained from fluorescence data. In acidic conditions, the emission intensity showed a three fold enhancement compared to the intensity in neutral media ($\lambda_{\text{exc}} = 304 \text{ nm}$). The same effect was observed for the fluorescence accompanied by a shift to longer wavelengths of 20 nm.

The data based on the experimental measurements fitted (using a non-linear iterative least squares fitting procedure operating under Excel[®] software) allowed the establishment of the acidity constant.



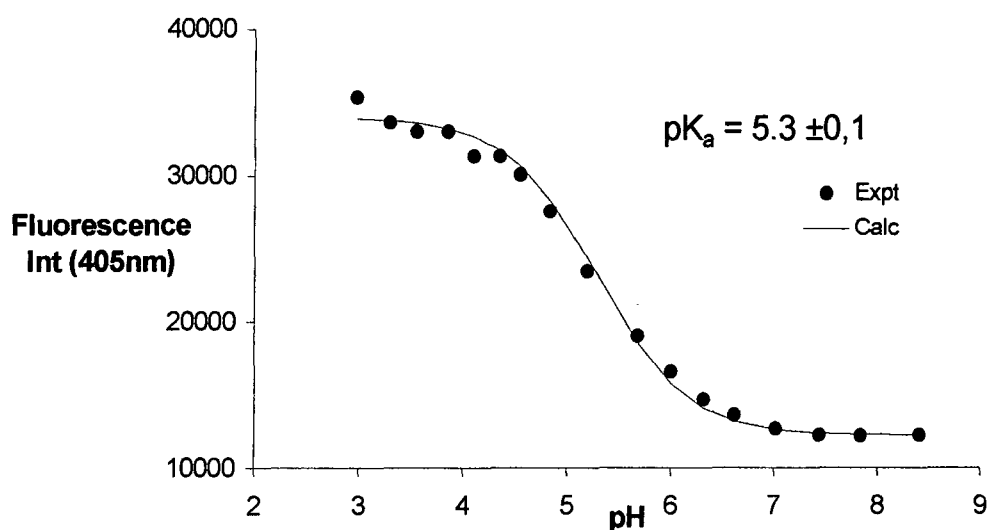
Scheme 2.13: Europium emission sensitised by phenanthridinyl excitation as a function of pH for **19** (295K, $\lambda_{\text{exc}} = 304 \text{ nm}$)

The europium emission spectra showed fairly precisely the different absorption bands corresponding to each transition from the 5D_0 level to the ground state 7F_n manifold. It was observed that no changes occurred in the form of these bands, consistent with the absence of any change in the Eu coordination environment following ligand protonation. The variations in intensity observed at different pH values are simply due to the pH dependent perturbation of the phenanthridine chromophore itself. Furthermore, the reversibility of the observed phenomenon also demonstrates the robustness of the system, which tolerates very low (\sim pH 1) as well as quite high pH (\sim pH 12). No alteration of the coordinating or linking functions was observed.

➤ *Terbium(III) tricarboxylate complex 20*

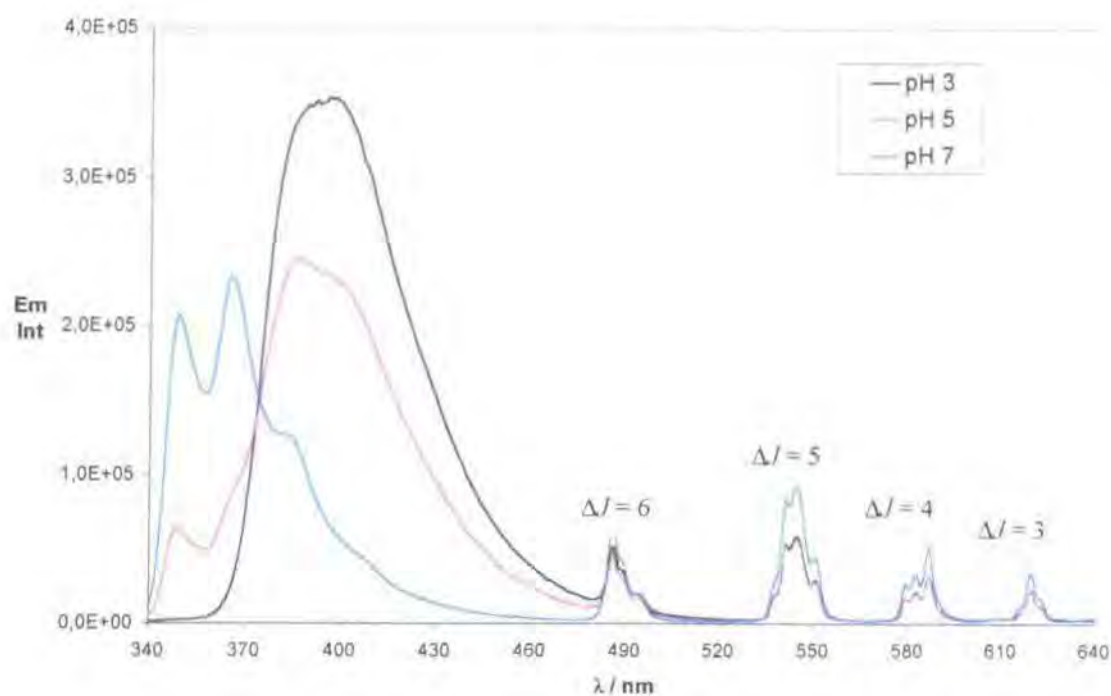
The ground state pK_a was measured to be 5.5 from the pH dependence of the absorption spectrum, in reasonable agreement with the value of 5.4 obtained for the analogous europium complex.

The emission based on the phenanthridine fluorescence was monitored to determine the protonation constant for the singlet excited state of the complex. A value of 5.3 was estimated after fitting of the increase in fluorescence intensity ($\lambda_{exc} = 304$ nm, $\lambda_{em} = 405$ nm) following variation of pH (Scheme 2.14).



Scheme 2.14: Variation of phenanthridine fluorescence intensity as a function of pH for **20**, showing the fit to the experimental data points (295K, $I = 0.1$ M NMe_4NO_3 , $\lambda_{exc} = 304$ nm)

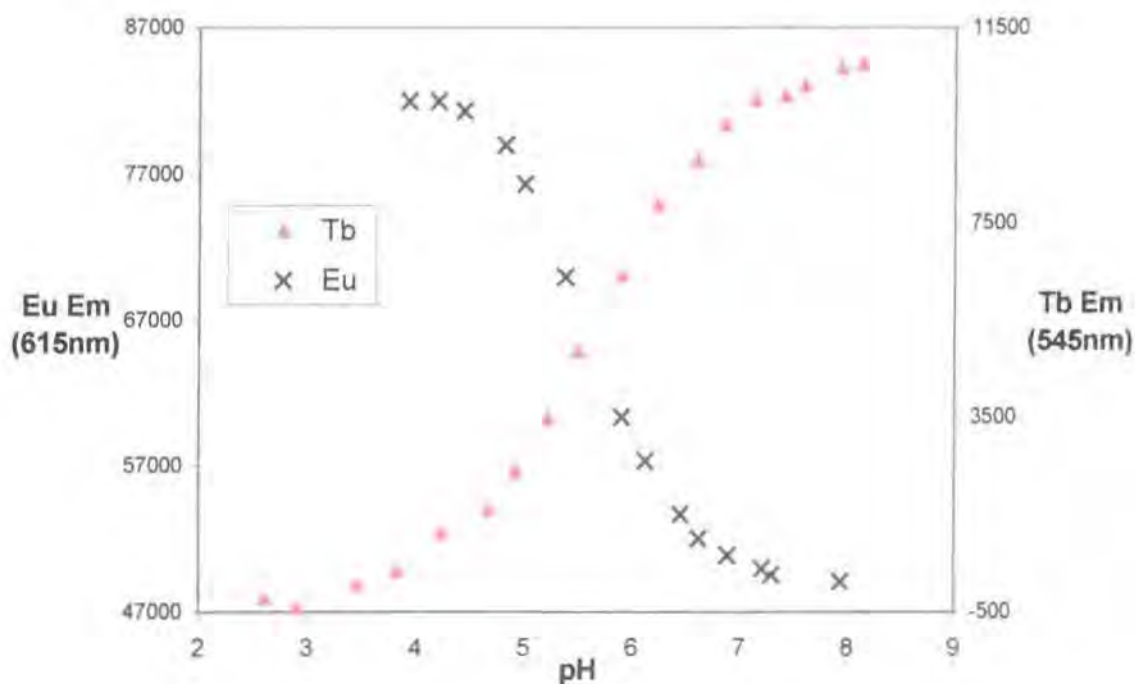
The analysis of the metal centred emission from the terbium complex showed different behaviour as a function of the acidity of the medium. Firstly, the phenanthridine fluorescence ($\lambda_{\text{em}} = 405 \text{ nm}$) decreased with increasing pH, like the europium analogue, from which data a protonation constant of 5.6 was found. Secondly, the terbium emission ($\lambda_{\text{exc}} = 304 \text{ nm}$, $\lambda_{\text{em}} = 545, 590 \text{ or } 620 \text{ nm}$, $\Delta J = 5, 4, 3$) behaved in the opposite direction by increase with alkaline pH. A value of 5.6 was determined by monitoring the 545 nm band associated with the $^5D_4 \rightarrow ^7F_5$ transition ($\Delta J = -1$). Scheme 2.15 illustrates how the ligand fluorescence based emission and the metal based emission vary in opposing senses dependent upon the acidity of the medium.



Scheme 2.15 : Variation of emission as a function of pH for Tb carboxylate complex 20 (295K, I = 0.1 M NMe_4NO_3 , $\lambda_{\text{exc}} = 304 \text{ nm}$)

The reason for this inversion is that the triplet excited state level of the protonated phenanthridine group is also populated by a back energy transfer process from the proximate terbium 5D_4 excited state. This process competitively deactivates the terbium 5D_4 level (20500 cm^{-1}). Under neutral conditions, the unprotonated phenanthridine triplet state is higher in energy, and therefore can populate the Tb excited level without significant back

energy transfer, leading to terbium emission bands. This process is the same as that reported with the original unsubstituted complex **II**.⁴



Scheme 2.16: Complementarity of the two lanthanide complexes **19** (x) and **20** (▲) for pH sensing ($\lambda_{exc} = 304 \text{ nm}$; $\lambda_{em} = 615 \text{ nm}$ for **19**; $\lambda_{em} = 545 \text{ nm}$ for **20**)

The two complexes Eu and Tb complexes exhibit opposite and complementary behaviour when they are submitted to variations in pH (Scheme 2.16). The excited state pK_a was estimated to be $5.6 (\pm 0.1)$ in each case.

➤ Europium(III) triphosphinate complexes

The pK_a of the phosphinate complexes was also investigated. Both methyl and benzyl phosphinate europium complexes **24** and **25** showed the same behaviour, suggesting that the nature of the phosphorus ligands does not affect the behaviour of the switching process. The singlet state pK_a value for these complexes was found to be 5.35 in each case. The pK_a values determined by monitoring changes in the europium emission intensity ($\lambda_{em} = 590 \text{ nm}$, $\Delta I = 1$) gave the same value of $5.4 (\pm 0.1)$.

2-3.2.2: Lifetimes and quantum yields

The lifetimes in H₂O and D₂O for the decay of the Eu excited state in unsubstituted phenanthridinyl monoamide triphosphinate complex **I** had revealed the presence of one water molecule bound to the lanthanide.⁹ For the complexes prepared in this study the coordination number at the lanthanide ion was not expected to change, given that the coordinating pendent arms are the same. Lifetimes in H₂O and D₂O have been measured for complex, **19**, aiming to identify the coordination number (Table 2.2).

	k _{H₂O}	k _{D₂O}
Neutral	1.48	0.41
Acidic	1.49	0.40

Table 2.2: Radiative rate constants (ms⁻¹) for complex **19** (295K)

An estimation of the hydration state, q, for **19**, using Eq 2.1, gave a value of 0.92, meaning that one water molecule binds the europium whatever the pH of the solution.

$$q^{\text{Eu}} = 1.2 [(k_{\text{H}_2\text{O}} - k_{\text{D}_2\text{O}}) - 0.25 - 0.075x] \quad (\text{Eq 2.1})$$

where x is the number of proximate NH oscillators which when equidistant are assumed to quench in an equivalent manner.

To quantify the efficiency of sensitised emission, the overall quantum yields for sensitised emission in **19** were measured in H₂O and D₂O under neutral and acidic conditions (Table 2.3).

	Φ _{H₂O}	Φ _{D₂O}
Neutral (pH 7)	0.014	0.055
Acidic (pH 2)	0.062	0.25

Table 2.3: Quantum yields (±20%) for the europium complex **19** (295K)

The values obtained in D₂O were consistently about three times larger than in H₂O, reflecting the deactivating effect of vibrational quenching by OH oscillators. This is also revealed by the higher rate constant for luminescence decay in H₂O.

As explained in part 2-1, the protonation of the phenanthridine nitrogen inhibits the quenching of the singlet excited state, leading to higher ϕ_{em} value in acidic media. In both H₂O and D₂O the quantum yields for complex **19** were four times larger in acidic media compared to the values obtained under neutral conditions. This reflects the ease of energy transfer from the excited triplet state of the ligand, when the sensitizer is protonated. Because the protonation lowers the triplet energy level by 600 cm⁻¹, the energy transfer is favoured, and the emission from the europium becomes more efficient.

It was also of interest to compare the efficacy of sensitised emission in the case where the phenanthridine is substituted by a butyl group, e.g. complex **19**, with the original unsubstituted complex **I**. As was described earlier, the butyl substitution allowed the increase of the acidity constant of the complex; the emission quantum yields could also be affected by such a chemical modification. The values of the quantum yields in H₂O are listed in Table 2.4.

	ϕ_{em}		ϕ_{em}
Eu- I	0.011	Eu- 19	0.014
[Eu- I]H ⁺	0.03	[Eu- 19]H ⁺	0.062

Table 2.4: Quantum yields in H₂O for complexes **I** and **19**

Very similar trends are noticed for both complexes. The efficiency of sensitised luminescence in the neutral complexes did not show any differences in terms of yield. The values are very similar. When the quantum yields in acidic media are compared, complex **19** seems to be more efficient by a factor of 2 over its unsubstituted analogue **I** (measured under the same conditions). This gain in efficiency is likely to be due to the decrease in the triplet state energy of the phenanthridinium antenna caused by the alkyl group substitution. As listed in table 2.1 (page 43), the triplet state energies, respectively under neutral and acidic

conditions, are 400 cm^{-1} and 300 cm^{-1} higher in the case of the phenanthridine compared to its substituted analogue.

As a reminder the energy of the triplet state of phenanthridine was found to be 22000 and $(21300)^*$ cm^{-1} and for 6-butylphenanthridine, 21600 and $(21000)^*$ cm^{-1} . Because the butyl group lowered the energy levels of the ligand, the quantum yields are likely to be increased by a more efficient energy transfer step, which has led to a more efficient overall lanthanide luminescence. In support of this argument, a recent study by Latva *et al.*¹⁰ examining over 40 europium complexes revealed that the highest quantum yields were obtained for complexes where the triplet state of the sensitiser lies between 21000 cm^{-1} and 22000 cm^{-1} .

The distance between the sensitiser and lanthanide ion is an important feature involved in the efficiency of the energy transfer process in the case of a Förster mechanism. This is reflected to the efficiency of the quantum yields as defined by Eq. 2.2.

$$\Phi_{\text{em}} = (\Phi_{\text{T}} \eta_{\text{ET}})(k_0 \tau_{\text{obs}}) \quad (\text{Eq. 2.2})$$

where Φ_{T} is the quantum yield for the triplet formation
 η_{ET} is the efficiency of the energy transfer process
 k_0 is the natural radiative rate constant for the ${}^5\text{D}_0$ state of the Eu complex
 τ_{obs} is the observed lifetime for europium decay

In the case of the Förster mechanism, the efficiency of the energy transfer process is proportional to the inverse of the distance to the sixth power, given by Eq. 2.3.

$$\eta_{\text{ET}} = k_{\text{ET}} / (k_{\text{ET}} + k_{\text{r}} + k_{\text{nr}}) = \frac{1}{[1 + (r/r_0)^6]} \quad (\text{Eq. 2.3})$$

where k_{ET} is the rate of energy transfer
 k_{r} is the radiative decay of the donor
 k_{nr} is the non-radiative decay of the donor
 r is the separation between the donor and the acceptor
 r_0 is the distance at which the energy transfer is 50% efficient

In these two complexes the distance between the phenanthridinyl donor and the europium ion is believed to remain unchanged. Consequently the difference between these

two systems only involves the photophysical aspects of the chromophore, i.e. the energy levels of its excited states.

A recent study carried out at Durham,¹¹ investigated the efficiency of the energy transfer as a function of the distance donor-acceptor in phenanthridinyl europium complexes, and revealed that efficient overall quantum yields can be found even if the phenanthridinyl chromophore is more than 5 Å distant from the europium centre.

Summary

To conclude, the substitution of a butyl group at the 6-position of the phenanthridine allowed the pK_a of the probe to be increased to 5.6, being consequently more suitable for pH sensing closer to the physiological range. The photophysical properties of the europium and terbium complexes were not significantly affected by this substitution. Furthermore in terms of efficiency of the sensitised emission, this substitution has a positive effect, allowing the complex to exhibit a stronger luminescence.

Recent studiesⁱ have been carried out immobilising such responsive complexes in a sol-gel matrix and studying their behaviour as a function of pH. The pK_a values obtained were all about 1.2 to 1.5 units higher than those found in homogenous solutions. They thus fall in the range 5.4 (unsubstituted) to 7.2 (6-butylphenanthridinium complexes), well suited to the analysis of biological samples. The higher pK_a may be simply be related to the enhanced polarity of the sol-gel medium.

* In italic characters are given the values for the protonated species.

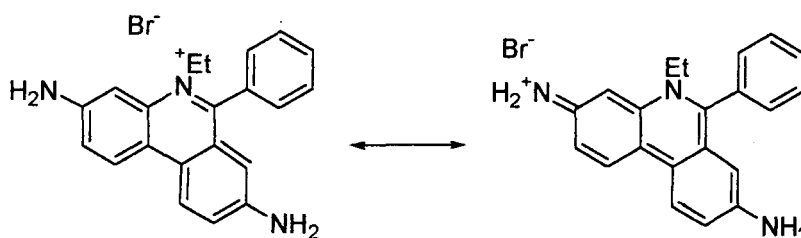
ⁱ This work has been carried out by Stephanie Blair in Durham.

-
- ¹ D. Parker, K. Senanayake, J. A. G. Williams, *Chem. Commun.*, **1997**, 1777-1778.
- ² B. R. T. Keene, P. Tissington, *J. Chem. Soc.*, **1965**, 4426.
- ³ D. Parker, J. A. G. Williams, *Chem. Commun.*, **1998**, 245-246.
- ⁴ D. Parker, K. Senanayake, J. A. G. Williams, *J. Chem. Soc., Perkin Trans. 2*, **1998**, 2129-2140.
- ⁵ a) H. Gilman, J. Eisich, *J. Org. Chem.*, **1963**, 28, 3007.
b) H. Gilman, J. Eisich, *J. Am. Chem. Soc.*, **1955**, 77, 6379.
c) H. Gilman, J. Eisich, *J. Am. Chem. Soc.*, **1957**, 79, 5479-5483.
- ⁶ G. M. Badger, J. H. Seidler, B. Thomson, *J. Chem. Soc.*, **1951**, 3207-3211.
- ⁷ a) C. B. Reese, *J. Chem. Soc.*, **1958**, 173, 895-899.
b) C. B. Reese, *J. Chem. Soc.*, **1958**, 174, 899-901.
- ⁸ T. J. Norman, D. Parker, K. Pulukkody, L. Royle, C. J. Broan, *J. Chem. Soc., Perkin Trans. 2*, **1993**, 605.
- ⁹ a) A. Beeby, I. M. Clarkson, R. S. Dickins, S. Faulkner, D. Parker, L. Royle, A. S. de Sousa, J. A. G. Williams, M. Woods, *J. Chem. Soc., Perkin Trans. 2*, **1999**, 493-503.
b) D. Parker, J. A. G. Williams, *J. Chem. Soc., Dalton Trans.*, **1996**, 3613.
- ¹⁰ M. Latva, H. Takalo, V.-M. Mukkala, C. Matachescu, J. C. Rodriguez-Ubis, J. Kankare, *J. Lumin.*, **1997**, 75, 149-169.
- ¹¹ I. M. Clarkson, A. Beeby, J. I. Bruce, L. J. Govenlock, M. P. Lowe, C. E. Mathieu, D. Parker, K. Senanayake, *New J. Chem.*, **2000**, 24, 377-386.

***2-Phenanthridinyl Based Ligands
for DNA Interaction***

The phenanthridine unit was shown to be an efficient sensitiser for lanthanide ions using the appropriate ligand system. The previous chapter was devoted to the interactions of various analytes, especially protons, with a phenanthridinyl conjugate. Changes in the local environment of the phenanthridine group can also affect the singlet and triplet energy levels of the phenanthridine which are reported by variations in the luminescence intensity, lifetime and quantum yield.

As a matter of fact, the molecular structure of the phenanthridine ring system is the same as that of ethidium bromide, which suggests that it could be incorporated in a lanthanide complex system with the aim of interacting with the DNA helix. Since 1970, ethidium bromide has been known to be a very efficient DNA intercalator, endowed with very interesting fluorescence properties toward intercalation between nucleobases.¹ Conjugation involving the two amino groups in position 3 and 8 of the aromatic ring defines its photophysical properties (Scheme 3.1). Because of this conjugated and relatively poor electron system, ethidium bromide is able to slide between the base pairs of the DNA helix and to form a strong complex.²



Scheme 3.1: Ethidium bromide

Upon intercalation, the electron transfer from the nucleobases to the electron deficient ethidium bromide gives rise to a marked hypochromism and a red shift in its absorption spectrum. The enhanced fluorescence from ethidium bromide, which has been monitored to evaluate the affinity of the binding,³ occurs as a result of reduced hydrogen-bonded solvent quenching interactions in the excited singlet state.

A chiral phenanthridinium lanthanide complex presents not only the interesting intercalative properties of a conjugated extended ring, but also possesses the appropriate energy levels to sensitise effectively europium, terbium or ytterbium, complexed in a chiral

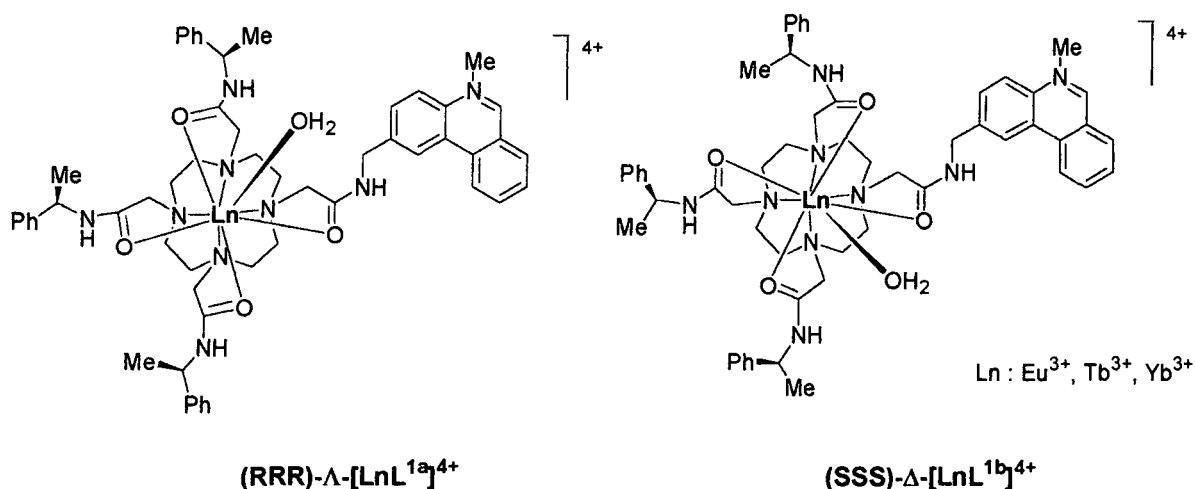
cyclen derivative. Monitoring the interactions of such a series of complexes with various oligonucleotides allows DNA structure to be probed.

3-1 Bases

3-1.1: Description of the chiral complexes

The introduction of a stereogenic centre δ to the ring N imparts considerable rigidity to the complex and leads to formation of an enantiopure complex. In the Eu, Tb and Yb complexes, the configuration of the chiral centre in the amide moiety determined both the macrocyclic ring configuration (δ or λ in each 5-ring chelate) and the helicity of the layout of the *N*-substituents (Δ vs. Λ).

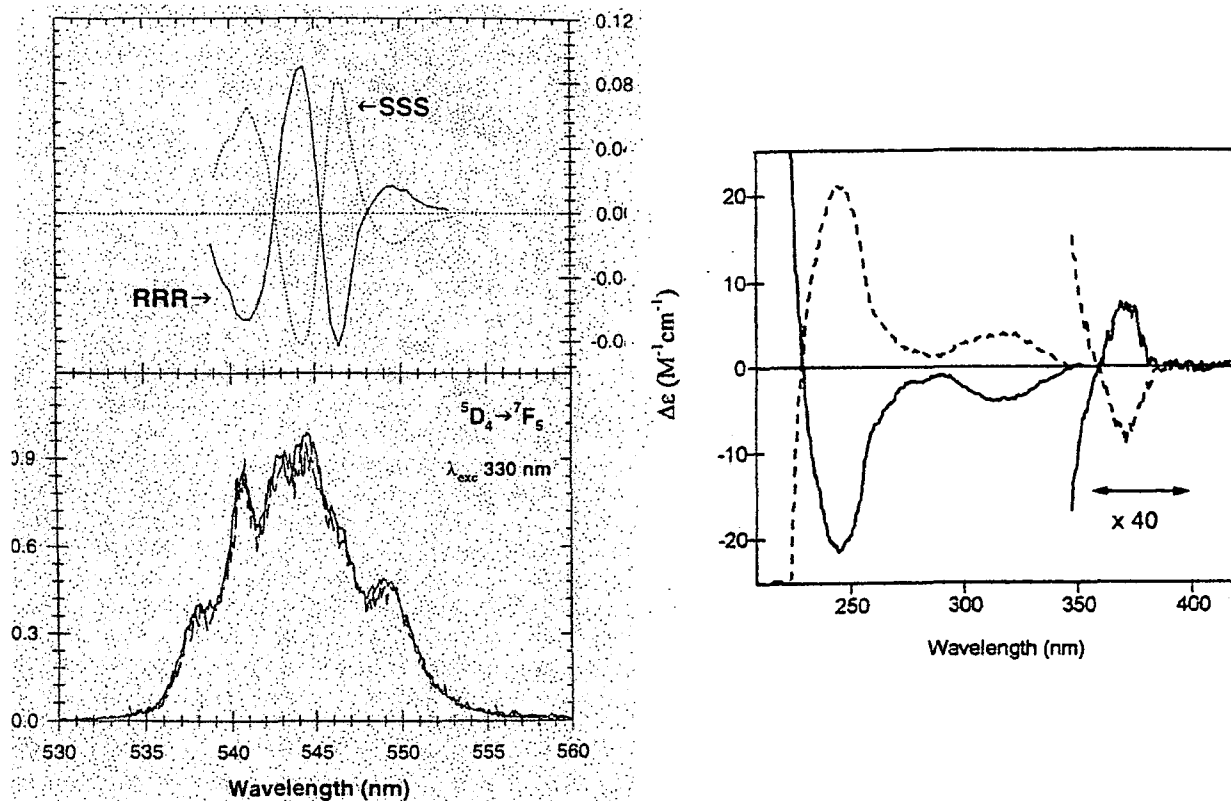
The functionalisation of the cyclen with three chiral amide arms defined two cationic enantiomeric lanthanide complexes. These tetra-amide complexes can also adopt either a left-handed Λ or a right-handed Δ configuration which is determined by the chirality of the three amide *N*-substituents of the cyclen (Scheme 3.2). The (*R*) and (*S*) amide arms give rise respectively to the Λ and the Δ configuration. The Δ and Λ lanthanide complexes give rise to equal and opposite CPL spectra.



Scheme 3.2: Enantiomeric 2-Phenanthridinium complexes

An example is given by the behaviour of the terbium complex: CPL spectra were recorded in methanol (298K) and the observed dissymmetry factors, g_{em} , were +0.17 ($\lambda_{em} = 545$ nm) for (RRR)-[TbL^{1a}]⁴⁺ and -0.17 for (SSS)-[TbL^{1b}]⁴⁺ (Scheme 3.3). Analysis of the ¹H

NMR spectra for (RRR)-[EuL^{1a}]⁴⁺ revealed only one set of shifted ring protons (H_{ax}) at +29.8, +29.0, +28.4 (1:2:1) ppm. Such behaviour is consistent with the preferred adoption in solution of a single stereoisomeric species and by analogy with the behaviour defined for the related (RRRR) tetra-amide lanthanide complexes,⁴ the (RRR)-[LnL^{1a}]⁴⁺ complexes exist as the (λλλλ)-Δ stereoisomer in solution.



Scheme 3.3: CPL (left) and CD spectra (right) of Δ and Λ -[TbL¹]⁴⁺ complexes

The phenanthridine moiety linked through the 2-position to the chiral macrocycle, allows the extended aromatic surface to slide deeply into the DNA helix. In addition to the triply charged lanthanide centre, the methylation of the phenanthridine produces an extra positive charge on the intercalative moiety, enhancing electrostatic attraction. The independent motion of the phenanthridinyl amide arm allows the complex to adopt a suitable geometry during complexation to the double helix, without profoundly affecting the macrocyclic complex.

The presence of the phenyl substituent in the 6-position of the phenanthridine chromophore is not required for increased affinity during binding to oligonucleotides or DNA. Comparative titrations were carried out with *N*-ethylphenanthridinium iodide and *N*-ethyl-6-

phenylphenanthridinium iodide binding to $[(CG)_6]_2$. The absorbance spectra revealed no sign of enhanced conjugation between the phenyl substituent and the actual phenanthridine ring. Furthermore, the affinity of the *N*-ethyl-6-phenylphenanthridinium iodide for the oligonucleotide was lower than that observed for the non-substituted compound. Thus, it was concluded that the phenyl ring has no significant influence on the intercalative binding.

3-1.2: Interaction with oligonucleotides

The interaction of such a chiral complex with the DNA helix is expected to be favoured for one enantiomer over the other. The DNA double strand being a chiral molecule, the association of the two enantiomers will give rise to a stronger diastereomeric complex, related to the principle of *diastereomeric resolution*. The A- and B-forms of DNA are right-handed helices, while the Z form is left-handed. The oligonucleotides chosen for studying these interactions are twelve deoxyribonucleotide units long, e.g. a succession of 6 pairs Cytosine-Guanine (dC-dG)₆ or 6 pairs Adenine-Thymine (dA-dT)₆. The duplex form is the strongly favoured structure in aqueous solution for these “short” oligonucleotide chains.

The driving force for the interaction of such complexes with DNA is related to their ability to intercalate the DNA *via* the phenanthridinium unit, and the recognition of the path of the helix *via* the chiral macrocycle. The backbone of the DNA is polyanionic due to the phosphate bridges pointing at the surface, which produces an electrostatic attraction for any positively charged species. This last feature is involved in the first step of the associative interaction, i.e. the approach of the complex close to the DNA.

3-1.3: Photophysical aspects of the interaction

Several parameters can be examined to characterise the interaction, and a study of changes to both the ligand and the DNA duplex can give information. Firstly the tertiary structure of the DNA double strand is expected to undergo changes in its length, degree of unwinding, helical twist or in its electronic parameters. Secondly, the ligand, especially when it is a lanthanide complex, is able to signal changes in its proximate environment, through perturbations to the antenna fluorescence or the metal luminescence.

The intercalation of the phenanthridinium moiety between the nucleobases can be signalled by a hypochromism and a red shift in its absorbance spectrum. The red shift is an

essential element to prove the intercalation of the ligand between the bases of the DNA: the excited states of the phenanthridine chromophore are lowered. This stabilisation is due to charge transfer from the nucleobases and this gives rise to an absorption of light at higher wavelengths. The fluorescence from the ligand is expected to be quenched by electron transfer from the nucleobases. This effect is often observed when aromatic fluorophores interact with DNA. Consequently the luminescence from the lanthanide being affected as the photophysical characteristics of the sensitiser change. Such changes are also directly related to the interaction between the sensitiser and the DNA aromatic bases.

As well as these traditional absorption techniques, chiroptical measurements, particularly Circular Dichroism gives information about the behaviour of the DNA during binding, about the helix, and by extension, about how a small molecule can determine such conformational changes.

The use of mass spectroscopy was also investigated to study these interactions, and allowed an evaluation of the stoichiometry of the binding.

3-1.4: McGhee and von Hippel method of binding constant determination

The titration data obtained in these studies were analysed using the McGhee and von Hippel method,⁵ which allows an estimation of the apparent binding constant and the size of the binding site, by relating the spectroscopic data to the concentration of oligonucleotide added. This method of analysis, in contrast to Scatchard method, was the first to account for the fact that a binding site might span more than one lattice point. The equilibrium binding constant establishing the strength of a ligand for a given oligonucleotide is defined as Eq 3.1:

$$K = \frac{L_b}{L_f S_f} \quad (\text{Eq 3.1})$$

where L_b is the concentration of bound ligand
 L_f is the concentration of free ligand
 S_f is the free site concentration

Free ligand + Empty binding site \rightleftharpoons Bound ligand

The total site concentration is determined in the case of the Scatchard method by Eq 3.2,

$$S_{tot} = C_M / n \quad (Eq\ 3.2)$$

where C_M is the concentration of DNA duplex

So the relation expressing K is defined by Eq 3.3 :

$$\frac{r}{L_f} = \frac{K S_f}{C_M} = \frac{K}{n} - rK \quad (Eq\ 3.3)$$

where $r = L_b / C_M$

But this analysis is too simplistic when the macromolecule can be considered as a lattice. The McGhee and von Hippel method takes account for the fact that a binding site may span more than one lattice point. In this method, the expression of K becomes Eq 3.4:

$$\frac{r}{L_f} = K \left(1 - \frac{r}{n}\right) \left[\frac{n-r}{n - (1-n)r} \right]^{1/n-1} \quad (Eq\ 3.4)$$

The starting point for the determination of equilibrium constant from spectroscopic data is usually given by Eq 3.5:

$$L_b = \alpha \rho \quad (Eq\ 3.5)$$

where ρ is the emission intensity of the ligand at a chosen wavelength
 α is a constant over the range of binding ratios being considered

If all of the ligand is bound, L_f is assumed to be zero, so Eq 3.5 becomes Eq 3.6:

$$\rho = \alpha / L_{tot} \quad (Eq\ 3.6)$$

where L_{tot} is the total ligand concentration

The first step of the analysis is the determination of α . Because it is not always possible to get data for either low or high binding ratio limits, the binding constant K from Eq 3.1, can be written as shown in Eq 3.7.

$$K = \frac{\alpha\rho}{(S_{tot} - \alpha\rho)(L_{tot} - \alpha\rho)} \quad (\text{Eq 3.7})$$

Rearranging Eq 3.7 gives Eq 3.8:

$$L_{tot} = \frac{L_{tot}S_{tot}}{\alpha\rho} - S_{tot} + \alpha\rho - K^{-1} \quad (\text{Eq 3.8})$$

So for two different total oligonucleotide concentration, ${}^jS_{tot}$ and ${}^kS_{tot}$, but the same concentration of ligand (complex), Eq 3.8 becomes Eq 3.9:

$$\frac{{}^kS_{tot} - {}^jS_{tot}}{\rho^k - \rho^j} = \frac{L_{tot}}{\alpha} \left(\frac{{}^kS_{tot} / \rho^k - {}^jS_{tot} / \rho^j}{\rho^k - \rho^j} \right) + \alpha \quad (\text{Eq 3.9})$$

Or equivalently

$$\frac{{}^kC_M - {}^jC_M}{\rho^k - \rho^j} = \frac{L_{tot}}{\alpha} \left(\frac{{}^kC_M / \rho^k - {}^jC_M / \rho^j}{\rho^k - \rho^j} \right) + \alpha \quad (\text{Eq 3.8})$$

So in the plot, the ideal straight line has a slope of L_{tot} / α and an intercept of $n\alpha$.

$$y = \frac{{}^kC_M - {}^jC_M}{\rho^k - \rho^j} \quad \text{versus} \quad x = \frac{{}^kC_M / \rho^k - {}^jC_M / \rho^j}{\rho^k - \rho^j}$$

The determination of α allows us to relate, for each point, the concentration of bound ligand, L_b , and then the concentration of free ligand, L_f .

The second step in the analysis following Eq 3.6, is to plot r / L_f versus r allowing the determination of the binding constant K , as the intercept on the y axis, and n , the number of bound ligand per duplex, as the intercept on the x axis.

N.B: An example illustrating such a method is given in *Appendix*.

3-2 Interaction of 2-phenanthridinium Δ and Λ complexes with oligonucleotides

3-2.1: Affinities towards [(CG)₆]₂ and [(AT)₆]₂

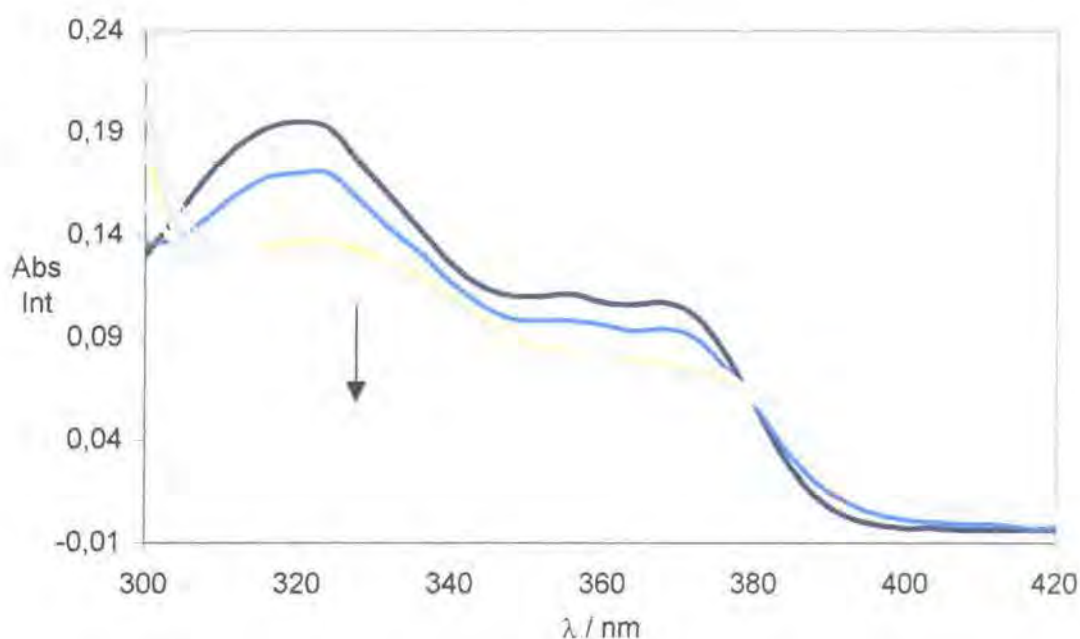
The affinity of the europium and ytterbium complexes for a given oligonucleotide, [(CG)₆]₂ and [(AT)₆]₂ was determined by monitoring changes in the absorbance and fluorescence spectra of the ligand upon addition of oligonucleotide. The advantages of using spectroscopic data for determining the binding affinity K include the short time scale of the experiment, meaning that the system does not have to be stable for any great length of time, and our ability to probe a signal due only to the bound ligand. The enantiopure complex of europium or ytterbium was solubilized in aqueous solution buffered at pH 7.4 (10 mM HEPES, 10 mM NaCl) at a concentration of 30 μ M and the HPLC-purified commercial oligonucleotide solution was used without any further operation.

3-2.1.1: Binding of Europium complexes Δ and Λ [EuL¹]⁴⁺

3-2.1.1.1: Absorbance spectroscopy

The affinity of the Δ and Λ [LnL¹]⁴⁺ complexes for [(CG)₆]₂ and [(AT)₆]₂ was investigated by absorbance and luminescence spectroscopies.

With the europium (SSS)- Δ and (RRR)- Λ complexes, two isosbestic points at 304 and 378 nm were observed in the absorbance spectra of the phenanthridinium moiety upon addition of oligonucleotide [(CG)₆]₂ and [(AT)₆]₂ (Scheme 3.4). The same trend was observed with Calf Thymus DNA, which is composed by 42% of CG base pairs.

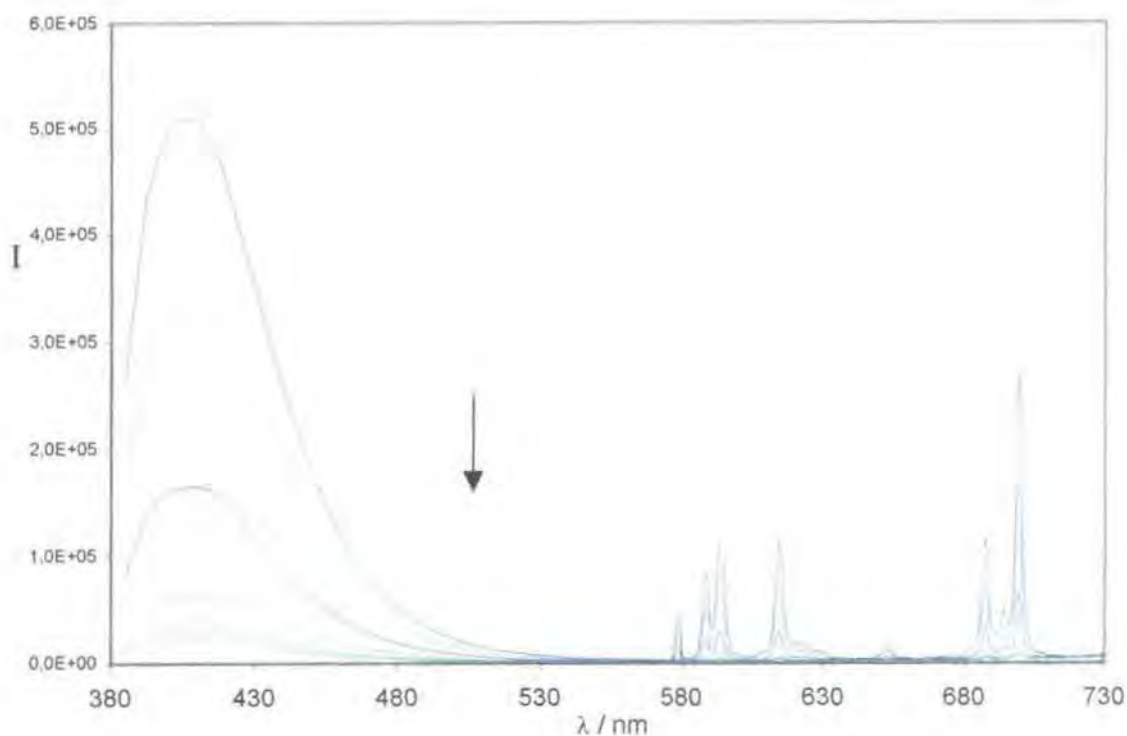


Scheme 3.4 : Absorbance spectra of Δ -[EuL^{Ia}]⁺ complex following addition of [(CG)₆]₂ (295K, pH 7.4, NaCl 10 mM, HEPES 10 mM)

The characteristic features of an intercalative binding mode, i.e. a pronounced hypochromism, a red shift and a long wavelength tail were noticed in each case. The hypochromism at 320 nm was measured and was more intense by a factor of two for both Δ and Λ complexes with [(CG)₆]₂ compared to [(AT)₆]₂. The spectra at saturation of oligonucleotide showed a shift to longer wavelengths of 10 nm, independent of the oligonucleotide used. The size of the red shift did not vary with the configuration of the complex remaining the same in each case within experimental error.

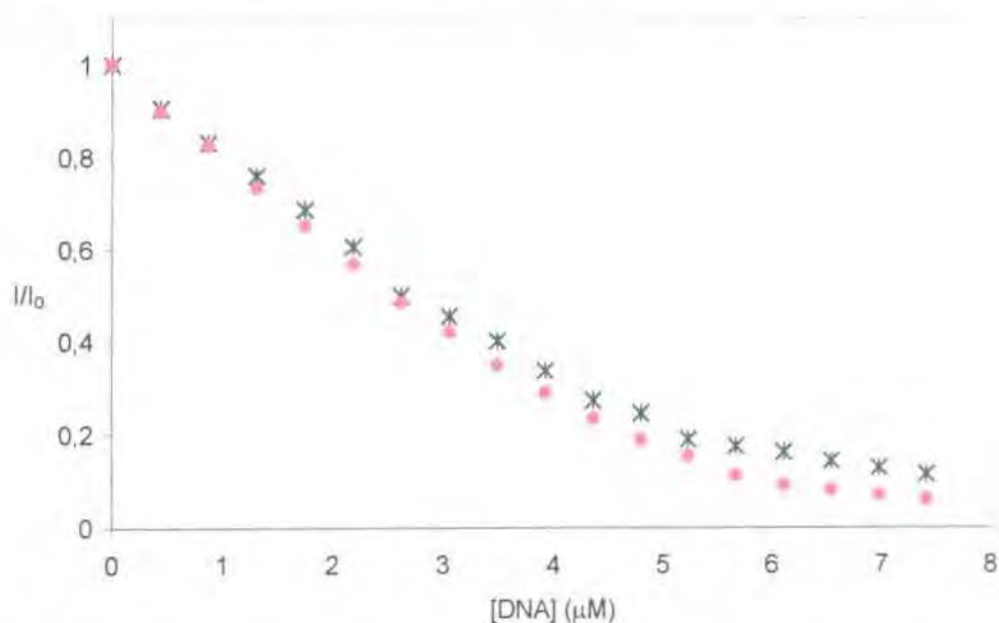
3-2.1.1.2: Luminescence spectroscopy

The fluorescence of the *N*-alkyl phenanthridinium moiety ($\lambda_{\text{exc}} = 378 \text{ nm}$, $\lambda_{\text{em}} = 415 \text{ nm}$) was monitored as a function of added oligonucleotide, and the observed variations allowed the affinity of the binding to be quantified by analysis with the McGhee and von Hippel method.⁵ The quenching of the phenanthridinium fluorescence ($\lambda_{\text{em}} = 415 \text{ nm}$) by the charge transfer between the phenanthridinium and the DNA bases was also followed by the decrease of the long-lived europium luminescence, following addition of the oligonucleotide (Scheme 3.5).



Scheme 3.5: Decay of the luminescence of $A-[EuL^{Ia}]^{d+}$ following addition of $[(CG)_6]_2$ ($295K$, $\lambda_{exc} = 378$ nm, pH 7.4, 10 mM NaCl, 10 mM HEPES)

The changes in Eu luminescence were monitored with parallel results to those observed for the fluorescence data analysis as shown in Scheme 3.6.

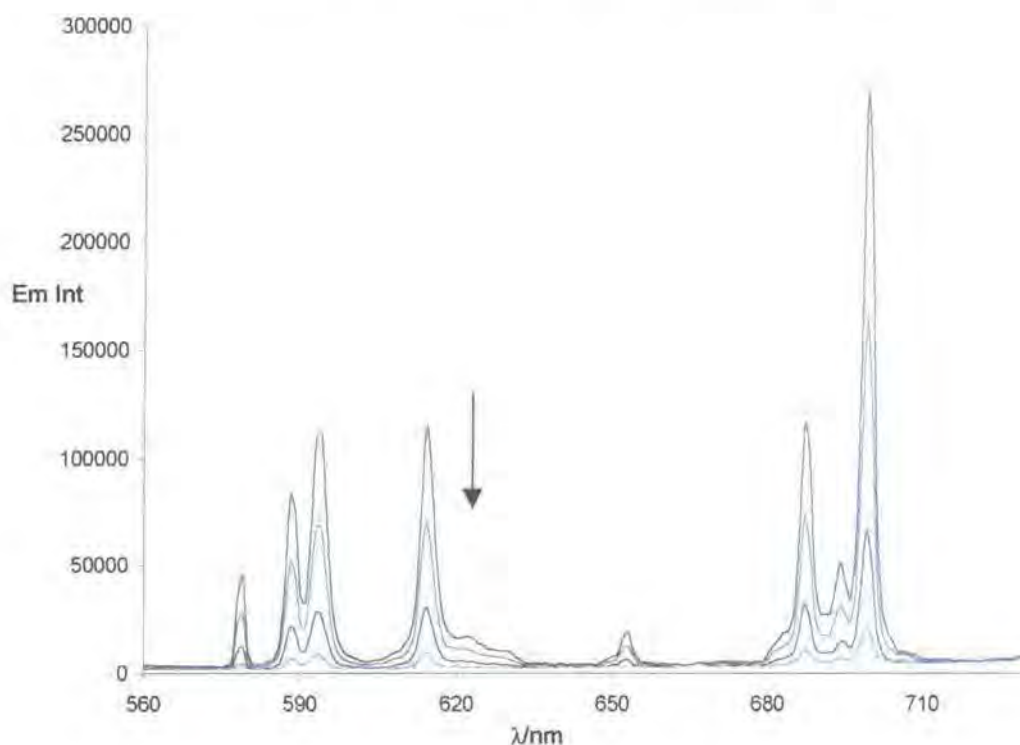


Scheme 3.6: Relative decay of phenanthridine fluorescence (●) at 410 nm and europium emission (x) at 614 nm as a function of the concentration of DNA added ($\lambda_{exc} = 378$ nm.)

The variation in intensity was slightly greater for the fluorescence ($\lambda_{em} = 410$ nm) than for the europium emission ($\lambda_{em} = 612$ nm, i.e. $\Delta J = 2$), so the former data set was used for the semi-quantitative analysis. Furthermore it seems more appropriate to monitor directly the changes undergone by the phenanthridinium fluorophore.

The general form and relative intensity of the europium luminescence spectra remained constant throughout the titration; only a decrease in total intensity was observed upon addition of oligonucleotide. The europium transitions sensitive to the local environment (i.e. transitions $\Delta J = 2$, $\Delta J = 4$) remained unchanged through the titration, indicating the coordination environment around the lanthanide was not distorted upon binding (Scheme 3.7).

No significant change in the lifetime of the europium emission was observed from its value of 0.55 ms in water in the absence of DNA, ruling out any direct quenching of the metal excited state by photoinduced electron transfer from the DNA bases.

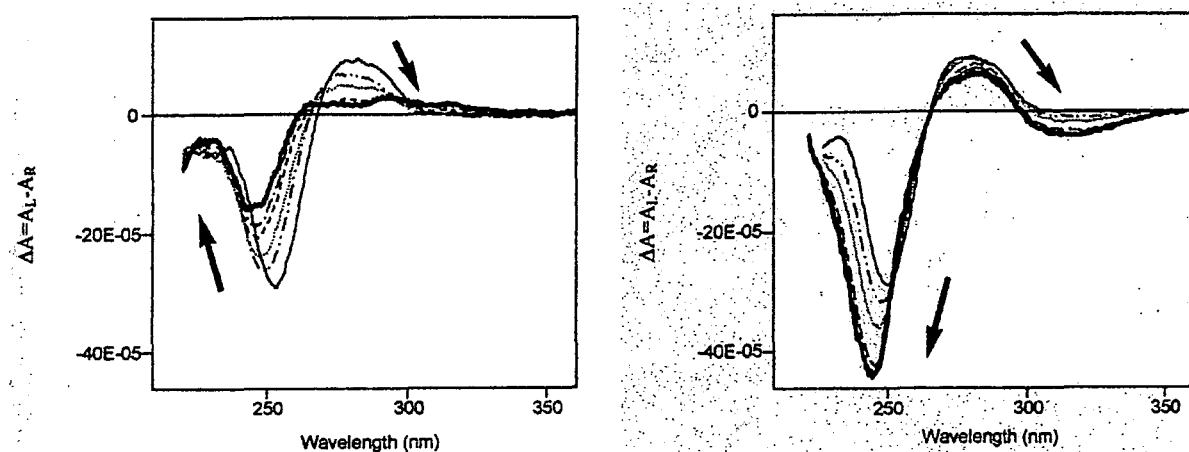


Scheme 3.7: Quenching of Eu emission for $A-[EuL^{1a}]^4$ following incremental addition of $[(CG)_6]_2$ (295K, $\lambda_{exc} = 378$ nm)

The observed spectroscopic changes suggested that binding involved intercalation of the phenanthridinium chromophore between the base pairs of the oligonucleotide.

3-2.1.1.3: Circular dichroism spectroscopy

To define whether the chirality of the complexes contribute to selectivity in binding to DNA, the interaction of these complexes with the oligonucleotides was also investigated by circular dichroism spectroscopy. This time the titrations were carried out differently. The effect of the binding of the complexes on the DNA structure was monitored by measuring the CD of the oligonucleotide as a function of added ligand (or complex). As the ligand was chiral as well, it gives rise to CD bands in the same range of the DNA absorption. Consequently there was a need to subtract the CD spectra of the ligand or complex from the spectra of the perturbed DNA. The resulting difference spectra therefore allowed observation of the 'DNA-bound complex' only.



Scheme 3.8 : Difference CD spectra of $[(CG)_6]_2$ in the presence of increasing ratios of Λ - $[EuL^{1a}]^{4+}$ (left) and of Δ - $[EuL^{1b}]^{4+}$ (right) (295K)

NB : The thin plain line is the spectrum of the DNA alone.

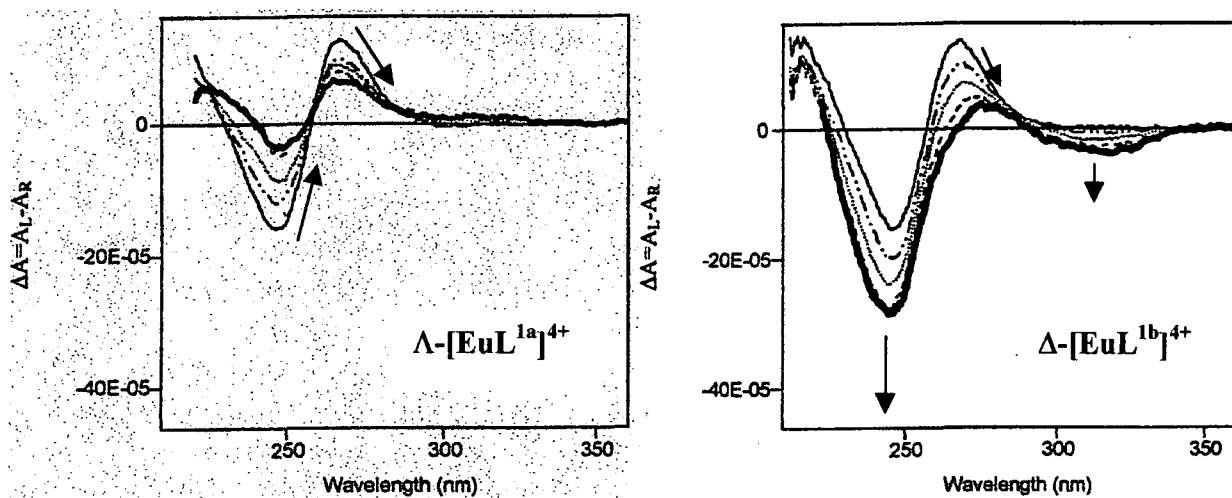
In the near UV region, the characteristic CD spectrum of the oligonucleotide $[(CG)_6]_2$ and of B-form of poly(dG-dC) exhibits a strong negative band at 250 nm and a positive band at 275 nm (thin plain line in Scheme 3.8).⁶ Upon addition of Λ - $[EuL^{1a}]^{4+}$ complex both bands decreased in intensity, and a shift of a few nm to lower wavelength was noticed for the 250 nm band. The positive band almost disappeared with the saturation of the oligonucleotide by the complex.

For the Δ - $[EuL^{1b}]^{4+}$ complex, addition to $d(CG)_6$ gave rise to an increase in intensity of the negative band, for which the maximum shifted to lower wavelength by 6 nm. The

positive band at 275 nm decreased slightly upon the addition of complex. At 320 nm a new negative band appeared and reached a saturation point at a ratio of three complexes per duplex.

With a different type of oligonucleotide $[(AT)_6]_2$ the CD titrations depicted a similar kind of event (Scheme 3.9). With the complex, both bands at 250 and 270 nm characteristic of d(A)-d(T) decreased upon the addition of complex. At 250 nm the intensity of the negative band became three times smaller while at 270 nm the positive band decreased by 50 %.

With the Δ -[EuL^{1b}]⁴⁺ enantiomer, the addition of complex to $[(AT)_6]_2$ induced an increase of 40 % of the 250 nm negative band while at 270 nm the band decreased and shifted by 5 nm to the red.

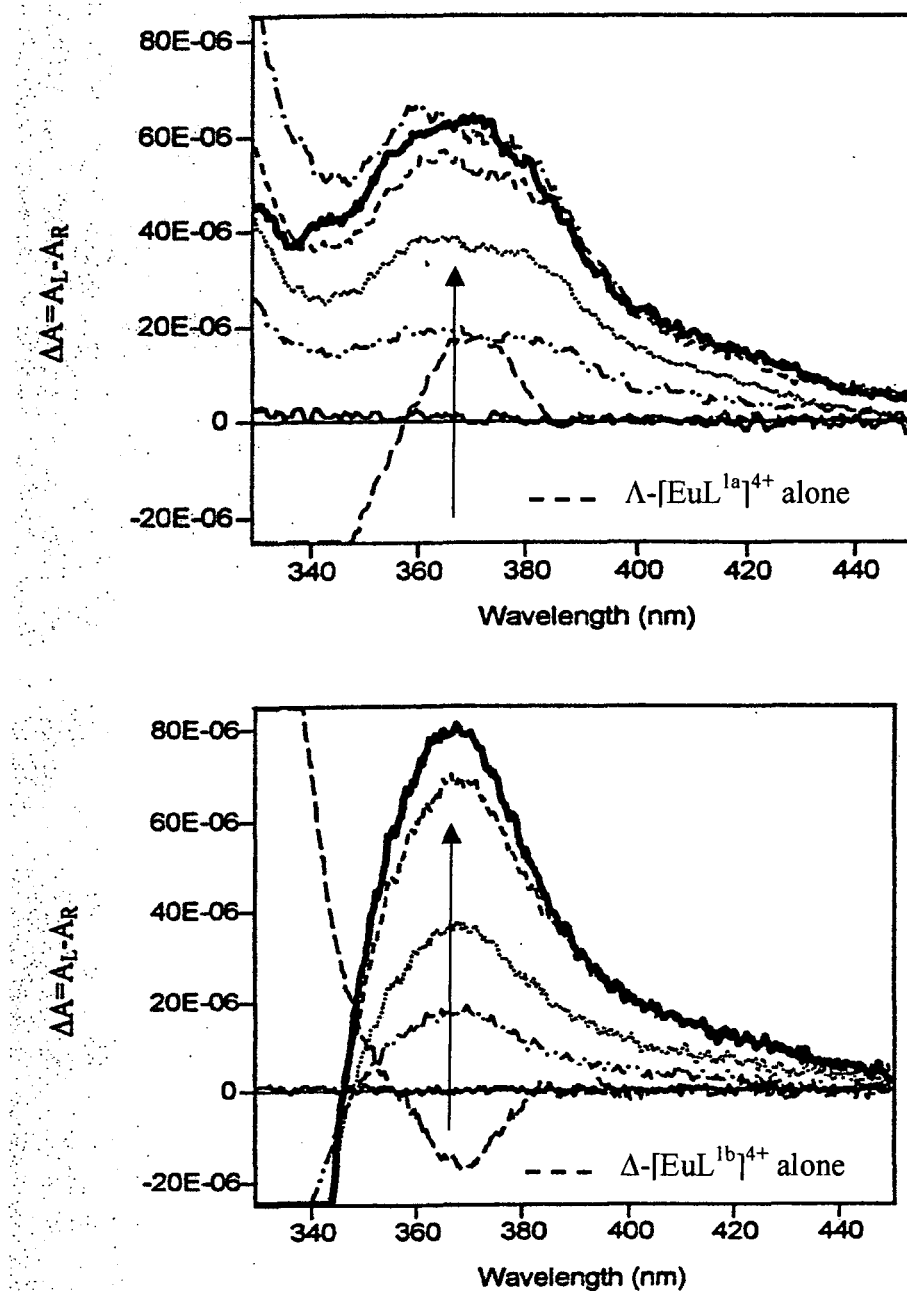


Scheme 3.9: Difference CD spectra for $[(AT)_6]_2$ upon the addition of the Λ (left) and Δ (right) Eu complexes (295K, pH 7.4, 10 mM NaCl, 10 mM HEPES).

In the UV region, the CD spectra of $[(CG)_6]_2$ and $[(AT)_6]_2$ showed the characteristic features of B-DNA, and this overall form persisted even after addition of a considerable amount of complex, ruling out the B \rightarrow Z transition which can occur in the presence of a highly charged metal complex.⁷

In the visible region, the CD signal arises exclusively from the phenanthridinium chromophore. This titration was processed in the same way as previously: the complex was added to the DNA, and its contribution was subtracted. Firstly, no absorption was observed

as the DNA does not absorb in this region (thin plain line in Scheme 3.10). Upon binding to $[(CG)_6]_2$ and $[(AT)_6]_2$ (i.e. ratio $[(CG)_6]_2/[\text{ligand}]$, [1;0.5]), a positive band increased in intensity at 370 nm which is the characteristic absorption of the phenanthridinium chromophore. This behaviour was observed for both the Δ and Λ complex (Scheme 3.10).



Scheme 3.10: Difference CD spectra of $[(CG)_6]_2$ upon the addition of Λ -[EuL^{1a}]⁴⁺ (above) and Δ -[EuL^{1b}]⁴⁺ (below) (295K, HEPES 10mM, NaCl 10mM, pH 7.4)

This positive 370 nm band, only observed for the bound complex, was of the same form for both oligonucleotides, suggesting that the chirality of the phenanthridinium binding site must be similar for both [(CG)₆]₂ and [(AT)₆]₂, as the sign of the induced CD was independent of the complex handedness.

The stoichiometry of the oligonucleotide-Eu complex binding was further investigated using the method of continuous variation, by plotting the CD intensity at a precise wavelength versus the mole fraction of the complex. Discontinuities at 0.5 and 0.67 were found, consistent with stepwise formation of 1:1 and 1:2 complexes for each oligonucleotide [(CG)₆]₂ and [(AT)₆]₂.

Both Λ-Eu and Δ-Eu complexes displayed the same induced CD bands when they bound to the DNA. Furthermore the spectra seem to show a saturation point at a DNA:ligand ratio of 1:3.

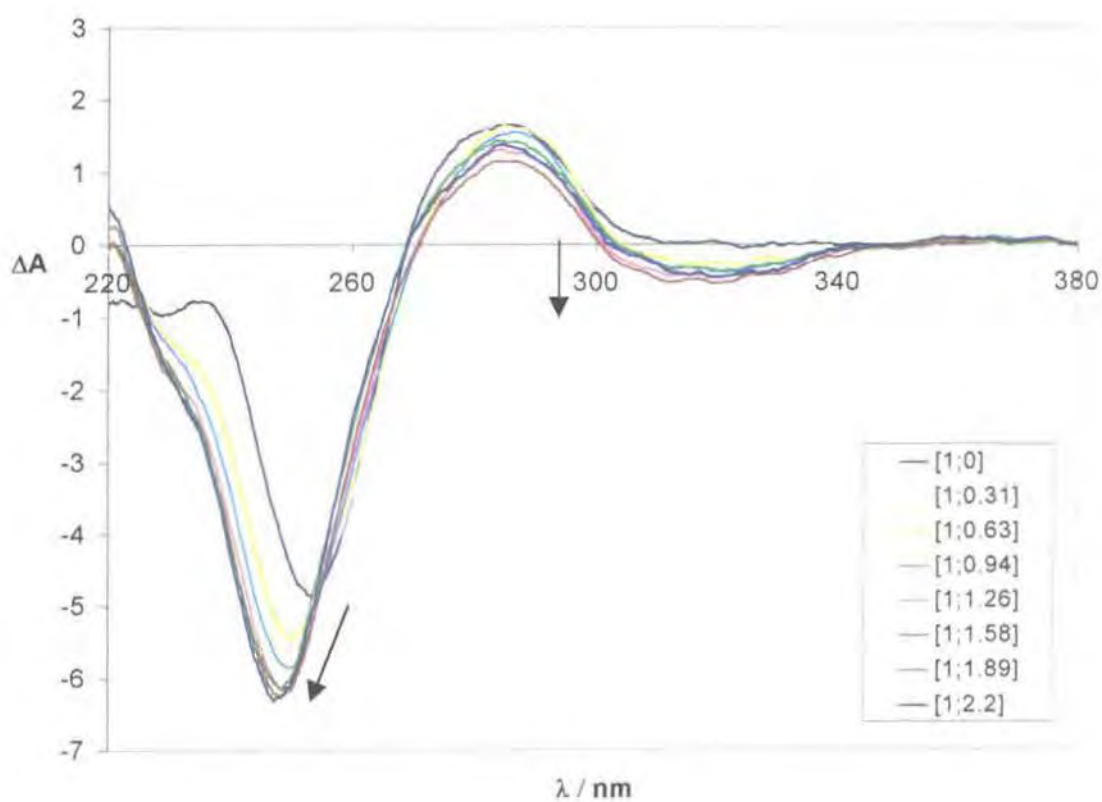
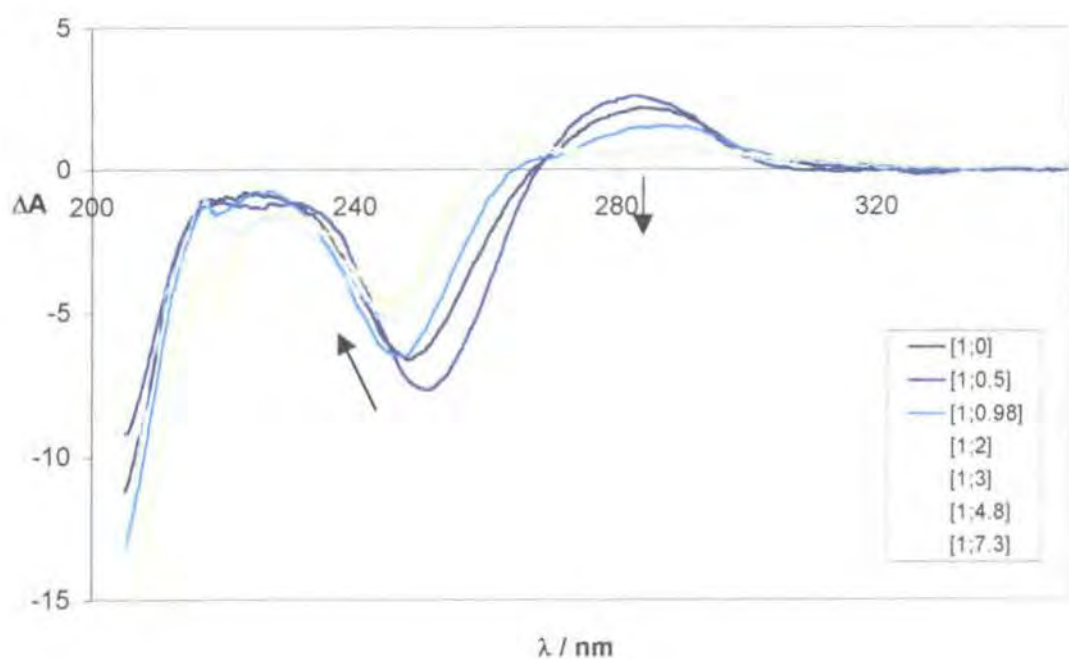
3-2.1.2: Binding of Ytterbium complexes: Δ and Λ [YbL¹]⁴⁺

To evaluate the influence of the lanthanide, the interaction of Δ and Λ ytterbium complexes [YbL¹]⁴⁺ with [(CG)₆]₂ and [(AT)₆]₂ was also investigated by spectroscopic techniques and mass spectrometry.

The absorbance spectra for this series of Λ complexes showed a red shift of 10 nm and the hypochromism at 320 nm was measured to be 32 %, upon the addition of [(CG)₆]₂. With the other oligonucleotide, [(AT)₆]₂, the hypochromism of 24 % was twice that observed with the Λ-Eu analogue although the shift of 8 nm to longer wavelength remained unchanged.

With the Δ-Yb complex, the titration monitored by absorbance revealed with each oligonucleotide a distinctive hyperchromism, but a small shift to the red was still noticed.

The fluorescence intensity from the phenanthridinium moiety ($\lambda_{exc} = 378$ nm, $\lambda_{em} = 415$ nm) decreased upon the addition of DNA. With this series of complexes, it was not possible to monitor the ytterbium emission as the instrument was not sufficiently sensitive beyond 800 nm. However the ytterbium luminescence changes were expected to be the same as those of the phenanthridinium fluorescence.



Scheme 3.11 : Difference CD spectra of $[(CG)_6]_2$ in the presence of increasing ratios of Δ -[YbL^{1a}]⁴⁺ (upper) and of Δ -[YbL^{1b}]⁴⁺ (lower) (295K, pH 7.4, 10 mM NaCl, 10mM HEPES)

The surprising behaviour of Δ -Yb revealed by the absorbance spectral changes suggested that a different type of interaction may be occurring. However the fluorescence decay characteristics and the CD spectral changes exhibited the same features observed in the binding of the Δ -Eu complex. Both titrations of $[(CG)_6]_2$ with Λ -[YbL^{1a}]⁴⁺ and Δ -[YbL^{1b}]⁴⁺ showed the same changes in the induced CD bands for the near UV region (Scheme 3.11). This suggests that the nature of the interaction of the complex with the oligonucleotide duplex is of a similar type for both the europium and the ytterbium complexes.

3-2.1.3: Mass spectrometry

The advantages of studying DNA interactions with short well-defined oligonucleotides relate not only to the ease of handling, but also to the potential application of mass spectrometry. Mild ionization techniques need to be employed to preserve the structure of the relatively weak non-covalent binding interactions.

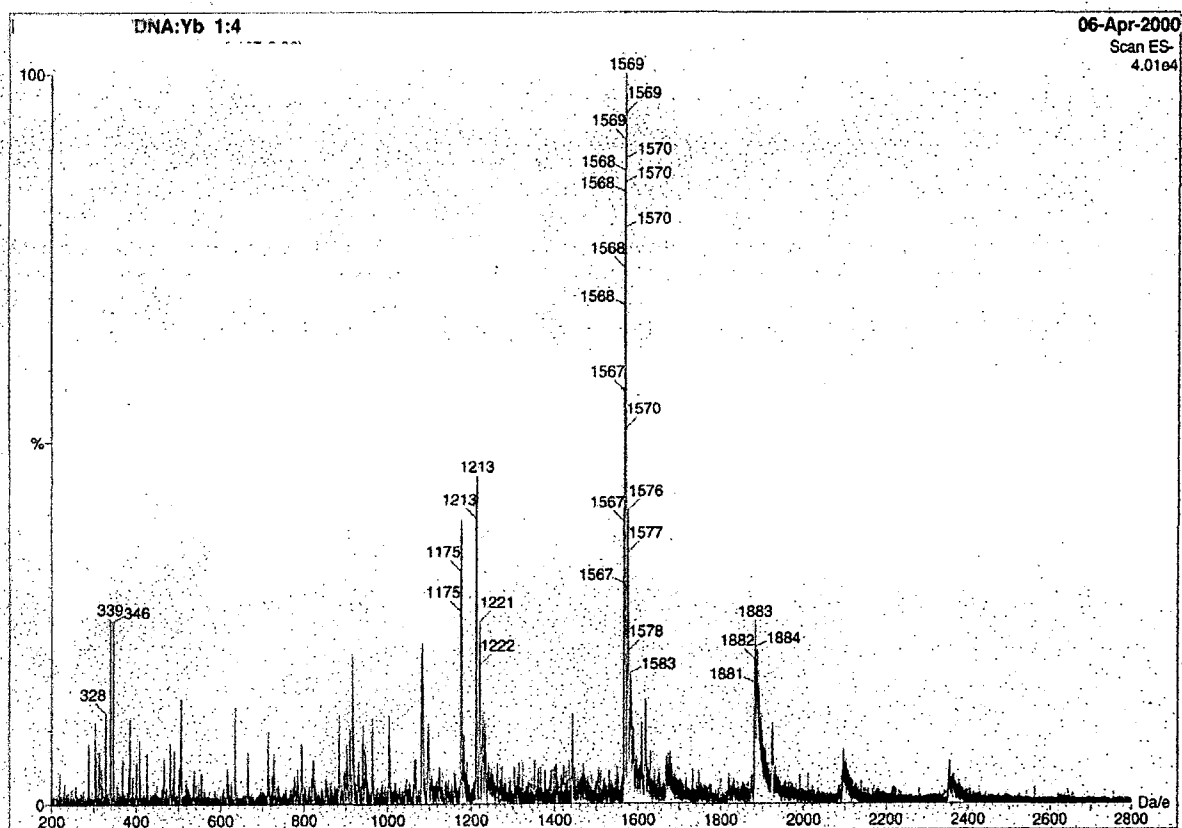
A different type of oligonucleotide was initially used to monitor the DNA interaction of Eu and Yb macrocyclic complexes. The Drew and Dickerson dodecamer $d(CGCGAATTCGCG)_2$ has already shown that it is stable towards electrospray ionization techniques.⁸ However mass spectral analysis of the non-covalent DNA binding of a given ligand must be treated with caution since the gas phase stability may be quite different to the stability in a solvated environment.

After assignment of the molecular peaks corresponding to the Drew and Dickerson oligonucleotide, i.e. monomer (M) and dimer (D), species with charges varying from -1 to -5, the Δ -[EuL^{1b}]⁴⁺ complex (C) was added with a precise ratio of duplex to metal complex. In addition to their masses, the spectral profiles of the DNA-complexes exhibited an irregular shape compared to those derived from the oligonucleotide alone, where the presence of ammonium counter ions was clearly depicted in the fine structure of the spectral envelope. The molecular peaks were separated by 9 m/z units one from each other (e.g. $M(NH_4)/2$). The major set of peaks were observed at 1853 m/z (20%) for $[D + 2C]^{5-}$, and at 2110 m/z (20%) for $[D + C]^{4-}$. There was no sign of peaks showing three complexes bound to the dodecamer.

The interaction of the isomeric Λ -[EuL^{1a}]⁴⁺ complex with this dodecamer also showed the presence of such mass spectral peaks corresponding to two complexes bound.¹

In contrast to the d(CGCGAATTCGCG)₂ dodecamer, for [(CG)₆]₂ a cluster was found with a maximum centred at 1498 m/z units for [D + 3C]⁷⁻ with 75 % relative intensity. Peaks for [D + 2C]⁵⁻ at 1883 m/z (40%), [D + 2C]⁴⁻ at 2345 m/z (10%) and [D + C]⁵⁻ at 1675 m/z (20%) were also observed. This result may be related to the stronger affinity of cationic complexes for the oligonucleotide composed of electron rich nucleobases like cytosine and guanine, compared to Adenine and Thymine.

With the Λ -[YbL^{1a}]⁴⁺ and Δ -[YbL^{1b}]⁴⁺ complexes, evidence for 2 and 3 complexes bound to [(CG)₆]₂ was also obtained. The observed peaks at 1893 (65%) and 2365 (30%) correspond respectively to two complexes bound [D + 2C]⁵⁻ and [D + 2C]⁴⁻. Evidence for the presence of three complexes bound to [(CG)₆]₂ was provided by the observation of peaks at 2110 (65%) [D + 3C]⁵⁻ and at 2643 (25%) [D + 3C]⁴⁻ (Scheme 3.12).



¹ This work involving the use of the Drew and Dickerson oligonucleotide was carried out in collaboration with Martin Smith during his Fourth year undergraduate project.

The chirality of the complex does influence the binding in various ways; it is especially noticeable in the strength of binding of Λ -[EuL^{1a}]⁴⁺ to AT-rich regions; binding of Δ -[EuL^{1b}]⁴⁺ was found to be 5 times weaker. This suggests that the complementary handedness of the complex favours the binding to an AT-rich region. Consequently Λ -[EuL^{1a}]⁴⁺ may present more favourable non-bonding contacts with the B-DNA compared to the Δ isomer. For ytterbium complexes, the Λ isomer was bound more strongly by both [(AT)₆]₂ and [(CG)₆]₂, exhibiting high binding constants in each case. This suggests that the chirality of oligonucleotide binding site must be similar for both [(CG)₆]₂ and [(AT)₆]₂ and is independent of the chirality of the complex. Clearly the binding of each of the complexes to the oligonucleotide involves a substantial intercalation of the phenanthridinium moiety between the DNA base pairs.

A last point of importance needs to be highlighted because the binding affinities are not only influenced by the nature of the oligonucleotide, and the chirality of the complex but also by the nature of the lanthanide ion. The Eu and Yb complexes do not behave in the same way, and the choice of the metal influences the strength of the binding. Where the stronger Eu complex-[(CG)₆]₂ association is with the Δ isomer, in the ytterbium case the binding affinities are higher for the Λ isomer. A possible explanation involving the different size of the metal ion inducing a different complex conformation has to be refuted since ¹H NMR studies showed that both the Eu and Yb complexes adopt a regular square-antiprismatic geometry with the same approximate twist angle of 40° for the arms.¹² A tentative suggestion for these variations relates to the acidity of the water molecule bound to the lanthanide. This will be more acidic in the ytterbium case, and this could affect the binding to the duplex through a differential hydrogen-bonding interaction.¹³

3-2.2: Control experiments

3-2.2.1: Quenching of fluorescence from complexes Δ and Λ

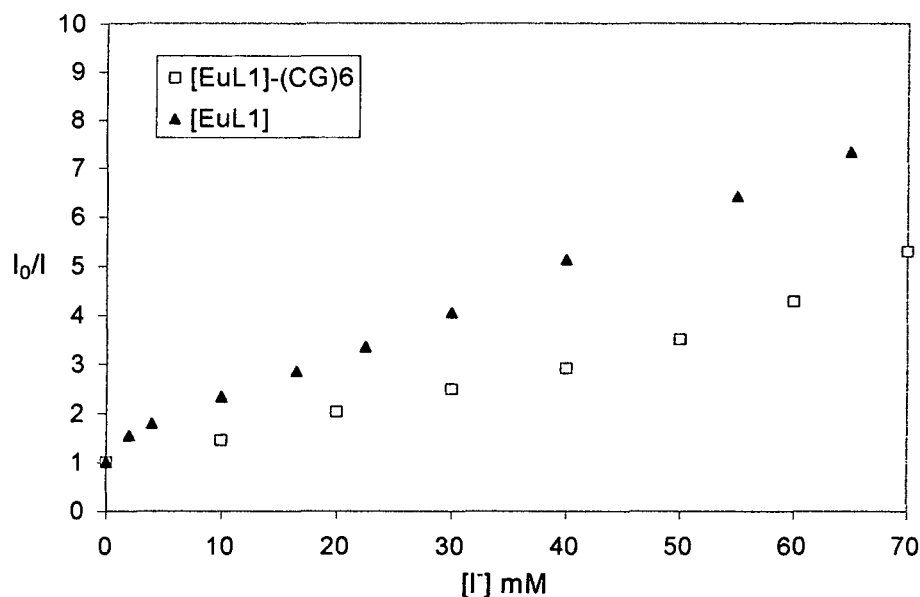
Halide ions are known to quench phenanthridinium fluorescence by an electron transfer mechanism. In evaluating the strength and the nature of the binding to DNA by such complexes, the competition between charge transfer quenching by nucleobase interaction and

quenching by electron transfer from X^- may give useful comparative information. By taking the saturated oligonucleotide-complexes in the presence of a known concentration of added iodide or chloride, the change in the fluorescence decay was observed. This competitive deactivation of the phenanthridinium singlet state by the halide, notwithstanding the partial quenching by charge transfer from the nucleobases, may be quantified in terms of apparent Stern-Volmer quenching constants. The reference points for such experiments are the Stern Volmer constants established for *N*-alkyl phenanthridinium fluorescence itself and for europium emission in the presence of added iodide or chloride (Table 3.2).

<i>Halide</i>	<i>Phenanthridine Fluorescence</i>	<i>Europium emission</i>
<i>Cl⁻</i>	6.0	26
<i>I⁻</i>	1.9	1.2

Table 3.2: Stern Volmer quenching constants (K_{SV}^{-1} , mmol.l^{-1}) for the effect of halide ions on $\Lambda\text{-[EuL}^1\text{]}^{4+}$ ($I = 0.1 \text{ M Me}_4\text{ClO}_4$, 295K)¹⁴

The first quenching experiment involving the $\Lambda\text{-[EuL}^1\text{]}^{4+}\text{-d(CG)}_6$ binding allowed an estimate of the Stern Volmer constants for the effect of chloride and iodide on the phenanthridinium fluorescence. The effect of iodide on the free complex resulted in a steeper curve (σ), that saturated more slowly compared to when the complex is bound to the DNA (\square). In the latter case the complex may be shielded from the iodide quenching effect. Therefore the observed fluorescence decay is a combination of 'DNA base' quenching and halide quenching.



Scheme 3.13: Decay of phenanthridinium fluorescence in Λ -[EuL^{1a}]⁴⁺ (\blacktriangle) and Λ -[EuL^{1a}]⁴⁺(RRR)/[(CG)₆]₂ (\square) as a function of increasing iodide concentration (295K)

In the case of added iodide, the observed decay of the fluorescence for the bound (CG)₆ complex was consistent with an apparent Stern Volmer constant of 15 mM. The bound complex is therefore up to 8 times less sensitive to iodide quenching when it is bound to the DNA than when free in solution.

The addition of chloride to the solution of $\{\Lambda$ -[EuL^{1a}]⁴⁺-d(CG)₆ $\}$ was also expected to quench the fluorescence. However the effect of increasing concentration of added chloride led only to an *enhancement* of the phenanthridinium emission ($K_{sv}^{-1} = -116$ mM). This behaviour was at first sight surprising, as chloride was supposed to deactivate the singlet excited state of the phenanthridinium. In this experiment, the effect of added sodium chloride salt not only increased the presence of chloride but also increased the ionic strength, affecting the strength of the binding at the same time. The higher ionic strength seems to lower the affinity of Λ -[EuL^{1a}]⁴⁺ for [(CG)₆]₂. This aspect will be further studied separately, see part 3.2-3.

The comparative quenching studies were extended to include the series of Yb complexes binding to [(CG)₆]₂ and [(AT)₆]₂, particularly examining the strength of their interaction in the presence of iodide (Table 3.3).

<i>Complex / oligonucleotide</i>	<i>K_{sv}⁻¹ by iodide (10⁻³ mol.l⁻¹)</i>	<i>K_{aff}[#] (10⁵ M¹.duplex⁻¹)</i>
Δ -[YbL ^{1b}] ⁴⁺ /[(CG) ₆] ₂	23	15
Λ -[YbL ^{1a}] ⁴⁺ /[(CG) ₆] ₂	107	57
Δ -[YbL ^{1b}] ⁴⁺ /[(AT) ₆] ₂	16	13
Λ -[YbL ^{1a}] ⁴⁺ /[(AT) ₆] ₂	22	30

The binding affinities taken from Table 2.1 are indicative of the overall apparent binding affinity.

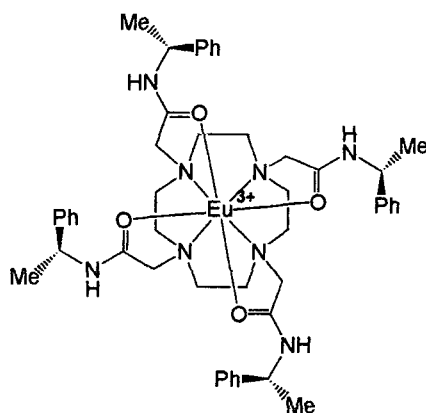
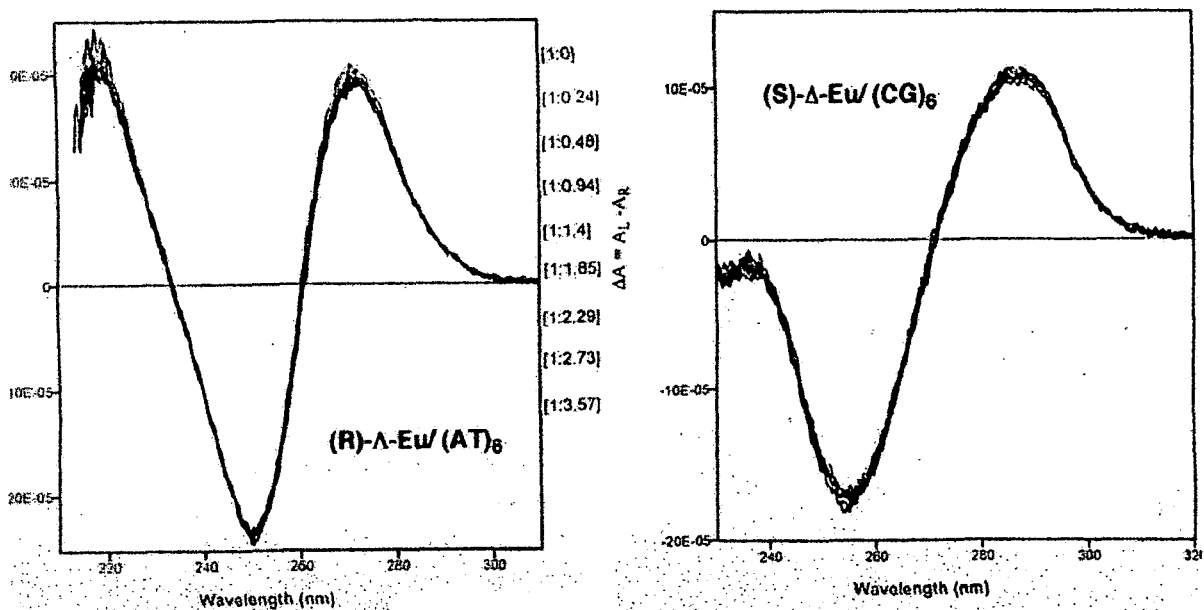
Table 3.3: Apparent Stern Volmer quenching constants (K_{sv}⁻¹, mM) for the effect of iodide ions on phenanthridinium fluorescence ($\lambda_{exc} = 378$ nm, $\lambda_{em} = 405$ nm) in [YbL¹]⁴⁺ bound to [(CG)₆]₂ and [(AT)₆]₂ (293K, pH 7.4, HEPES 10mM, NaCl 10mM)

The apparent Stern Volmer quenching constants for iodide were at least 10 times higher when the complexes are in the presence of added oligonucleotide. This fact suggests that the phenanthridinium moiety is shielded by the DNA helix from the quenching effect of iodide. The Stern Volmer constant for Λ -[YbL^{1a}]⁴⁺/[(CG)₆]₂ was 6 times higher than any other. Such behaviour is consistent with the fact that its binding affinity with [(CG)₆]₂ was found to be the strongest for this series of complexes. The decay of phenanthridinium fluorescence in the case of Λ -[YbL^{1a}]⁴⁺/[(CG)₆]₂ was anomalous: a break in the Stern Volmer plot above 30 mM iodide was observed. This suggests that there are two types of binding interaction (with differing sensitivities to added iodide or salt) involved in this interaction of Λ -[YbL^{1a}]⁴⁺ with [(CG)₆]₂. This may explain the apparent size of the Stern-Volmer quenching constant.

The other quenching constants are all of the same order, suggesting the strength of the complex-oligonucleotide association was fairly similar in each case.

3-2.2.2: Control CD studies of the Δ and Λ -tetra-amide L^2 complexes

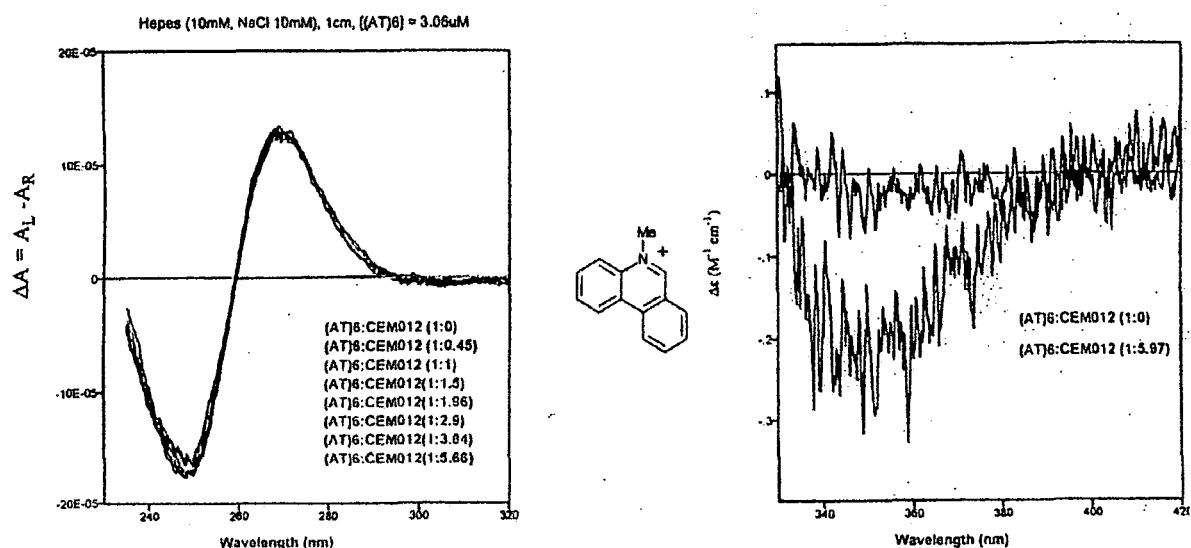
Any positively charged ligand or complex is likely to bind to a negatively charged DNA backbone. To further probe the nature of the interaction of the complex, CD experiments were carried out with a parent complex lacking the intercalative moiety, i.e. without the phenanthridinium group (Scheme 3.14). Both Δ and Λ of $[\text{EuL}^2]^{3+}$ were titrated against oligonucleotide, and changes were monitored by circular dichroism.

Scheme 3.14: Δ - $[\text{EuL}^{2a}]^{3+}$ 

Scheme 3.15: Difference CD spectra for $[(\text{CG})_6]_2$ following addition of Λ - $[\text{EuL}^{2b}]^{3+}$
(295K, pH 7.4, NaCl 10mM, HEPES 10 mM)

No significant change occurred in the CD spectra of the oligonucleotide following addition of increasing concentrations of complex. This behaviour was found for both Δ and Λ complexes. The absence of change in the CD difference spectra of both the Δ and Λ isomers suggests that the changes observed with the corresponding phenanthridinium complexes are predominantly due to the binding of the phenanthridinium moiety. A complex lacking the intercalative unit cannot bind to the DNA in this manner. The DNA conformation is also not affected by the presence in solution of increasing concentrations of the positively charged complexes. So the presence of an intercalative moiety is crucial for the interaction with DNA and especially for an intercalation binding mode.

Following these observations, a simple phenanthridinium chromophore was also examined by circular dichroism in its interaction with $[(CG)_6]_2$, to evaluate its effect on the DNA structure. Nordén *et al.* have previously described changes and selectivity in the binding of a related chiral phenanthridinium chromophore to DNA.¹⁵



Scheme 3.16: Difference CD spectra for $[(CG)_6]_2$ in the presence of increasing amounts of N-methyl phenanthridinium iodide (295K, pH 7.4, NaCl 10mM, HEPES 10mM)

The slight changes observed (Scheme 3.16) in the CD titration were comparable in magnitude to those found following addition of $[EuL^2]^{3+}$. Only a very weak and negative induced CD band was observed at 370 nm, contrasting with the stronger positive induced CD

band found for $[\text{LnL}^{1a}]^{4+}$. This suggests that while the phenanthridinium moiety alone can bind to DNA, it does not promote significant variation in the DNA helical structure. The intercalation phenomenon increases the DNA pitch and the extent of unwinding; the helical twist is also likely to be slightly modified. However in this case, the combined presence of an intercalator and a strongly helical cationic complex which may interact selectively with the DNA groove gives rise to the major observed perturbations of DNA structure.

3-2.3: Dependence of affinity on salt concentration

The interaction of the positively charged complexes with the negatively charged oligonucleotides must also involve a strongly stabilising electrostatic interaction.¹⁶ The CD titrations involving the parent tetra-amide complexes have suggested that this component may not dominate the binding of these phenanthridinium complexes to DNA. A consequence of the cooperativity between ion pairing and intercalation in these complexes is that the association binding constant must be strongly dependent on the ionic strength of the solution and is expected to decrease with increasing salt concentration.¹⁷ To determine the contribution of the electrostatic interaction in the case of the binding of tetra-positive complexes to DNA, the salt concentration of the medium has been varied.¹⁸

The quenching of the fluorescence of $\Lambda\text{-[EuL}^{1a}]^{4+}$ complex upon binding to $[(\text{CG})_6]_2$ ⁱⁱ was studied under relatively high salt conditions (50 and 100 mM sodium chloride) to estimate the relative binding affinities. The titrations were monitored by absorbance and fluorescence spectroscopy to evaluate the effect.

The absorbance spectra showed the same characteristic features of intercalation at a sodium chloride concentration of 10 mM, 50 mM and 100 mM. A hypochromism of 30 % was noticed in each case, accompanied by a red shift of 7-8 nm. A long wavelength tail was observed as well. The fluorescence decay from the phenanthridinium group was analysed and the results are listed in Table 3.4.

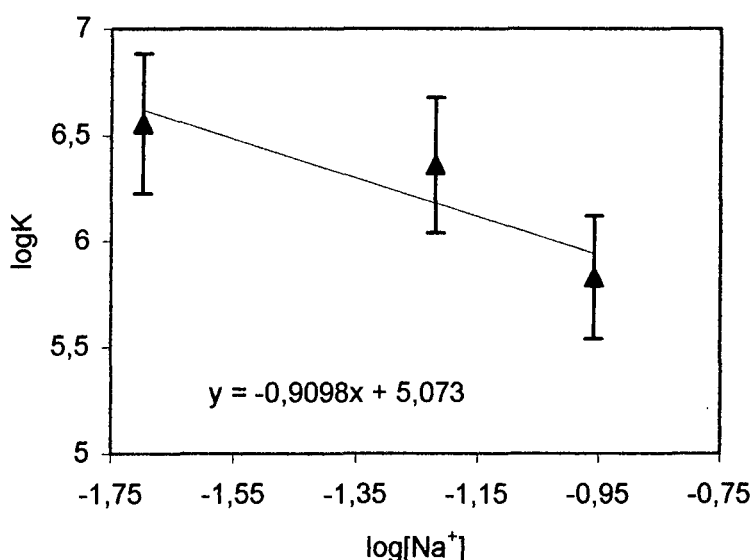
ⁱⁱ $[(\text{CG})_6]_2$ was chosen in this study as the complexes exhibit a stronger affinity compared to $[(\text{AT})_6]_2$.

Concentration of Na ⁺ (mM)	K [#] (10 ⁵) (M ⁻¹ .duplex ⁻¹)	n [#] (duplex ⁻¹)	% Hypochromism (320nm)
20	36	3.9	33
60	23	1.9	35
110 ^a	6.9	2	33
110 ^b	5.9	2.3	36

^a Using from 100 mM NaCl. ^b Using from 100 mM NaOAc.

Table 3.4: Intrinsic binding constants (*K*), site sizes (*n*), and degree of hypochromism measured for Λ -[EuL^{1a}]⁴⁺ complex with [(CG)₆]₂ (295K, pH 7.4, HEPES 10mM)

Because the presence of a high concentration of chloride in solution leads to competitive quenching of the fluorescence signal, a comparative titration was also carried out in the presence of 100 mM sodium acetate (110 mM Na⁺). The resulting binding constant was the same as that obtained in 100 mM sodium chloride. This observation suggests that the constant presence of chloride does not affect the apparent binding affinity, even though the fluorescence signal is partially reduced in intensity.

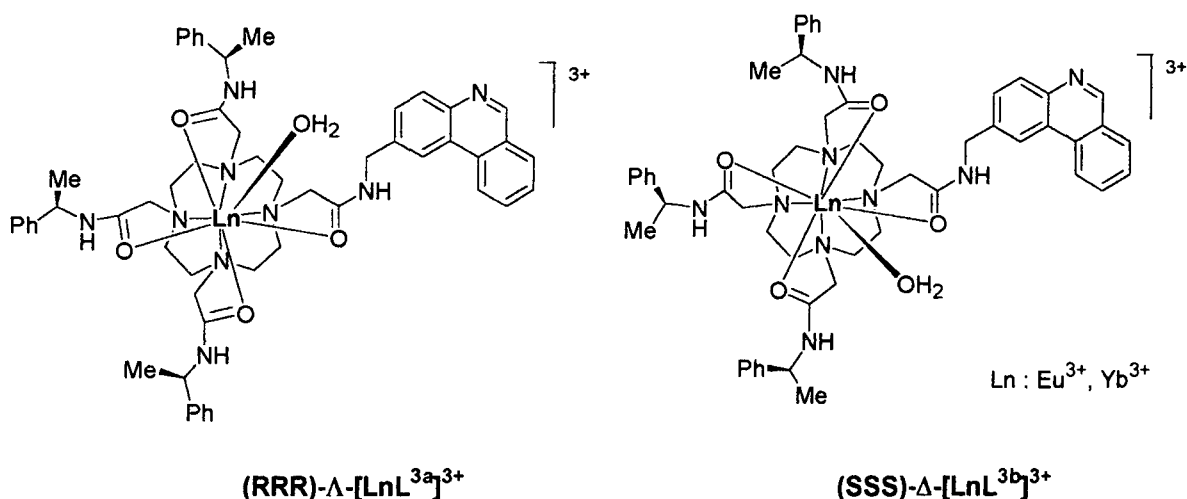


Scheme 3.17: Salt dependence of Λ -[EuL^{1a}]⁴⁺-[(CG)₆]₂ binding (295K, [Na⁺] = 20, 60 and 110 mM)

The linear dependence of the logarithm of the apparent binding constant as a function of the logarithm of the salt concentration suggests that the binding of those complexes does involve an electrostatic interaction (Scheme 3.17). However the shallowness of the slope of this relationship suggests that a major component in the overall free energy of binding must involve an intercalative binding mode (i.e. involving a singly charged chromophore), in association with a stereochemically sensitive non-covalent interaction with the DNA groove.

3-3 Control studies examining the unmethylated complexes, Δ and Λ -[LnL³]³⁺

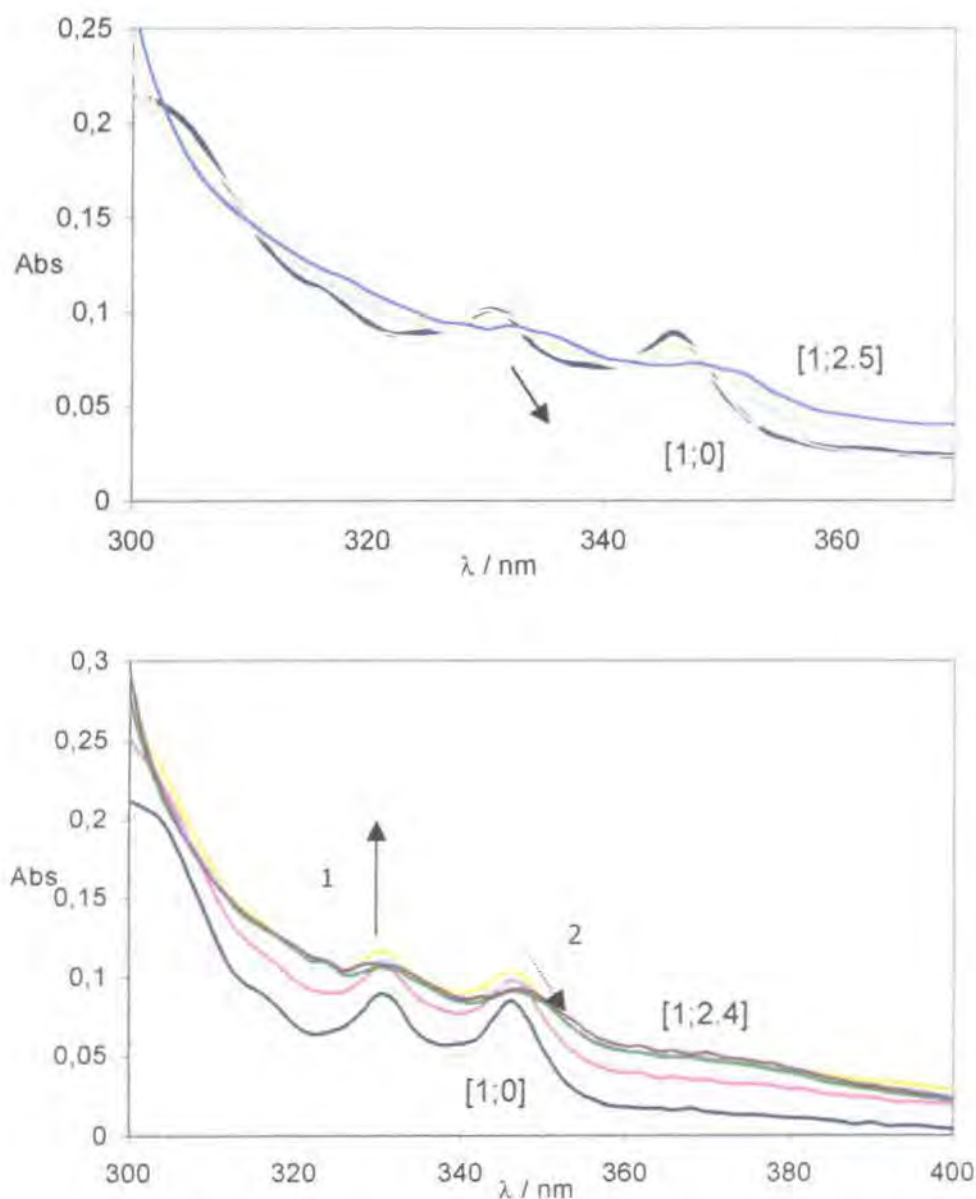
The previous series of complexes involved systems where the intercalating moiety itself bore a single positive charge. Aiming to investigate the importance of a positively charged chromophore in the intercalation process, complexes were also examined where the phenanthridinium nitrogen was not quaternized (Scheme 3.18). The helicity at the lanthanide centre remained Λ or Δ as a function of the chirality of the amide pendent arms. The overall charge of the complex is reduced by one, and consequently the binding affinities were expected to be lowered. Nevertheless, the lower charge may give rise to modified selectivity in the chiral recognition of the DNA by the macrocycle.



Scheme 3.18: Λ and Δ phenanthridinyl lanthanide complexes

3-3.1: Binding affinities: absorbance, fluorescence quenching and CD studies

The absorbance spectral titration of Λ and Δ Eu complexes with $[(CG)_6]_2$ and $[(AT)_6]_2$ revealed surprising behaviour. With the Λ isomer, a red shift and hypochromism was noticed, whereas for the Δ isomer the spectra showed first a hyperchromism and then a hypochromism upon the addition of oligonucleotide, with both $[(CG)_6]_2$ and $[(AT)_6]_2$. The Λ isomer exhibited two isosbestic points at 310 and 348 nm. For the Δ isomer, no well-defined isosbestic point was apparent (Scheme 3.19).



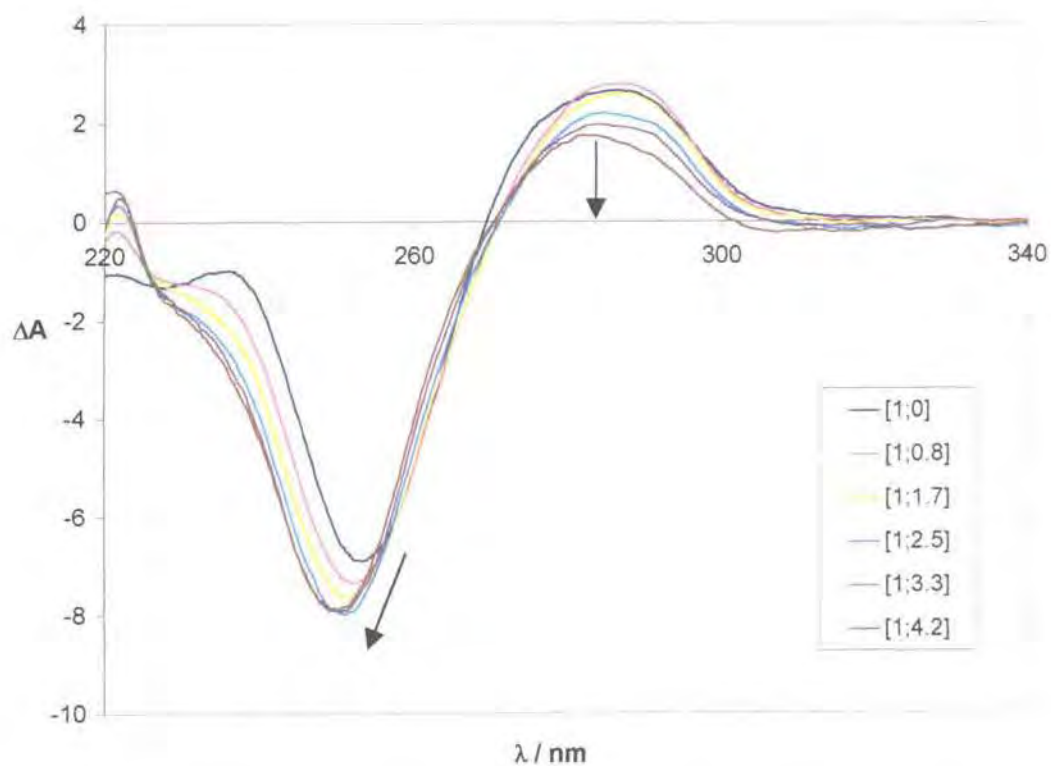
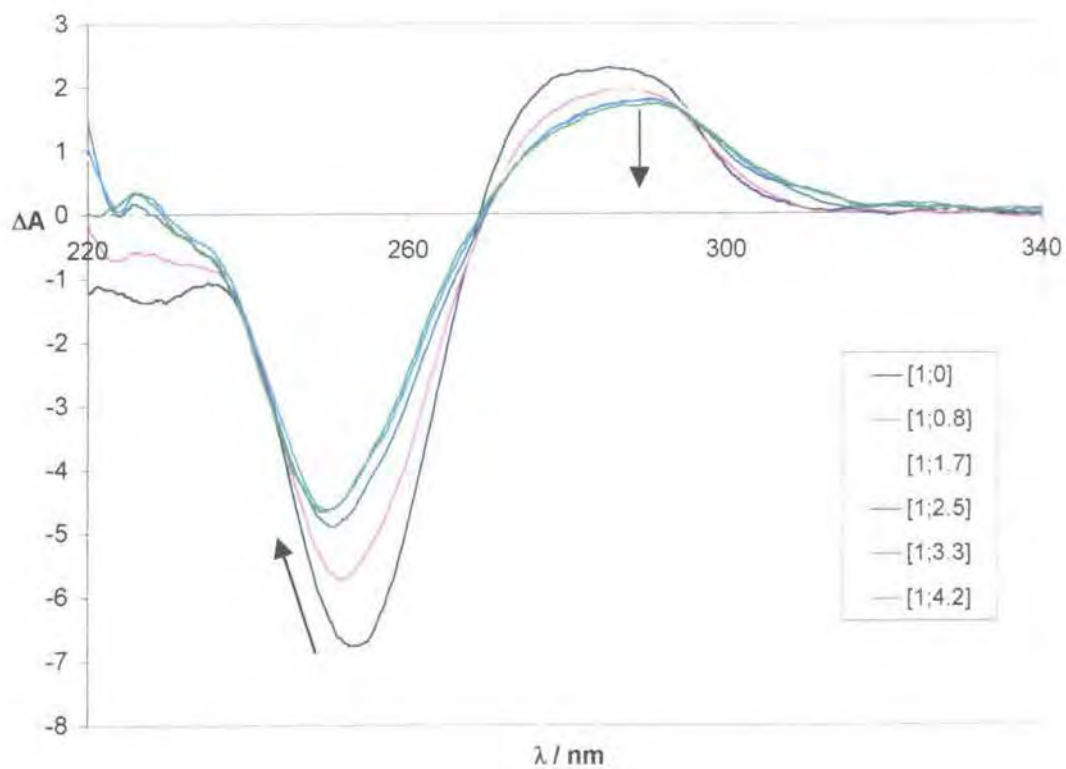
Scheme 3.19: Absorbance spectra of Λ -[EuL^{3a}]³⁻ (upper) and Δ -[EuL^{3b}]³⁻ (lower) following addition of $[(CG)_6]_2$ (295 K, NaCl 10 mM, HEPES 10mM, pH 7.4)

For Λ -[EuL^{3a}]³⁺ the characteristic features of an intercalative binding mode were compared to those observed previously in the case of *N* methylated complexes (Scheme 3.19). The red shift was 6 nm and a hypochromism of 21 % (345 nm) was noted.

For the Δ -[EuL^{3b}]³⁺ isomer, a modest hyperchromism was found together with a slight shift to the red and the appearance of a long wavelengths tail (Scheme 3.19). The absorbance spectra of Λ -[YbL^{3a}]³⁺ showed only a hyperchromism and no shift to lower energy was observed. Those features, revealed by the absorbance spectra, were also characteristic of the binding of Δ -[YbL^{1b}]⁴⁺ to both oligonucleotides, [(CG)₆]₂ and [(AT)₆]₂.

The nature of the interaction revealed by the absorbance spectra was further investigated by circular dichroism studies. The CD difference spectra were acquired for the oligonucleotide [(CG)₆]₂ following addition of Λ and Δ complexes (Scheme 3.20).

The binding of Λ -[EuL^{3a}]³⁺ to [(CG)₆]₂ induced the same changes in the oligonucleotides as observed with the *N*-alkylated complex Λ -[EuL^{1a}]⁴⁺. A decrease in the intensity of both bands was observed to a similar extent. For the Δ isomer, similar CD difference spectra were obtained compared to the *N*-alkylated analogue. These observations suggest that both series of complexes bind to [(CG)₆]₂ in a comparable manner in which the stereoselectivity of the binding interaction is primarily determined by the handedness of the lanthanide complex.



Scheme 3.20: Difference CD spectra for $[(CG)_6]_2$ in the presence of increasing ratio of $\Delta-[EuL^{3a}]^{3-}$ (upper) and $\Delta-[EuL^{3b}]^{3-}$ (lower) (295K, NaCl 10 mM, HEPES 10mM, pH 7.4)

Estimates of the apparent binding affinities were obtained by monitoring the phenanthridine fluorescence intensity decay ($\lambda_{\text{exc}} = 304 \text{ nm}$, $\lambda_{\text{em}} = 385 \text{ nm}$). Data sets were analysed as before using the McGhee and von Hippel approximation (Table 3.5). The europium luminescence changes echoed the decay in intensity found for the phenanthridinium fluorescence.

<i>Complex</i>	$K^{\#} (10^5)$ ($M^1 \cdot \text{duplex}^{-1}$)	$n^{\#}$ (duplex^{-1})	% Hypochromism (345nm)
$\Delta\text{-[EuL}^{3b}\text{]}^{3+}/[(\text{CG})_6]_2$	30	5	6
$\Lambda\text{-[EuL}^{3a}\text{]}^{3+}/[(\text{CG})_6]_2$	35	5	18
$\Delta\text{-[EuL}^{3b}\text{]}^{3+}/[(\text{AT})_6]_2$	35	3.5	7
$\Lambda\text{-[EuL}^{3a}\text{]}^{3+}/[(\text{AT})_6]_2$	37	5	21
$\Lambda\text{-[YbL}^{3a}\text{]}^{3+}/[(\text{CG})_6]_2$	10	3	nd

[#] Typically $[\text{LnL}] = 20\text{-}30 \mu\text{M}$; the binding value showed a dependence on the concentration of complex; data from fluorescence intensity changes with added oligonucleotide were analysed using the method of McGhee and von Hippel.⁵

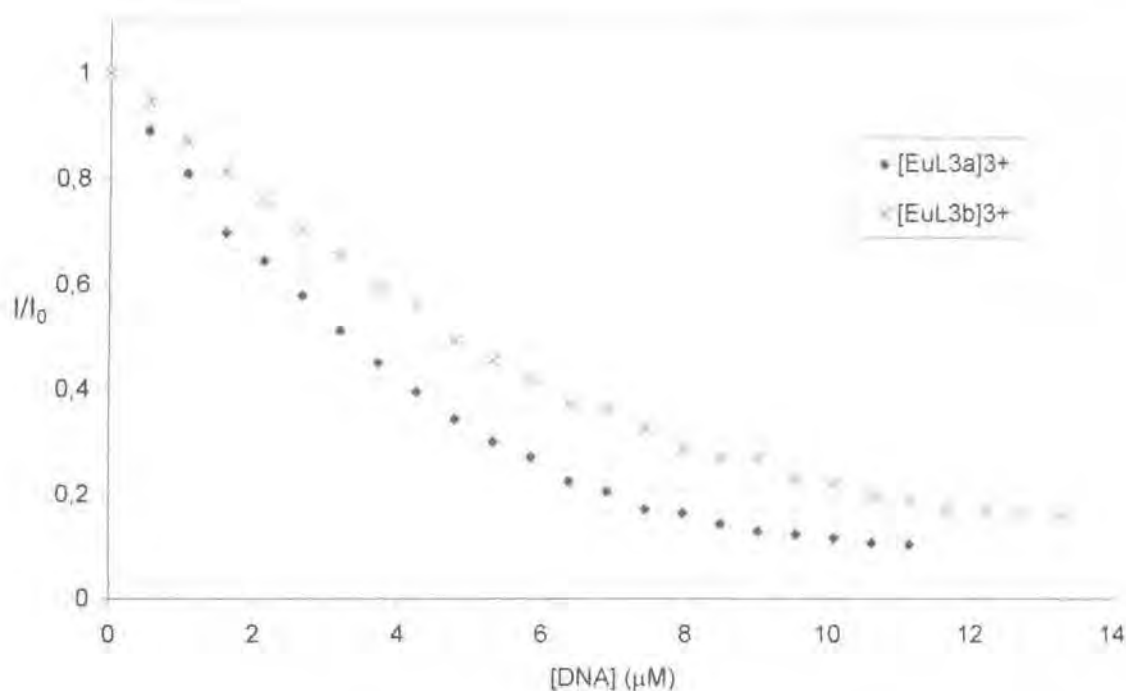
Table 3.5: Intrinsic binding constants (K), site sizes (n), and degree of hypochromism measured for complexes of $[(\text{CG})_6]_2$ and $[(\text{AT})_6]_2$ with $\Lambda[\text{LnL}^{3a}]^{3+}$ and $\Delta[\text{LnL}^{3b}]^{3+}$

The estimated binding affinities all fall in the same range indicating that the complexes bind to the oligonucleotide without any distinctive stereodifferentiation. As a consequence of fitting problems associated with relatively small variations of fluorescence intensity (overall changes in fluorescence intensity were <80%, compared to 95% for $\Lambda\text{-[EuL}^{1a}\text{]}^{4+}$), these values, especially the number of 'ligand' per duplex n , are subject to a significant error. Thus it may be misleading to compare fluorescence intensity changes with those of the previous series of *N*-alkylated complexes. To observe a decrease of 50% of the fluorescence intensity, for example, the DNA concentration needed to be 3.7 times higher for

tri-cationic complexes.ⁱⁱⁱ So this observation itself suggests that the binding of the tri-cationic complexes is approximately 4 times lower than those of the corresponding tetra-cationic complexes.

The absence of a positive charge on the phenanthridine moiety in these tri-cationic complexes has a considerable effect. Evidently the positive charge on the phenanthridine chromophore constitutes a significant driving force for the intercalative interaction, consistent with a predominantly charge-transfer binding mode.

In term of the differences observed in the absorbance spectral titrations, a stronger association for Λ -[EuL^{3a}]³⁺ was suggested compared to the Δ isomer, for both [(CG)₆]₂ and [(AT)₆]₂. However the data in Table 3.5 indicate that both complexes exhibit comparable affinity. Nevertheless, the intensity changes can be compared for equivalent concentrations of complex and added oligonucleotide (Scheme 3.21).



Scheme 3.21 : Fluorescence intensity changes ($\lambda_{exc} = 304 \text{ nm}$, $\lambda_{em} = 385 \text{ nm}$) in Λ -[EuL^{3a}]³⁺ and Δ -[EuL^{3b}]³⁺ following addition of [(CG)₆]₂ ([EuL] = 24 μM, 295K, pH 7.4, NaCl 10 mM, HEPES 10 mM)

ⁱⁱⁱ This calculation is based on the fluorescence data from titrations with Λ -[EuL^{1a}]⁴⁺ and Λ -[EuL^{3a}]³⁺.

The absorbance data had suggested a more distinctive binding mode for the Λ isomer. Here the normalised intensity decay curve also suggested that a more efficient quenching mechanism occurred with the Λ complex. This observation leads to the conclusion that in the binding of the Λ isomer there may exist a more complementary interaction between the DNA groove and the complex allowing more favourable non-bonding interactions than with the Δ isomer. Given the sense of this interaction this could plausibly involve an interaction from the minor groove, as suggested for the binding of certain chiral ruthenium complexes.¹⁹

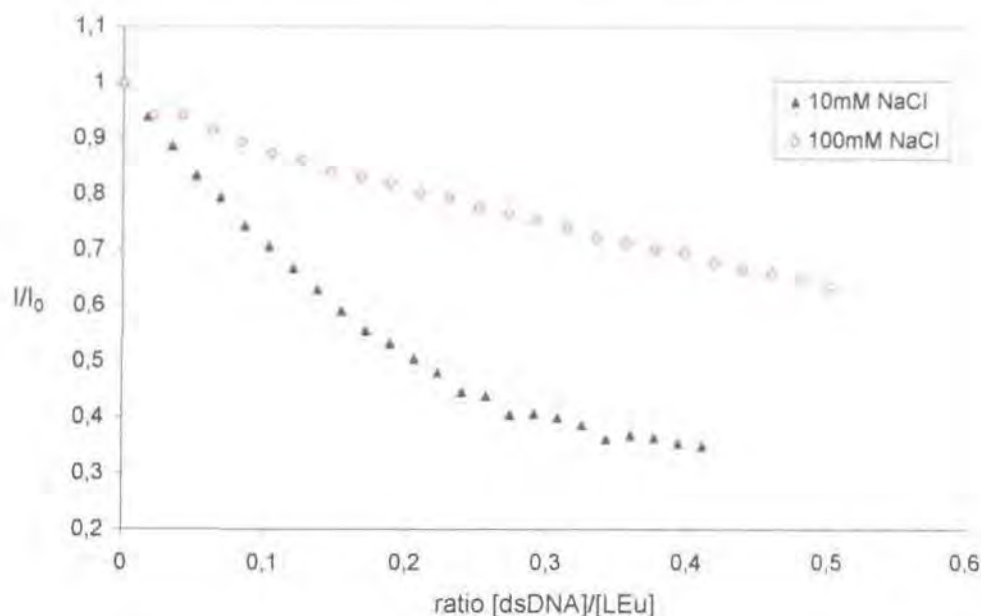
3-3.2: Salt concentration effect

In section 3.2-3, it was shown that the ionic strength modulated the binding affinities of these complexes for the oligonucleotide duplex via changes to the electrostatic contribution to the binding. The electrostatic attraction energy varies as $1/r$ and so is very likely to be involved in the first step of the binding process. As this contribution has been defined for the tetra-cationic complexes, an investigation of the effect of higher ionic strength on the binding of these series of triply charged complexes was also undertaken. The estimation of apparent binding affinities was not considered possible in the case of complexes bound to DNA under high salt concentration conditions, due to the absence of a well defined limiting intensity value.

The absorbance spectra for the titration Λ -[EuL^{3a}]³⁺ with [(CG)₆]₂ at 100 mM NaCl showed the same behaviour at high salt as in 10 mM sodium chloride. The Λ -[EuL^{3a}]³⁺ exhibited a marked hypochromism and a small red shift, while for the Δ isomer, a small hyperchromism was discerned.

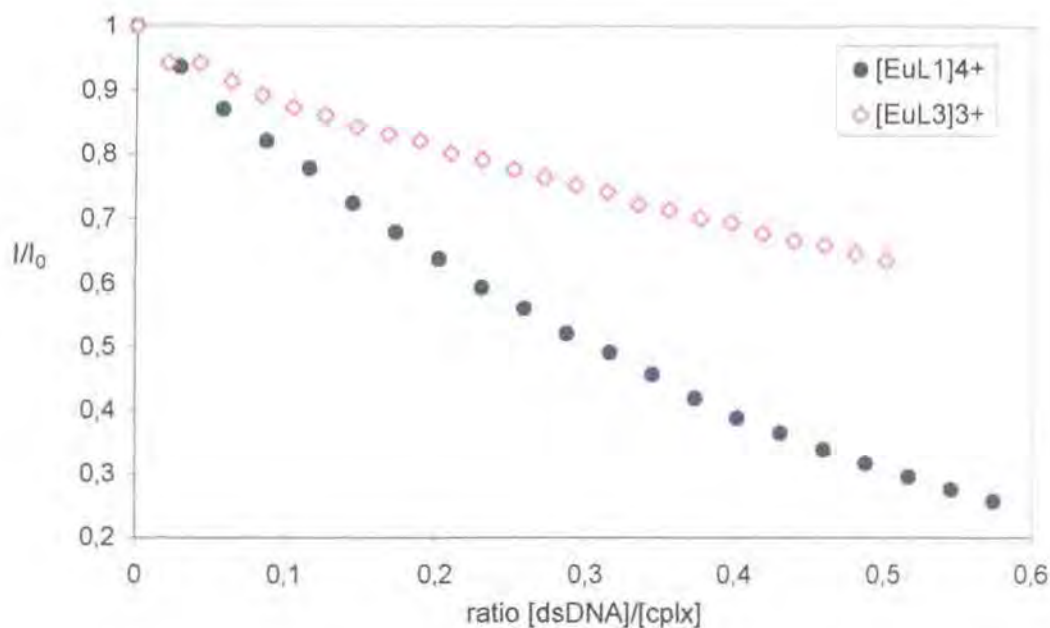
The approximate values found were 0.5 and 0.8 $10^5 \text{ M}^{-1} \cdot \text{duplex}^{-1}$, for the binding of Λ -[EuL^{3a}]³⁺ and Δ -[EuL^{3b}]³⁺, respectively bound to [(CG)₆]₂ in high salt media (100 mM NaCl). It is more appropriate to compare the fluorescence decay titration curves to evaluate the strength of the binding.

The fluorescence decay of Λ -[EuL^{3a}]³⁺ under normal (10 mM NaCl) and high salt (100 mM NaCl) concentrations were compared (Scheme 3.22). To obtain a quenching effect of 25 %, the concentration of added DNA needed to be more than 3 times higher under conditions of high ionic strength. Furthermore, no evidence for a saturation limit was found, contrary to the fluorescence intensity decay changes in 10 mM NaCl solution.



Scheme 3.22: Fluorescence intensity changes ($\lambda_{exc} = 304 \text{ nm}$, $\lambda_{em} = 385 \text{ nm}$) of $\Lambda\text{-}[\text{EuL}^{3a}]^{3-}$ following addition of $[(\text{CG})_6]_2$ in 10 mM (\blacktriangle) and 100 mM (\diamond) sodium chloride (295K)

A comparison of the binding of $\Lambda\text{-}[\text{EuL}^{1a}]^{4+}$ and $\Lambda\text{-}[\text{EuL}^{3a}]^{3+}$ shows that the presence of high salt concentration reduced the binding affinity of both complexes to $[(\text{CG})_6]_2$ (Scheme 3.23).



Scheme 3.23: Fluorescence intensity changes of $\Lambda\text{-}[\text{EuL}^{1a}]^{4+}$ (\bullet) and $\Lambda\text{-}[\text{EuL}^{3a}]^{3-}$ (\diamond) following addition of $[(\text{CG})_6]_2$ in 100 mM sodium chloride solution ($\lambda_{exc} = 378 \text{ nm}$, $\lambda_{em} = 410 \text{ nm}$; $\lambda_{exc} = 304 \text{ nm}$, $\lambda_{em} = 385 \text{ nm}$) (295 K, HEPES 10 mM)

This inhibitory effect is manifested by the near linearity of the decay profiles. As the binding of the triply charged complex is already relatively weak, the effect is more evident in this case. A decay in the fluorescence intensity of 30% was attained for the triply charged complex with a DNA concentration that is 2.5 times higher than for Λ -[EuL^{1a}]⁴⁺.

Summary of binding of Δ and Λ -[EuL³]³⁺:

This series of complexes exhibits a particular affinity for DNA that is dependent upon whether the phenanthridine N is alkylated or not. The binding of the Λ isomer seems to involve at least partially, an intercalative interaction of the phenanthridinyl unit, as shown by changes in absorbance spectra. It is estimated that the binding affinity of the tri-cationic complexes is at least three times less than those of the corresponding phenanthridinium tetra-cationic complexes.

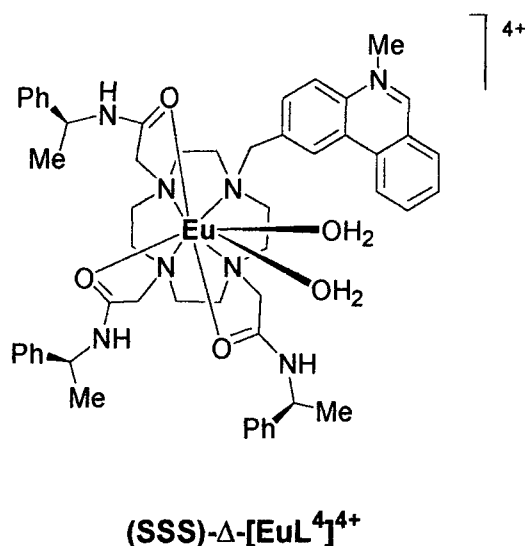
There is some evidence suggesting a slightly favoured binding for Λ -[EuL^{3a}]³⁺ complex compared to the Δ isomer. Differences between europium and ytterbium complexes in their binding to each oligonucleotide were also evident with the unmethylated series, although it is not clear why this should be so.

3-4 Diaqua Δ -L⁴ Europium complex

The design of new nucleic acid probe requires systems that possess both a high association constant with the biomolecule and also exhibit good recognition of the substrate structure. The previous series of tri-cationic complexes presented a neutral intercalative chromophore, which inhibits strong binding. Consequently a cationic intercalative moiety was regarded as essential in a search for novel DNA probes.

In the tetra-cationic europium complex Δ -[EuL⁴]⁴⁺ (Scheme 3.24), the linking arm between the chiral macrocycle and the intercalating phenanthridinium group has been shortened with the aim of improving the stereoselectivity in the binding by bringing the element of chirality of the complex closer to the chromophore. The complex possesses two bound water molecules at least one of which may be displaced by interaction with a phosphate group of a nucleotide residue. Such a change in the local lanthanide coordination

environment may be signalled by changes to the europium emission spectrum. Evidence for such effects has recently been obtained in the binding of Δ -[EuL⁴⁺]⁴⁺ with carbonate, and monohydrogen phosphate anions, amongst others.²⁰

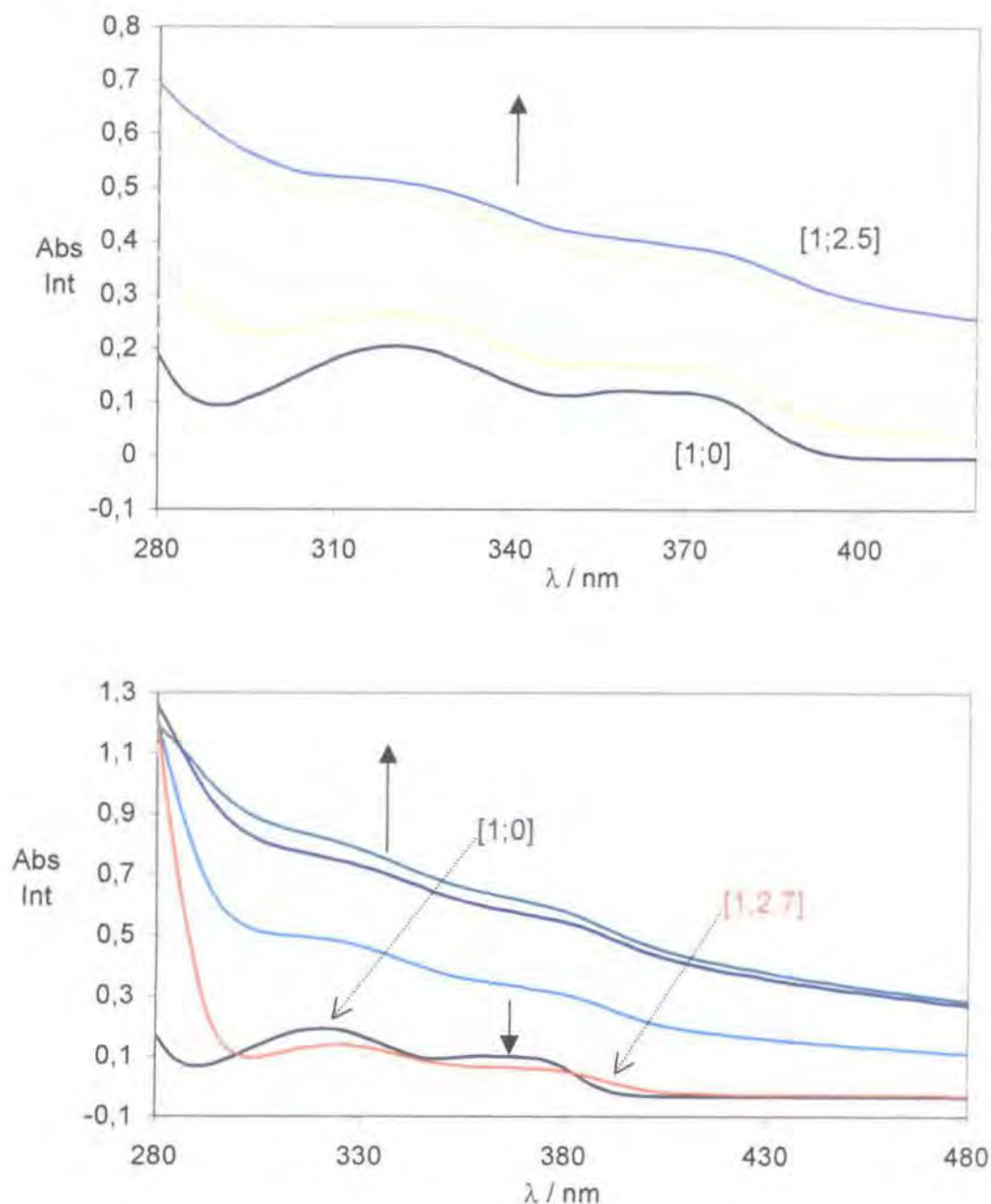


Scheme 3.24: Diaqua phenanthridinium europium complex^{iv}

3.4-1: Spectroscopic titrations

The absorbance spectrum of the complex following addition of oligonucleotide showed a pronounced hyperchromism of 160% ($\lambda_{\text{abs}} = 320 \text{ nm}$) for [(CG)₆]₂ (Scheme 3.25). With [(AT)₆]₂ the changes in absorption spectra suggested a stepwise interaction with the DNA bases. A marked hyperchromism was noticed at the early stage of the titration (very high complex concentration). Then, once the ratio complex:DNA had reached [5:1], the absorbance decreased. At oligonucleotide saturation, two isosbestic points at 304 and 378 nm, and a red shift of 7 nm were observed. However the behaviour of the absorbance spectra is not reliable due to the non-zero baseline.

^{iv} This complex was synthesised by Dr L. J. Govenlock.

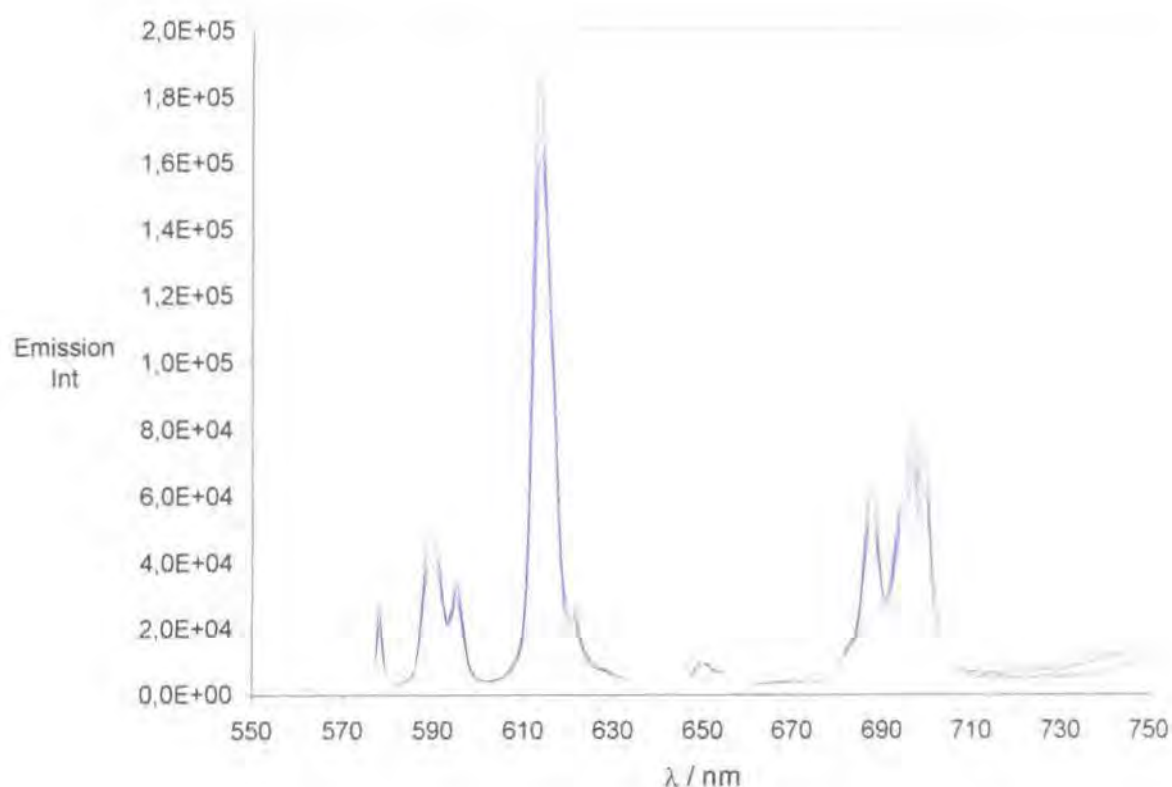


Scheme 3.25: Absorbance spectra of Δ -[EuL₄]⁴⁻ following addition of [(CG)₆]₂ (upper) and [(AT)₆]₂ (lower) (295K, pH 7.4, NaCl 10mM, HEPES 10mM)

With the oligonucleotide [(AT)₆]₂, the intercalative interaction with the cationic complexes was expected to be weaker than for the more electron-rich [(CG)₆]₂. Unfortunately solubility problems occurred during these titrations: a white solid precipitated, inhibiting further detailed analysis.

In the Eu emission spectra similar behaviour was noticed with each oligonucleotide model. The classical quenching of phenanthridine fluorescence ($\lambda_{em} = 409$ nm) by the nucleobases was accompanied by a parallel decrease in the Eu emission intensity (Scheme 3.26).

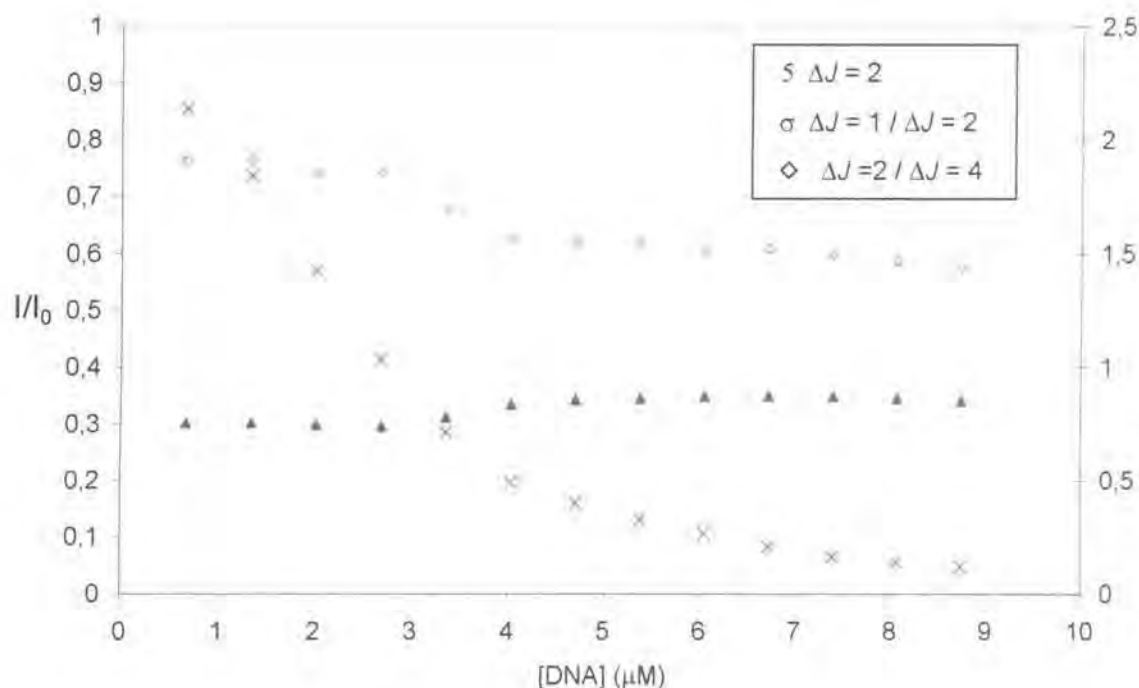
The spectra behaviour depicted in Scheme 3.25 may be interpreted in terms of a stepwise binding process with a markedly different effect on the nature and extent of phenanthridine charge transfer.



Scheme 3.26: Quenching of $\Delta-[EuL^A]^4^{+}$ emission following addition of $[(CG)_6]_2$
(295 K, $\lambda_{exc} = 378$ nm, pH 7.4, NaCl 10mM, HEPES 10mM)

The shape of the emission spectrum is determined by the local coordination environment and aids definition of the type of interaction involved between the complex and the DNA helix. The binding of DNA to the complex was monitored by variations of emission intensity and the ratio of intensities ($\Delta I = 2 / \Delta I = 4$; 615/697 nm) as a function of the concentration of

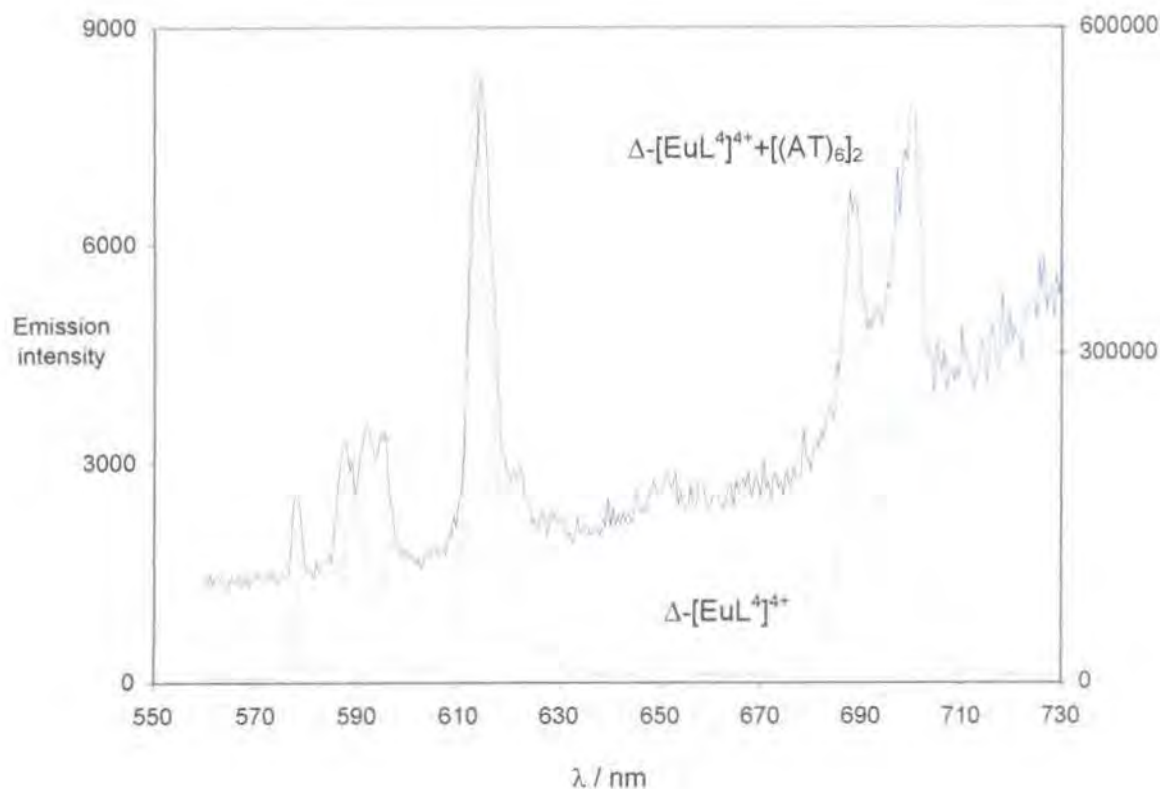
added oligonucleotide. The $\Delta J = 2$ and $\Delta J = 4$ transitions of the europium emission spectrum are hypersensitive and so are perturbed significantly by variations in the Eu coordination environment.¹⁸



Scheme 3.27: Quenching of europium emission ($\lambda_{exc} = 378$ nm, $\lambda_{em} = 615$ and 697 nm) in $[\Delta\text{-EuL}^4]^{3+}$ by $[(AT)_6]_2$ (293K, NaCl 10mM, HEPES 10mM, pH 7.4)

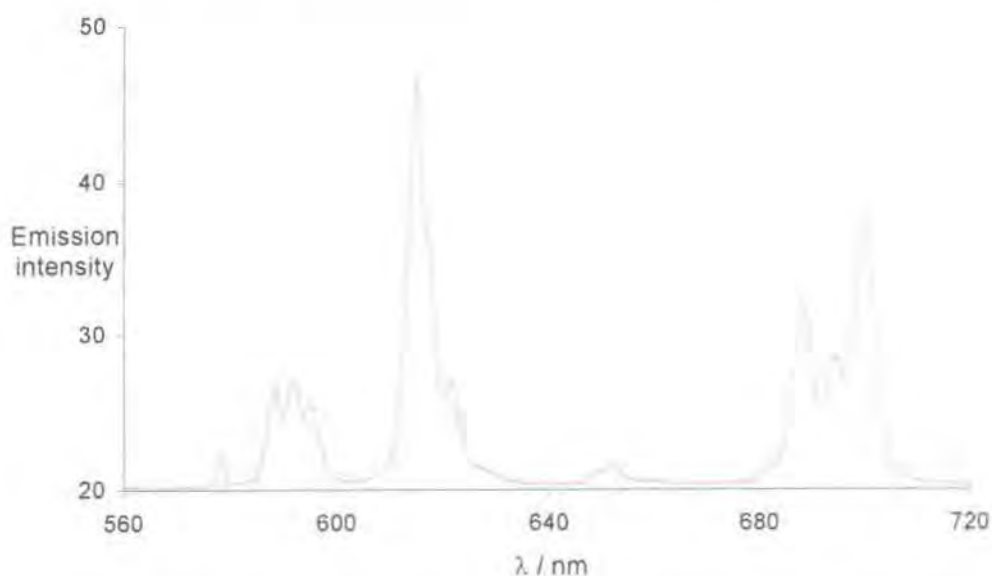
As the concentration of added $[(AT)_6]_2$ increased, the relative ratio of the transitions $\Delta J = 2$ and $\Delta J = 4$ decreased but not in a constant manner. Beyond a relative concentration of DNA duplex:complex [1:5] (concentration of $[(AT)_6]_2$ of $3.5 \mu\text{M}$; see Scheme 3.27), the intensity ratio remained constant. Such a discontinuity is also apparent in the changes to the $\Delta J = 2 / \Delta J = 1$ ratio.

By comparing the emission spectrum from the complex alone (diaqua) to that saturated with DNA, a change in the form and relative intensity of the transitions $\Delta J = 1$, $\Delta J = 2$ and $\Delta J = 4$, was noted suggesting a change in the coordination environment of the lanthanide ion (Scheme 3.28). The splitting of the $\Delta J = 1$ transition manifold is a complex function of the nature of the ligand and axial donor atoms, their polarisability and the local site symmetry. The $\Delta J = 4$ manifold also exhibits a markedly different fine structure in the complex bound form.



Scheme 3.28: Europium emission spectra ($\lambda_{exc} = 378 \text{ nm}$) for diaqua $\Delta\text{-[EuL}^4\text{]}^{4+}$ (lower) and in the presence of excess $[(AT)_6]_2$ (upper) (295 K, NaCl 10mM, HEPES 10mM, pH 7.4)

The Eu emission spectrum of the complex with $[(AT)_6]_2$ is rather similar to the spectrum observed following addition of HPO_4^{2-} to $\Delta\text{-[EuL}^4\text{]}^{4+}$ (scheme 3.29).^{19b}



Scheme 3.29: Europium emission spectra ($\lambda_{exc} = 370 \text{ nm}$) for $[\Delta\text{-EuL}^4]^{4+}$ in the presence of excess HPO_4^{2-} (295 K, NaCl 10mM, HEPES 10mM, pH 7.4)

3-4.2: Binding affinities of Δ -[EuL⁴]⁴⁺ to [(CG)₆]₂ and [(AT)₆]₂

Estimations of apparent binding affinities were made from the luminescence decay titration curves using the McGhee and von Hippel method.⁵ With [(CG)₆]₂, the apparent binding constant of the complex has been found to be $20 \times 10^6 \text{ M}^{-1} \cdot \text{duplex}^{-1}$ with a value for n of 5. Its binding to [(AT)₆]₂ was estimated to be 15 times weaker with an apparent affinity of $1.3 \times 10^6 \text{ M}^{-1} \cdot \text{duplex}^{-1}$ ($n = 2.5$). The difference in affinity between the two oligonucleotides was partially foreseen by the distinctive behaviour of each absorbance titration. Yet it is fairly surprising to observe such a large difference between the two oligonucleotides compared to the more modest differences in affinity defined in the tetra-amide series of complexes.

One very important qualification about these values needs to be mentioned: the excitation wavelength chosen was 378 nm in each of the luminescence titrations as it constituted an isosbestic point. However at high complex/DNA ratios, for both titrations the absorbance was not constant at 378 nm throughout. Therefore the extent of quenching of the phenanthridinium fluorescence is also a function of the extinction coefficient of the complex. The erroneous quenching intensity values leads to binding affinities that may not be reliable.

3-4.3: Lifetime measurements

The displacement of water molecules by a coordinating anion, e.g. phosphate, is signalled by an increase in the lifetime of the lanthanide excited state and an increase in its emission intensity. Such a phenomenon can be demonstrated by measuring the Eu emission lifetimes in H₂O and D₂O for the complex free and bound to the oligonucleotide. These values are listed in Table 3.6.

	$k_{\text{H}_2\text{O}}$	$k_{\text{D}_2\text{O}}^{(c)}$	$q^{\text{Eu (b)}}$
Δ -[EuL ⁴] ⁴⁺	1.42 ^(a)	0.28	0.8
Δ -[EuL ⁴] ⁴⁺ /[(CG) ₆] ₂	1.40	0.76	0 (0.2)

Table 3.6: Rate constants (ms)⁻¹ for Δ -[EuL⁴]⁴⁺ free and bound to [(CG)₆]₂ (295 K)

- (a) Bi-exponential decay was observed with both direct and indirect excitation of the Eu centre, suggesting that both $q=1$ and $q=2$ species may be present.
- (b) Hydration states are estimated using methods defined in the reference 21, wherein the quenching effect of closely diffusing OH oscillators and static amide NH vibrators is accounted for.
- (c) Complex was allowed to undergo H/D exchange for 3h prior to measurement.

The hydration state of Eu when the complex is in the presence of oligonucleotide was determined, using the relation given in Eq 3.9.²¹ Apparently no water molecule is bound, consistent with the displacement by an oligonucleotide phosphate group of the water molecules.

$$q^{\text{Eu}} = 1.2 [(k_{\text{H}_2\text{O}} - k_{\text{D}_2\text{O}}) - 0.25 - 0.075x] \quad (\text{Eq 3.9})$$

where x is the number of proximate NH oscillators which when equidistant are assumed to be quenched in an equivalent manner.

This reorganisation of the coordination sphere around the europium was observed to be time dependent. Rate constants for the complex in the presence of excess oligonucleotide rose to 1.40 ms^{-1} after 30 min, and remained unchanged thereafter-equivalent to a 'resting' hydration state of 0.2.

This time dependent problem inhibited the possibility of examining the interaction by circular dichroism; the time scale of a typical CD acquisition being superior to 30 minutes.

Summary of the binding behaviour of $\Delta\text{-[EuL}^4\text{]}^{4+}$:

The binding behaviour of the complex to each oligonucleotide presents novel features, whose complexity has not allowed the exact nature of the interaction to be defined. No unequivocal evidence for an intercalative binding of the phenanthridinium unit nor improvement of the stereoselectivity has been found. Nevertheless the interaction of the europium with an oligonucleotide phosphate group presents some attractive features as a potentially reactive complex. Many articles dealing about DNA cleavage arise from hydrolytic properties of the lanthanide (III) ions, occurring on the phosphate backbone.²² Thus further studies are warranted to examine the possibility of cleavage in a complex where the lanthanide possesses displaceable water molecules.

- ¹ J.-B. Le Pecq, *Methods of Biochemical Analysis*, Vol.20, Wiley Interscience, New York, 1971.
- ² a) J. Markovits, B. P. Roques, J.-B. Le Pecq, *Analytical Biochemistry*, 1979, 94, 259-264.
b) T.-C. Tang, H.-J. Huang, *Electroanalysis*, 1999, 11, 16, 1185-1190.
- ³ T. Tao, J. H. Nelson, C. R. Cantor, *Biochemistry*, 1970, 9, 18, 3514-3524.
- ⁴ R. S. Dickins, J. A. K. Howard, C. L. Maupin, J. M. Moloney, D. Parker, J. P. Riehl, G. Siligardi, J. A. G. Williams, *Chem. Eur. J.*, 1999, 5, 1095.
- ⁵ a) J. D. McGhee, P. H. von Hippel, *J. Mol. Biol.*, 1974, 86, 469.
b) A. Rodger, B. Nordén, *Circular Dichroism and Linear Dichroism*, Oxford University Press, 1997.
- ⁶ a) R. Lyng, A. Rodger, B. Nordén, *Biopolymers*, 1991, 31, 1709-1720.
b) C. Zimmer, G. Luck, *Advances in DNA Sequence Specific Agents*, 1992, vol. 1, 51-88.
c) W. C. Johnson, *Circular Dichroism : Principles and Applications*, 2nd Ed., 2000, Chap 24, 703-718.
- ⁷ S. L. Klakamp, W. deW. Horrocks, *Biopolymers*, 1990, 30, 33.
- ⁸ A. Triolo, F. M. Arcamone, A. Raffaelli, P. Salvadori, *J. Mass Spectrometry*, 1997, 32, 1186-1194.
- ⁹ C. Hiort, B. Nordén, A. Rodger, *J. Am. Chem. Soc.*, 1990, 112, 1971-1982.
- ¹⁰ J. K. Barton, A. T. Danishefsky, J. M. Goldberg, *J. Am. Chem. Soc.*, 1984, 106, 2172-2176.
- ¹¹ M. T. Carter, M. Rodriguez, A. J. Bard, *J. Am. Chem. Soc.*, 1989, 111, 8901-8911.
- ¹² a) A. S. Balsanov, A. Beeby, J. I. Bruce, J. A. K. Howard, A. M. Kenwright, D. Parker, *Chem. Commun.*, 1999, 1011-1012.
b) L. S. de Bari, G. Pintacuda, R. S. Dickins, D. Parker, P. Salvadori, *J. Am. Chem. Soc.*, 2000, 122, 9257.
- ¹³ a) D. T. Richens, 'The Chemistry of Aqua Ions', Wiley, Chichester, 1997.
b) S. Aime, A. Barge, M. Botta, J. A. K. Howard, J. M. Moloney, D. Parker, A. S. de Sousa, M. Woods, *J. Am. Chem. Soc.*, 1999, 121, 5762-5772.
- ¹⁴ D. Parker, K. Senanayake, J. A. G. Williams, *J. Chem. Soc., Perkin Trans. 2*, 1998, 2129-2140.
- ¹⁵ G. Colmenarejo, A. Holmén, B. Nordén, *J. Phys. Chem. B*, 1997, 101, 5196-5204.
- ¹⁶ B. Honig, A. Nicholls, *Science*, 1995, 268, 1144-1149.
- ¹⁷ a) J. Sartorius, H.-J. Schneider, *J. Chem. Soc., Perkin Trans. 2*, 1997, 2319-2327.
b) H. W. Zimmermann, *Angew. Chem. Int. Ed. Engl.*, 1986, 25, 115-130.
- ¹⁸ R. Mahtab, H. H. Harden, C. J. Murphy, *J. Am. Chem. Soc.*, 2000, 122, 14-17.
- ¹⁹ a) J. K. Barton, *Science*, 1986, 233, 727.
b) N. Grover, N. Gupta, H. H. Thorp, *J. Am. Chem. Soc.*, 1992, 114, 3390.
- ²⁰ a) R. S. Dickins, T. Gunnlaugsson, D. Parker, R. D. Peacock, *Chem. Commun.*, 1998, 1643.
b) J. I. Bruce, R. S. Dickins, T. Gunnlaugsson, S. Lopinski, M. P. Lowe, D. Parker, R. B. Peacock, J.B.B. Perry, S. Aime, M. Botta, *J. Am. Chem. Soc.*, 2000, 122, 9674-9684.
- ²¹ a) A. Beeby, I. M. Clarkson, R. S. Dickins, S. Faulkner, D. Parker, L. Royle, A. S. de Sousa, J. A. G. Williams, M. Woods, *J. Chem. Soc., Perkin Trans. 2*, 1999, 493-503.
b) D. Parker, J. A. G. Williams, *J. Chem. Soc., Dalton Trans.*, 1996, 3613.
- ²² a) M. Komiyama, N. Takeda, H. Shigekawa, *Chem. Commun.*, 1999, 1443-1451.
b) R. Hettich, H.-J. Schneider, *J. Chem. Soc., Perkin Trans. 2*, 1997, 2069-2072.



***6-Phenanthridinyl Based Ligands
for DNA Interaction***

The previous series of complexes involving the phenanthridine chromophore exhibited a particular affinity for nucleic acids, and allowed certain characteristics required for intercalative DNA probes to be defined. The charge and the length of the link between the chiral macrocycle element and the intercalative moiety appeared to be important features for the effective intercalation of the complex into the DNA double strand. In the previous series of complexes, the phenanthridinyl chromophore was linked to the chiral macrocycle via its 2 position. Such a linkage constrained the interaction of the phenanthridine group with the nucleobases.

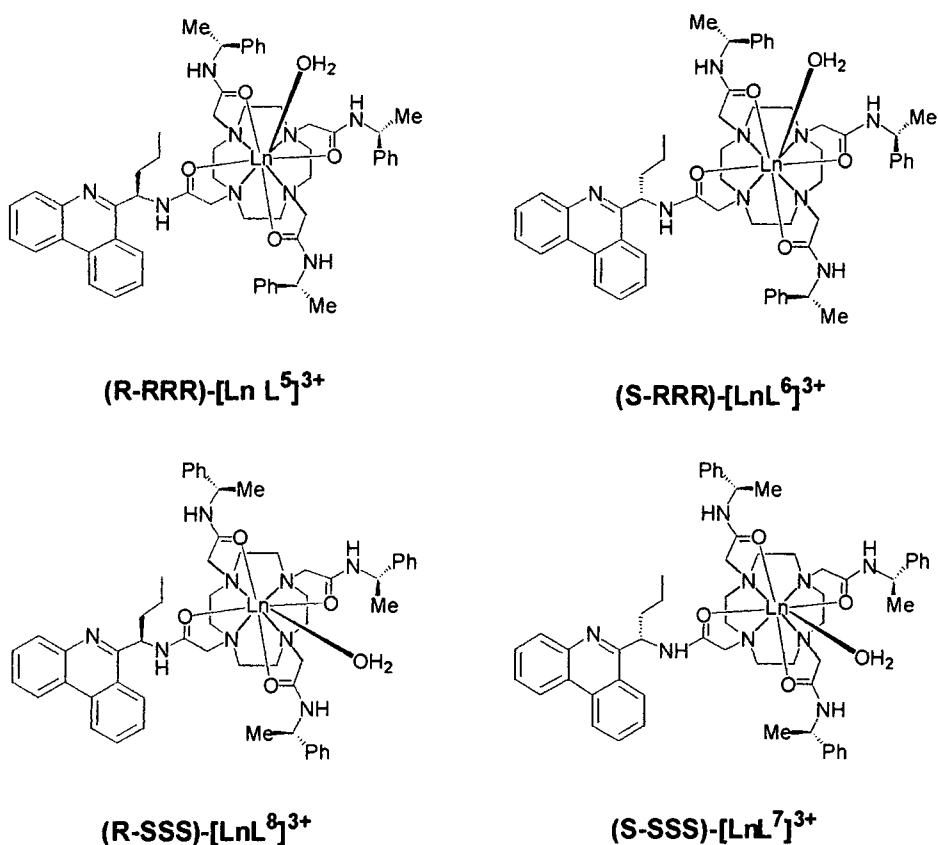
The possibility to link the intercalative chromophore via another position of the aromatic ring may offer alternative geometries to be adopted, depending on whether the delocalised surface is able to interact more favourably with the nucleobases.

In the search for such new DNA probes, the stereoselectivity of the binding represents a fundamental aspect in the selective recognition of the helix. It has been shown that the chiral amide pendent arms, which determine the helicity of the complex, constitute an important issue in this recognition. The design of a new series of complexes was extended in scope by the idea that an additional chiral centre on the intercalative unit arm may help to tune the selectivity of the complex towards the oligonucleotides, by a more appropriate 'fitting' to the DNA backbone.¹

4-1 A new series of chiral phenanthridinyl complexes

4-1.1: Aims and objectives

The salient feature of the chiral complex $[\text{EuL}^1]^{4+}$ was its three chiral pendent arms which conferred a Λ or Δ helicity to the complex. The addition of a fourth arm bearing an additional chiral centre, leads to two sets of diastereoisomers which bear the same major element of helicity but differ in the local chromophore arm chirality. Accordingly, the series of complexes $[\text{LnL}^n]^{3+}$, ($n = 5,6,7,8$), were prepared (Scheme 4.1).

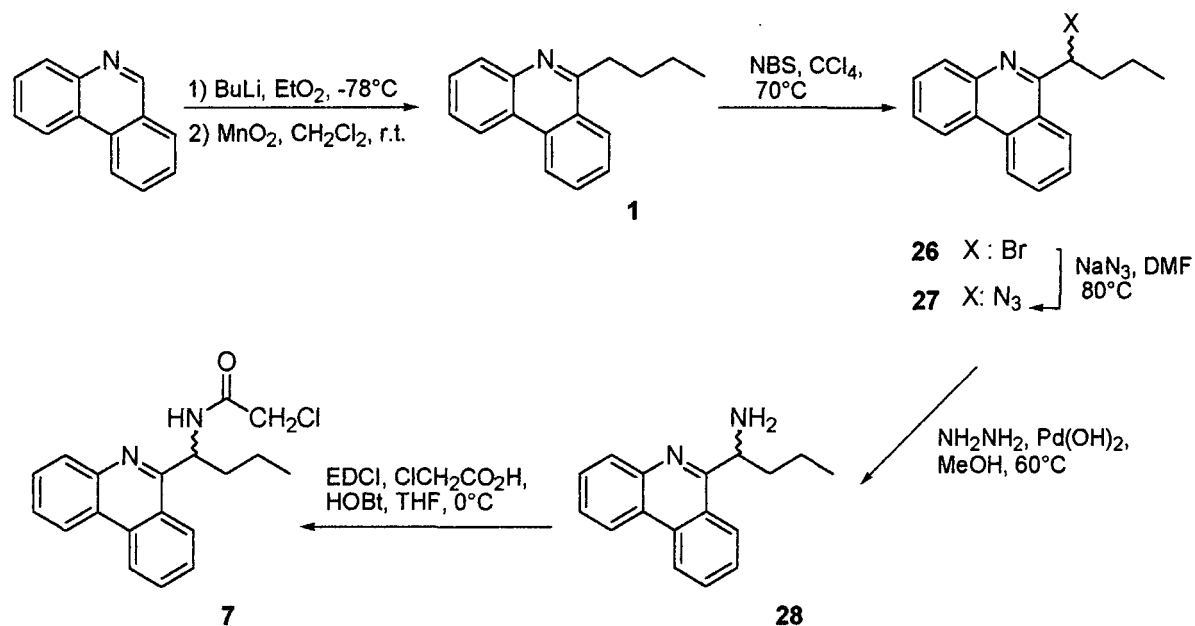
Scheme 4.1: $[LnL^n]^{3+}$ complexes ($n = 5, 6, 7, 8$)

4-1.2: Synthesis of a series of chiral complexes

The synthesis of the enantiopure ligands begins with the functionalization of the phenanthridine chromophore in a racemic α -haloamide, followed by the coupling with the trisubstituted enantiopure cyclen derivative (**29** and **30**). The ligands which are obtained in each case were a mixture of two diastereoisomers, which were separated by column chromatography, giving rise to enantiopure ligands.

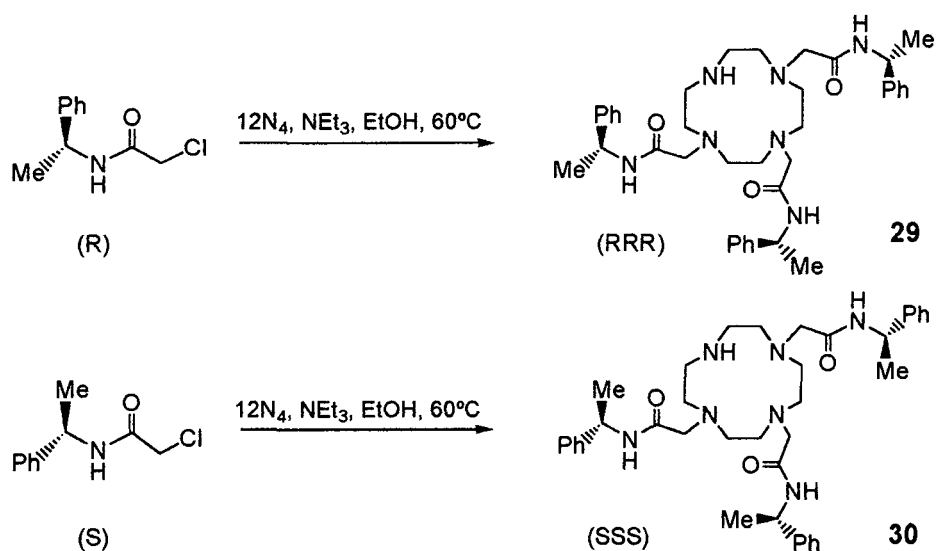
Firstly the phenanthridine was C-alkylated following an established procedure.² Nucleophilic attack of butyl lithium occurs selectively at the 6-position, i.e. α to the phenanthridine nitrogen. The chromophore was re-aromatized using manganese(IV) dioxide. The bromination of **1** occurs preferentially at the benzylic position on the butyl chain, and gave rise to the two enantiomers of **26** as a racemic mixture. Nucleophilic attack (with inversion of configuration) by sodium azide produced **27**, which was then reduced to the amine **7** by a transfer hydrogenation over $Pd(OH)_2/C$. The resultant mixture of (*R*)- and (*S*)-

primary amines were coupled to α -chloroacetic acid in the presence of EDCI and 1-hydroxybenzotriazole, leading to the racemic amide **7**.



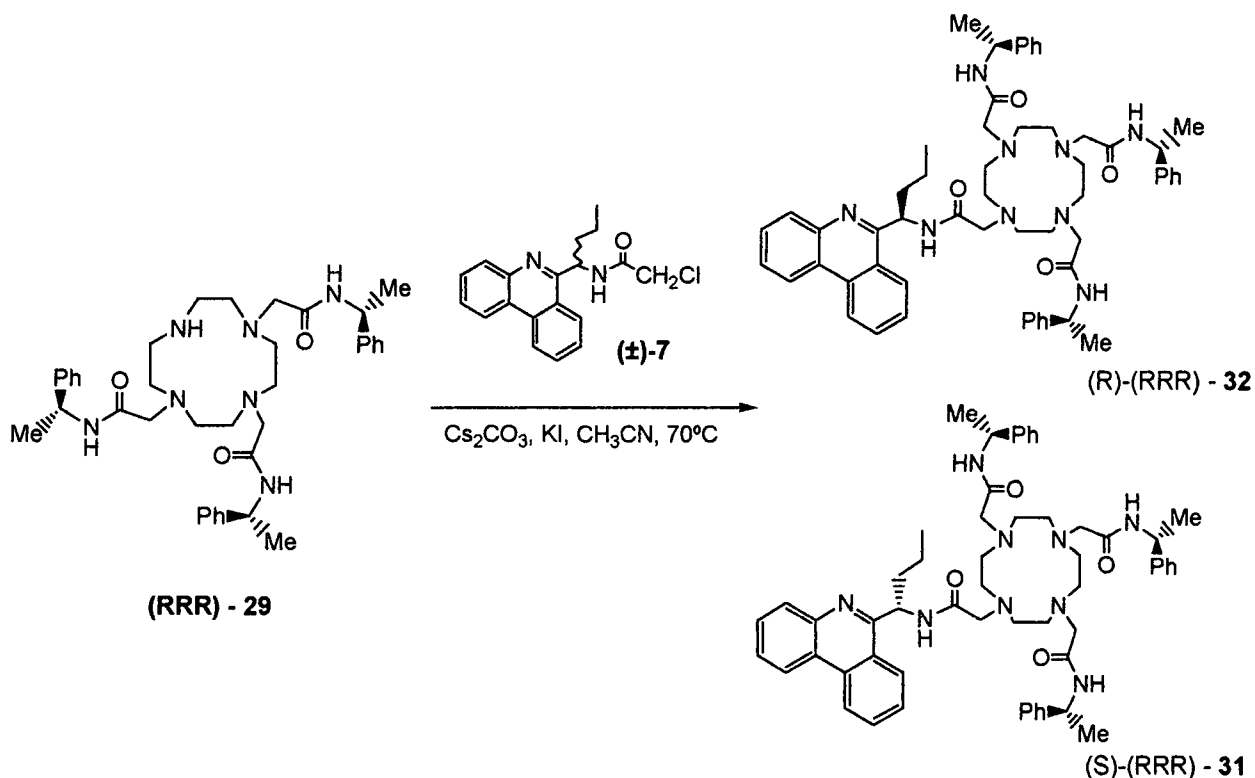
Scheme 4.2: Synthesis of the α -haloamide **7**

The (RRR) or (SSS) chiral trisamides were obtained by reaction of 3 equivalents of the appropriate (*R*)- or (*S*)- α haloamide with cyclen. The reaction was monitored by ESMS and showed the formation of trisubstituted and tetrasubstituted compounds, which were separated by aqueous washing and column chromatography on silica.



Scheme 4.3: Synthesis of the chiral trisamides **29** and **30**

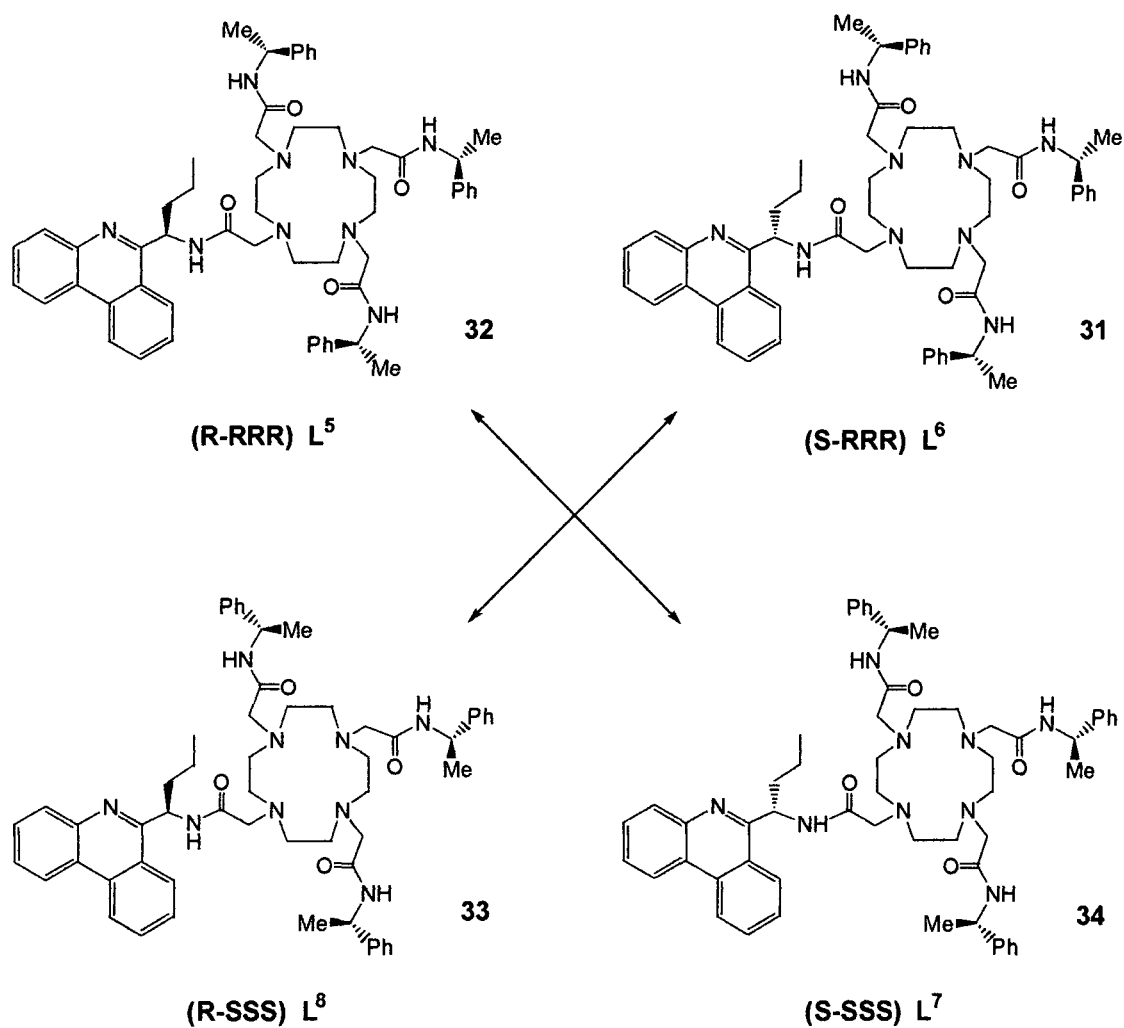
The coupling reaction of racemic **7** with the macrocycles **29** and **30** led to formation of a pair of diastereoisomers, e.g. **31** & **32** and **33** & **34** respectively, which were separated chromatographically, thereby using the chiral macrocyclic element as a chiral auxiliary.



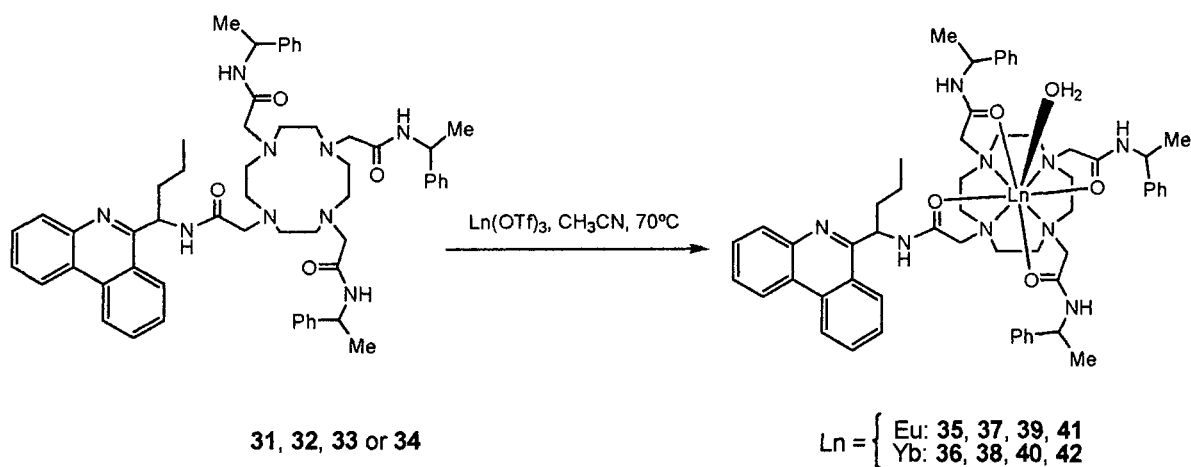
Scheme 4.4: Synthesis of the ligands **31** and **32**

The two diastereoisomers exhibited a different retention factor on neutral alumina. Thus repetitive chromatography column allowed the separation of the enantiopure ligands. The process was repeated using (SSS)-**30** to yield ligands **33** and **34**. Scheme 4.5 depicts the four diastereoisomeric ligands **31**, **32**, **33**, and **34**, that were isolated following this procedure. The assignment of the chirality for each of the four ligands was carried out by comparison of their NMR spectra. Each enantiomeric pair exhibited the same pattern of couplings.

The complexation of lanthanide ions was carried out using the appropriate lanthanide triflate salt in acetonitrile. The europium complexes **35**, **37**, **39**, **41**, and ytterbium complexes **36**, **38**, **40**, **42** were purified by precipitation of the triflate salt in 10% aqueous methanol (Scheme 4.6).



Scheme 4.5: Four diastereoisomeric ligands L⁵, L⁶, L⁷ and L⁸ showing the enantiomeric relationships



Scheme 4.6: Synthesis of the lanthanide complexes of the stereoisomeric tetra-amides

Attempts to quaternise the phenanthridine nitrogen were unsuccessful. Diverse alkylating agents like methyl triflate, dimethyl sulfate, or benzyl chloride were used in dipolar solvents (MeCN, PhNO₂) over a range of temperatures but without any success.

An explanation for the absence of reaction is the lower nucleophilicity of the phenanthridinium nitrogen; hydrogen-bonding between the amide NH and the phenanthridine N may inhibit nucleophilic attack. Furthermore the α -substitution sterically hinders the approach of any alkylating agent.

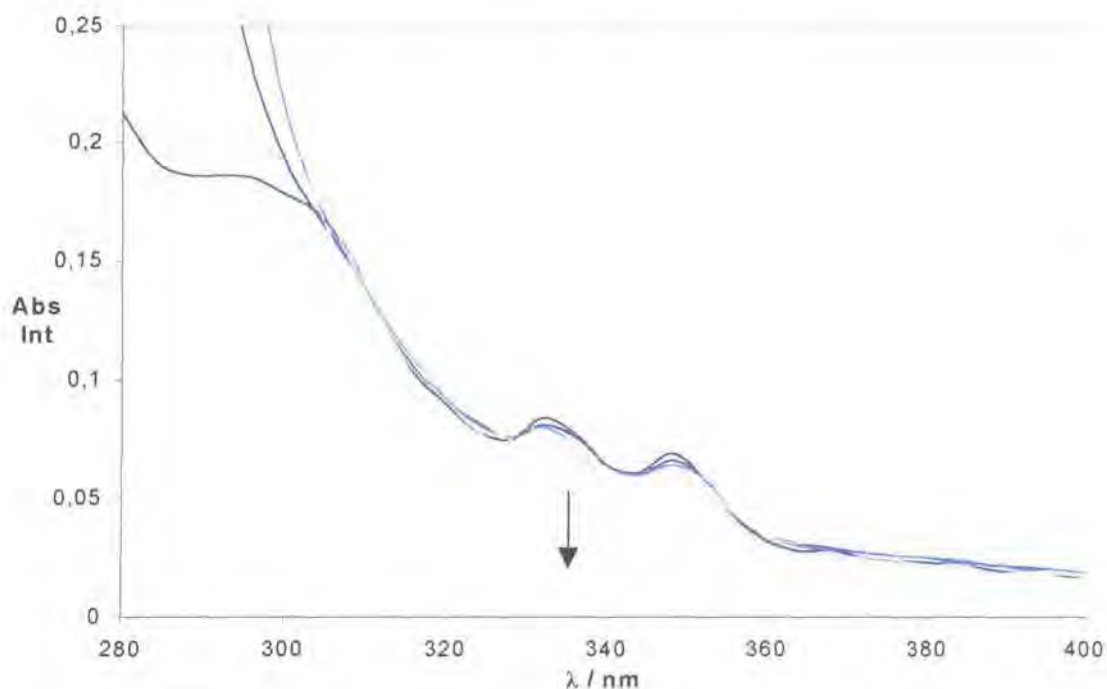
Some pK_a titrations were carried out to measure the basicity of the phenanthridine nitrogen, for compound 7, and in the complexes 37 and 40. A pK_a value of under 3 was measured by monitoring changes on the absorption and emission spectra as a function of pH. The low basicity of the nitrogen suggests that both steric inhibition of solvation and intramolecular hydrogen-bonding may be occurring.

The ¹H NMR spectra of the europium and ytterbium complexes (295K, 400 MHz) exhibited a set of 5 singlets (1:3:2:1:1) for the four most shifted macrocycle axial ring protons between +30 and +26 ppm for europium complexes and +111 and +103 ppm for ytterbium complexes. This behaviour is consistent with the existence of two stereoisomers in solution for each complex. The macrocyclic ring may adopt different conformations around the lanthanide ion, in each of these isomers. Usually and as revealed by several X-ray analyses, for an (*S*)- stereocentre each of the -NCCN- chelates adopts a λ conformation. In this case ($\lambda\lambda\lambda\lambda$) and ($\delta\lambda\lambda\lambda$) may exist. Such a situation is not unprecedented: Morrow has reported such examples in the structural analysis of europium tetra-amide complexes with four simple -CH₂CONH₂ side arms.³

4-1.3: Interaction with nucleic acids

4-1.3.1: Absorbance and fluorescence spectroscopies

To evaluate the affinity of these complexes for nucleic acids, they were titrated against [(CG)₆]₂ under the same conditions as described previously. As the phenanthridine nitrogen is not alkylated, the absorbance spectra exhibits three bands at 295, 333 and 348 nm to shorter wavelength of the phenanthridinium chromophore, and the maximum intensity of absorption was noted at 270 nm.

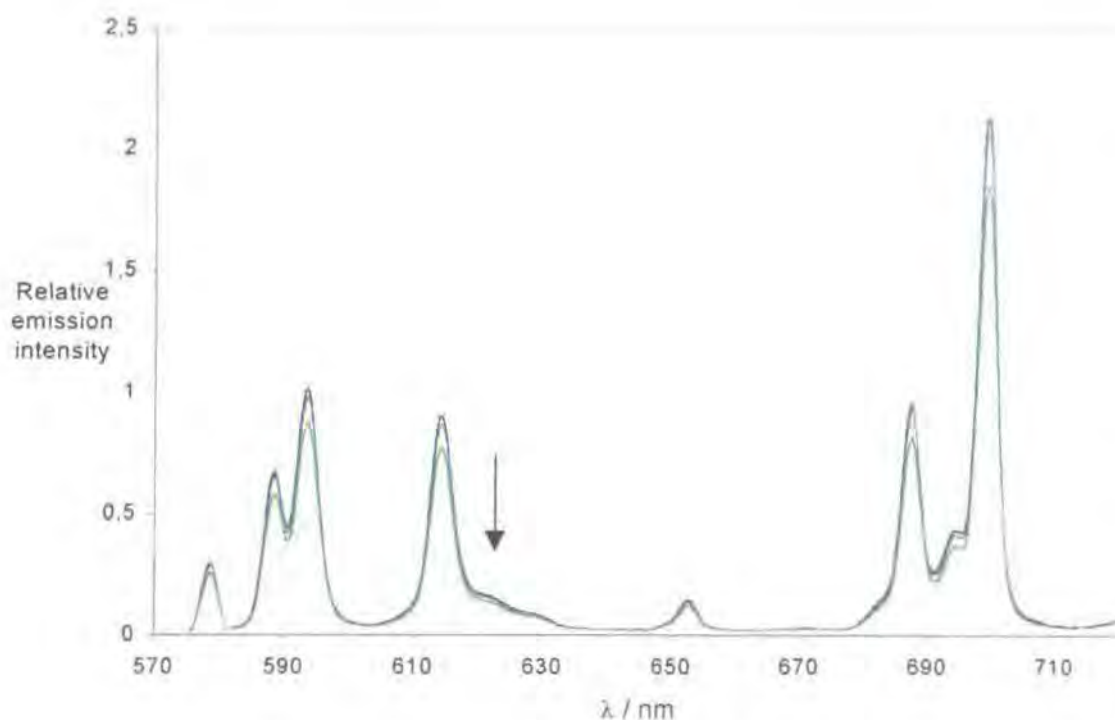


*Scheme 4.7: Absorbance spectra of complex $[EuL^7]^{3+}$ **39** following addition of $[(CG)_6]_2$
Final ratio $[(CG)_6]_2/\text{complex}$ [1;2.3] (295K, pH 7.4, 10 mM NaCl, 10 mM HEPES)*

Upon addition of $[(CG)_6]_2$ each complex saw its absorbance decrease slightly for the two bands at 333 and 348 nm with an isosbestic point at 310 nm, as shown Scheme 4.7. The hypochromism at 348 nm was calculated to range between 10 and 20% for each complex examined.

A slight shift of the spectrum to the red was observed when the complex was saturated with $[(CG)_6]_2$ but this is not as pronounced as the effect observed in the cases of previous complexes described in Chapter 3. Nevertheless, the same small red shift of 3 nm was measured for each complex of the series, i.e. the shift was independent of the chirality and was the same for Eu and Yb complexes.

The affinity towards $[(CG)_6]_2$ was investigated by luminescence spectroscopy, by monitoring the phenanthridine fluorescence at 385 nm and the europium emission at 615 nm for the $\Delta J = 2$ transition. The quenching of the fluorescence upon addition of oligonucleotide results in a quenching of the emissive state of europium as well. Both phenomena undergo the same variation, and the same quenching effect was observed in each of the Eu transitions, indicating that no perturbation of the Eu coordination environment occurred on complexation (Scheme 4.8).



*Scheme 4.8: Luminescence of complex $[EuL^5]^{3+}$ **35** following addition of $[(CG)_6]_2$ (295K, $\lambda_{exc} = 304$ nm, 10 mM NaCl, 10 mM HEPES pH 7.4)*

The evaluation of the apparent binding affinities using the McGhee and von Hippel method was rather difficult to interpret. The observed fluorescence decay was such that rather weak emission was observed near the end-point which may account for the non-linearity seen in the McGhee-von Hippel analysis. Such behaviour suggests a binding mechanism involving more than one step or more than one binding mode. Nevertheless the apparent binding affinities found for the interaction of the four europium complexes with $[(CG)_6]_2$ fell in the same range of 10^6 $M^{-1} \cdot duplex^{-1}$ (Table 4.1). The apparent binding site size remains in all cases fairly similar, but is unusually high considering that these complexes do not bind very strongly. The larger degree of hypochromism of the $[EuL^5]^{3+}$ complex **35** is suggestive of a stronger binding in this case. This was corroborated by the fluorescence quenching behaviour (63 % diminution, $\lambda_{em} = 615$ nm). This parameter cannot be of course used as a determinant for the evaluation of the binding strength.

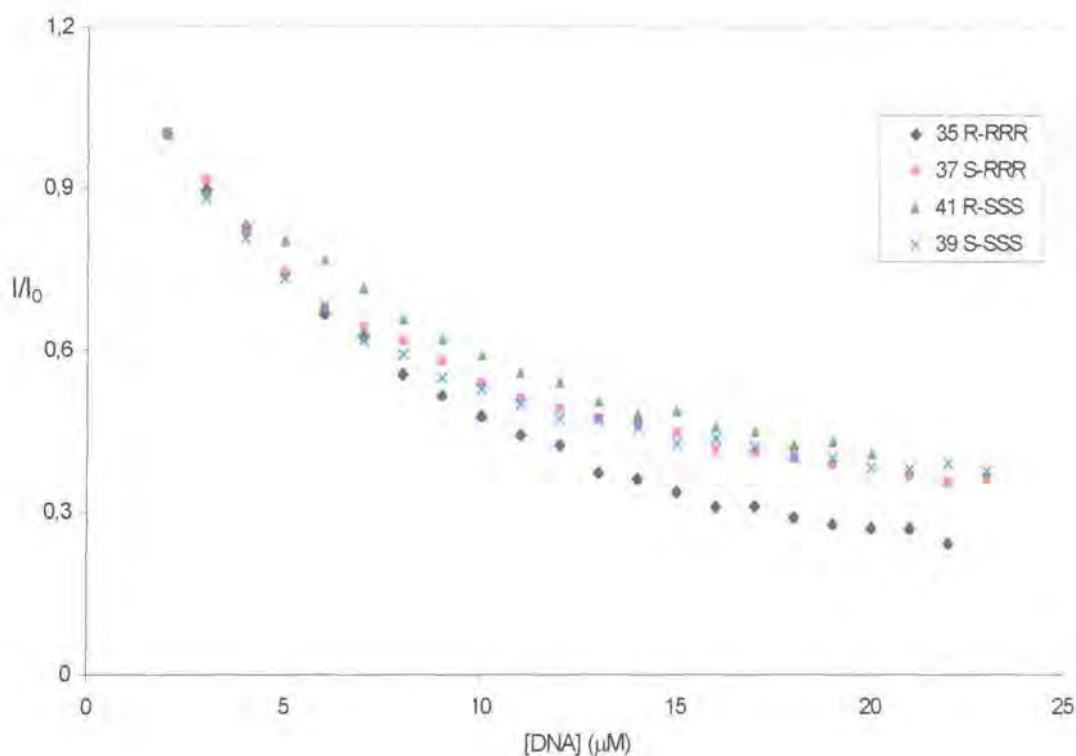
<i>Complex</i>	$K^{\#}$ (10^5) ($M^{-1} \cdot \text{duplex}^{-1}$)	$n^{\#}$ (duplex^{-1})	% Hypochromism (348nm)
(<i>R</i> -RRR)- 35 [EuL^5] $^{3+}$ /[(CG) $_6$] $_2$	16	7.7	20
(<i>S</i> -RRR)- 37 [EuL^6] $^{3+}$ /[(CG) $_6$] $_2$	13	8	12
(<i>S</i> -SSS)- 39 [EuL^7] $^{3+}$ /[(CG) $_6$] $_2$	9	9.8	13
(<i>R</i> -SSS)- 41 [EuL^8] $^{3+}$ /[(CG) $_6$] $_2$	16	6.6	8

[#] Typically [LnL] = 20-30 μM ; the binding value showed a dependence on the concentration of complex; data from fluorescence intensity changes with added oligonucleotide were analyzed with the method of McGhee and von Hippel.

Table 4.1: Intrinsic binding constants (K), site sizes (n), and degree of hypochromism measured for complexes of [(CG) $_6$] $_2$ with [EuL^5] $^{3+}$, [EuL^6] $^{3+}$, [EuL^7] $^{3+}$, and [EuL^8] $^{3+}$

Because the values obtained by the analysis of McGhee and von Hippel were not considered to be sufficiently accurate to establish the real effect of the additional chiral chromophore arm for the four diastereoisomeric europium complexes, their relative fluorescence decay curves were analysed (Scheme 4.9).

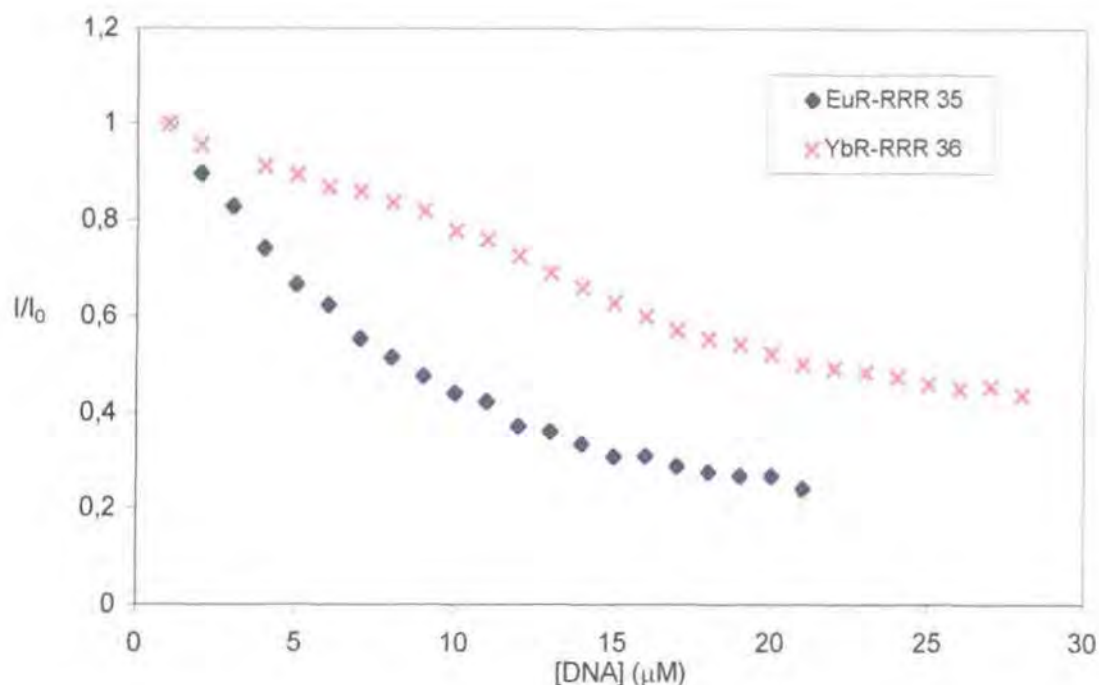
The [EuL^5] $^{3+}$ complex **35** showed the largest reduction in its fluorescence intensity being quenched 10% more than the three other complexes. This difference may be tentatively associated with a more suitable geometry in the binding to [(CG) $_6$] $_2$ compared to the other complexes. The phenanthridine chromophore in **35** may take up a more favourable binding geometry with respect to the oligonucleotide and give rise to a more efficient excited state quenching involving the DNA bases. In terms of affinity, the *chiral link* to the chromophore does not appear to influence binding selectivity, although the quenching of the emission intensity revealed a different pattern of behaviour for the (*S*-RRR) and (*R*-SSS) complexes **37** and **41**. They both exhibited a modest discontinuity, which could be related to a stepwise binding process.



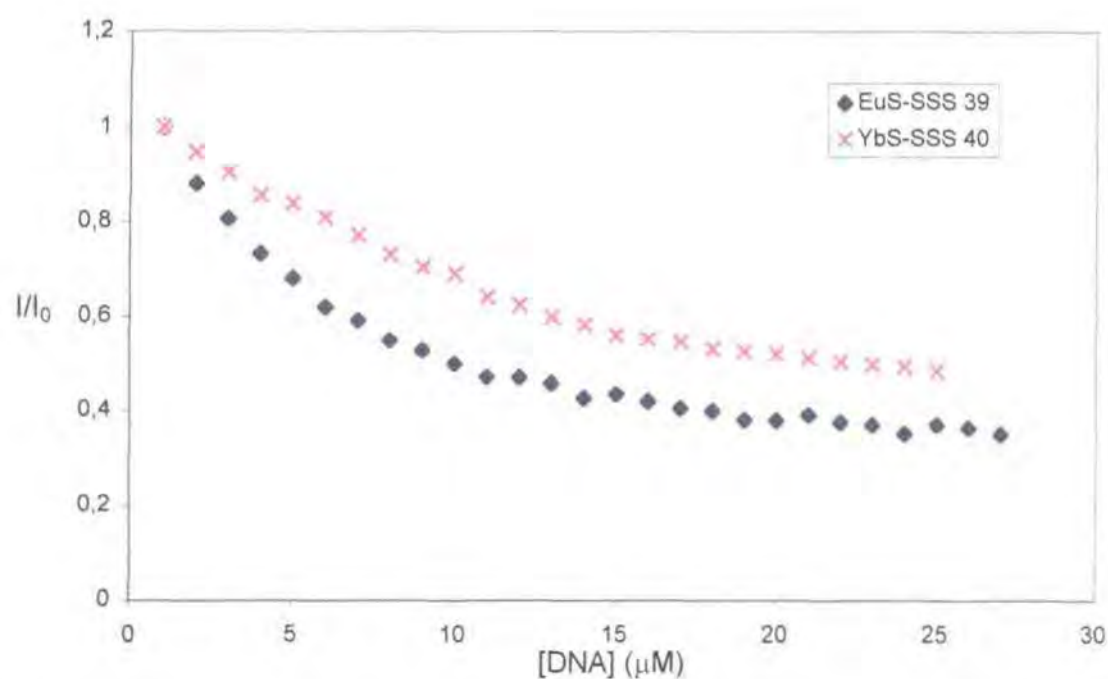
Scheme 4.9: Fluorescence quenching decay curves for Eu complexes 35, 37, 39, and 41 as a function of [(CG)₆]₂ concentration (295K, $\lambda_{exc} = 304$ nm, pH 7.4, 10 mM NaCl, 10 mM HEPES)

Comparison of europium and ytterbium complexes

Despite the unchanged geometry of the complex the nature of the lanthanide is likely to influence the binding with these series of complexes as well. Thus the behaviour of ytterbium complexes was investigated and compared to the analogous europium complexes.



Scheme 4.10: Phenanthridine fluorescence decay of $[EuL^5]^{3+}$ **35** and $[YbL^5]^{3+}$ **36** following addition of $[(CG)_6]_2$ (295K, $\lambda_{exc} = 304$ nm, $\lambda_{em} = 385$ nm, pH 7.4, 10 mM NaCl, HEPES)



Scheme 4.11: Phenanthridine fluorescence decay of $[EuL^7]^{3+}$ **39** and $[YbL^7]^{3+}$ **40** following addition of $[(CG)_6]_2$ (293K, $\lambda_{exc} = 304$ nm, $\lambda_{em} = 385$ nm, 10 mM NaCl, HEPES pH 7.4)

Firstly the quenching of ytterbium complexes appeared in each case to be less significant than was observed for europium. For the L^5 isomer the change of lanthanide from europium to ytterbium results in a 20% reduction in quenching, and for the S-SSS isomer the difference in quenching was 10%. The ytterbium complexes appeared to bind less strongly than the europium complexes to the oligonucleotide.

Secondly the ytterbium complexes were more likely to exhibit a discontinuity in their quenching decay profile. This is more marked for $[\text{YbL}^{5}]^{3+}$, **36**, than for $[\text{YbL}^{7}]^{3+}$, **40**, which is consistent with the assumption that a stepwise binding process is more likely to be observed for the weakest complex [DNA-ligand].

One possible reason for the difference of affinity between europium and ytterbium complexes is the acidity of the water molecule bound to the lanthanide. In the case of the more charge dense ytterbium complexes, this water is more acidic.⁴ It is possible that the bound water at Yb is significantly ionised, forming a $[\text{YbLOH}]^{2+}$ complex at ambient pH. The lower residual charge on the complex offers a simple explanation for the difference in affinity.

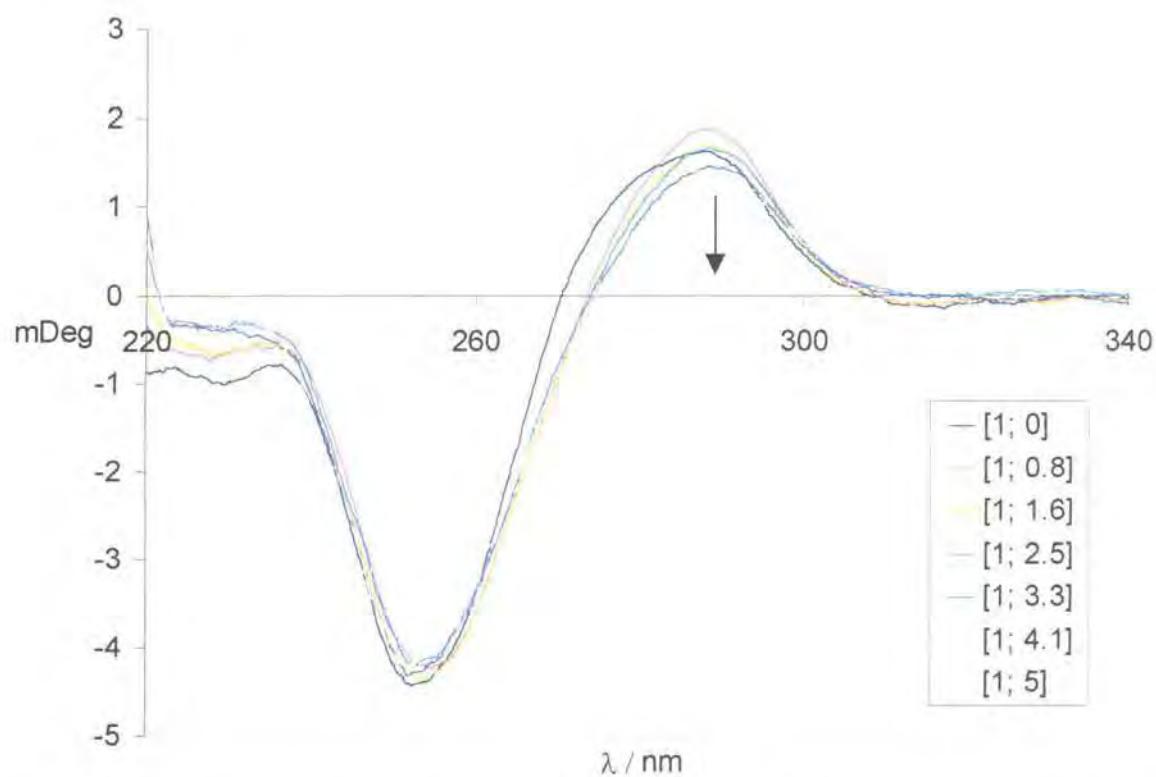
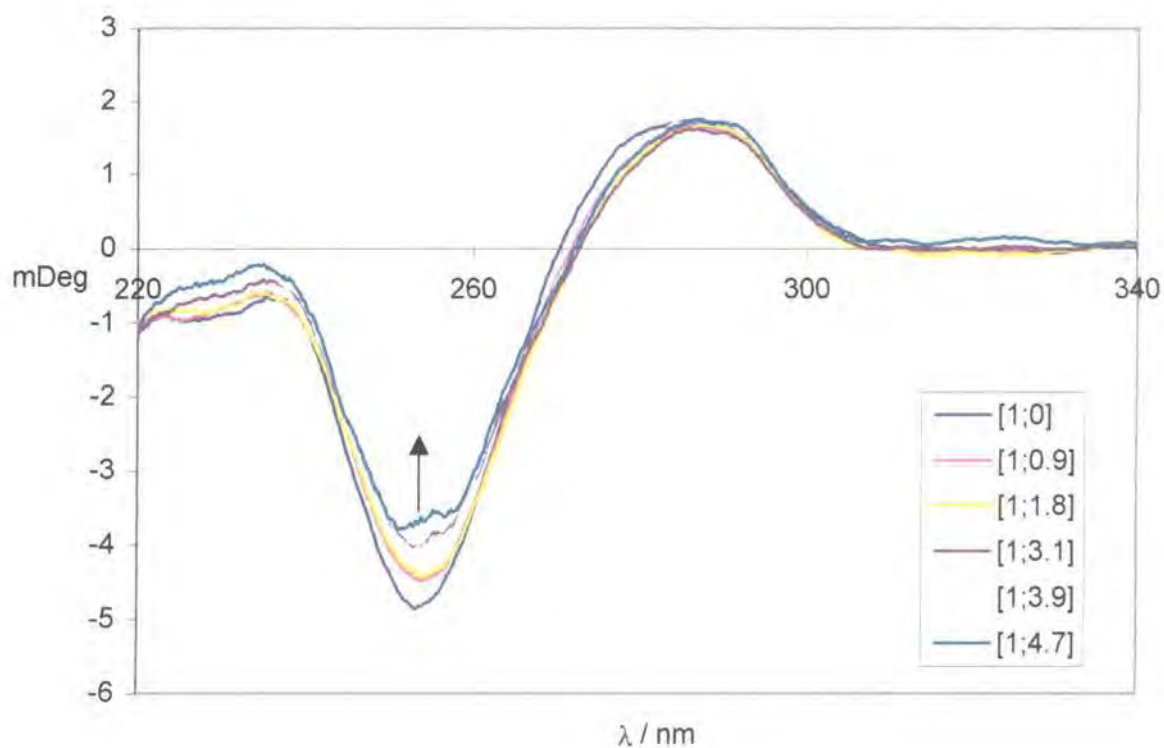
This difference is also highlighted with the CD experiments in the following part 4.1-2.2.

For the simple reason of lack of affinity, the interaction of these complexes with $[(\text{AT})_6]_2$ was studied qualitatively only for the $[\text{EuL}^{5}]^{3+}$ complex, **35**. The fluorescence and absorbance measurement revealed only slight variations, which precluded a more detailed analysis.

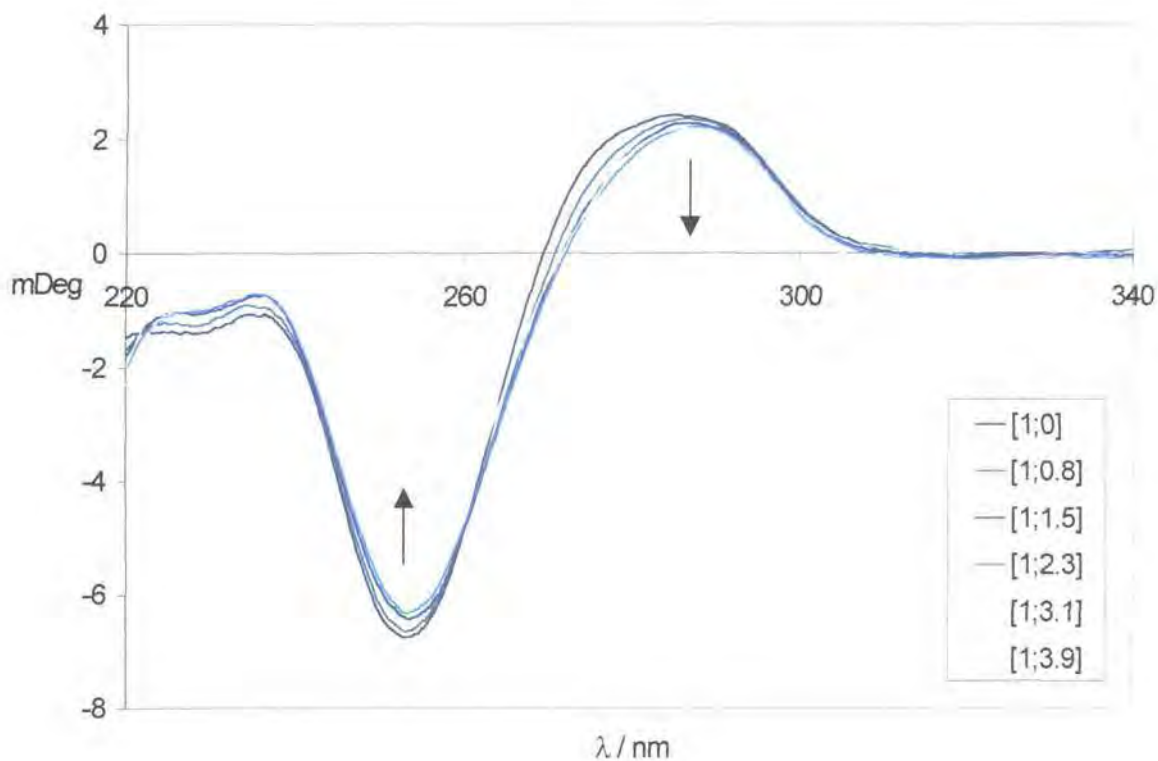
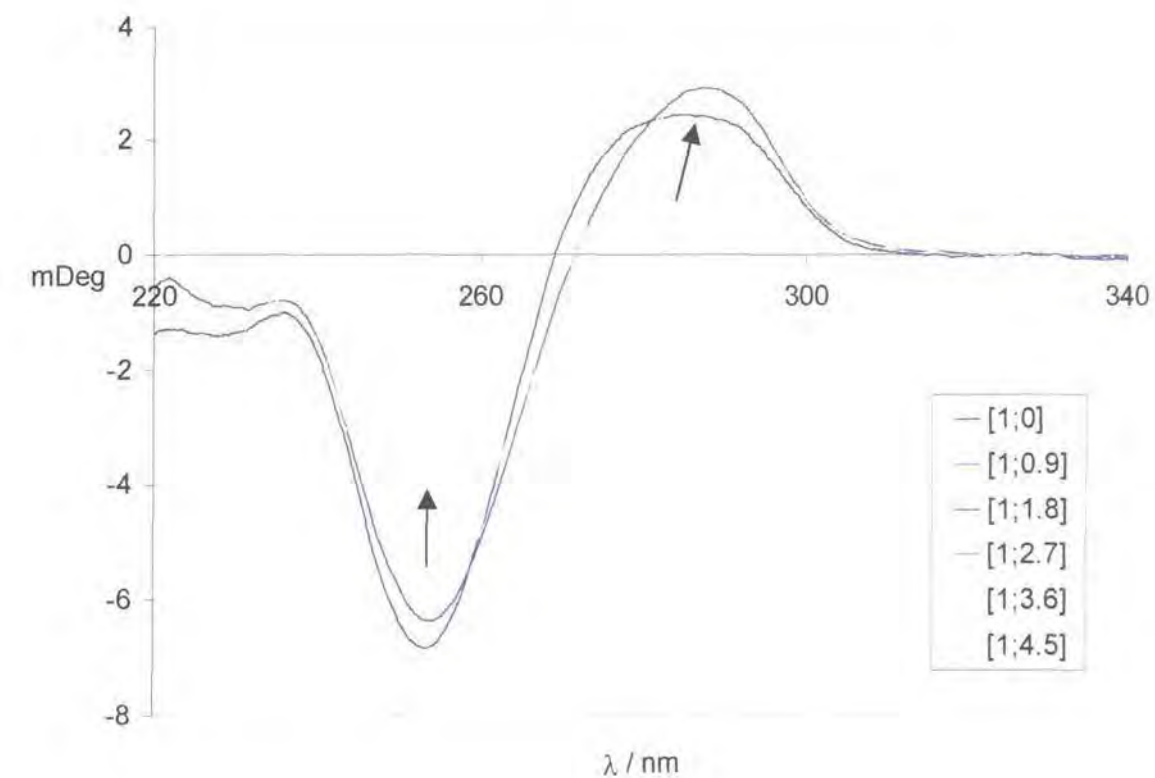
4-1.3.2: CD titrations

The difference between europium and ytterbium complexes was also investigated by circular dichroism studies. The small variations observed by absorption and emission spectroscopy even in the case of the (R-RRR) and (S-SSS) isomers did not allow firm conclusions to be reached concerning the selectivity upon binding of the different complexes. Only the (R-RRR) and (S-SSS) enantiomers of europium and ytterbium complexes were examined in their binding to $[(\text{CG})_6]_2$.

The difference CD spectra were recorded following the addition of each of the enantiomeric complexes. Thus the importance of the complex helicity was investigated as well as the influence of the lanthanide complexed.



Scheme 4.12: Difference CD spectra of $[(CG)_6]_2$ following addition of complexes $[EuL^7]^{3-}$ **39** (upper) and $[EuL^5]^{3+}$ **35** (lower) (295K, 10 mM NaCl, 10 mM HEPES pH 7.4)



Scheme 4.13: Difference CD spectra of $[(CG)_6]_2$ following addition of complexes $[YbL^7]^{3+}$ **40** (upper) and $[YbL^5]^{3+}$ **36** (lower) (295K, 10 mM NaCl, 10 mM HEPES pH 7.4)

Spectra were recorded following addition of the Δ and Λ europium complexes to $[(CG)_6]_2$. Different behaviour was observed in each case (Scheme 4.12). The negative band at 265 nm decreased in intensity when the complex Δ -[EuL⁷]³⁺, **39**, saturated the oligonucleotide. A slight shift to higher wavelength was also observed for the positive band at 285 nm. In the case of the Λ -[EuL⁵]³⁺ complex, **35**, the negative band at 265 nm remained unchanged while the positive band at 285 nm decreased in intensity and shifted slightly to the red. Thus each complex induces different changes in the conformation of the dodecamer $d(CG)_6$. The chirality of the europium complex indeed determines the nature of the binding interaction, as expected for such diastereoisomeric complexes.

Secondly, the case of the ytterbium complexes Λ -**36** and Δ -**40** was examined (Scheme 4.13). Upon the addition of either complex, a decrease in intensity was observed for both bands at 265 and 290 nm, and thus suggested a similar type of chiral interaction.

The effect of varying the lanthanide ion was revealed by comparing the CD difference spectra for the same ligand complexed by either europium or ytterbium. The changes induced in the oligonucleotide duplex upon addition of ligand L⁷ are of different nature for europium or ytterbium. Decreases in intensity were observed in 285 and 255 bands in the case of the ytterbium complex, **40**, while for the corresponding europium complex, **39**, only the 255 nm band was affected.

With the Λ -(R-RRR) complexes, the position of the band at 255 nm does not change for the europium complex, **35**, only the positive band at 285 nm exhibit an intensity decrease which was also observed for the ytterbium complex, **36**.

With both enantiomeric ligands, the nature of the complexed metal affected the DNA conformation in such a way that the characteristic pair of transitions of a B-form $d(CG)_6$ were reduced in intensity or remained unmodified. The chirality of the ligand also promoted a variation of intensity for the negative band for the Δ -complexes, while the Λ -complex perturbed (lowering and red shift) the 290 nm positive band.

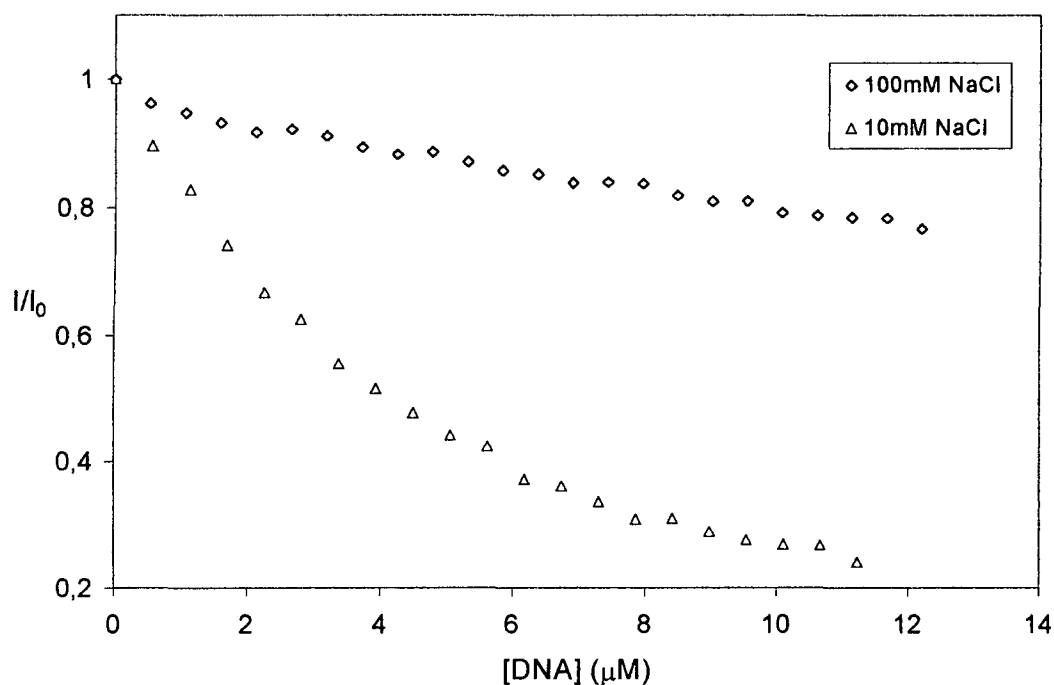
With these series of tricationic complexes the possibility of examining induced CD bands in the visible region cannot be investigated. This experiment which proved valuable in

the case of the tetracationic complexes, i.e. those bearing a quaternized nitrogen on the phenanthridine chromophore, was not possible with this series as the absorption bands were much reduced in intensity in this region.

4-1.3.3: Ionic strength influence

The effect of ionic strength on the binding of the $[\text{Eu-L}^5]^{3+}$ complex was investigated in the same way as for the tri-cationic complex $\Lambda\text{-}[\text{EuL}^{3a}]^{3+}$, by absorbance and fluorescence spectroscopy. An estimation of apparent binding affinities was not considered possible due to the small changes observed. Consequently, comparative fluorescence decay curves were plotted for qualitative analysis.

The interaction of the more strongly bound complex $[\text{EuL}^5]^{3+}$ with $[(\text{CG})_6]_2$ was studied in low salt (10 mM NaCl) and at higher ionic strength (100 mM NaCl) (Scheme 4.14).

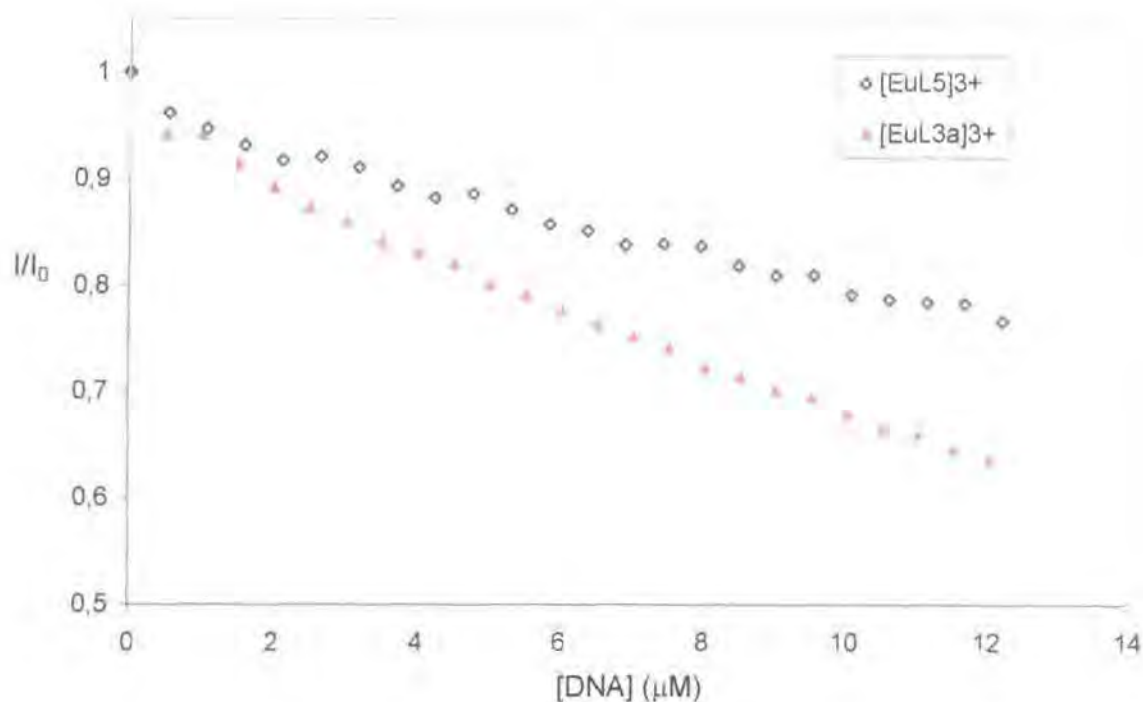


Scheme 4.14: Fluorescence intensity changes ($\lambda_{exc} = 304 \text{ nm}$, $\lambda_{em} = 385 \text{ nm}$) of $[\text{EuL}^5]^{3+}$ following addition of $[(\text{CG})_6]_2$ in 10 mM and 100 mM sodium chloride (295K)

The intensity of the fluorescence was lowered by up to 75% in 10 mM added salt, while in the presence of 100 mM NaCl, the intensity was only quenched by 20%. Such a

large change suggests a binding mode to $[(CG)_6]_2$ for this complex predominantly involving a large electrostatic component.

To assess the influence of the high ionic strength on the tri-cationic complex $[EuL^5]^{3+}$, its fluorescence decay curve was also compared to that obtained with $[EuL^{3a}]^{3+}$ under the same conditions (Scheme 4.15).



Scheme 4.15: Fluorescence intensity changes ($\lambda_{exc} = 304 \text{ nm}$, $\lambda_{em} = 385 \text{ nm}$) of $[EuL^{3a}]^{3+}$ and of $[EuL^5]^{3+}$ following addition of $[(CG)_6]_2$ in 100 mM sodium chloride (295K)

Both curves show a similar form suggesting that the behaviour of the two complexes $[EuL^{3a}]^{3+}$ and $[EuL^5]^{3+}$ in their binding to $[(CG)_6]_2$ under high salt concentration may be similar. The quenching of the fluorescence from the phenanthridine apparently decays almost linearly, and does not show the marked curvature revealed under lower ionic strength conditions.

The fluorescence of the complex $[EuL^{3a}]^{3+}$ is quenched by 15 % more upon binding to $[(CG)_6]_2$ compared to the $[EuL^5]^{3+}$ complex. This observation suggests a stronger association for $[EuL^{3a}]^{3+}$ - $[(CG)_6]_2$ than for $[EuL^5]^{3+}$ - $[(CG)_6]_2$. The reasons for this difference can only be the linking direction or the greater degree of steric hindrance around the phenanthridine

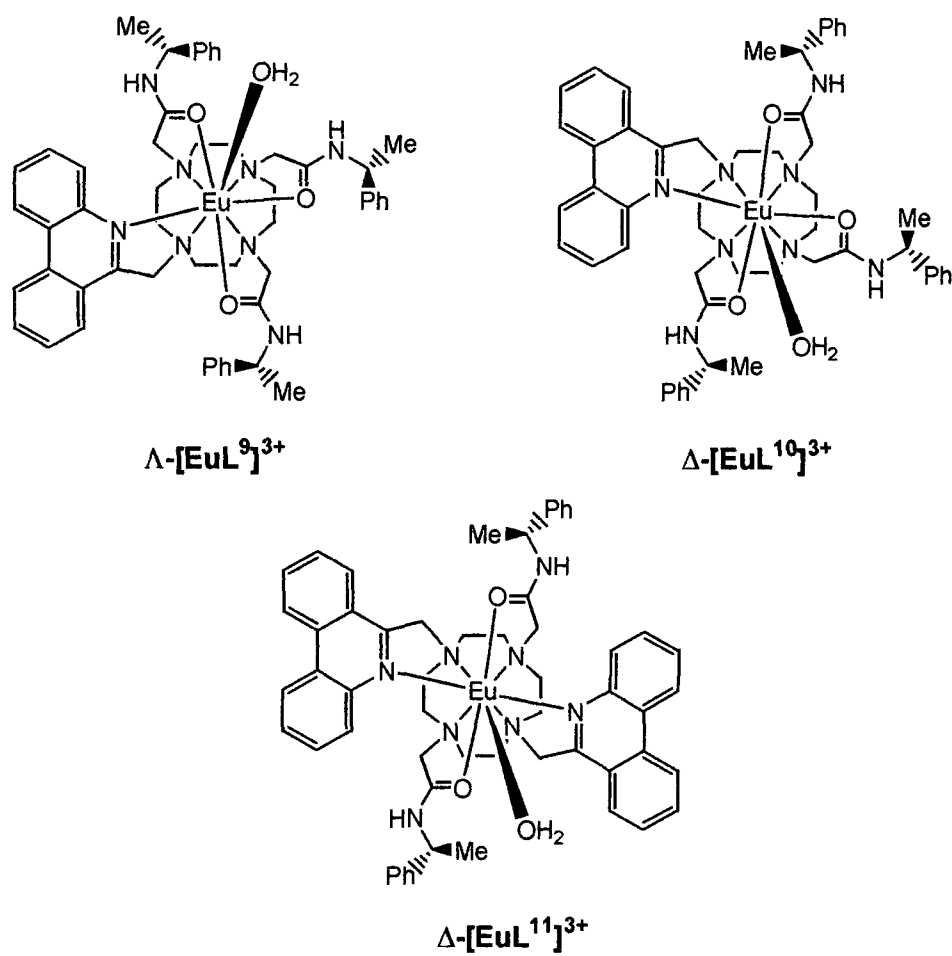
group, which may limit the degree of contact with the DNA bases. The electrostatic contribution seems to constitute an important part component in the binding of these complexes to oligonucleotides, since no definitive evidence of intercalation of the phenanthridine moiety has been found.

Summary of the binding behaviour of $[LnL^{5-8}]^{3+}$:

The presence of the additional chiral centre on the linking arm did not improve the selectivity upon binding. It also lowered the nucleophilicity of the phenanthridine nitrogen which inhibited *N*-alkylation. Nevertheless a common point emerged: the Λ -isomers for both of the tri-cationic series of complexes Λ -[EuL^{3a}]³⁺ and Λ -[EuL⁵]³⁺ showed the strongest affinity possibly suggesting a binding mode involving a more complementary interaction with the minor groove. Such a conclusion needs to be substantiated by additional experiments however.

4-2 Mono and bis chiral phenanthridinyl complexes

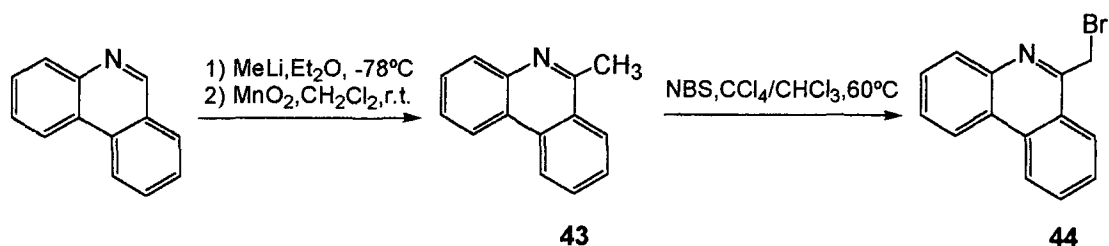
In the third chapter, the chiral lanthanide complexes incorporating an *N*-phenanthridinium moiety were shown to exhibit some CG base-pair selectivity. The element of helicity around the lanthanide ion was also important in this recognition process, so consideration was given to bringing it closer to the intercalative moiety aiming to try and improve the selectivity of this interaction. The shortening of the linking arm led to a complex where the phenanthridine nitrogen itself acts as a coordinating atom for the lanthanide, thereby satisfying a coordination number of 8. Thus the potentially intercalative chromophore was once again a neutral phenanthridine moiety. The effect of such a modification was studied by examining the series of complexes Δ - and Λ -[EuL⁹⁻¹⁰]³⁺ and the bis phenanthridine analogue Δ -[EuL¹¹]³⁺ (scheme 4.16).



Scheme 4.16: The 6-substituted phenanthridine-bound complexes Λ -[EuL⁹]³⁺, Δ -[EuL¹⁰]³⁺ and Δ -[EuL¹¹]³⁺

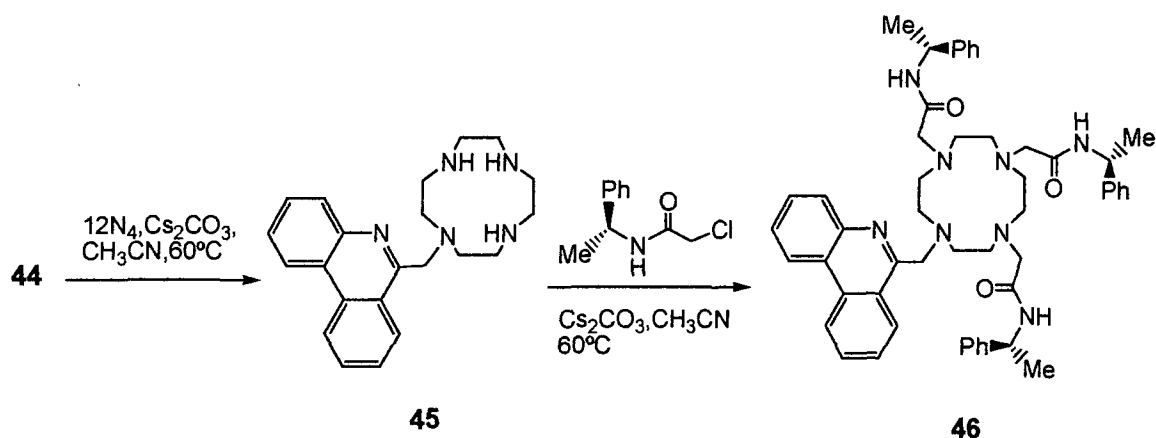
4-2.1: Synthesis of a series of chiral complexes

The substitution of the phenanthridine in the 6-position was carried out following established methods,² involving nucleophilic attack by methyl lithium in THF at low temperature (Scheme 4.17). The re-aromatization of the ring was performed using manganese dioxide in dichloromethane. Bromination of **43** using *N*-bromosuccinimide in a mixture of chloroform and dichloromethane occurred exclusively at the benzylic position and led to the desired mono-bromo product **44**.



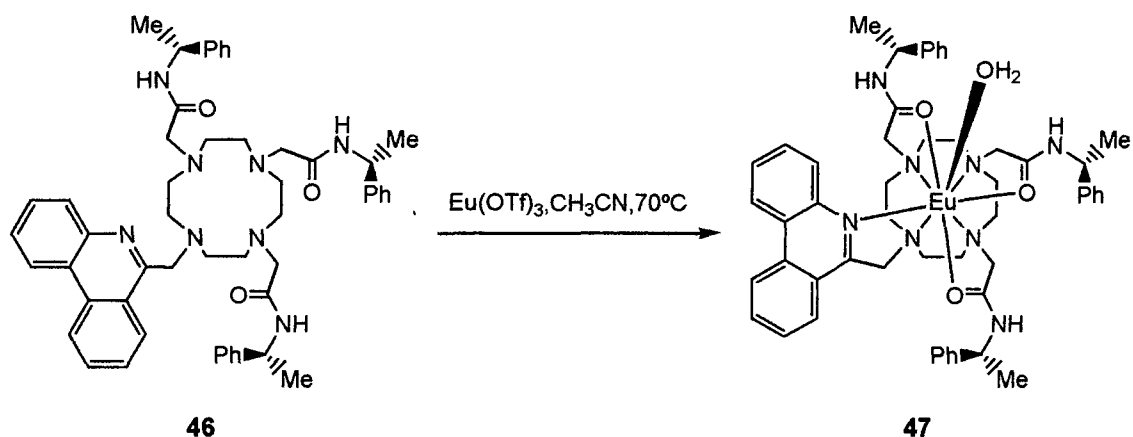
Scheme 4.17: Synthesis of the 6-bromomethylphenanthridine

The coupling of **44** with the cyclen was performed in acetonitrile in the presence of caesium carbonate to give the tetra-amide **45**. The ligand **46** was obtained by the functionalization of the macrocyclic unit with the chiral α -chloroamide (Scheme 4.18).



Scheme 4.18: Synthesis of the ligand *L*⁹

Complexation of a lanthanide occurred easily by reaction of the metal triflate salt in dry acetonitrile. The complexes were purified by precipitation of their triflate salt in aqueous methanol. The phenanthridine nitrogen may not be alkylated here, due its involvement in the coordination of the lanthanide.



Scheme 4.19: Synthesis of the complex (RRR)-[EuL⁹]³⁺

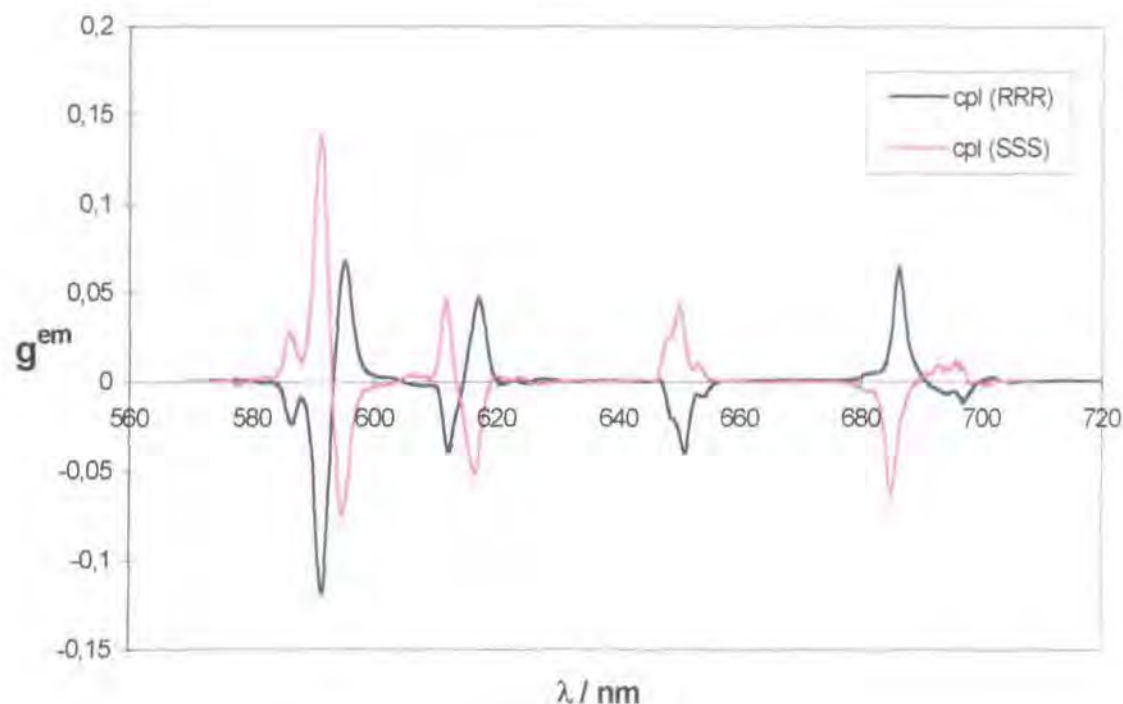
Following the same procedure,⁵ the ligand enantiomer L¹⁰ bearing three (S)-amide pendent arms was obtained.ⁱ For purposes of comparison, the synthesis of a *bis* analogue⁶ was also carried out to investigate the possibility of such a complex spanning two oligonucleotides. The distance between the phenanthridine group in [EuL¹¹]³⁺ is about 5.5 Å (N-Eu-N), compared to an 11 Å width in the major groove of B-DNA.

4-2.2: Characterisation of the complexes [EuL⁹]³⁺, [EuL¹⁰]³⁺ and [EuL¹¹]³⁺

4-2.2.1: Circularly Polarized Luminescence

For each of these complexes, the circularly polarized luminescence emission spectrum was measured. The two enantiomeric complexes [EuL⁹]³⁺ and [EuL¹⁰]³⁺ gave rise to equal and opposite CPL spectra (Scheme 4.20).

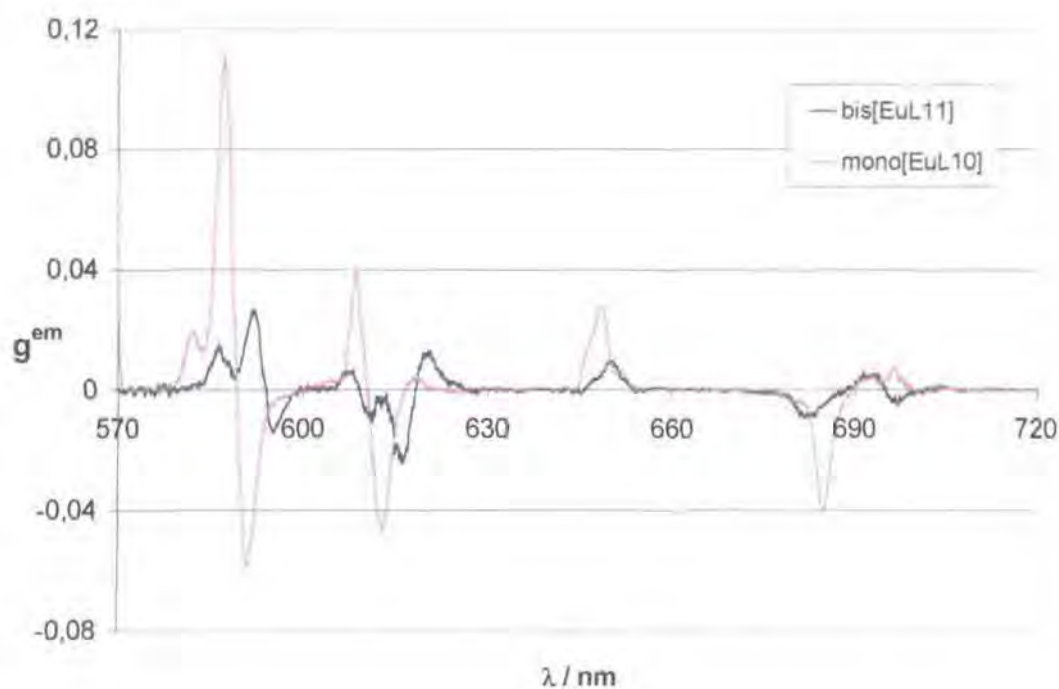
ⁱ The synthesis of [EuL¹⁰]³⁺ was carried out by Dr Linda J. Govenlock, and for [EuL¹¹]³⁺ by Alessandra Badari.



Scheme 4.20: Circularly Polarized Luminescence spectra for $(RRR)\text{-}\Lambda\text{-[EuL}^9\text{]}^{3+}$ and $(SSS)\text{-}\Delta\text{-[EuL}^{10}\text{]}^{3+}$ (295K, MeOH, $\lambda_{exc} = 355\text{nm}$)

The comparison of these spectra with those reported for analogous chiral complexes, e.g. $\Delta\text{-[EuL}^2\text{]}^{3+}$,⁷ reveals a similar spectral form and the observed dissymmetry factors (g^{em}) value for $[\text{EuL}^{10}]^{3+}$ of +0.14 (586 nm), -0.07 (591 nm) ($\Delta J = 1$ transition), +0.04 (648 nm, $\Delta J = 3$) and -0.07 (685 nm, $\Delta J = 4$) were also similar in both magnitude and sign. This suggests that $(SSS)\text{-[EuL}^{10}]^{3+}$ adopts a right-handed helicity in the layout of the ring nitrogen substituents. Therefore the complexes are denoted $\Lambda\text{-[EuL}^9\text{]}^{3+}$ and $\Delta\text{-[EuL}^{10}\text{]}^{3+}$.

The CPL spectra of the complex $[\text{EuL}^{11}]^{3+}$ showed the same overall spectral form. However the intensity of the emission was at least 10 times weaker, suggesting that the metal centred Δ helicity is much less pronounced in the C_2 -symmetric *bis* $[\text{EuL}^{11}]^{3+}$ complex compared to the mono substituted one, $\Delta\text{-[EuL}^{10}\text{]}^{3+}$. Evidently the presence of two trans-related substituents bearing the stereogenic centres at C induces a less marked helicity around the lanthanide ion.



Scheme 4.21: Circularly Polarized Luminescence spectra for the mono Δ -[EuL¹⁰]³⁺ and for bis Δ -[EuL¹¹]³⁺ complexes (295K, MeOH, $\lambda_{exc} = 355\text{nm}$)

4-2.2.2 : Halide effect quenching

The distinguishing feature of these complexes is the coordination of the phenanthridine nitrogen to the lanthanide ion. Consequently the resulting complex is likely to become more rigid, and so could possess a somewhat electron-deficient and potentially intercalative chromophore. A cationic aromatic chromophore is considered as an important factor for efficient intercalation, but is not essential for a charge-transfer interaction between the DNA bases and the chromophore. In the complex Λ -[EuL^{3a}]³⁺ for example, it has been shown that the neutral phenanthridine group shows evidence for intercalation between the DNA bases.

The electronic structure of these complexes Λ -[EuL⁹]³⁺, Δ -[EuL¹⁰]³⁺, Δ -[EuL¹¹]³⁺ therefore presents a compromise between a neutral and a cationic phenanthridyl moiety, and so the quenching effect of halide on the luminescence is expected to be less pronounced than for [EuL¹]³⁺.⁸

To quantify the effect of added halide on the emission characteristics of such complexes, the phenanthridine fluorescence and the europium emission were monitored in presence of increasing concentration of iodide and chloride. The resulting Stern-Volmer quenching constants are listed Table 4.2, and reveal similar behaviour for the mono and bis-phenanthridine complexes.

	$\Delta\text{-[EuL}^{10}\text{]}^{3+}$		$\Delta\text{-[EuL}^{11}\text{]}^{3+}$	
	<i>Phenanthridine Fluorescence</i>	<i>Europium emission</i>	<i>Phenanthridine Fluorescence</i>	<i>Europium emission</i>
<i>Iodide</i>	23	40	16	34
<i>Chloride</i>	124	144	80	>250

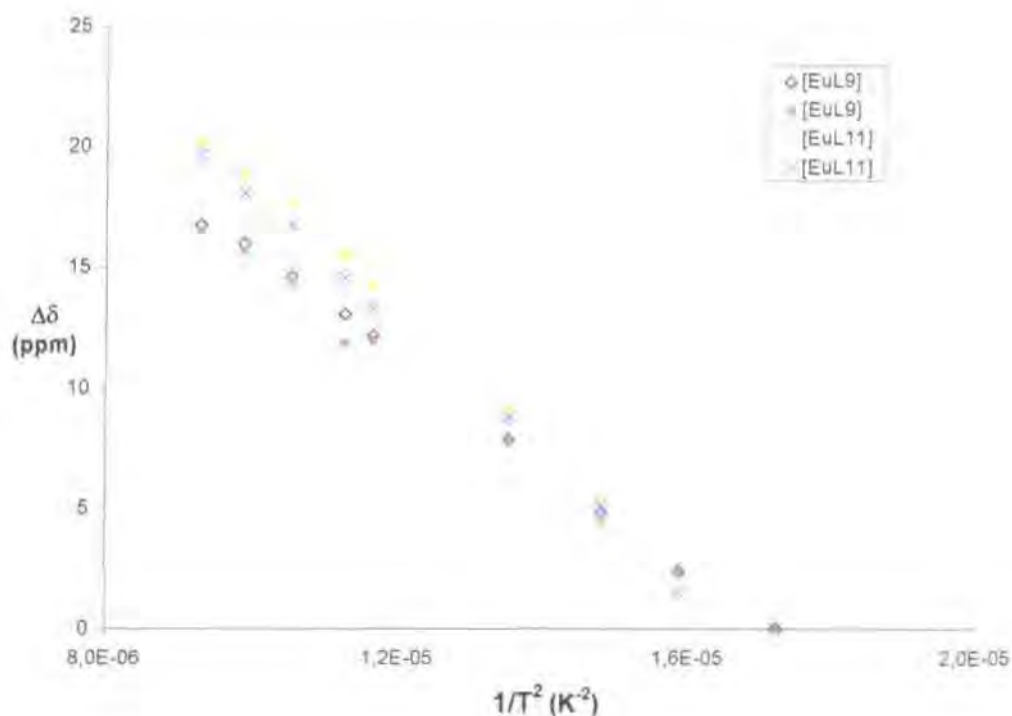
Table 4.2: Stern-Volmer quenching constants (K_{sv}^{-1} , mmol.l^{-1} , $\pm 10\%$) for the effect of halide ions on phenanthridinium fluorescence ($\lambda_{em} = 405\text{ nm}$) and europium emission ($\lambda_{em} = 615\text{ nm}$) in $\Delta\text{-[EuL}^{10}\text{]}^{3+}$ and $\Delta\text{-[EuL}^{11}\text{]}^{3+}$ (295 K, $\lambda_{exc} = 365\text{ nm}$)

The comparison of the values found for the complexes $\Delta\text{-[EuL}^{10}\text{]}^{3+}$ and $\Delta\text{-[EuL}^{11}\text{]}^{3+}$ and those of $[\text{EuL}^1]^{4+}$ (Table 4.2) showed that the quenching was less effective for the phenanthridinyl bound complexes. A simple explanation is provided by the ease of charge transfer from an halide to the more readily reduced cationic phenanthridinium compared to a transfer to the electron-deficient phenanthridine moiety in $\Delta\text{-[EuL}^{10}\text{]}^{3+}$ and $\Delta\text{-[EuL}^{11}\text{]}^{3+}$. The stronger quenching occurred each time with the iodide halide, which is easier to oxidise than chloride.

4-2.2.3: Variable temperature NMR

The paramagnetic shifted ^1H NMR spectra of $[\text{EuL}^9]^{3+}$ and $[\text{EuL}^{11}]^{3+}$ were recorded in methanol at various temperatures from 240 to 330 K.

The analysis of the chemical shift of the most shifted ring axial protons revealed one set of four singlets (39.0, 35.6, 25.1 and 22.3 ppm, 295 K), which is consistent with the presence in solution of one major stereoisomeric species (>95%). Such behaviour was also observed in the case of Δ -[EuL⁹]³⁺ and Λ -[EuL¹¹]³⁺ tetra-amide complexes.^{7a}



Scheme 4.22: Chemical shift of the macrocycle axial protons for Λ -[EuL⁹]³⁺ and Δ -[EuL¹¹]³⁺ at 241, 251, 260, 272, 293, 298, 308, 318, 328 K (CD₃OD)

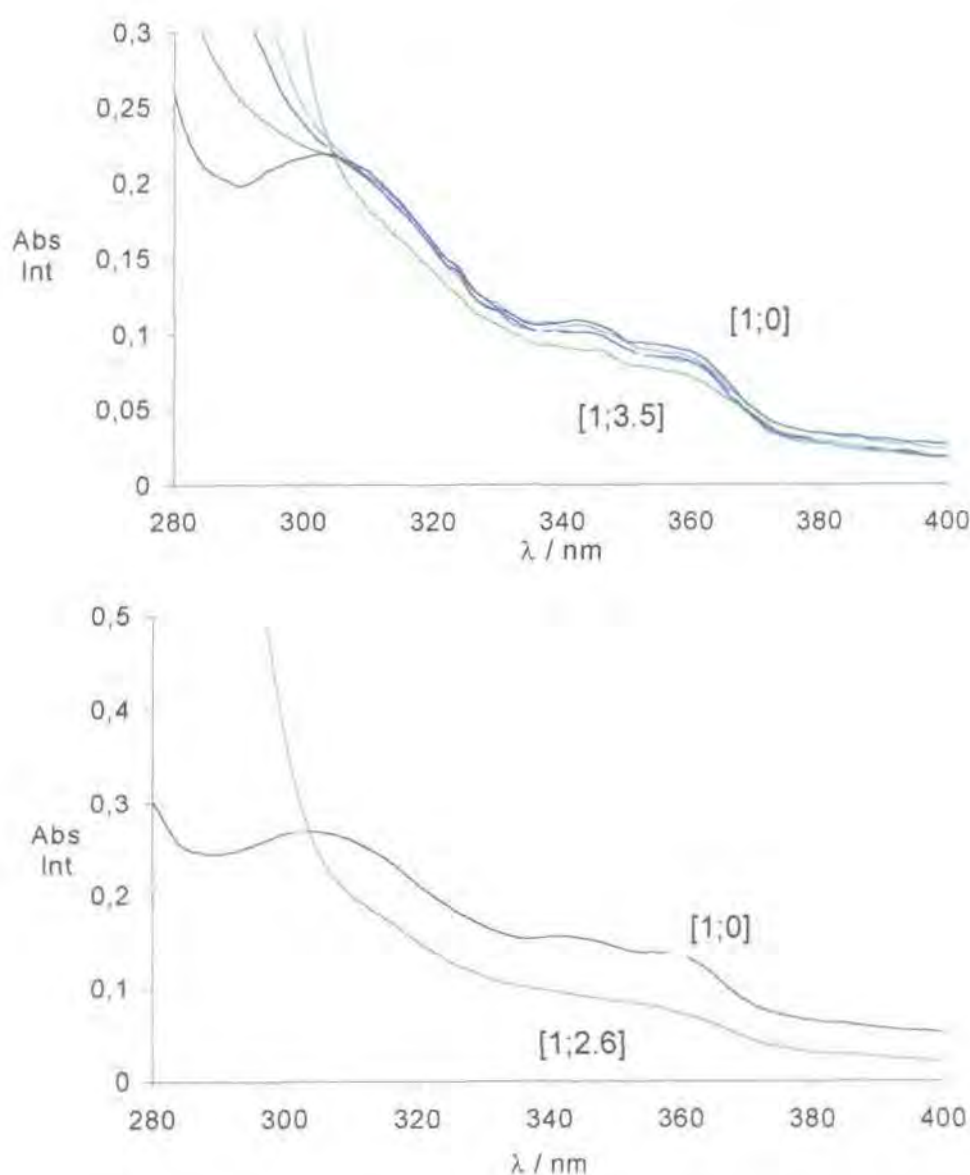
The approximately linear variation of the chemical shift $\Delta\delta$ of ring axial protons and the inverse of the temperature squared suggests the existence of a predominant dipolar or pseudocontact shift. The ring axial proton is quite remote from the Eu centre, so that any contact shift, operating through the bonds, is likely to be small. The T^{-2} dependence of the chemical shift of the bound water represents a good approximation for the dipolar term.⁹ The near-linearity of the relation between $\Delta\delta$ and $1/T^2$ was observed for both the mono and bis complexes.

The implication of the observed temperature variation and the absence of any other significant line broadening phenomena is that there are no significant chemical dynamic exchange processes occurring below 300K. This suggests that each of the complexes is relatively rigid on the NMR time scale and to a similar extent.

4-2.3: Interaction with nucleic acids

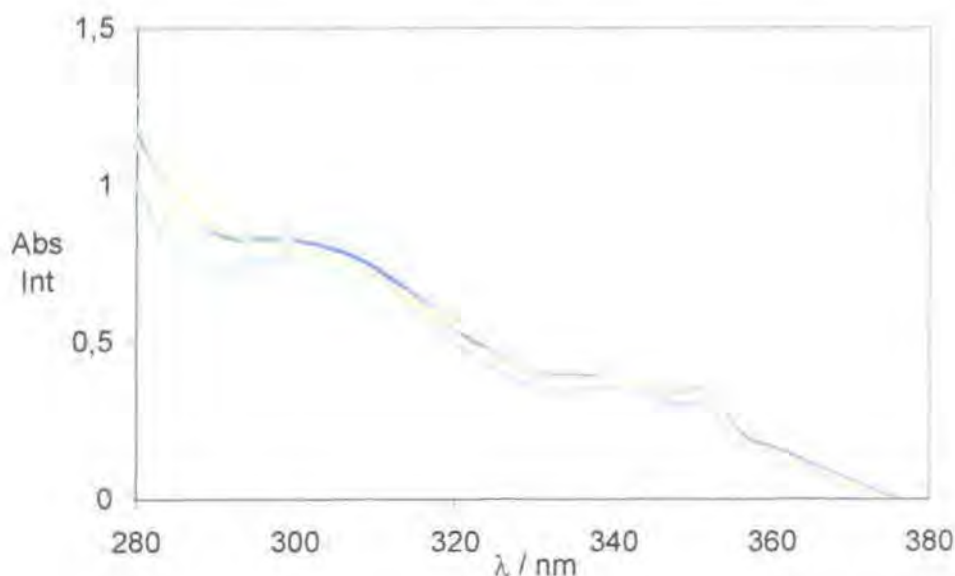
4-2.3.1: Absorbance spectroscopy

The interaction of the bound phenanthridinyl complexes was investigated by absorbance spectroscopy. The absorbance spectra of each complex exhibited long wavelength maxima at 310, 345 and 365 nm, figures which are intermediate in value between the absorption spectrum of an alkylated (or protonated) phenanthridinium group and a neutral phenanthridine.



Scheme 4.23: Absorbance of complex $[EuL^9]^{3+}$ (upper) and $[EuL^{10}]^{3+}$ (lower) following addition of $[(CG)_6]_2$ (295K, pH 7.4, 10mM NaCl, 10mM HEPES) [ratio $[(CG)_6]_2$ complex]

The absorbance spectra of the complex Λ -[EuL⁹]³⁺ and Δ -[EuL¹⁰]³⁺ following addition of CT-DNA or [(CG)₆]₂ exhibit one isosbestic point at 304 nm. The hypochromism at 358 nm was 20% and 41% respectively for Λ -[EuL⁹]³⁺ and Δ -[EuL¹⁰]³⁺, and no red shift was observed for either enantiomer. The titration curves seemed to indicate the existence of an interaction, but an intercalative binding mode was not suggested by this behaviour. However a more well-defined interaction seems to occur with the Δ complex [EuL¹⁰]³⁺.



Scheme 4.24: Absorbance of complex [EuL¹¹]³⁺ following addition of CT-DNA (295K, pH 7.4, 10 mM NaCl, 10 mM HEPES) (Final ratio DNA base pair complex [1;0.3])

In the case of the bis complex Δ -[EuL¹¹]³⁺, the absorbance spectra changed even less, any variation presumably may even be due to the tail absorption of the added DNA itself. No sign of an intercalative binding mode was found with this complex. The behaviour observed for the *mono* complexes was clearly different for the *bis* complex [EuL¹¹]³⁺.

4-2.3.2: Luminescence spectroscopy

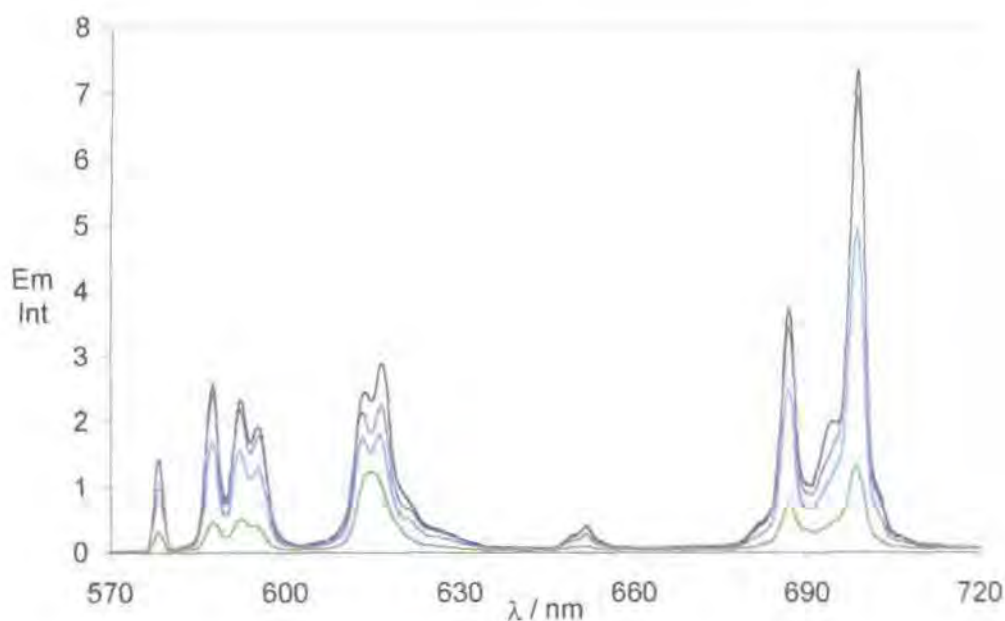
Luminescence titration with *mono* and *bis* complexes Λ -[EuL⁹]³⁺, Δ -[EuL¹⁰]³⁺ and Δ -[EuL¹¹]³⁺ revealed some surprising behaviour. While the absorbance spectral study had suggested the presence of a binding interaction for Λ -[EuL⁹]³⁺ and Δ -[EuL¹⁰]³⁺, there was only a small change in the europium emission intensity ($\lambda_{em} = 615$ nm). The phenanthridine

fluorescence intensity ($\lambda_{exc} = 304 \text{ nm}$, $\lambda_{em} = 385 \text{ nm}$) from both complexes $\Lambda\text{-[EuL}^9\text{]}^{3+}$ and $\Delta\text{-[EuL}^{10}\text{]}^{3+}$ decreased by 36%, which constitutes a small variation compared to any of the other complexes studied. The europium emission intensity exhibited a slightly greater variation of 44% ($\lambda_{em} = 615 \text{ nm}$) for both complexes.

Moreover the phenanthridine fluorescence ($\lambda_{exc} = 304 \text{ nm}$, $\lambda_{em} = 385 \text{ nm}$) from the complex $\Delta\text{-[EuL}^{11}\text{]}^{3+}$ remained almost unchanged following addition of CT-DNA. Thus no evidence for quenching of the phenanthridine fluorescence by charge transfer from the electron rich CG-base pairs was found.

In the case of the complexes $\Lambda\text{-[EuL}^9\text{]}^{3+}$ and $\Delta\text{-[EuL}^{10}\text{]}^{3+}$, the emission spectra showed slight variation in the form of the $\Delta J = 2$ transition. The shoulder of the $\Delta J = 4$ band also seems to disappear at saturation of the oligonucleotide. These two transitions are sensitive to the environment of the europium ion, slight changes in coordination geometries around the europium ion may occur following addition of the oligonucleotide.

For $\Delta\text{-[EuL}^{11}\text{]}^{3+}$ however, the transitions in the europium emission spectra retained the same form, consistent with the existence of the same coordination environment around the lanthanide ion with and without added DNA.



Scheme 4.25: Europium emission of complex $[\text{EuL}^{10}]^{3+}$ following addition of $[(\text{CG})_6]_2$

(295K, $\lambda_{exc} = 304 \text{ nm}$, pH 7.4, 10 mM NaCl, 10 mM HEPES)

Nb: The same spectrum was observed for $\Lambda\text{-[EuL}^9\text{]}^{3+}$

Summary of the binding behaviour of Λ -[EuL⁹]³⁺, Δ -[EuL¹⁰]³⁺ and Δ -[EuL¹¹]³⁺:

This series of complexes apparently does not possess suitable properties for an efficient binding interaction. The lack of flexibility in their structure appeared to inhibit their interaction with nucleic acids. It may be that the complex is too bulky to bring its positive charge closer to the DNA polyanionic phosphate backbone. Thus the first step of the binding interaction, e.g. the electrostatic interaction, may not be occurring efficiently. Furthermore, no evidence for any stereoselectivity in the binding interaction was observed. The phenanthridine unit itself may also not be sufficiently electron-deficient to interact strongly with the nucleobases by an intercalative process.

-
- ¹ A. R. Al Rabaa, F. Tfibel, F. Merola, P. Pernot, M.-P. Fontaine-Aupart, *J. Chem. Soc., Perkin Trans. 2*, **1999**, 341-351.
- ² H. Gilman, J. Eisch, *J. Am. Chem. Soc.*, **1957**, 79, 5479-5483.
- ³ S. Amin, D.A. Voss, W. D. Horrocks, C. H. Lake, M. R. Churchill, J. R. Morrow, *Inorg. Chem.*, **1995**, 34, 3294.
- ⁴ a) D. T. Richens, 'The Chemistry of Aqua Ions', Wiley, Chichester, **1997**.
b) S. Aime, A. Barge, M. Botta, J. A. K. Howard, J. M. Moloney, D. Parker, A. S. de Sousa, M. Woods, *J. Am. Chem. Soc.*, **1999**, 121, 5762-5772.
- ⁵ I. M. Clarkson, A. Beeby, J. I. Bruce, L. J. Govenlock, M. P. Lowe, C. E. Mathieu, D. Parker, K. Senanayake, *New J. Chem.*, **2000**, 24, 377-386.
- ⁶ Alessandra Badari, University of Torino, Final Year Report, **1999**.
- ⁷ a) R. S. Dickins, J. A. K. Howard, C. L. Maupin, J. M. Moloney, D. Parker, J. P. Riehl, G. Siligardi, J. A. G. Williams, *Chem Eur. J.*, **1999**, 5, 1095.
b) A. Casani, C. Fischer, M. Guardigli, A. Isernia, I. Manet, N. Sabbatini, R. Ungaro, *J. Chem. Soc., Perkin Trans. 2*, **1996**, 395.
- ⁸ D. Parker, K. Senanayake, J. A. G. Williams, *J. Chem. Soc., Perkin Trans. 2*, **1998**, 2129-2140.
- ⁹ B. McGarvey, *J. Magn. Resonance*, **1979**, 33, 445.

Experimental

Solvents were dried from an appropriate drying agent when required and water was purified by the « Purite^{STILL} plus » system. Thin layer chromatography was carried out using neutral aluminium oxide plates (Merck Art 5550) or silica plates (Merck Art 5554), both being fluorescent on irradiation at 254 nm. Preparative column chromatography was carried out using silica (Merck silica gel 60, 230-400 mesh) or alumina (Merck neutral alumina). IR spectra were recorded with a Perkin Elmer 1600 FT-IR spectrometer operating with a GRAMS Analyst software using a “Golden Gate” accessory.

Mass spectra (CI) were recorded using a VG 7070E spectrometer using ammonia as the impinging gas. Electrospray mass were recorded using a VG II Platform spectrometer (Fisons Instruments) with methanol or H₂O as the carrier solvent. Accurate masses were measured by EPSRC Mass Spectroscopy Service at the University of Wales at Swansea.

Mass Spectrometry of oligonucleotides : The oligonucleotides were prepared by stirring at 60°C in ammonium acetate (0.1 M) for 10 min and then left cooling down at room temperature overnight. The concentration of oligonucleotide was adjusted to 18 µM (duplex) by addition of Purite water. Measurements of oligonucleotide mass spectra were carried out in negative mode, (ES⁻), over a mass range from 200 to 2800 with a cone voltage of 79 V (295 K). The complex solutions established in purite water were added directly to the oligonucleotide solution, and the mixture injected without any further preparation.

Proton NMR spectra were recorded on a Varian VXR 400 (65.26 MHz), Varian VXR 200 (199.99 MHz), Varian Gemini 200 (199.99 MHz), Varian Mercury 200 (199.99 MHz) or Varian Unity 300 (299.91 MHz). Carbon NMR spectra using the Varian Mercury 200 (50.29 MHz), Varian Unity 300 (75.4 MHz), Varian VXR 400 (100.58 MHz) or Bruker AMX 500 spectrometer (125.77 MHz). Spectra were referenced to solvent residual proton resonances. All chemical shifts (δ) are reported in ppm and coupling constants reported in Hz.

Melting points were measured using a Reichart-Köfler block and are uncorrected.

Ultraviolet absorbance spectra were recorded on a Unicam UV2 spectrometer operating with a Unicam Vision software, with extinction coefficients reported in parentheses, in units of M⁻¹cm⁻¹. Luminescence spectra were recorded either using a Perkin Elmer LS 50B or an Instruments SA Fluorolog 3-11 equipped with a SPX 1934D3 phosphorimeter. Corrected spectra were obtained taking into account the wavelength-dependent response of the instrument.

Non-zero baseline effects were allowed for by running a blank sample and subtracting this from the obtained spectra. Second order diffraction effects were obviated by using a cut-off filter to remove the scattered light before it enters the emission monochromator, e.g. by use of a 380 nm cut-off filter when acquiring Eu emission spectra.

Excited state lifetime measurements for europium and terbium were made on either the Perkin Elmer LS 50B (using Phlemming data acquisition written by Dr. A. Beeby, University of Durham) or the Instruments SA Fluorolog (using DataMax for Windows v2.1). Lifetimes were measured by excitation of a sample by short pulse of light (397 nm for europium) followed by monitoring the integrated intensity of light (594 or 616 nm for europium) emitted during a fixed gate time, t_g , a delay time, t_d , later. At least 20 delay times were used covering 3 or more lifetimes. Typically gate times of between 100 and 250 μ s were used, and the excitation and emission slits were set to 5-15 nm bandpass. The obtained decay curves were fitted to a simple mono-exponential decay curve using either Grafit 3.0 (Erithacus software) or Microsoft Excel.

Quantum yield measurements were made relative to two known standards. For europium complexes these were Rhodamine 101 in ethanol ($\phi = 1$) and Cresyl violet in methanol ($\phi = 0.54$). These standards were chosen as they emit in a similar spectral window to europium and possess a similar absorbance to the aromatic antenna, at the excitation wavelength used in the studied complexes. For each of the standards and the unknown, five solutions with absorbances between 0.02 and 0.1 were used. For each of these solutions the absorbance at the excitation wavelength and the total integrated emission was determined. Errors in quantum yield determinations can arise due to the inner filter effect or errors in the amount of absorbed light. The first of these can be very important when using references such as Rhodamine 101 and Cresyl violet as these are both strongly absorbing in the emission region. This effect was minimised by only using samples with absorbances below 0.2. Errors in the amount of light absorbed by each sample were minimised by choosing the excitation wavelength to be on a relatively flat area of the absorption curve (i.e. ca. 270 nm) and by a small band pass for excitation.

pH measurements were made using a Jenway 3320 pH meter (fitted with a BDH Glass + combination electrode - microsample) calibrated with pH 4, 7 and 10 buffer solutions.

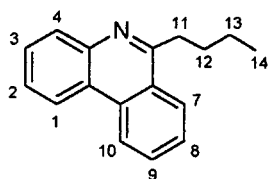
pH Titrations: Luminescence pH titrations were carried out in a background of constant ionic strength ($I = 0.1$ M NMe_4ClO_4 , 295 K) on solutions with absorbances of < 0.3

at wavelengths $\geq \lambda_{\text{ex}}$ in order to avoid any errors due to the inner filter effect. Solutions were made basic by addition of 1M KOH and titrated to acidic pH using small aliquots (typically 0.5 μL) of 1M or 0.1 M TFA. The luminescence spectra were recorded at each point (30 - 40 points per titration). Excitation wavelengths of 304 or 378 nm (sensitisation via phenanthridine chromophore) were used to obtain the luminescence spectra. Excitation and emission slits were 1 nm and 1.5 nm bandpass respectively. Points were recorded at 1 nm intervals with a 0.5s integration time. Standard least squares fitting techniques were used to determine protonation constants from the luminescence intensity data.

Oligonucleotide titrations : Luminescence DNA titrations were carried out in a background of buffered medium (pH 7.4, NaCl 10, 50 or 100 mM, HEPES 10mM, 295 K) on complexes solutions with absorbances of 0.2 at wavelengths 304 or 320 nm (typically a complex concentration between 20 and 30 μM). The oligonucleotide solutions were incremented by addition of aliquots of 10 μl of commercial solution (concentration of single strand typically 0.3 mM) purchased from Oswel company, Southampton. The luminescence spectra were recorded at each point. Excitation wavelengths of 304 or 378 nm (sensitisation via phenanthridine chromophore) were used to obtain the luminescence spectra. Excitation and emission slits were 1.5 nm bandpass. Points were recorded at 1 nm intervals with a 0.5 s integration time. Second order diffraction effects were obviated by using a 375 nm cut-off filter in the case of the luminescence spectra recorded after excitation at 304 nm (neutral phenanthridine chromophore).

Circular Dichroism spectra were recorded using a Jasco J-810 Spectropolarimeter.

Circular dichroism titrations : Difference CD titrations were carried out in a background of buffered medium (pH 7.4 NaCl 10 mM HEPES 10mM, 295 K) in a 1 cm path quartz cell. The concentration of oligonucleotide solutions was 3.06 μM and the complex solution was incremented to the oligonucleotide solution by addition of aliquots of 20 μl of a 0.16 mM solution concentration. The spectra were recorded with a sensitivity of 5 mDeg, in 4 successive scans. A spectra of the buffered background was deduced from each row spectra. A spectrum of the complex at its highest concentration was recorded, normalized and proportionally deduced from each normalized spectra of DNA-complex after each addition, to show the CD difference spectra. Dilution factors were considered at the time of the normalisation step included in the calculation of coefficients.

6-Butylphenanthridine¹

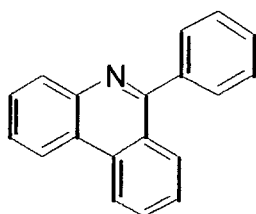
Phenanthridine (1 g, 5.6 mmol) was dissolved in dry diethyl ether under argon. The solution was cooled down to -78°C and *n*-butyllithium (4.1 ml, 6.1 mmol) was added dropwise. The yellow solution was stirred at -78°C for one hour, then quenched using an aqueous solution of potassium hydroxide (0.1 M, 5 ml). The product was extracted using dichloromethane (4×20 ml), the organic layers washed using brine (3×20 ml), dried over potassium carbonate, filtered and the solution was concentrated to one third of the volume. Manganese (IV) dioxide (2 g) was added, and stirred at room temperature overnight. The manganese residue was filtered and the solvent removed. The residue was purified by column chromatography on silica using dichloromethane as the eluent ($R_f = 0.3$), to give a colourless oil (1.1 g; 85%).

¹H NMR (CDCl₃, 300 MHz) : δ 8.59 (1H, d, *J* 8, H4) ; 8.50 (1H, d, *J* 8, H1) ; 8.23 (1H, d, *J* 8, H7) ; 8.15 (1H, d, *J* 8, H10) ; 7.78 (1H, t, *J* 7.1, H2) ; 7.65 (3H, m, H8H9H3) ; 3.37 (2H, t, *J* 7.9, H11) ; 1.91 (2H, m, H12) ; 1.57 (2H, m, H13) ; 1.00 (3H, t, *J* 7.5, H14).

¹³C NMR (CDCl₃, 75.4 MHz) : δ 160.3 (C6) ; 158.5 (C-Ar) ; 130.5, 129.7, 129.0, 128.8, 127.5, 127.1, 127.1, 126.5, 123.4, 122.7, 122.1, 118.9, 115.6 (C-Ar) ; 36.6 (C11) ; 28.2 (C12) ; 22.1 (C13) ; 12.9 (C14).

M/z (ES⁺) : 235 [M+H]⁺

Elemental analysis : Found C 84.7, H 7.53, N 5.80% ; C₁₇H₁₇N.0.25H₂O requires : C 85.2, H 7.31, N 5.84.

6-Phenylphenanthridine¹ 2

¹ H. Gilman, J. Eisch, *J. Am. Chem. Soc.*, 1957, 79, 5479.

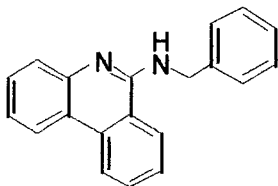
Phenanthridine (0.15 g, 0.86 mmol) was dissolved in dry diethyl ether under argon. The solution was cooled down to -78°C . Phenyllithium (1.2 ml; 1M, 1 mmol) was added dropwise. The yellow solution was maintained at -78°C for one hour. Then the solution was quenched using aqueous solution of potassium hydroxide (0.1 M, 5 ml). The product was extracted using dichloromethane (4×20 ml), the organic layers washed using brine (3×20 ml), dried over potassium carbonate, and filtered off. The solution was concentrated and manganese (IV) dioxide was added, and stirred at room temperature overnight. The manganese residue was filtered and the solvent removed. The residue was purified on silica chromatography column using dichloromethane as eluent ($R_f = 0.25$), to yield a white solid (0.26 g; 78%), m.p. $95-96^{\circ}\text{C}$ (litt. $103-106^{\circ}\text{C}$).

^1H NMR (CDCl_3 , 200 MHz): δ 8.74 (1H, d, J 8.3, H1); 8.66 (1H, d, J 7.8, H4); 8.27 (1H, d, J 7.8, H7); 8.13 (1H, d, J 8.3, H10); 7.88 (1H, t, J 7.3, H2); 7.77-7.53 (8H, m, H3H8H9, PhH).

^{13}C NMR (CDCl_3 , 50 MHz): δ 161.5 (C6); 159.5 (C-Ar); 140.2, 135.6, 133.5, 132.1, 131.3, 130.2, 129.7 (C-Ar); 125.1, 124.8 (CH-Ph), 124.6, 124.2, 124.1, 123.8, 122.9 (C-Ar).

M/z (ES^+): 256 $[\text{M}+\text{H}]^+$.

6-Benzylamine phenanthridine² **3**



6-Chlorophenanthridine **11** (0.1 g, 0.46 mmol) was solubilized in dimethylformamide (5 ml), benzylamine (2 ml) was added and the mixture was heated at 150°C for 2d. After cooling down the solution was poured into ice. The product was extracted using CH_2Cl_2 (4×30 ml), washed with sodium carbonate solution (0.1 M, 30 ml), dried over potassium carbonate, filtered off. The solvent was removed to yield a yellow oil (82 mg; 63%).

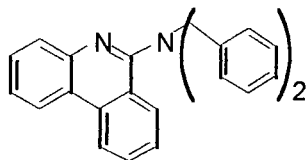
^1H NMR (CDCl_3 , 200 MHz): δ 8.55 (1H, d, H1); 8.46 (1H, d, H4); 8.15 (1H, d, H7); 8.07 (1H, d, H10); 7.78 (1H, t, H2); 7.65 (3H, m, H3H8H9); 7.20 (5H, m, PhH); 2.99 (2H, s, NCH_2 -), 1.52 (1H, br s, NH).

² a) C. B. Reese, *J. Chem. Soc.*, **1958**, 173, 895-899.

b) C. B. Reese, *J. Chem. Soc.*, **1958**, 174, 899-901.

^{13}C NMR (CDCl_3 , 75.4 MHz): δ 154.3 (C6); 150.8, 135.6, 129.5, 128.5, 127.5, 127.1 (C-Ar); 128.8, 125.3 (CH-Ph); 124.9, 124.8, 124.4, 122.9, 118.2, 116.7, 115.8 (C-Ar); 47.5 (CH_2NH).
M/z (ES^+): 285 [$\text{M}+\text{H}$] $^+$.

6-Dibenzylamine phenanthridine² **4**



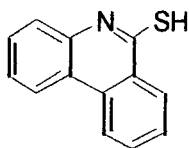
6-Chlorophenanthridine **11** (0.2 g, 0.93 mmol) was heated in dibenzylamine (5 ml) at 150°C overnight. The solution was poured into water. The product was extracted using CH_2Cl_2 (4 \times 20 ml), washed using potassium carbonate solution (0.1 M, 20 ml), dried over potassium carbonate, and filtered off. The oily residue was used without any further purification.

^1H NMR (CDCl_3 , 200 MHz): δ 8.59 (1H, d, H1); 8.50 (1H, d, H4); 8.48 (1H, d, H7); 7.97 (1H, d, H10); 7.79 (1H, t, H2); 7.65 (2H, q, H3H8); 7.49 (5H, m, H9, Ph Hortho); 7.33 (6H, m, Ph Hmeta,para); 4.77 (4H, s, NCH_2 -).

^{13}C NMR (CDCl_3 , 50 MHz): δ 155.2 (C6); 150.4, 134.8, 130.8, 130.1, 129.4, 129.6, 129.3 (C-Ar); 127.9, 127.2, 126.1 (C-Ph); 125.9, 117.1, 114.2, 112.7 (C-Ar), 55.1 (CH_2N).

M/z (ES^+): 375 [$\text{M}+\text{H}$] $^+$, 397 [$\text{M}+\text{Na}$] $^+$.

6-Thiophenanthridine **8**



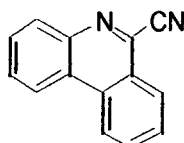
6-Chlorophenanthridine **11** (1 g, 4.6 mmol) was heated in ethanol for 2 h, then thiourea (0.38 g, 5 mmol) was added and the mixture was stirred at 60°C for 2hrs. The solvent was removed and the product was recrystallized from ethanol to yield a yellow solid (0.91 g; 94%).

^1H NMR (CDCl_3 , 300 MHz): δ 11.07 (1H, br s, SH); 9.10 (1H, d, H1); 8.32 (2H, t, H4 H7); 7.85 (1H, d, H10); 7.65 (1H, d, H2); 7.54 (1H, t, H3); 7.40 (2H, m, H8H9).

^{13}C NMR (CDCl_3 , 75.4 MHz): δ 165.4 (C6), 147.1, 133.7, 133.1, 130.0, 128.8, 127.9, 127.4, 125.1, 123.3, 116.5 (C-Ar).

M/z (ES^+): 210 $[\text{M}+\text{H}]^+$.

6-Cyanophenanthridine 9



6-Chlorophenanthridine **11** (1 g, 4.6 mmol) was solubilized in DMF (10 ml), with potassium cyanide (1 g, 12 mmol) and the mixture was heated at 100°C overnight. The mixture was cooled down to room temperature, and poured into ice. The product was extracted using CH_2Cl_2 (4 \times 30 ml), washed using water (3 \times 30 ml) and potassium carbonate solution (0.1 M, 20 ml), dried over potassium carbonate and filtered off. The solvent was removed and the residue recrystallized twice from aqueous ethanol, to give a pale yellow solid (0.6g ; 64%), m.p. 104-106°C.

^1H NMR (CDCl_3 , 300 MHz): δ 8.70 (1H, d, H1); 8.64 (1H, d, H4); 8.48 (1H, d, H7); 8.27 (1H, d, H10); 8.00 (1H, t, H2); 7.86 (3H, m, H3H8H9).

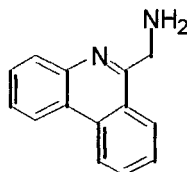
^{13}C NMR (CDCl_3 , 75.4 MHz): δ 152.5 (C6), 132.5; 131.3; 130.2; 129.1; 127.0; 122.6; 122.5; 112.7 (C aromatic); 106.7 (CN).

M/z (ES^+): 205 $[\text{M}+\text{H}]^+$.

Elemental analysis: Found C 80.97, H 3.82, N 13.00%; $\text{C}_{14}\text{H}_8\text{N}_2 \cdot 0.25\text{H}_2\text{O}$ requires C 80.6, H 4.08, N 13.4%

IR (thin film) : ν_{max} 2015 (CN).

6-Aminomethylphenanthridine 10



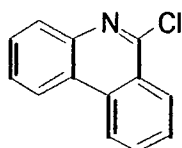
6-Cyanophenanthridine **9** (0.6 g; 2.9 mmol), hydrazine hydrate (3 ml, excess), palladium hydroxide (Pearlman's catalyst) (0.5 g) were stirred in methanol (30 ml) at room temperature overnight. The solid was filtered off and the solvent was removed under reduced pressure to yield a pale yellow oil (0.59 g; 98 %).

$^1\text{H NMR}$ (CDCl_3 , 300 MHz): δ 8.59 (1H, d, H1), 8.50 (1H, d, H7), 8.20 (1H, d, H10), 8.15 (1H, d, H4), 7.84 (1H, t, H2), 7.72-7.67 (3H, m, H3H9H8), 3.06 (2H, s, CH_2), 1.65 (2H, br.s, NH_2).

$^{13}\text{C NMR}$ (CDCl_3 , 75.4 MHz): δ 158.9 (C6); 144.5, 129.6, 127.9, 127.2, 126.4, 126.0, 125.1, 123.0, 121.3 (C-Ar); 45.7 (CH_2N).

M/z (ES^+): 209 [$\text{M}+\text{H}$] $^+$.

6-Chlorophenanthridine³ **11**



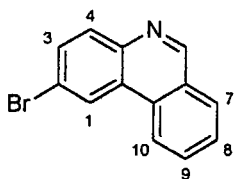
Phenanthridinone (5 g, 25 mmol) was solubilized in phosphorus oxychloride (60 ml) in the presence of *N,N*-dimethylaniline (2 ml) and the mixture was heated at reflux for 3hrs. The solvent was removed under reduced pressure and the residue poured into ice and the product was extracted using CH_2Cl_2 (4 \times 20ml). The organic layers were washed using an aqueous solution of K_2CO_3 (0.1 M, 2 \times 20ml), dried over K_2CO_3 , filtered and the solvent was removed. The product was recrystallised twice from ethanol-water, to yield beige crystals (3.8 g; 72%) mp : 90-92°C (lit. 113-114°C).

$^1\text{H NMR}$ (CDCl_3 , 300 MHz): δ 8.65 (1H, d, J 8.4, H1) ; 8.57 (1H, d, J 8.1, H7) ; 8.52 (1H, d, J 8.1, H4) ; 8.12 (1H, d, J 7.6, H10) ; 7.94 (1H, t, J 7.2, H2), 7.82-7.71 (3H, m, H3H9H8).

$^{13}\text{C NMR}$ (CDCl_3 , 75.4 MHz): δ 149.7 (C6); 131.8, 130.8, 130.3, 130.0, 128.9, 127.8, 126.9, 125.4, 123.9, 122.8, 118.9 (C-Ar).

Elemental analysis: Found C 70.01, H 3.57, N 5.84%; $\text{C}_{14}\text{H}_8\text{N}_2$ requires C 73.07, H 3.77, N 6.55%.

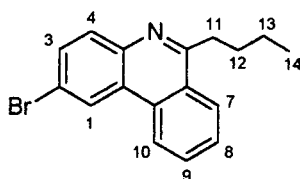
³ G. M. Badger, J. H. Seidler, B. Thomson, *J. Chem. Soc.*, **1951**, 3207-3211.

2-Bromophenanthridine 12

Title compound was prepared according to the literature method.⁴ Phenanthridine (5 g, 28 mmol) and *N*-bromosuccinimide (5 g, 29 mmol) were taken into carbon tetrachloride (50 ml) and the suspension was heated at reflux for 2 days, to give a bright yellow red solution. A small amount of solid adhered to the sides of the reaction flask. The solution was decanted and benzene (20 ml) was added. The solvent was reduced to about one third of the initial volume and left to crystallise from ethanol. The solid was purified using column chromatography (silica, dichloromethane, $R_f = 0.25$, 10% EtOH-CH₂Cl₂) to yield a yellow solid, 4.8 g (54%), m.p.: 156-158°C (lit.⁴ 160-162°C).

¹H NMR (CDCl₃, 200 MHz): δ 9.29 (1H, s, H6), 8.72 (1H, d, H1), 8.57 (1H, d, J 7.5, H4), 8.09 (1H, d, J 8, H3), 8.06 (1H, d, J 8, H7), 7.91 (1H, d, J 7, H10), 7.85 (1H, dd, J 7.5, J 7.5, H8), 7.79 (1H, dd, J 7, J 7, H9)

M/z (ES⁺): 258/260 [M+H]⁺

2-Bromo 6-butylphenanthridine 13

2-Bromophenanthridine **12** (0.98 g, 3.8 mmol) was dissolved in dry diethyl (20 ml) ether under argon. The suspension was cooled down to -10°C. Butylmagnesium chloride (2.2 ml, 4.0 mmol) was added dropwise and the mixture stirred for 2hrs at -10°C. The solution was allowed to warm up to room temperature overnight. The orange solution was treated with hydrochloric acid (5 ml, 0.1 M solution) and the solution extracted with ether (3 × 20 ml) and with dichloromethane (4 × 20 ml). The organic layers were combined, washed using brine (2 ×

⁴ H. Gilman, J. Eisch, *J. Am. Chem. Soc.*, **1955**, *77*, 6379.

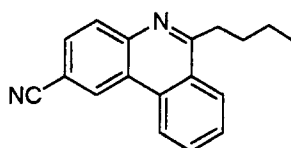
20 ml), and dried over potassium carbonate. Solvent was removed under reduce pressure, the residue dissolved in dichloromethane (50 ml) and manganese (IV) dioxide (1 g) was added. After stirring the suspension overnight at room temperature, the solid was filtered off and the residue was purified by chromatography on silica gel ($R_f = 0.3$, CH_2Cl_2) to give a pale yellow solid ($m = 0.93$ g, 78%), mp. 118-119°C.

^1H NMR (CDCl_3 , 300 MHz): δ 8.66 (1H, d, J 2, H1), 8.56 (1H, d, J 8, H4), 8.26 (1H, d, J 8, H7), 7.80 (1H, d, J 8.6, H10), 7.85-7.73 (3H, m, H3H9H8), 3.35 (2H, t, J 8, H11), 1.90 (2H, m, H12), 1.55 (2H, tq, H13), 1.01 (3H, t, H14).

M/z (ES^+): 314/316 $[\text{M}+\text{H}]^+$.

HR-ESMS (m/z): Found 314.0545. $\text{C}_{17}\text{H}_{16}\text{BrN}$ requires 314.0546.

2-Cyano 6-butyl phenanthridine 14



2-Bromo-6-butyl-phenanthridine **13** (0.9 g, 2.8 mmol) was dissolved in anhydrous dimethylformamide (20 ml). The solution was heated at 100°C for 1h and copper(I) cyanide (0.55 g, 5.7 mmol) was added. The reduced solution was stirred at 140°C under argon for 2 days. Solvent was removed under reduced pressure and the residue was taken in concentrated hydrochloric acid (30 ml, 6 M) to give a yellow solution. The pH of the solution was increased up to 12 by addition of potassium hydroxide pellets. The product was extracted using dichloromethane (4×20 ml). The combined organic layers were washed with aqueous potassium carbonate solution (0.1 M, 2×20 ml), dried over potassium carbonate and the residue was recrystallised twice from ethanol to give a pale yellow solid (0.57 g, 77%), m.p. 110-111°C.

^1H NMR (CDCl_3 , 300 MHz): δ 8.83 (1H, d, J 1, H1), 8.56 (1H, d, J 5.4, H4), 8.28 (1H, d, J 5.6, H7), 8.15 (1H, d, J 6, H10), 7.90-7.78 (3H, m, H3H9H8), 3.37 (2H, t, J 5.2, H11), 1.90 (2H, m, H12), 1.55 (2H, tq, H13), 1.01 (3H, t, H14).

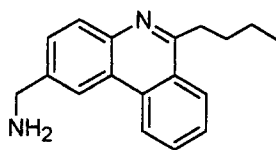
^{13}C NMR (CDCl₃, 75.4 MHz): δ 164.8 (C6), 144.3 (C-CN), 130.5, 130.2, 129.6, 129.0, 127.5, 126.6, 125.5, 124.4, 122.6, 121.3, 118.1 (Ar-C), 108.4 (CN), 35.1 (C11), 30.3 (C12), 22.0 (C13), 12.9 (C14).

M/z (ES⁺): 260.9 [M+H]⁺.

Elemental analysis: Found: C, 81.79; H, 6.08; N, 10.48. C₁₈H₁₆N₂ (+1/4H₂O) requires C, 80.7; H, 6.25; N, 10.60.

IR, cm⁻¹ (thin film): ν_{max} 2940 (CH), 2215 (CN).

2-Aminomethyl 6-butyl phenanthridine 15

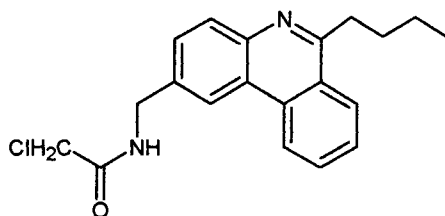


2-Cyano 6-butyl-phenanthridine **14** (0.1 g, 0.38 mmol) was dissolved in borane-tetrahydrofuran solution (15 ml, 1 M) under argon and the mixture heated at 70°C for 4 days. The reaction was monitored by analysis of a quenched sample by IR spectroscopy. The solution was cooled to room temperature and methanol (20 ml) was added carefully, dropwise. The solvent was removed and the residue was taken up in methanol (20 ml). This procedure was repeated three times and finally the residue was dissolved in hydrochloric acid (20 ml, 1 M) and heated at 80°C for 1 h. The temperature was maintained at 60°C overnight. The acid solution was washed using ether (30 ml). The pH was raised up to 13 and the product extracted using dichloromethane (5 × 20 ml). The combined extracts were washed using brine (2 × 20 ml), dried over potassium carbonate and the solvent removed under pressure to yield a brown solid, 91 mg (90%), which was used directly without further purification.

^1H NMR (CDCl₃, 200 MHz): δ 8.53 (1H, d, *J* 8, H4), 8.36 (1H, s, H1), 8.13 (1H, d, *J* 8.2, H7), 7.98 (1H, d, *J* 6, H10), 7.70 (1H, t, H3), 7.90-7.78 (2H, m, H9H8), 4.0 (2H, br.s, NH₂), 3.37 (2H, s, CH₂N), 3.23 (2H, t, *J* 5.2, H11), 1.80 (2H, m, H12), 1.45 (2H, tq, *J* 3.2, H13), 0.91 (3H, t, H14).

^{13}C NMR (CDCl₃, 75.4 MHz): δ 162.2 (C6), 142.9, 132.9, 130.3, 129.7, 128.2, 127.3, 126.4, 125.3, 123.7, 122.6, 120.0 (Ar-C), 50.5 (C11), 36.2 (C2'), 31.9 (C12), 23.3 (C13), 14.3 (C14).

M/z (ES⁺): 264.9 [M+H]⁺.

N-Chloroacetyl-2-aminomethyl-6-butyl phenanthridine 16

2-Aminomethyl-6-butyl-phenanthridine **15** (0.32 g, 1.24 mmol) was dissolved in tetrahydrofuran (30 ml) under argon. Chloroacetic acid (0.068 ml, 1.26 mmol) and 1-hydroxybenzotriazole (0.116 g, 1.26 mmol) were added and the solution was cooled at 0°C. EDC [1-(3-Dimethylaminopropyl)-3-ethyl-carbodiimide hypochloride] (0.245 g, 1.29 mmol) was added then and the solution stirred at 0°C for 1 h and at room temperature for 3 hrs. The solvent was removed and the residue washed with cold tetrahydrofuran (20 ml). The product was extracted using dichloromethane (3 × 25 ml), washed using a saturated solution of sodium carbonate (2 × 20 ml) and finally dried over potassium carbonate. Solvent was removed to yield a white solid, 0.33 g (78%), m.p.>250°C.

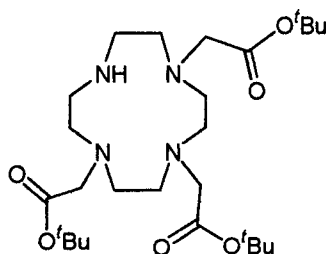
¹H NMR (CDCl₃, 300 MHz): δ 8.63 (1H, d, *J* 8, H4), 8.39 (1H, s, H1), 8.20 (1H, d, *J* 8.2, H7), 8.03 (1H, d, *J* 6, H10), 7.80 (2H, t, H3), 7.65-7.50 (2H, m, H9H8), 6.95 (1H, br. s, NH), 4.67 (2H, d, *J* 6, CH₂NH), 4.10 (2H, s, CH₂Cl), 3.30 (2H, t, *J* 5.2, H11), 1.83 (2H, m, H12), 1.45 (2H, m, H13), 0.93 (3H, t, H14).

¹³C NMR (CDCl₃, 75.4 MHz): δ 165.9 (C6), 162.6, 143.1, 135.1, 132.4, 130.2, 130.0, 128.1, 127.4, 126.3, 125.2, 123.5, 122.3, 121.1 (Ar-C); 44.0 (CH₂Cl), 42.6 (CH₂N), 36.1 (C11), 31.6 (C12), 23.0 (C13), 14.0 (C14).

M/z (ES⁺): 340.9, 342.9 [M+H]⁺

HR-ESMS (m/z): Found 341.1421; C₂₀H₂₂ClN₂O requires 341.1421 [M+H]⁺.

IR, cm⁻¹ (thin film): ν_{max} 3103, 1637, 1539, 1226, 1051.

1,4,7-Tris-(*t*-butoxycarbonylmethyl)-1,4,7,10-tetraazacyclododecane 17a

Sodium hydrogen carbonate (0.81 g, 9.6 mmol) and cyclen (0.55 g, 3.2 mmol) were placed into a flask containing 4Å molecular sieves under argon. A solution of *tert*-butyl bromoacetate (1.88 g, 9.6 mmol) in acetonitrile (15 ml) was added at room temperature under argon. The reaction was left to stir for 18hrs at room temperature. The inorganic material and the molecular sieves were removed by filtration. The solvents were removed under vacuum and the residue purified by chromatography on silica gel. The column was first washed with dichloromethane, then 30% THF in CH₂Cl₂ before the title compound was eluted using 5% ammonia, 5% methanol, 30% CH₂Cl₂, 60% THF (R_f = 0.5, SiO₂). The pale oil obtained was crystallised from acetonitrile and diethylether to give small colourless crystals (0.41 g, 25%), mp. 166-168°C.

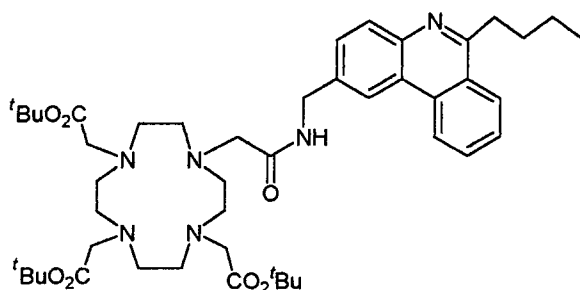
¹H NMR (CDCl₃, 300 MHz): δ 3.34 (s, 4H, 2x acetate CH₂'), 3.26 (s, 2H, acetate CH₂), 2.95 (br m, 16H, cyclen ring), 1.42 (s, 27H, *t*-Bu).

¹³C NMR (CDCl₃, 75.4 MHz): δ 172.2 (2 C=O), 171.4 (C=O), 83.8 (C(CH₃)₃), 83.6 (2 C(CH₃)₃), 60.4 (CH₂ ring), 53.6 (CH₂ ring), 51.2 (CH₂ acetate), 50.4 (CH₂ acetate), 49.5 (CH₂ ring), 30.2 (9 CH₃).

M/z (ES+): 515 [M+H]⁺, 537 [M+Na]⁺.

IR, cm⁻¹ (thin film): ν_{max} 1715 (C=O).

1-[[2-aminomethyl-(6-butyl-phenanthridine)]-carbamoylmethyl]-4,7,10-tris-(*t*-butoxycarbonylmethyl)-1,4,7,10-tetraazacyclododecane 17b



1,4,7-Tris-(*t*-butoxycarbonylmethyl)-1,4,7,10-tetraazacyclododecane **17** (0.15 g, 0.29 mmol) and *N*-chloroacetyl-2-aminomethyl-6-butyl phenanthridine (0.1 g, 0.2 mmol) were dissolved in dry acetonitrile (20 ml). Potassium carbonate (0.02 g, 0.15 mmol) was added and the mixture was heated at 70°C for 4 hrs. Solvent was removed under reduced pressure and the residue

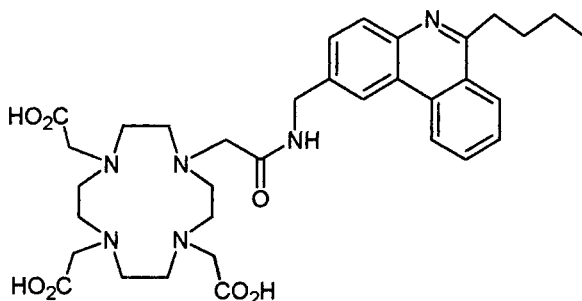
taken in dichloromethane (20 ml), washed with water (2 x 20 ml), dried over potassium carbonate, filtered and the solvent removed. The product was purified by chromatography column on alumina ($R_f = 0.2$, 5% EtOH-CH₂Cl₂), to give a colourless solid (0.1 g, 62%).

¹H NMR (CDCl₃, 300 MHz) : δ 10.2 (1H, t), 8.70 (1H, d, *J* 8.4, H4), 8.57 (1H, s, H1), 8.18 (1H, d, *J* 8.2, H7), 7.93 (1H, d, *J* 8.4, H10), 7.80-7.58 (3H, m, H3H9H8), 4.64 (2H, d, *J* 5.7, CH₂NH), 3.31 (2H, t, *J* 8.1, H11), 2.60-2.2 (16H, br m, CH₂ring), 1.80 (2H, m, H12), 1.50 (2H, m, H13), 1.29 (27H, m, *tert*-Bu), 0.97 (3H, t, H14).

¹³C NMR (CDCl₃, 75.4 MHz) : δ 172.4 (C=O), 161.8 (C6), 142.8, 138.7, 133.3, 130.4, 129.3, 129.1, 127.2, 126.2, 125.2, 123.6, 123.3, 121.3 (Ar-C); 82.0, 81.9 (C(CH₃)₃), 58.2 (CH₂NH), 56.3-55.8 (8C, Cring), 43.3 (C2'), 36.4 (C11), 31.5 (C12), 28.3, 28.1, 28.0 (C(CH₃)₃), 23.3 (C13), 14.2 (C14).

M/z (ES⁺): 842 [M+Na]⁺.

1-{Methylcarbonyl-[2-aminomethyl-(6-Butyl-Phenanthridine)]}-4,7,10-tris-(carboxymethyl)-1,4,7,10-tetraazacyclododecane 18



Tert-butyl ester **17b** (0.1 g, 0.12 mmol) was dissolved in a solution of 80% trifluoroacetic acid in dichloromethane (10 ml). The mixture was stirred at room temperature for 3hrs. The solvents were removed under reduced pressure and the residue taken in water. Solvent was removed on the freeze-drier to yield a colourless solid (0.073 g ; 95%).

¹H NMR (D₂O, 200 MHz): δ 8.40 (1H, d, *J* 8.4, H4), 8.16 (2H, m, H1H7), 7.90 (1H, d, H10), 7.75-7.55 (3H, m, H3H9H8), 4.39 2H, (br d, CH₂NH), 3.85 (1H, br s, NH), 3.2-2.8 (16H, br m, CH₂ring), 1.45 (2H, m, H12), 1.15 (2H, m, H13), 0.64 (3H, m, H14).

M/z (ES⁺): 647 [M+H]⁺

Europium complex of 18 : 19

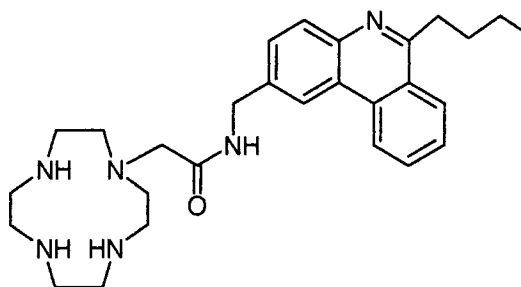
Europium acetate (15 mg, 45 μmol) and compound **18** (25 mg, 38 μmol) were dissolved in water (3 ml). The pH was adjusted to 5.5 and the solution heated at 80°C for 2 hrs. The product was purified on a short alumina chromatography column (eluent 10% methanol in CH_2Cl_2), to give a white solid (27 mg, 90%).

^1H NMR (D_2O , pD = 5.5): δ 33.8 (1H), 32.1 (2H), 31.6 (1H) (ring H_{ax}); 8.1-7.0 (m, 7H, Phen-H), 4.0-1.0 (m, 11H, CH_2N + Butyl chain), 0.1 (br s, 2H, H_{eq}), -2.4 (1H, H_{eq}), -3.1 (2H, H_{eq}), -4.8 (1H, H_{eq}), -6.0 (1H, H_{eq}), -7.2 (2H, H_{ax} , H_{eq}), -7.6 (1H, H_{ax}), -11.5 (2H, H_{ax}); -11.9 (1H, CHCO), -12.4 (1H, CHCO), -14.8 (2H, CHCO), -15.6 (1H, CH'CO), -16.0 (1H, CHCO), -17.0 (1H, CH'CO), -17.5 (1H, CHCO).

M/z (ES+): 801 $[\text{M}+\text{H}]^+$, 839 $[\text{M}+\text{K}]^+$.

HR-ESMS (m/z): Found 800.2270; $\text{C}_{34}\text{H}_{44}\text{N}_6\text{O}_7\text{Eu}$ requires 800.2272 $[\text{M}+\text{H}]^+$.

1-{Methylcarbonyl-[2-aminomethyl-(6-butyl-phenanthridine)]}-4,7,10-tetraazacyclododecane **21**



Freshly prepared 12N_4 -molybdenum tricarbonyl complex (0.22 g, 0.61 mmol) was solubilized in degassed DMF under argon. Potassium carbonate (0.13 g, 0.61 mmol) was added and the suspension was heated up to 80°C. *N*-Chloroacetyl-2-aminomethyl-6-butyl phenanthridine **16** (0.20 g, 0.61 mmol) was solubilized in degassed DMF (10 ml) under argon and added to the suspension. Heating was continued for 2 hrs at 80°C. The solvent was removed under vacuum. The residue was taken in hydrochloric acid (20 ml, 1 M), stirred overnight and the pH was raised up to 14 using potassium hydroxide pellets. The product was extracted using

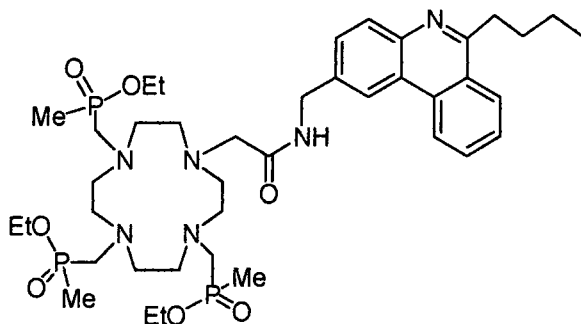
dichloromethane (4 × 30 ml), washed with brine (2 × 30 ml) and dried over potassium carbonate to yield a yellow oil, 0.26 g (89%), which was used without any further purification.

¹H NMR (CDCl₃, 200 MHz): δ 8.59 (1H, d, *J* 8.4, H4), 8.39 (1H, d, *J* 1.5, H1), 8.16 (1H, d, *J* 8.2, H7), 7.98 (1H, d, *J* 8.4, H10), 7.74 (2H, t, H3), 7.63-7.57 (2H, m, H9H8), 6.95 (1H, br.s, NH), 4.64 (2H, d, CH₂NH, *J* 5.7), 3.27 (2H, t, *J* 8.1, H11), 2.86 (s), 2.79 (2H, s), 2.58 (2H, s), 2.53 (s), 2.43 (m,), 2.35(m,), 1.60 (2H, m, H12), 1.45 (2H, m, H13), 0.93 (3H, t, H14).

¹³C NMR (CDCl₃, 75.4 MHz): δ 171.8 (C=O), 162.6 (C6), 162.6, 143.1, 136.9, 132.7, 130.5, 130.4, 129.8, 128.7, 127.5, 126.4, 125.4, 123.7, 122.7, 121.3, 59.3 (CH₂NH), 47.2-45.8 (8C, Cring), 43.6 (2-CH₂Phen), 36.6 (C11), 31.5 (C12), 23.2 (C13), 14.2 (C14).

M/z (ES⁺): 477.3 [M+H]⁺

1-{Methylcarbonyl-[2-aminomethyl-(6-butyl-phenanthridine)]}-4,7,10-tris-(ethoxymethylphosphinyl)methyl}-1,4,7,10-tetraazacyclododecane 22a



1-{Methylcarbonyl-[2-aminomethyl-(6-butyl-phenanthridine)]}-4,7,10-tetraazacyclododecane **21** (0.23 g, 0.55 mmol) and paraformaldehyde (0.08 g, 2.67 mmol) were taken into anhydrous tetrahydrofuran (20 ml) and the reaction mixture heated up to 60°C. Methyl-diethoxyphosphine (0.26 g, 1.92 mmol) was added and the solution was refluxed over 4Å molecular sieves according to the general procedure described previously.⁵ The product was purified by column chromatography on alumina (gradient elution from dichloromethane to 2% ethanol-dichloromethane, *R_f* = 0.3 by TLC using 5% ethanol-dichloromethane) to give a pale yellow oil, 0.25g, 55%.

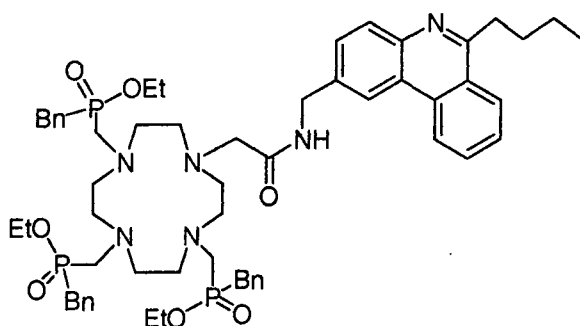
⁵ a) T. J. Norman, D. Parker, K. Pulukkody, L. Royle, C. J. Broan, *J. Chem. Soc., Perkin Trans. 2*, **1993**, 605.
b) S. Aime, M. Botta, D. Parker, J. A. G. Williams, *J. Chem. Soc., Dalton Trans.*, **1995**, 2259.

^1H NMR (CDCl₃, 200 MHz): δ 8.57 (1H, d, J 8.4, H4), 8.45 (1H, d, J 1.5, H1), 8.20 (1H, d, J 8.2, H7), 7.98 (1H, d, J 8.4, H10), 7.80 (1H, t, H3), 7.62 (2H, m, H9H8), 7.14 (15H, m, Ph), 4.64 (2H, m, CH₂-Phen), 4.06 (6H, m, P-OCH₂), 2.60-2.20 (22H, br m, CH₂ ring, N-CH₂-P), 3.25 (2H, t, H11), 1.78 (2H, m, H12), 1.42 (2H, m, H13), 1.16 (9H, t, CH₂ CH₃), 0.97 (3H, t, H14).

^{31}P NMR (CDCl₃): δ 53.1-51.7 (m, P-OEt)

M/z (ES⁺): 859.1 [M-Na]⁺, 837.1 [M-H]⁺.

1-{Methylcarbonyl-[2-aminomethyl-(6-butyl-phenanthridine)]}-4,7,10-tris-
{(ethoxymethylphosphinyl)benzyl}-1,4,7,10-tetraazacyclododecane 22b



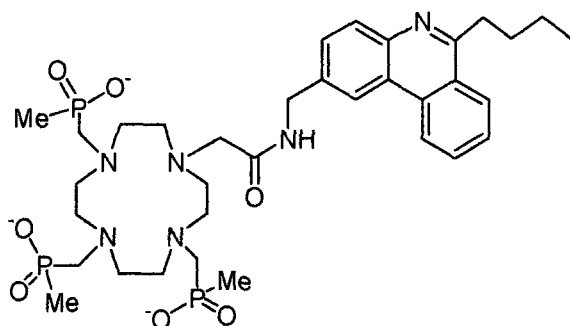
1-{Methylcarbonyl-[2-aminomethyl-(6-butyl-phenanthridine)]}-4,7,10-tetraazacyclododecane **21** (0.23 g, 0.55 mmol) and paraformaldehyde (0.08 g, 2.67 mmol) were taken into anhydrous tetrahydrofuran and the reaction mixture heated upto 60°C. Benzyl-diethoxyphosphine (0.4 g, 1.92 mmol) was added and the solution was refluxed over 4Å molecular sieves according to the general procedure described previously.⁵ The product was purified by column chromatography on alumina (gradient elution from dichloromethane to 2% EtOH-dichloromethane, $R_f = 0.33$ by TLC using 10% EtOH-dichloromethane) to give a pale yellow oil (0.35 g, 60%).

^1H NMR (CDCl₃, 300 MHz): δ 8.59 (1H, d, J 8.4, H4), 8.45 (1H, d, J 1.5, H1), 8.20 (1H, d, J 8.2, H7), 7.98 (1H, d, J 8.4, H10), 7.80 (1H, t, H3), 7.62 (2H, m, H9H8), 7.14 (15H, m, Ph), 4.64 (2H, m, CH₂-Phen), 3.90 (6H, m, P-OCH₂), 2.55-2.70 (22H, br m, CH₂ ring, N-CH₂-P), 3.25 (2H, t, H11), 1.78 (2H, m, H12), 1.42 (2H, m, H13), 1.19 (9H, t, CH₂ CH₃), 1.01 (3H, t, H14).

^{31}P NMR (CDCl₃): δ 49.8, 49.0.

M/z (ES⁺): 1088 [M+Na]⁺.

1-{Methylcarbonyl-[2-aminomethyl-(6-butyl-phenanthridine)]}-4,7,10-tris-
 {(methylphosphinyl)methyl}-1,4,7,10-tetraazacyclododecane 23a

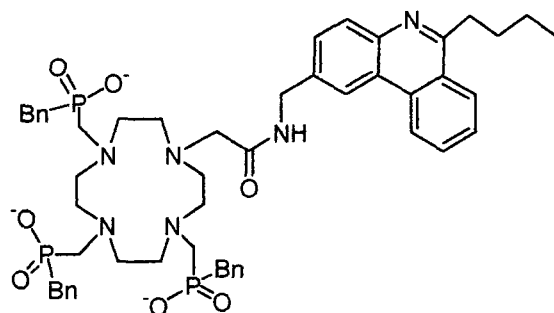


A solution of potassium deuterioxide in D₂O (15 ml) was added to the phosphinate ester **22a** (0.13 g, 0.16 mmol) and the mixture stirred at room temperature for 16 h to give clear solution. The reaction was monitored by ³¹P NMR. The solution was neutralized by addition of dilute hydrochloric acid and the solvent removed under low pressure to give a hygroscopic glassy solid (0.10g, 87%).

δ ³¹P NMR (CDCl₃): 40.4, 37.1-36.5 (m, P-OH)

1-{Methylcarbonyl-[2-aminomethyl-(6-butyl-phenanthridine)]}-4,7,10-tris-
 {(methylphosphinyl)benzyl}-1,4,7,10-tetraazacyclododecane 23b

Ligand **23b** was prepared similarly to ligand **23a**.



³¹P NMR (D₂O): δ 32.1.

Europium complex of 23a : 24

Europium nitrate was added to a solution of compound **23a** (0.10 g, 0.14 mmol) in water and the mixture heated at 70°C for 16hrs to give a clear solution. The progress of the reaction was monitored using ^{31}P NMR. The solvent was removed and the product was purified by chromatography on a short alumina column (eluent 10% MeOH- CH_2Cl_2 , $R_f = 0.3$) to give a colourless solid.

M/z (ES⁺): 903 [M-H]⁺, 452 [M-H]²⁺.

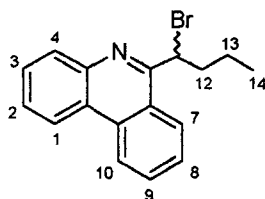
Europium complex of 23b : 25

Same procedure as described before .

^1H NMR (CD₃OD): δ 31.6, 31.6, 29.2, 19.2, 15.9, 14.6, 12.8, 12.2 (ringH_{ax}); -0.60, -1.3 (ringH_{eq}); -3.4 (ringH_{ax}); -6.8 (PCH₃); -11.1, -11.8, -12.3, -13.1, -15.8 (ring H and NCH₂CO).

^{31}P NMR (D₂O): δ 91.1, 87.2, 74.0.

M/z (ES⁻): 1130 [M+H]⁺

(±)(1'-Bromo) 6-butyl phenanthridine 26

6-Butyl phenanthridine **1** (1.1 g, 4.7 mmol) and *N*-bromosuccinimide (1.1 g, 6.2mmol) were dissolved in carbon tetrachloride and heated at reflux (80°C) for 4 hrs. The warm suspension was filtered over Celite, washed with a mixture of carbon tetrachloride/benzene and the solvents were removed. The product was recrystallized twice from ethanol to give white needle-shaped crystals (1.26 g, 83%), m.p. 158-159°C.

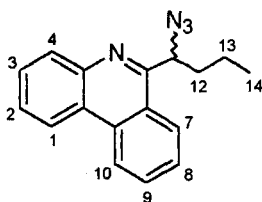
^1H NMR (CDCl₃, 300 MHz) : δ 8.62 (1H, d, *J* 8.4, H4); 8.50 (1H, d, *J* 8, H1); 8.36 (1H, d, *J* 8, H7); 8.13 (1H, d, *J* 8, H10); 7.79 (1H, t, *J* 7.1, H2); 7.65 (3H, m, H8H9H3); 5.77 (1H, t, *J* 8, H11); 2.61 (2H, m, H12); 1.62 (2H, m, H13); 0.97 (3H, t, *J* 7.5, H14).

^{13}C NMR (CDCl₃, 75.4 MHz) : δ 157.8 (C6); 130.4 (Ar-C); 128.7 (Ar-C); 127.4 (Ar-CH); 127.2 (Ar-CH); 125.5 (Ar-CH); 124.7 (Ar-C); 124 (Ar-CH); 122.6 (Ar-CH); 121.9 (Ar-CH); 77.2 (C11); 37.5 (C12); 21.5 (C13); 13.7 (C14).

M/z (ES⁺) : 313 [M+H]⁺, 233 [M-(Br)]⁺

HR-ESMS (m/z): Found 314.0540 ; C₁₇H₁₆BrN requires 314.0544

(±) 6-(1'-Azido) butyl phenanthridine 27



(±)(1'-Bromo) 6-butyl phenanthridine **26** (1 g, 3.2 mmol) and sodium azide (0.57 g, 9 mmol) were dissolved in dimethylformamide. The solution was heated at 70°C overnight. The solution was poured into ice and extracted using dichloromethane (3 × 20 ml), the organic layers washed using distilled water (4 × 20 ml) and sodium carbonate solution (3 × 20 ml), dried over potassium carbonate, and filtered off. The solvent was removed and the residue purified on silica column (*R_f* = 0.3, eluent dichloromethane/hexane 60:40), to give a white solid (0.84 g, 96%).

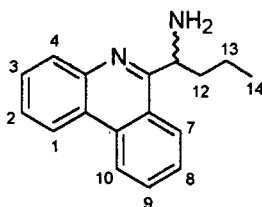
^1H NMR (CDCl₃, 300 MHz) : δ 8.69 (1H, d, *J* 6.2, H4); 8.58 (1H, d, *J* 6, H1); 8.31 (1H, d, *J* 6, H7), 8.22 (1H, d, *J* 8, H10); 7.86 (1H, t, *J* 7.1, H2); 7.72 (m, 3H, H8H9H3); 5.16 (t, 1H, *J* 7, H11); 2.22 (m, 2H, H12); 1.66-1.55 (m, 2H, H13); 1.03 (3H, t, *J* 7.5, H14).

^{13}C NMR (CDCl₃, 75.4 MHz) : δ 162.7 (C6); 130.8 (2C, Ar-C); 128.9 (1C, Ar-C); 127.4 (1C, Ar-CH); 125.6 (2C, Ar-CH); 122.9 (2C, Ar-C); 122.1 (2C, Ar-CH); 36.7 (C11); 31.6 (C12); 20.2 (C13); 14.1 (C14).

Elemental analysis : Found (C 74.0, H 5.82); C₁₇H₁₆N₄·0.5H₂O requires (C 73.9, H 5.83).

M/z (ES⁺) : 249 [M-HN₂]⁺.

IR ν_{max} (cm⁻¹): ν_{max} 2098 (-N₃).

(±)6-(1'-Amino) butyl phenanthridine 28

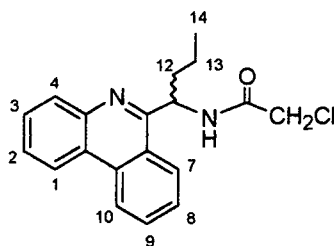
(±)(1'-Azido)6-butyl phenanthridine **27** (0.84 g, 3 mmol), hydrazine hydrate (3 ml, excess), palladium hydroxide (Pearlman's catalyst) (0.5 g) were heated in methanol (20 ml) at 60°C overnight. The suspension was filtered and the solvent removed. The residue was dissolved in dichloromethane, washed using sodium carbonate solution, dried over potassium carbonate, filtered and the solvent was removed to give a colorless oil (0.54 g, 73%).

¹H NMR (CDCl₃, 300 MHz) : δ 8.69 (1H, d, *J* 6.2, H4) ; 8.58 (1H, d, *J* 6, H1) ; 8.31 (1H, d, *J* 6, H7) ; 8.22 (1H, d, *J* 8, H10) ; 7.86 (2H, t, *J* 7.1, H2) ; 7.72 (3H, m, H8H9H3) ; 4.87 (t, 1H, *J* 8, H11) ; 2.22 (2H, m, H12) ; 1.76 (2H, broad s, -NH₂) ; 1.55 (m, 2H, H13) ; 0.96 (3H, t, *J* 7.5, H14).

¹³C NMR (CDCl₃, 75.4 MHz) : δ 157.8 (C6) ; 131.3 (2C, Ar-C) ; 130.3 (1C, Ar-C) ; 129.0 (1C, Ar-CH) ; 128.3 (1C, Ar-CH) ; 127.7 (1C, Ar-CH) ; 127.3 (1C, Ar-C) ; 123.3 (1C, Ar-CH) ; 122.3 (2C, Ar-CH) ; 122.1 (2C, Ar-CH) ; 42.6 (C11) ; 31.2 (C12) ; 17.8 (C13) ; 14.1 (C14).

Elemental analysis : Found (C 77.48, H 6.50, N 9.86) ; C₁₇H₁₈N₂·0.75H₂O requires (C 77.4, H 7.40, N 10.60)

M/z (ES⁺) : 251 [M+H]⁺

(±)6-(N-Chloroacetyl-1'-amino)-butyl phenanthridine 7

Chloroacetic acid (0.151 g, 1.6 mmol), and 1-hydroxybenzotriazole (0.22 g, 1.6 mmol) were dissolved in anhydrous THF, and the solution cooled down to 0°C. EDCI (0.36 g, 1.9 mmol)

was added. (1'-Amino) 6-butyl phenanthridine **28** (0.4 g, 1.6 mmol) was dissolved in THF (2 ml) and added dropwise. The solution was stirred at 0°C for one hour and warmed up to room temperature for 2 hrs. After filtration, the solvent was removed and the residue taken up in dichloromethane (20 ml), washed using sodium carbonate solution (3 × 20ml), dried over potassium carbonate, and filtered off. The solvent was removed and the residue purified on silica column ($R_f = 0.3$, eluent dichloromethane/ethyl acetate 60/20), to give a beige solid (0.33 g, 63%), m.p. : 140-141°C.

$^1\text{H NMR}$ (CDCl_3 , 300 MHz) : δ 8.69 (1H, d, J 6.2, H4) ; 8.58 (1H, d, J 6, H1) ; 8.31 (1H, d, J 6, H7) ; 8.22 (1H, d, J 8, H10) ; 7.86 (1H, t, J 7.1, H2) ; 7.72 (3H, m, H8H9H3) ; 4.87 (1H, q, J 3, H11) ; 2.22 (2H, m, H12) ; 1.76 (2H, broad s, $-\text{NH}_2$) ; 1.55 (2H, m, H13) ; 0.96 (3H, t, J 7.5, H14).

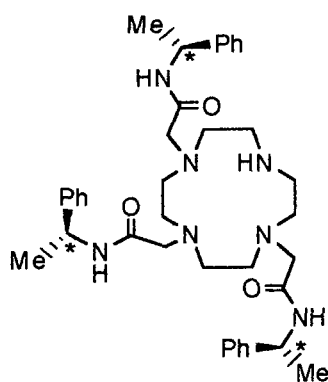
$^{13}\text{C NMR}$ (CDCl_3 , 75.4 MHz) : δ 169.2 (CO) ; 162.4 (C6) ; 137.0 (C, Ar-CH) ; 134.6 (C, Ar-CH) ; 133.66 (C, Ar-CH) ; 132.6 (C, Ar-CH) ; 131.4 (C, Ar-C) ; 130.8 (C, Ar-C) ; 129.0 (2C, Ar-CH) ; 127.6 (C, Ar-CH) ; 126.5 (C, Ar-CH) ; 125.8 (2C, Ar-CH) ; 53.9 (C11) ; 46.8 (CH_2Cl) ; 42.4 (C12) ; 22.4 (C13) ; 17.8 (C14).

M/z (ES^+) : 348 [$\text{M}+\text{Na}$] $^+$

Elemental analysis : Found C 69.8, H 5.86, N 8.57% ; $\text{C}_{19}\text{H}_{19}\text{ClN}_2\text{O}$ requires C 69.9, H 5.84, N 8.60%

IR $\nu_{\text{max}}(\text{cm}^{-1})$: ν_{max} 1664 (CO)

1,4,7-Tris[(*R*)-1-(1-phenyl)methyl-carbamoylmethyl]-1,4,7,10-tetraazacyclododecane **29**



(*R*)-*N*-(2-Chloroethanoyl)-2-phenylethylamine (1.13 g, 5.67 mmol) in dry ethanol (10 ml) was added dropwise over 8 hrs to a stirred solution of 1,4,7,10-tetraazacyclododecane (0.30 g, 1.77 mmol) and triethylamine (0.80 ml, 5.7 mmol) in dry ethanol (30 ml) at 60°C. The mixture was boiled under reflux for 18 hrs, concentrated to small volume, poured into aqueous hydrochloric acid (0.1M, 40 ml) and washed with diethyl ether (3 × 30 ml). The aqueous phase was neutralised by careful addition of sodium hydroxide (1M) the pH adjusted to 13 and the solution extracted with dichloromethane (3 × 30 ml). Extracts were dried (K_2CO_3) and solvent removed to yield an oily residue which was purified by chromatography on neutral alumina (100% CH_2Cl_2 to 2% MeOH/ CH_2Cl_2), R_f (Al_2O_3 ; 10% MeOH/ CH_2Cl_2) = 0.5 to yield a pale yellow solid (430 mg, 37%), m.p. 60-61°C.

1H NMR ($CDCl_3$, 400 MHz): δ 7.32 (3H, s, NHCO), 7.29-7.20 (15H, m., 3Ph), 3.8 (3H, dq+dq, C*H), 2.96 (4H, s, CH_2CO), 2.91 (2H, s, $CH_2C'O$), 2.70 (16H, br m., CH_2N_{ring}), 2.05 (1H, br s, NH), 1.50 (9H, d, J 7.2, 3 CH_3).

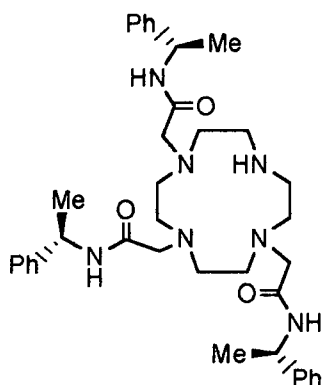
^{13}C NMR ($CDCl_3$, 75.4 MHz): δ 170.8, 170.6, 143.7 (C quater.), 129.1 (meta Ph-C), 127.8 (para Ph-C), 127.0, 59.9 (CH_2CO), 58.0 (CH_2CO), 54.5 (CH_2N), 53.6 (CH_2N), 48.9 (CHN), 48.6 (CHN), 22.1, 21.9 (CH_3).

M/z (ES^+): 348 $[M+H]^{2+}$, 656 $[M+H]^+$.

HR-ESMS (m/z): Found 656.4284. $C_{38}H_{54}N_7O_3$ requires $[M+H]^+$, 656.4288.

Elemental analysis : Found C 68.2; H 8.18; N 14.6 ; $C_{38}H_{53}N_7O_3 \cdot 0.5H_2O$ requires C 68.66; H 8.13; N 14.76.

1,4,7-Tris[(*S*)-1-(1-phenyl)methyl-carbamoylmethyl]-1,4,7,10-tetraazacyclododecane 30



(*S*)-*N*-(2-Chloroethanoyl)-2-phenylethylamine (1.17 g, 5.9 mmol) in dry ethanol (10 ml) was added dropwise over 8 hrs to a stirred solution of 1,4,7,10-tetraazacyclododecane (0.34 g, 2.0 mmol) and triethylamine (0.83 ml, 5.9 mmol) in dry ethanol (30 ml) at 60°C. The mixture was boiled under reflux for 18 hrs, concentrated to small volume, poured into aqueous hydrochloric acid (0.1M, 40 ml) and washed with diethyl ether (3 × 30 ml). The aqueous phase was neutralised by careful addition of sodium hydroxide (1M) the pH adjusted to 13 and the solution extracted with dichloromethane (3 × 30 ml). Extracts were dried (K₂CO₃) and solvent removed to yield an oily residue which was purified by chromatography on neutral alumina (100% CH₂Cl₂ to 2% MeOH/CH₂Cl₂), R_f (Al₂O₃; 10% MeOH/CH₂Cl₂) = 0.5 to yield a pale yellow solid (380 mg, 29%), m.p. 63-65°C.

¹H NMR (CDCl₃, 400 MHz): δ 7.30 (3H, s, NHCO), 7.29-7.21 (15H, m., PhH), 5.12 (3H, dq+dq, C*H), 2.97 (4H, s, CH₂CO), 2.93 (2H, s, CH₂C'O), 2.58 (16H, br m., CH₂N_{ring}), 1.80 (1H, br s, NH), 1.48 (6H, d, *J* 7.2, CH₃), 1.45 (3H, d, CH₃).

¹³C NMR (CDCl₃, 75.4 MHz): δ 170.8, 168.1 (CO), 143.4 (Ar-C), 128.8 (ortho Ar-C), 127.9 (meta ArC), 126.5 (para ArC), 58.4 (CH₂CO), 53.1 (CH₂N_{ring}), 50.6 (CH₂N_{ring}), 49.2 (C*H), 47.6 (C*H), 22.0, 21.7 (CH₃).

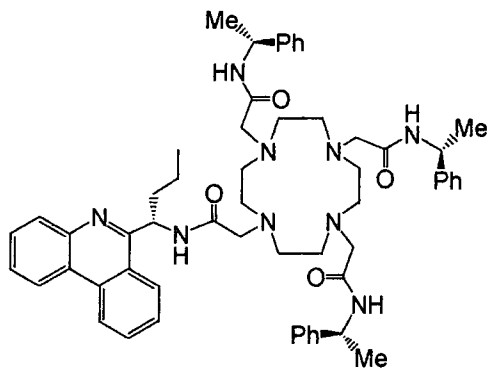
HR-ESMS (m/z): Found 656.4287. C₃₈H₅₄N₇O₃ requires [M+H]⁺, 656.4288.

Elemental analysis : Found (C 65.7; H 8.54; N 14.0) ; C₃₈H₅₃N₇O₃·2H₂O requires C 66.0; H 8.30; N 14.2.

Ligands R-RRR (L⁵), S-RRR (L⁶), S-SSS (L⁷), R-SSS (L⁸) :

6-(*N*-Chloroacetyl-1'-amino)-butyl phenanthridine (0.2 g, 0.61 mmol), the (RRR) **29** or (SSS) **30** tris-amide (0.4 g, 0.61 mmol), caesium carbonate (0.2 g, 0.6 mmol), potassium iodide (0.02 g, 0.12 mmol) were heated at 70°C in acetonitrile for 2d. The formation of product was followed by ESMS. The reaction was quenched using water, the product was extracted using CH₂Cl₂ (4 × 20 ml), washed using potassium carbonate aqueous solution, dried over K₂CO₃, filtered off and the solvent was removed. The two diastereoisomers were purified and separated on an alumina chromatography column (gradient eluent from 1% to 4% MeOH in CH₂Cl₂), R_f(Al₂O₃, 10% MeOH/CH₂Cl₂) (A) = 0.58, (B) = 0.27, to yield pale yellow solids : A (S-RRR or R-SSS) (95 mg, 17%) and B (R-RRR or S-SSS) (90 mg, 15%).

• (S-RRR)-(L⁶) : 31



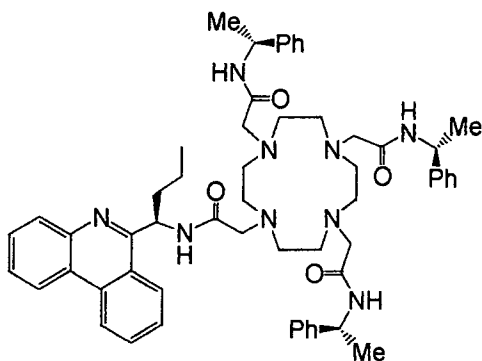
¹H NMR (CDCl₃, 300 MHz) : δ 8.60 (1H, t, *J* 6.2, H1) ; 8.54 (1H, t, *J* 6, H7) ; 8.15 (1H, d, *J* 6, H10) ; 8.06 (1H, m, H4) ; 7.82 (1H, m, *J* 6, H2) ; 7.77-7.60 (3H, m, H8H9H3) ; 7.30-7.10 (16H, m, Ph, NH) ; 6.78 (2H, m, NH) ; 5.98 5.90 (1H, 2br m, C*H) ; 5.06-4.80 (3H, m, C*HMePh) ; 2.90-2.40 (14H, m, ring H, CH₂ arms) ; 2.10-1.84 (4H, m, H12H13) ; 1.45 (9H, m, Me arms) ; 0.84 (3H, t, *J* 7.5, H14).

¹³C NMR (CDCl₃, 75.4 MHz) : δ 170.6 170.4, 170.0 (CO) ; 159.5 (C6) ; 144.4, 142.9, 143.6, 133.4 (C, Ar-CH) ; 131.2 (C, Ar-CH) ; 129.7 (C, Ar-CH) ; 129.1 (C, Ar-CH) ; 128.8 (C, Ph) ; 128.3 (C, Ar-C) ; 127.4 (C, Ph) ; 126.6 (C, Ph) ; 125.5 (C, Ar-C) ; 124.1 (2C, Ar-CH) ; 123.8 (C, Ar-CH) ; 122.9 (C, Ar-CH) ; 122.4 (2C, Ar-CH) ; 59.5, 59.21, 57.6, 57.32 (4CH₂CO) ; 51.2-49.8 (Cring) ; 47.06 (C*HNH) ; 38.8 (C11) ; 25.6 (C12) ; 22.2-21.7 (CH₃) ; 19.2 (C13) ; 14.2 (C14).

M/z (ES⁺) : 493 [M+Ca]²⁺, 968 [M+Na]⁺

Elemental analysis : Found C 70.75, H 7.6, N 13.0 ; C₅₇H₇₃N₉O₄·0.5H₂O requires C 71.5, H 7.8, N 13.2.

• (R-RRR)-(L⁵) : 32



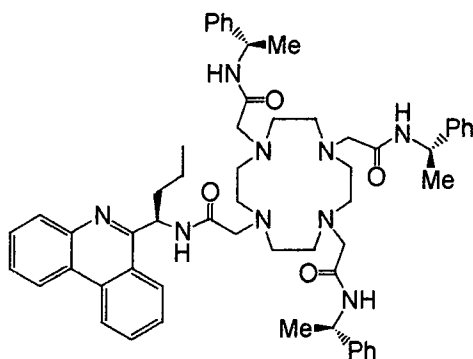
^1H NMR (CDCl_3 , 300 MHz) : δ 8.66 (1H, d, J 6.2, H1) ; 8.55 (1H, d, J 6, H7) ; 8.28 (1H, d, J 6, H10) ; 8.08 (1H, t, J 3, H4) ; 7.85 (1H, t, J 6, H2) ; 7.73-7.64 (3H, m, H8H9H3) ; 7.28-7.14 (17H, m, Ph, NH) ; 6.94 (2H, br.m, NH) ; 6.12 (1H, br., C*H) ; 5.15 (3H, m, CHMePh) ; 2.87 (8H, m, CH₂ pendent arms) ; 2.60 (16H, br. m, ring H) ; 2.08 (2H, m, H12) ; 1.70 (2H, m, H13) ; 1.43 (9H, dd, Me arms) ; 0.87 (3H, t, J 7.5, H14).

^{13}C NMR (CDCl_3 , 75.4 MHz) : δ 169.9 (CO) ; 162.4 (C6) ; 143.3, 143.0, 133.4 (C, Ar-CH) ; 131.2 (C, Ar-CH) ; 129.7 (C, Ar-CH) ; 129.1 (C, Ar-CH) ; 128.8 (C, Ph) ; 128.0 (C, Ar-C) ; 127.7 (C, Ph) ; 126.6 (C, Ph) ; 126.5 (C, Ar-C) ; 125.6 (C, Ar-CH) ; 124.1 (2C, Ar-CH) ; 122.8 (C, Ar-CH) ; 122.4 (2C, Ar-CH) ; 59.6, 59.45, 59.1, 58.8 (4CH₂CO) ; 53.6-53.1 (Cring) ; 49.5, 48.5, 48.4 (C*HNH) ; 38.7 (C11) ; 25.6 (C12) ; 21.7-21.5 (CH₃) ; 19.3 (C13) ; 14.3 (C14).

M/z (ES^+) : 493 [$\text{M}+\text{Ca}$]²⁺, 968 [$\text{M}+\text{Na}$]⁺

Elemental analysis : Found C 70.8, H 7.51, N 12.9 ; C₅₇H₇₃N₉O₄.0.5H₂O requires C 71.5, H 7.8, N 13.2.

• (R-SSS)-(L⁸) : **33**



^1H NMR (CDCl_3 , 400 MHz) : δ 8.68 (1H, t, J 6.2, H1) ; 8.57 (1H, t, J 6, H7) ; 8.20 (1H, d, J 6, H10) ; 8.08 (1H, m, H4) ; 7.90 (1H, m, J 6, H2) ; 7.80-7.65 (3H, m, H8H9H3) ; 7.33-7.19 (15H, m, Ph) ; 6.9 (3H, m, NH) ; 6.06 5.96 (1H, 2br m, C*H) ; 5.09 (3H, m, CHMePh) ; 2.80-2.50 (14H, m, ring H, CH₂ pendent arms) ; 2.10 (2H, m, H12) ; 1.84 (2H, m, H13) ; 1.43 (9H, m, Me arms) ; 0.89 (3H, t, J 7.5, H14).

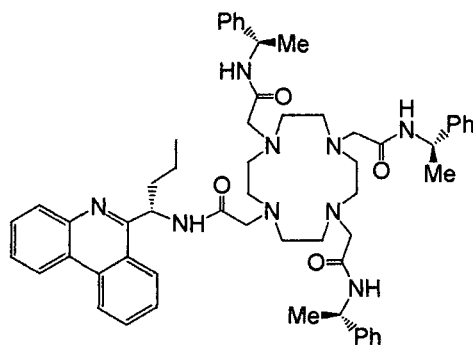
^{13}C NMR (CDCl_3 , 75.4 MHz) : δ 170.7 170.5, 170.0 (CO) ; 159.7 (C6) ; 143.6, 133.4 (C, Ar-CH) ; 131.2 (C, Ar-CH) ; 129.7 (C, Ar-CH) ; 129.1 (C, Ar-CH) ; 128.8 (C, Ph) ; 128.3 (C, Ar-C) ; 127.4 (C, Ph) ; 126.6 (C, Ph) ; 125.5 (C, Ar-C) ; 124.1 (2C, Ar-CH) ; 123.8 (C, Ar-CH) ; 122.9 (C, Ar-CH) ; 122.4 (2C, Ar-CH) ; 59.6, 59.45, 57.46, 57.3 (4CH₂CO) ; 51.3-49.7

(Cring); 47.1 (C*HNH); 39.1 (C11); 25.6 (C12); 22.3-21.9 (CH₃); 19.3 (C13); 14.3 (C14).

M/z (ES⁺) : 493 [M+Ca]²⁺, 968 [M+Na]⁺

Elemental analysis : Found C 70.4, H 7.9, N 12.8; C₅₇H₇₃N₉O₄.H₂O requires C 70.85, H 7.82, N 13.04.

• (S-SSS)-(L⁷) : **34**



¹H NMR (CDCl₃, 400 MHz) : δ 8.65 (1H, d, *J* 6.2, H1); 8.55 (1H, d, *J* 6, H7); 8.30 (1H, d, *J* 6, H10); 8.08 (t, *J* 3, H4); 7.86 (t, 1H, *J* 6, H2); 7.72 (m, 3H, H8H9H3); 7.28-7.14 (m, 17H, Ph, NH); 6.94 (br., 2H, NH); 6.06 (br., 1H, C*H); 5.15-4.85 (m, 3H, CHMePh); 2.88 (m, 8H, CH₂); 2.60 (br. m, ring H); 2.10 (m, 2H, H12); 1.84 (m, 2H, H13); 1.22 (m, 9H, Me arms); 0.89 (t, 3H, *J* 7.5, H14).

¹³C NMR (CDCl₃, 75.4 MHz) : δ 170.0 169.9 (CO); 160.0 (C6); 143.3, 133.3 (C, Ar-CH); 131.2 (C, Ar-CH); 129.7 (C, Ar-CH); 129.1 (C, Ar-CH); 128.9 (C, Ph); 128.0 (C, Ar-C); 127.6 (C, Ph); 126.6 (C, Ph); 125.6 (C, Ar-C); 124.1 (2C, Ar-CH); 122.8 (C, Ar-CH); 122.4 (2C, Ar-CH); 59.6, 59.5, 59.1, 58.9 (4CH₂CO); 53.6-53.1 (Cring); 49.5, 48.5, 48.4 (C*HNH); 38.7 (C11); 25.6 (C12); 21.6 21.5 (CH₃); 19.3 (C13); 14.2 (C14).

M/z (ES⁺) : 493 [M+Ca]²⁺, 968 [M+Na]⁺

Elemental analysis : Found C 70.7, H 7.7, N 12.8; C₅₇H₇₃N₉O₄.H₂O requires (C 70.8, H 7.82, N 13.0).

Lanthanide Complexes of L⁵, L⁶, L⁷, L⁸

The Eu(III) and Yb(III) complexes were prepared by stirring each of the isomeric ligands with one equivalent of the appropriate lanthanide triflate salt in dry CH₃CN (1-2 ml) at 80°C

overnight. The CH₃CN was then removed under vacuum and the oily residue taken up into a mixture of methanol (1 ml) and purified water (10 ml). The solvents were removed by lyophilisation to give the complexes as pale yellow solids.

• R-RRR [Eu-L⁵](CF₃SO₃)₃.H₂O 35

¹H NMR (CD₃OD, 300 MHz): δ 29.7, 28.9, 28.6, 28.1, 26.9 (4H, H_{ax}); 11.13, 10.59, 10.06, 9.96, 9.42 (4H, H'_{eq}); 8.30, 8.10, 7.91, 7.66, 7.47 (4H, H_{eq}); -1.76, -1.85, -2.15, -2.44 (4H, NH_{amide}); -6.69, -6.64, -7.08 (4H, CH'₂N_{ring}); -7.76, -7.86 (4H, H_{ax'}); -13.4, -13.5, -13.9, -14.2, -14.7, -15.1 (4H, CH₂N_{ring}).

M/z (ES⁺): 366 [M-H]³⁺, 549 [M-H]²⁺, 624 [M-OTf]²⁺

HR-ESMS (m/z): Found 623.7181 C₆₀H₇₁F₉N₉O₁₃S₃Eu requires [M-(OTf)₂]²⁺, 623.7181.

• R-RRR [Yb-L⁵](CF₃SO₃)₃.H₂O 36

¹H NMR (CD₃OD, 200 MHz): δ 110.4, 108.3, 106.6, 104.1, 103.3 (4H, H_{ax}); 20.1, 19.4, 18.7, 18.1 (4H, H'_{eq}); 16.5, 14.4, 12.8, 12.1 (4H, H_{eq}); -13.5, -14.2, -14.8, -15.0 (4H, NH_{amide}); -27.1, -27.7, -28.4, -28.9 (4H, CH'₂N_{ring}); -35.5, -36.2, -37.2, -38.2 (4H, H_{ax'}); -64.3, -65.3, -66.3, -67.7, -68.4 (4H, CH₂N_{ring}).

M/z (ES⁺): 373 [M-H]³⁺, 559 [M-H]²⁺, 634 [M-OTf]²⁺

HR-ESMS (m/z): Found 634.2268 C₆₀H₇₁F₉N₉O₁₃S₃Yb requires [M-OTf₂]²⁺, 634.2269.

• S-RRR [Eu-L⁶](CF₃SO₃)₃.H₂O 37

¹H NMR (CD₃OD, 300 MHz): δ 29.6, 28.4, 28.3, 27.6, 26.7 (4H, H_{ax}); 10.63, 10.14, 9.51, 8.92 (4H, H'_{eq}); 8.14, 7.89, 7.70, 7.45, 7.21 (4H, H_{eq}); -2.26, -2.60, -2.94, -3.53 (4H, NH_{amide}); -7.11, -7.24, -7.48 (4H, CH'₂N_{ring}); -8.05, -8.22 (4H, H_{ax'}); -13.88, -14.6, -15.2, -15.5 (4H, CH₂N_{ring}).

M/z (ES⁺): 366 [M-H]³⁺, 549 [M-H]²⁺, 624 [M-OTf]²⁺

HR-ESMS (m/z): Found 623.7183 C₆₀H₇₁F₉N₉O₁₃S₃Eu requires [M-(OTf)₂]²⁺, 623.7181.

• S-RRR [Yb-L⁶](CF₃SO₃)₃.H₂O 38

¹H NMR (CD₃OD, 200 MHz) : δ 112.6, 110.6, 108.7, 106.1, 101.1 (4H, H_{ax}); 21.1, 20.0, 18.9, 18.6 (4H, H'_{eq}); 17.2, 14.8, 13.08, 12.4 (4H, H_{eq}); -13.5, -14.2, -14.8, -15.0 (4H, NH_{amide}); -27.2, -28.5, -30.6, -31.9 (4H, CH'₂N_{ring}); -35.7, -36.3, -37.3, -38.4 (4H, H_{ax'}); -65.0, -66.1, -66.7, -68.4, -69.1 (4H, CH₂N_{ring}).

M/z (ES⁺) : 373 [M-H]³⁺, 559 [M-H]²⁺, 634 [M-OTf]²⁺

HR-ESMS (m/z) : Found 634.2268 C₆₀H₇₁F₉N₉O₁₃S₃Yb requires [M-OTf₂]²⁺, 634.2269.

• S-SSS [Eu-L⁷](CF₃SO₃)₃.H₂O 39

¹H NMR (CD₃OD, 300 MHz) : δ 28.2, 27.3, 26.9, 26.5, 25.4 (4H, H_{ax}); 9.58, 9.42, 8.56, 8.10 (4H, H'_{eq}); 7.84, 7.75, 7.40, 7.27 (4H, H_{eq}); -0.94, -1.17, -1.49 (4H, NH_{amide}); -2.17, -2.3, -3.36, -3.67 (4H, CH'₂N_{ring}); -8.2, -8.3, -8.5, -8.9, -9.4, -9.9 (4H, H_{ax'}); -14.8, -14.9, -15.1, -15.4, -15.6, -15.8, -16.3, -16.5 (4H, CH₂N_{ring}).

M/z (ES⁺) : 366 [M-H]³⁺, 549 [M-H]²⁺, 624 [M-OTf]²⁺

HR-ESMS (m/z) : Found 1394.3887 C₆₀H₇₁F₉N₉O₁₃S₃¹⁵¹Eu requires [M-OTf]⁺, 1394.3869.

• S-SSS [Yb-L⁷](CF₃SO₃)₃.H₂O 40

¹H NMR (CD₃OD, 200 MHz) : δ 110.5, 108, 106, 104, 99.5 (4H, H_{ax}); 20.6, 19.2, 18.4, 17.9 (4H, H'_{eq}); 14.9, 14.2, 13.4, 12.4 (4H, H_{eq}); -13.9, -14.2, -14.5, -14.7 (4H, NH_{amide}); -26.8, -27.4, -28.3, -28.6 (4H, CH'₂N_{ring}); -35.3, -35.9, -37.8, -38.4 (4H, H_{ax'}); -64.0, -65.1, -66.0, -68.1 (4H, CH₂N_{ring}).

M/z (ES⁺) : 373 [M-H]³⁺, 559 [M-H]²⁺, 634 [M-OTf]²⁺

HR-ESMS (m/z) : Found 1417.4044 C₆₀H₇₁F₉N₉O₁₃S₃Yb requires [M-OTf]⁺, 1417.4058.

• R-SSS [Eu-L⁸](CF₃SO₃)₃.H₂O 41

¹H NMR (CD₃OD, 300 MHz) : δ 29.8, 28.9, 28.5, 28.1, 26.9 (4H, H_{ax}); 11.3, 11.26, 10.42, 10.06, 9.96 (4H, H'_{eq}); 8.28, 8.09, 7.95, 7.51, 7.27 (4H, H_{eq}); -1.72, -1.80, -2.21, -2.45 (4H,

NH_{amide}); -6.76, -6.91, -7.08, -7.12 (4H, CH₂N_{ring}); -7.62, -7.68, -7.97 (4H, H_{ax}); -13.5, -13.74, -13.98, -14.24, -14.75, -15.13 (4H, CH₂N_{ring}).

M/z (ES⁺) : 366 [M-H]³⁺, 549 [M-H]²⁺, 624 [M-OTf]²⁺

HR-ESMS (m/z) : Found 1394.3863 C₆₀H₇₁F₉N₉O₁₃S₃¹⁵¹Eu requires [M-OTf]⁺, 1394.3869.

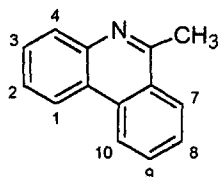
• R-SSS [Yb-L⁸](CF₃SO₃)₃·H₂O 42

¹H NMR (CD₃OD, 200 MHz) : δ 110.6, 108.3, 106.8, 104.3, 99.5 (4H, H_{ax}); 20.6, 19.4, 18.4, 17.9 (4H, H_{eq}); 14.5, 14.2, 13.4, 12.4 (4H, H_{eq}); -9.0, -9.26, -10.3, -10.6 (4H, NH_{amide}); -26.2, -27.4, -28.8, -29.2 (4H, CH₂N_{ring}); -34.2, -34.6, -35.6, -37.3 (4H, H_{ax}); -60.4, -62.0, -64.1, -64.6 (4H, CH₂N_{ring}).

M/z (ES⁺) : 373 [M-H]³⁺, 559 [M-H]²⁺, 634 [M-OTf]²⁺

HR-ESMS (m/z) : Found 1417.4040 C₆₀H₇₁F₉N₉O₁₃S₃Yb requires [M-OTf]⁺, 1417.4058.

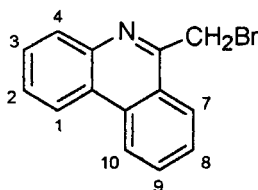
6-Methylphenanthridine 43



Phenanthridine (1.09 g, 6.08 mmol) was dissolved in dry THF (50 ml) under argon and the solution cooled to -78°C. Methyl lithium (solution 1.0 M in THF, 12 ml) was added dropwise with stirring. After the addition was complete the yellow-green solution was stirred at -78°C for 1 h then warmed to room temperature. The reaction was quenched with KOH solution (3 M, 30 ml) and the solution extracted with CH₂Cl₂ (50 mL). The organic layer was washed with water (100 ml), dried (Na₂SO₄) and the solvent removed under vacuum. The oily residue was re-dissolved in CH₂Cl₂ (50 ml) and stirred with excess MnO₂ (1 g) overnight. The mixture was filtered through a bed of celite and the filtrate evaporated to dryness under vacuum to give the title compound (1.11 g, 96%) as an orange oil.

¹H NMR (CDCl₃, 200 MHz): δ 8.61 (1H, d, *J* 8.0, H1), 8.53 (1H, d, *J* 8.0, H7), 8.20 (1H, d, *J* 8.0, H4) 8.09 (1H, d, *J* 8.0, H10), 7.56-7.87 (4H, m, H2H3H8H9), 3.04 (3H, s, CH₃).

M/z (ES⁺) : 195 [M+H]⁺

6-Bromomethylphenanthridine 44

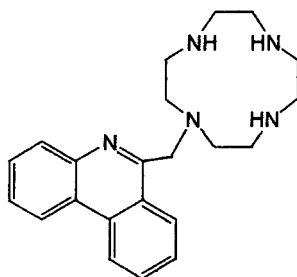
6-Methylphenanthridine **43** (1.4 g, 7.18 mmol) was dissolved in a mixture of CCl_4 (10 ml) and CHCl_3 (50 ml). *N*-Bromosuccinimide (1.5 g, 8.42 mmol, 1.1 eq.) and a catalytic amount of benzoyl peroxide were added and the resultant orange solution stirred at reflux for 5 hrs. The solution was cooled, filtered (to remove residual succinimide) and the solvent removed under vacuum. The residue was purified by chromatography over silica (CH_2Cl_2 /hexane; 3:1, R_f 0.3) to afford the title compound (1.6 g, 82%) as a pale yellow solid, mp. 107-108°C.

$^1\text{H NMR}$ (CDCl_3 , 200 MHz): δ 8.67 (1H, d, J 8.0, H1), 8.56 (1H, d, J 8.0, H7), 8.36 (1H, d, J 8.0, H4) 8.18 (1H, d, J 8.0, H10), 7.89 (1H, t, H2), 7.80-7.72 (3H, m, H3H8H9), 4.98 (2H, s, CH_2Br).

$^{13}\text{C NMR}$ (CDCl_3 , 75.4 MHz): δ 156.2 (C6), 142.8 (4°C), 133.6 (Cquatern.), 131.1, 130.3, 129.1, 127.8, 127.6, 126.5, 124.6 (Cquatern.), 124.2 (Cquatern.), 122.8, 122.2 (C aromatic), 32.3 (CH_2).

M/z (ES^+): 272/274 [$\text{M}+\text{H}$] $^+$, 295/297 [$\text{M}+\text{Na}$] $^+$

Elemental analysis: Found C, 61.6; H, 3.96; N, 5.01. $\text{C}_{14}\text{H}_{10}\text{BrN}$ requires C, 61.6; H, 3.70; N, 5.15%.

1-(6'-Methylphenanthridine)-1,4,7,10-tetraazacyclododecane 45

6-Bromomethylphenanthridine (220 mg, 0.809 mmol), cyclen (443 mg, 2.57 mmol, 3.2 eq.) and caesium carbonate (805 mg, 2.47 mmol) were stirred in acetonitrile (3 ml) overnight

under argon at room temperature. The solvent was removed under vacuum and the residue taken up into CHCl_3 (20 ml) and washed with purite water (3×30 ml), dried (Na_2SO_4), filtered and the solvent removed under vacuum to give a pale yellow oil (230 mg, 78%) which was used without purification, m.p. 60-61°C.

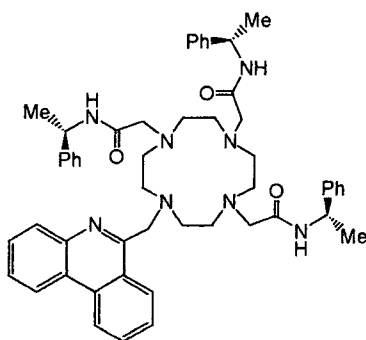
$^1\text{H NMR}$ (CDCl_3 , 200 MHz): δ 8.53 (1H, d, J 8.2, H1), 8.49-8.43 (2H, m, H7H4), 8.05 (1H, d, J 8.2, H10), 7.73 (1H, t, J 8.2, H2), 7.64-7.52 (3H, m, H3H8H9), 4.26 (2H, s, CH_2), 2.37-2.76 (16H, m, ring CH_2).

$^{13}\text{C NMR}$ (CDCl_3 , 75.4 MHz): δ 158.8 (C6), 143.0, 133.3, 130.1, 130.1, 128.7, 127.3, 127.2, 127.0, 125.6, 124.6, 122.5, 122.2 (Caromatic), 62.28 (Ar- CH_2), 53.09, 47.27, 46.27, 45.45 (C ring).

M/z (ES⁺): 364 [M+H]⁺

HR-ESMS (m/z): [M+H]⁺ found 364.2499; $\text{C}_{22}\text{H}_{29}\text{N}_5$ requires 364.2501.

1-(6'-Methylphenanthridine)-4,7,10-tris-[(*R*)-1-(1-phenyl)ethylcarbamoyl-methyl]-1,4,7,10-tetraazacyclododecane L⁹ 46



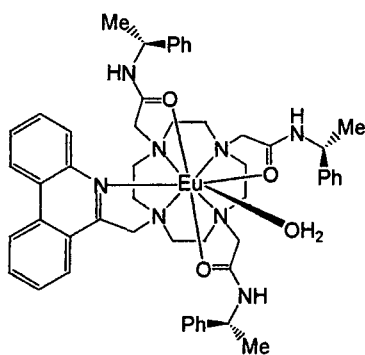
1-(6'-Methylphenanthridine)-1,4,7,10-tetraazacyclododecane (0.2 g, 0.554 mmol), (*R*)-*N*-2-chloroethanoyl-1-phenylmethylamine (0.34 g, 1.72 mmol, 3.1 eq.) and caesium carbonate (550 mg, 1.68 mmol) were stirred overnight in a mixture of CH_3CN (2 ml) and CH_2Cl_2 (2 ml) at 60°C under argon. The solvent was removed under vacuum and the residue taken up into CH_2Cl_2 (20 ml), washed with purite water (70 ml), dried (Na_2SO_4), filtered and evaporated to dryness to afford compound **46** (340 g, 73%) as an orange oily residue.

$^1\text{H NMR}$ (CDCl_3 , 200 MHz): δ 8.56 (1H, d, J 8, H1), 8.48 (1H, d, J 7.2, H7), 8.30 (1H, d, J 8, H4), 8.00 (1H, d, J 8, H10), 7.75 (1H, t, J 7.7, H2), 7.67-7.50 (3H, m, H3H8H9), 7.26-6.80 (18H, m, Ph, amide NH), 5.08-4.85 (3H, m, C*H), 3.88-3.91 (4H, m, pendent arms CH_2), 2.40-2.83 (20H, m, ring H, pendant arm CH_2), 1.33-1.43 (6H, m, CH_3), 1.24 (3H, d, J 6.8, CH_3).

M/z (ES^+): 444 $[\text{M}]^{2+}$, $[\text{M}+\text{Ca}]^{2+}$, 847 $[\text{M}+\text{H}]^+$, 869 $[\text{M}+\text{Na}]^+$

HR-ESMS (m/z): Found $[\text{M}+\text{H}]^+$ 847.5011. $\text{C}_{52}\text{H}_{62}\text{N}_8\text{O}_3$ requires 847.5023.

(RRR)-[EuL⁹](CF₃SO₃)₃·H₂O 47



The Eu(III) complex was prepared by stirring compound **46** (L^9) with 1 equivalent of $\text{Eu}(\text{OTf})_3$ in CH_3CN (1-2 mL) at 80°C overnight. The CH_3CN was then removed under vacuum and the oily residue taken up into a mixture of methanol (1 mL) and Purite water (10 mL) and the solvents removed on the freeze drier to give the complex as a pale yellow solid.

$^1\text{H NMR}$ (CD_3OD , 200 MHz): δ 39.4, 36, 25.3, 22.8 (s, 1H each, ring Hax), 16 (br s, 1H, phen H), 8.9-0 (30H, aromatic, CH, CH_3), 12.7 (1H), 11.5 (3H), 10.2 (1H), -1.3 (2H), -2.1 (2H), -2.9 (1H), -3.1 (1H), -7.7 (2H), -11.3 (2H), -12.6 (1H), -13.2 (1H), -15.3 (1H), -16.5 (1H), -18.8 (1H), -20.5 (1H), -20.9 (1H, NCHCO).

M/z (ES^+): 499 $[\text{M}+\text{H}]^{2+}$, 574 $[\text{M}+\text{OTf}]^{2+}$.

HR-ESMS (m/z): Found: $[\text{M} - (-\text{OTf})_3]^{2+}$ 499.2038 ; $\text{C}_{52}\text{H}_{62}\text{N}_8\text{EuO}_3$ requires 499.2040.

Therefore for monocharged ion, found $[\text{M} - (-\text{OTf})_3]^+$ 998.4076 ; requires 998.4075.

Elemental analysis : Found: C 44.85, H 4.28, N 7.02%. $\text{C}_{55}\text{H}_{62}\text{N}_8\text{EuF}_9\text{O}_{12}\text{S}_3 \cdot 2\text{H}_2\text{O}$ requires C 44.6, H 4.4, N 7.55%.

Conclusion

The thesis presents the synthesis and characterisation of chiral lanthanide complexes and their complexation behaviour with selected oligonucleotides and DNA.

In the second chapter the elaboration of complexes exhibiting pH-dependent luminescence was undertaken, with an appropriate chromophore chosen to sensitise efficiently the europium or terbium ion. The photophysical properties of each proposed chromophore were investigated under neutral and acidic conditions, and the ligand bearing a 6-butyl phenanthridine chromophore linked to a macrocyclic core was synthesised on this basis. The protonation constants for the europium and terbium tri-acetate and tri-phosphinate complexes were measured using ligand fluorescence and metal emission changes. The substitution by the 6-butyl group allowed the apparent protonation constant to be increased by 1.2 units compared to the parent.

The third and fourth chapters deal with the interaction of well-defined chiral lanthanide complexes with oligonucleotides. Fundamental aspects of the recognition process were evaluated. An intercalative binding mode was defined for several complexes, to which systematic structural or electronic variations were effected. Thus the different factors that may influence the binding of a given complex were studied: its helicity, the length of the linking arm, the degree of steric hindrance, the electron deficiency of the intercalative unit and the choice of the complexed lanthanide ion.

Firstly the helicity at the metal centre was shown to determine the strength and the stereoselectivity of the binding. This was demonstrated for the complexes $[\text{LnL}^1]^{4+}$, $[\text{LnL}^3]^{3+}$, and $[\text{LnL}^{5-8}]^{3+}$. For the tetracationic L^1 complexes, the Δ isomer showed the greatest affinity for $[(\text{CG})_6]_2$, while for the tricationic complexes L^3 and L^{5-8} , the Λ isomer was found to bind more strongly. The tuning of the helicity by an additional chiral centre introduced in $[\text{LnL}^{5-8}]^{3+}$ complexes appeared to enhance the selectivity in binding.

Secondly, the length of the linking arm between the phenanthridine chromophore and the chiral macrocyclic unit was modified both in series of 2-phenanthridyl and 6-phenanthridyl complexes. Bringing the element of helicity closer to the intercalative unit was postulated to enhance the selectivity of interaction with the DNA helix. Unfortunately, such complexes,

i.e. $[\text{LnL}^4]^{4+}$ and $[\text{LnL}^9]^{3+}$ & $[\text{LnL}^{10}]^{3+}$ each possessed considerable inflexibility in their structure, which may have inhibited their efficient interaction with the oligonucleotides.

However, the shortening of the linking arm in the complex $[\text{LnL}^4]^{4+} \cdot (\text{H}_2\text{O})_2$ (a complex of a heptadentate ligand) led to complexation behaviour in which more marked changes occurred at the metal centre. The form of the hypersensitive transitions in the Eu emission spectra suggested the ligation of a DNA phosphate oxygen in the binding of the complex.

In addition to the rigidity of the complex, steric inhibition of binding with $[\text{LnL}^{5-8}]^{3+}$ may have inhibited the phenanthridine chromophore from sliding between the DNA base pairs. No evidence for intercalation was found for these tricationic complexes. An electrostatic binding mode coupled to some degree of groove binding are more probable interactions, given that the phenanthridine-conjugate linked via its 6-position offered only a restricted aromatic surface to interact with the nucleic acids. The significant lipophilicity of the complex as well as the possibility of stabilising hydrogen bonding interactions, e.g. with the phenanthridine nitrogen, may also contribute to the putative groove-binding mode.

Thirdly the electron deficiency of the phenanthridine moiety served to influence the strength and the selectivity of the intercalative binding. A cationic chromophore favoured a charge-transfer interaction with the more electron-rich base pairs. Intercalative binding occurred preferentially to CG base pairs for the tetra- and, to a lesser extent, the tri-cationic phenanthridine complexes, $[\text{LnL}^1]^{4+}$ and $[\text{LnL}^3]^{3+}$.

Finally the choice of the lanthanide ion europium and ytterbium gave rise to distinctly different behaviour in the binding of $[\text{LnL}^1]^{4+}$, $[\text{LnL}^3]^{3+}$, and $[\text{LnL}^{5-8}]^{3+}$ with the oligonucleotides used in this study. A tentative suggestion for the difference relates to the acidity of the water molecule bound to the lanthanide. This is likely to be more acidic in ytterbium complex, and therefore may affect the binding to the duplex through a differential hydrogen-bonding interaction.

The studies carried out with the complexes studied herein are preliminary in nature and certainly not exhaustive! Further work may embrace the development of reactive complexes, in which either singlet oxygen is produced by a DNA-bound Tb complex, or wherein hydrolytic cleavage is facilitated by cooperative intercalation and phosphate oxygen-Ln(III) binding.

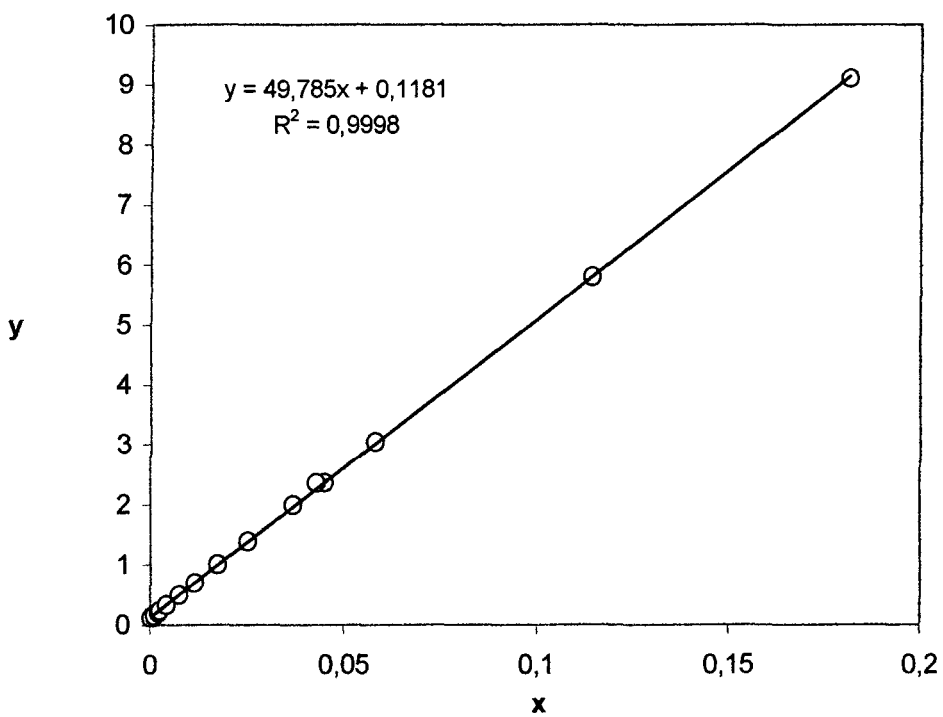
Appendix

Determination of apparent binding constants

1. Representative data set for titration of Λ -[YbL^{1a}]⁴⁺ with [(CG)₆]₂.

Data handling using intrinsic methods to determine the concentration of bound complex (see part 3.1.4):

Flu (408nm)	$r_j = o - l $	r_k	$r_k - r_j$	$[DNA]_2 = C_j$	C_k	$C_k - C_j$	x	y
51		6	6	0				
45	6	12	6	0,6374	1,2748	0,6374	0	0,1062333
39	12	17	5	1,2748	1,9122	0,6374	0,0012498	0,12748
34	17	23	6	1,9122	2,5496	0,6374	-0,0002717	0,1062333
28	23	28	5	2,5496	3,187	0,6374	0,00059385	0,12748
23	28	33	5	3,187	3,8244	0,6374	0,0004139	0,12748
18	33	37	4	3,8244	4,4618	0,6374	0,00117457	0,15935
14	37	40	3	4,4618	5,0992	0,6374	0,00229694	0,2124667
11	40	42,69	2,69	5,0992	5,7366	0,6374	0,00256434	0,2369517
8,31	42,69	44,63	1,94	5,7366	6,374	0,6374	0,00435085	0,3285567
6,37	44,63	45,92	1,29	6,374	7,0114	0,6374	0,00765004	0,4941085
5,08	45,92	46,84	0,92	7,0114	7,6488	0,6374	0,01153157	0,6928261
4,16	46,84	47,48	0,64	7,6488	8,2862	0,6374	0,01753667	0,9959375
3,52	47,48	47,94	0,46	8,2862	8,9236	0,6374	0,0252635	1,3856522
3,06	47,94	48,21	0,27	8,9236	9,561	0,6374	0,04510682	2,3607407
2,79	48,21	48,53	0,32	9,561	10,1984	0,6374	0,03695766	1,991875
2,47	48,53	48,74	0,21	10,1984	10,8358	0,6374	0,05796249	3,0352381
2,26	48,74	48,85	0,11	10,8358	11,4732	0,6374	0,11406811	5,7945455
2,15	48,85	48,92	0,07	11,4732	12,1106	0,6374	0,18133378	9,1057143
2,08	48,92	49,19	0,27	12,1106	12,748	0,6374	0,04295957	2,3607407



Intrinsic method for determination of α

slope = L_{tot} / α with $L_{tot} = 24.4 \mu\text{M}$

hence $\alpha = 0.490$

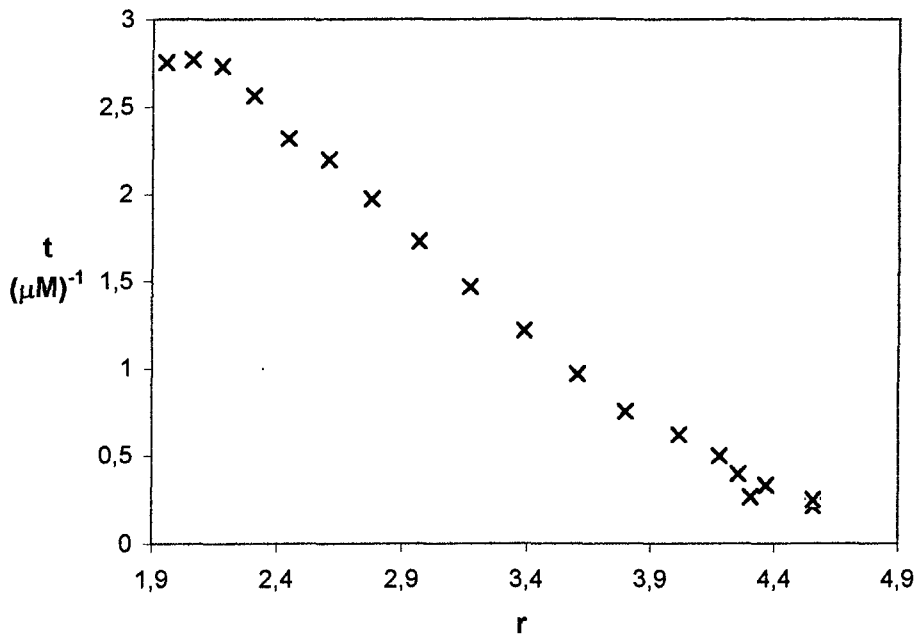
So the concentration of bound complex can determined:

$$L_b = \alpha \cdot r_j$$

where r_j is variation of fluorescence

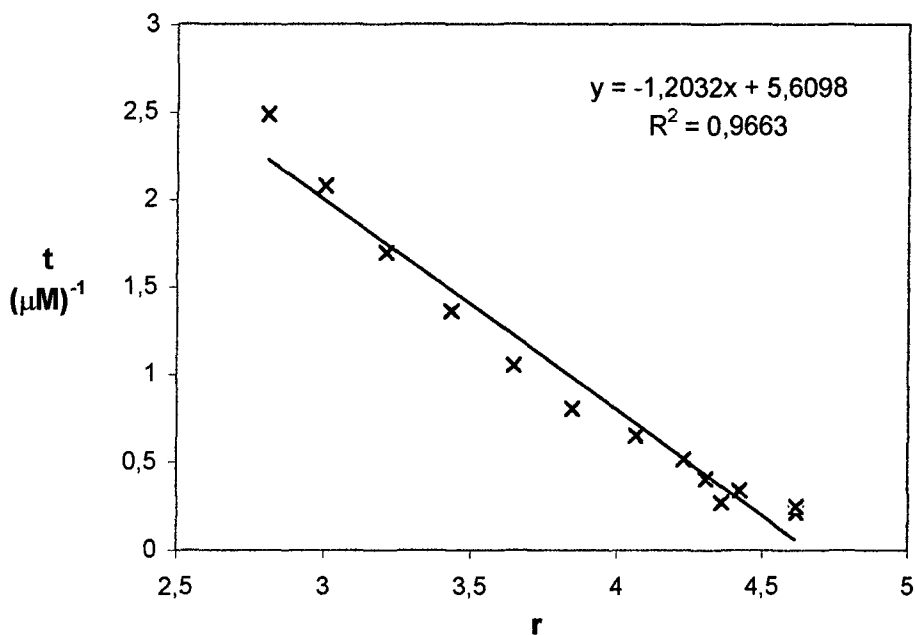
2. Handling of data using McGhee/von Hippel approach

r_j	$[DNA]_2=c_j$	$L_b=\alpha \cdot r_j$	$l_f=24,4-l_b$	$r=l_b/c_j$	$t=r/l_f$
6	0,6374	2,940645	21,45936	4,6135	0,214988
12	1,2748	5,88129	18,51871	4,6135	0,249126
17	1,9122	8,331827	16,06817	4,357194	0,271169
23	2,5496	11,27247	13,12753	4,421271	0,336794
28	3,187	13,72301	10,67699	4,305933	0,403291
33	3,8244	16,17355	8,226454	4,229041	0,514078
37	4,4618	18,13398	6,266024	4,064274	0,648621
40	5,0992	19,6043	4,795702	3,844583	0,801673
42,69	5,7366	20,92269	3,477312	3,647228	1,048864
44,63	6,374	21,8735	2,526504	3,431675	1,35827
45,92	7,0114	22,50573	1,894265	3,209877	1,694524
46,84	7,6488	22,95663	1,443366	3,001338	2,079401
47,48	8,2862	23,2703	1,129698	2,80832	2,485904
47,94	8,9236	23,49575	0,904248	2,63299	2,9118
48,21	9,561	23,62808	0,771919	2,471298	3,201498
48,53	10,1984	23,78492	0,615085	2,33222	3,791705
48,74	10,8358	23,88784	0,512162	2,204529	4,304357
48,85	11,4732	23,94175	0,45825	2,086754	4,553742
48,92	12,1106	23,97606	0,423943	1,979758	4,669869
49,19	12,748	24,10839	0,291614	1,89115	6,485117



McGhee von Hippel plot with all data

K value ($x = 0; K = t$) was fairly insensitive to the fitted value of n . The major error seems to be associated with determination of n' : e.g. at low values of t , n' can be 4 or 4.5, with little change in K .



McGhee-von Hippel plot – approximation of the central portion of 'curve'

The value for K is $5.6 \mu\text{M}^{-1} \cdot \text{duplex}^{-1}$, with 4-4.5 complexes bound to the duplex of $(\text{CG})_6$. Obviously an additional approximation, but iterative least squares fitting gives values for K , n' which are within 10-15% of the value given here.

